CONTRACTOR REPORT ARLCD-CR-81018

EXPLOSIVE FRAGMENTATION OF DIVIDING WALLS

L. M. VARGAS
J. C. HOKANSON
SOUTHWEST RESEARCH INSTITUTE
6220 CULEBRA ROAD
SAN ANTONIO, TX 78284

R.M. RINDNER
PROJECT LEADER
ARRADCOM

JULY 1981

US ARMY ARMAMENT RESEARCH AND DEVELOPMENT COMMAND
LARGE CALIBER
WEAPON SYSTEMS LABORATORY
DOVER, NEW JERSEY

UNCLASSIFIED

SECURITY CLASSIFICATION OF THIS PAGE (When Data Entered)

REPORT DOCUMENTATION PAGE

READ INSTRUCTIONS BEFORE COMPLETING FORM

1. REPORT NUMBER CONTRACTOR REPORT ARLCD-CR-81018	2. GOVT ACCESSION NO. AD-A104348	3. RECIPIENT'S CATALOG NUMBER
4. TITLE (and Subtitle) EXPLOSIVE FRAGMENTATION OF DIVIDING WALLS		5. TYPE OF REPORT & PERIOD COVERED Final Report
		6. PERFORMING ORG. REPORT NUMBER 02-5793
7. AUTHOR(s) L. M. Vargas and J. C. Hokanson, Southwest Research Institute R. M. Rindner, Project Leader, ARRADCOM		8. CONTRACT OR GRANT NUMBER(s) DAAK10-79-C-0325
9. PERFORMING ORGANIZATION NAME AND ADDRESS Southwest Research Institute 6220 Culebra Road San Antonio, TX 78284		10. PROGRAM ELEMENT, PROJECT, TASK AREA & WORK UNIT NUMBERS
11. CONTROLLING OFFICE NAME AND ADDRESS ARRADCOM, TSD STINFO Div (DRDAR-TSS) Dover, NJ 07801		12. REPORT DATE July 1981
		13. NUMBER OF PAGES 200
14. MONITORING AGENCY NAME & ADDRESS (if different from Controlling Office) ARRADCOM, LCWSL Energetic Systems Process Division, LCWSL Dover, NJ 07801 (DRDAR-LCM-SP)		15. SECURITY CLASS. (of this report) Unclassified
		15a. DECLASSIFICATION/DOWNGRADING SCHEDULE

16. DISTRIBUTION STATEMENT (of this Report)

Approved for public release; distribution unlimited.

17. DISTRIBUTION STATEMENT (of the abstract entered in Block 20, if different from Report)

18. SUPPLEMENTARY NOTES

19. KEY WORDS (Continue on reverse side if necessary and identify by block number)

Dividing wall fragmentation	Impulse	Masonry walls
Reinforced concrete	Explosive loading	Scale model
Spalling	Blast loading	
Fragmentation	Fragment velocity	

20. ABSTRACT (Continue on reverse side if necessary and identify by block number)

A study to determine the fragmentation characteristics of reinforced concrete and masonry dividing walls subjected to close-in blast effects has been performed. This study concentrated its efforts on obtaining data on the following parameters: fragment velocity, fragment shape and size, and fragment density down range.

(Cont)

DD FORM 1 JAN 73 1473 EDITION OF 1 NOV 65 IS OBSOLETE

UNCLASSIFIED

SECURITY CLASSIFICATION OF THIS PAGE (When Data Entered)

UNCLASSIFIED

SECURITY CLASSIFICATION OF THIS PAGE(When Data Entered)

20. ABSTRACT (Cont)

A test plan for validation tests was developed based on the results of the literature search and the model analysis. Thirty-six tests using 1/6th-scale model reinforced concrete dividing walls and four full-scale masonry dividing wall tests were performed. Charge weight, standoff distance, wall thickness, reinforcement spacing and restraint conditions were varied for the reinforced concrete wall tests; charge weight, standoff distance, and type of block were varied for the masonry wall tests. Fragments were recovered, sized, and weighed, and fragment velocities were measured for all tests.

A procedure was developed for estimating the total impulse imparted to the dividing wall during an explosion. An empirical prediction model, which adequately correlated the experimental data for the number of fragments produced, the highest velocity, the longest range, and the largest mass with the total impulse was developed. Statistical distributions for fragment mass and range were prepared in the format of arena tests of bombs and large caliber projectiles.

UNCLASSIFIED

SECURITY CLASSIFICATION OF THIS PAGE(When Data Entered)

ACKNOWLEDGMENTS

The authors would like to express their appreciation to Mr. E. P. Bergmann for his guidance and assistance during the course of this program. The authors would also like to express their appreciation to Messrs. M. Ray Burgamy, Kirtland W. Thistlethwaite, and Richard A. Cervantes of SwRI for their assistance in conducting the experiments and to Mlles. Donna K. Wauters and Norma Sandoval for their assistance in reducing the data.

CONTENTS

		Page
1.0	Introduction	1
2.0	Experimental Program	2
	2.1 General	2
	2.2 Fabrication of Reinforced Concrete Model Walls	2
	2.3 Fabrication of Masonry Block Dividing Walls	7
	2.4 Test Setup and Procedures	7
3.0	Test Results	16
	3.1 General	16
	3.2 Reinforced Concrete Panel Test Results	16
	3.3 General Summary of Test Results	18
	3.4 Fragment Mass Distributions	21
	3.5 Fragment Range Distributions	36
	3.6 Velocity Distributions	36
	3.7 Maximum Responses	52
	3.7.1 Largest Velocity	56
	3.7.2 Largest Range	56
	3.7.3 Number of Fragments Produced	61
	3.7.4 Largest Mass	61
	3.8 Masonry Wall Test Results	61
4.0	Conclusions	70
5.0	Recommendations	73
6.0	References	75
Appendixes		
	A - Results of Literature Search and Model Analysis	77
	B - Test Summaries	93
	C - General Summary of Test Results	119
	D - Fragment Maps	159
Distribution List		199

LIST OF TABLES

Table		Page
2-1.	Concrete Mixes	5
2-2.	Program Test Plan	12
3-1.	Fragment Velocity Computation Summary	51
3-2.	Summary of Single Side Support Tests	53
3-3.	Summary of Three Side Support Tests	54
3-4.	Masonry Dividing Wall Test Results	66

LIST OF ILLUSTRATIONS

Figure		Page
2-1.	Deformed Wire Used to Simulate Reinforcement Bars	4
2-2.	Fabrication Mold for Reinforced Concrete Panels	6
2-3.	Schematic Drawing of the Reinforced Concrete Panel Mounting Fixture	8
2-4.	Photograph of the Test Fixture for a Single Side Supported Test	9
2-5.	Photograph of the Test Fixture for a Three Side Supported Test	10
2-6.	Test Arrangement for a Masonry Block Wall	11
2-7.	Test Setup	14
2-8.	Typical Camera Setup	15
3-1.	Dual Hinge Failure of a Single Side Supported Reinforced Concrete Panel	17
3-2.	Multiple Hinge Failure of a Three Side Supported Panel at Low Impulse Levels	19
3-3.	Failure Pattern of a Three Side Supported Panel at High Impulse Levels	20
3-4a.	Mass Distribution for Test Series 1CW	22
3-4b.	Mass Distribution for Test Series 2CW	23
3-5a.	Mass Distribution for Test Series 1W	24
3-5b.	Mass Distribution for Test Series 2W	25
3-5c.	Mass Distribution for Test Series 3W	26
3-6a.	Mass Distribution for Test Series 1S	27
3-6b.	Mass Distribution for Test Series 2S	28
3-6c.	Mass Distribution for Test Series 3S	29
3-6d.	Mass Distribution for Test Series 4S	30
3-7.	Mass Distribution for Test Series 8W	31

LIST OF ILLUSTRATIONS (Con't)

Figure		Page
3-8a.	Mass Distribution for Test Series 5S	32
3-8b.	Mass Distribution for Test Series 6S	33
3-8c.	Mass Distribution for Test Series 7S	34
3-8d.	Mass Distribution for Test Series 8S	35
3-9a.	Range Distribution for Test Series 1CW	37
3-9b.	Range Distribution for Test Series 2CW	38
3-10a.	Range Distribution for Test Series 1W	39
3-10b.	Range Distribution for Test Series 2W	40
3-10c.	Range Distibution for Test Series 3W	41
3-11a.	Range Distribution for Test Series 1S	42
3-11b.	Range Distribution for Test Series 2S	43
3-11c.	Range Distribution for Test Series 3S	44
3-11d.	Range Distribution for Test Series 4S	45
3-12.	Range Distribution for Test Series 8W	46
3-13a.	Range Distribution for Test Series 5S	47
3-13b.	Range Distribution for Test Series 6S	48
3-13c.	Range Distribution for Test Series 7S	49
3-13d.	Range Distribution for Test Series 8S	50
3-14.	Scaled Specific Impulse Distribution	55
3-15a.	The Largest Fragment Velocity as a Function of the Impulse Factor for Single Side Supported Panels	57
3-15b.	The Largest Fragment Velocity as a Function of the Impulse Factor for Three Side Supported Panels	58
3-16a.	The Largest Fragment Range as a Function of the Scaled Impulse Factor for Single Side Supported Panels	59
3-16b.	The Largest Fragment Range as a Function of the Impulse Factor for Three Side Supported Panels	60

LIST OF ILLUSTRATIONS (Con't)

Figure		Page
3-17a.	Number of Fragments Produced as a Function of the Scaled Impulse Factor for Single Side Supported Panels	62
3-17b.	Number of Fragments Produced as a Function of the Impulse Factor for Three Side Supported Panels	63
3-18a.	Largest Recovered Mass as a Function of the Scaled Impulse Factor for Single Side Supported Panels	64
3-18b.	Largest Recovered Mass as a Function of the Impulse Factor for Three Side Supported Panels	65
3-19.	Failure Pattern for a Haydite Block Dividing Wall Test	68
3-20.	Failure Pattern for a Concrete Block Dividing Wall Test	69
5-1.	Suggested Dividing Wall Concepts	74

1.0 INTRODUCTION

In munition manufacturing facilities, reinforced concrete dividing walls are used as shields for personnel protection and as physical barriers between explosive production steps. If an explosion should occur, the dividing wall may break up under the overpressure loading. Fragments emerging from the back side of the wall may impact an adjacent explosive source with sufficient energy to cause a secondary initiation, or may be a hazard for nearby inhabited buildings. The sensitivity of selected munitions and explosives to fragment impact is being investigated and sufficient data are available to predict threshold initiation conditions. However, the fragment hazard associated with wall breakup under blast loadings is an area which has not been extensively studied. Current predictive techniques for determining wall fragmentation are based solely on analytical studies which have limited scopes and few practical design applications. For these reasons, the current safety regulations which have evolved are quite conservative:

1) building must be located such that less than one fragment per 55.7 m^2 (600 ft^2) exposed building area with an energy greater than 78.6 J (58 foot pounds) strikes the structure;

2) if the above criteria (1) cannot be met, then inhabited building distance of 381 m (1250 ft) minimum is required for siting quantities greater than 45.4 kg (100 lb).

In the majority of design applications, the spall fragment density is not known, so the second and most costly requirement is usually enforced.

The objective of this program was to determine the fragmentation characteristics of reinforced concrete and masonry dividing walls subjected to close-in blast effects. A literature search and review of related programs was performed. A model analysis was also developed as part of this program. A test plan was developed based on the model analysis and on a review of the pertinent data. Validation tests using 1/6th-scale reinforced concrete dividing wall models and full scale masonry walls were performed and the pertinent data recorded. Comparisons of the experimental versus the predicted results were performed and predictive models developed.

This report is divided into five major sections. Section 2.0 describes the experimental program, including the development of the test plan, the test set-up, fabrication of the 1/6th-scale model walls, and the data collection and reduction procedures. Section 3.0 presents the results of the experimental program for both the reinforced concrete and masonry walls. The effects of varying wall thickness, reinforcement, concrete strength, charge location and impulse on the fragmentation characteristics of reinforced concrete are all discussed in this section. Section 4.0 presents conclusions, while Section 5.0 presents recommendations and Section 6.0 is the list of references. The results of the literature search and review of related programs as well as the details of the model analysis are presented in Appendix A.

2.0 EXPERIMENTAL PROGRAM

2.1 General

The objective of this test program was to obtain the fragmentation characteristics of reinforced concrete dividing walls and masonry dividing walls subjected to transient air shocks. Fragment data such as fragment velocities, shapes, sizes, and density downrange were obtained for 1/6th-scale model reinforced concrete dividing walls and for full-scale masonry block dividing walls. The tests on the reinforced concrete walls were performed varying the wall thickness, reinforcement bar spacing, wall support conditions, charge weight, and standoff distance. The tests on the masonry block walls were performed varying only the charge size and standoff distance. Fragment velocities were measured for all tests using high-speed cameras, and the fragments themselves were recovered using a fine sand runway. Fragment downrange positions were recorded and each individual fragment was weighed and sized.

2.2 Fabrication of Reinforced Concrete Model Walls

In selecting a representative scale model dividing wall, considerable research was performed to obtain the physical dimensions of a full-scale dividing wall. It was found that dividing walls range in thickness from 15.24 cm (6.0 inches) to several feet, in height from 2.44 to 4.57 m (8.0 to 15.0 feet) and in width from 2.44 to 6.1 m (8.0 to 20.0 feet). Most dividing walls have vertical and horizontal reinforcement bars [No. 4 rebar at 30.48 cm (12 inches) centers] and may or may not have lacing. TM 5-1300 (Reference 1) requires that newer walls have lacing; however, for this program it was decided to limit the study to walls with vertical and horizontal reinforcements without lacing. Four full-scale wall designs were selected as being representative of dividing walls and they include the following:

1) 2.44 m x 2.44 m x 0.3 m (8 ft x 8 ft x 1 ft) with No. 4 rebar at 30.5 cm (12 in) centers
2) 2.44 m x 2.44 m x 0.3 m (8 ft x 8 ft x 1 ft) with No. 4 rebar at 15.2 cm (6 in) centers
3) 2.44 m x 2.44 m x 0.46 m (8 ft x 8 ft x 1.5 ft) with No. 4 rebar at 30.5 cm (12 in) centers
4) 2.44 m x 2.44 m x 0.46 m (8 ft x 8 ft x 1.5 ft) with No. 4 rebar at 15.2 cm (6 in) centers.

As previously mentioned, it was decided to use 1/6th-scale model walls and the corresponding 1/6th-scale model walls had the following dimensions:

1) 0.46m x 0.46 m x 5.1 cm (18 in x 18 in x 2 in) with 0.21 cm (0.083 in) wire at 5.1 cm (2 in) centers (Design No. 1)

2) 0.46 m x 0.46 m x 5.1 cm (18 in x 18 in x 2 in) with 0.21 cm (0.083 in) wire at 2.54 cm (1 in) centers (Design No. 2)
3) 0.46 m x 0.46 m x 7.62 cm (18 in x 18 in x 3 in) with 0.21 cm (0.083 in) wire at 5.1 cm (2 in) centers (Design No. 3)
4) 0.46 m x 0.46 m x 7.62 cm (18 in x 18 in x 3 in) with 0.21 cm (0.083 in) wire at 2.54 cm (1 in) centers (Design No. 4).

In fabricating the 1/6th-scale model walls, 14 gage [0.21 cm (0.083 in) diameter] galvanized steel wire was used to simulate the reinforcing bars. It was felt that the bond between the rebar and the concrete in the full-scale walls was important enough that an attempt to model the deformations on the full-scale rebar should be made. Therefore, a knurling tool was used to deform the 14 gage wire. Figure 2-1 presents a picture of the deformed wire. Yield and tensile strength tests were performed on the deformed wire and the yield strength was found to be 404.4 MPa (58,700 psi) and the ultimate strength was 451.3 MPa (65,500 psi) with a percent elongation of approximately 14 percent. These strengths were judged to be acceptable and this particular type of wire was used in all of the scaled reinforced concrete walls.

A number of concrete mixes were also evaluated in an effort to obtain a concrete and scaled aggregate which would give the necessary compressive strength of approximately 27.6 MPa (4,000 psi). Table 2-1 presents a summary of the various mixes which were tested. Included in this table are the results of the compressive strength tests performed on each type concrete. Initially, the decision was made to use a Portland Type III concrete which is a fast setting, high strength concrete. However, the compressive strengths for the mixes using Type III concrete were either too high or the mix was too thick and would not flow. It was decided to use Type I concrete instead of Type III because the Type I would attain lower strengths than the Type III, i.e., in the neighborhood of 27.6 MPa (4,000 psi) after a seven day cure, and the strength would not increase appreciably over a several month time span. Tests No. 3, 4 and 5 were performed using different aggregate, sand, and concrete ratios and also by varying the amount of water. The resulting mixes were found to be either too thick or the strength was too low. Two more concrete mixes were tested, Tests No. 6 and 7. These mixes were fluid enough to allow for easy pouring into the molds for the scale walls and the strengths; specifically Test No. 7 was acceptable.

Molds for the reinforced concrete walls were composed of a rectangular plywood frame which was designed to be reusable. Each mold had a series of holes drilled into the sides which accepted the scale rebar and held it in position at the proper depth in the wall, about 6.35 mm (0.25 in) from the surface of the wall. Figure 2-2 shows a completed mold with both vertical and horizontal rebar. The concrete was poured into the molds such that an approximate layer of concrete, 6.35 mm (0.25 in) thick, covered the rebar on both the front and back sides of the wall. Compression test coupons were poured every time

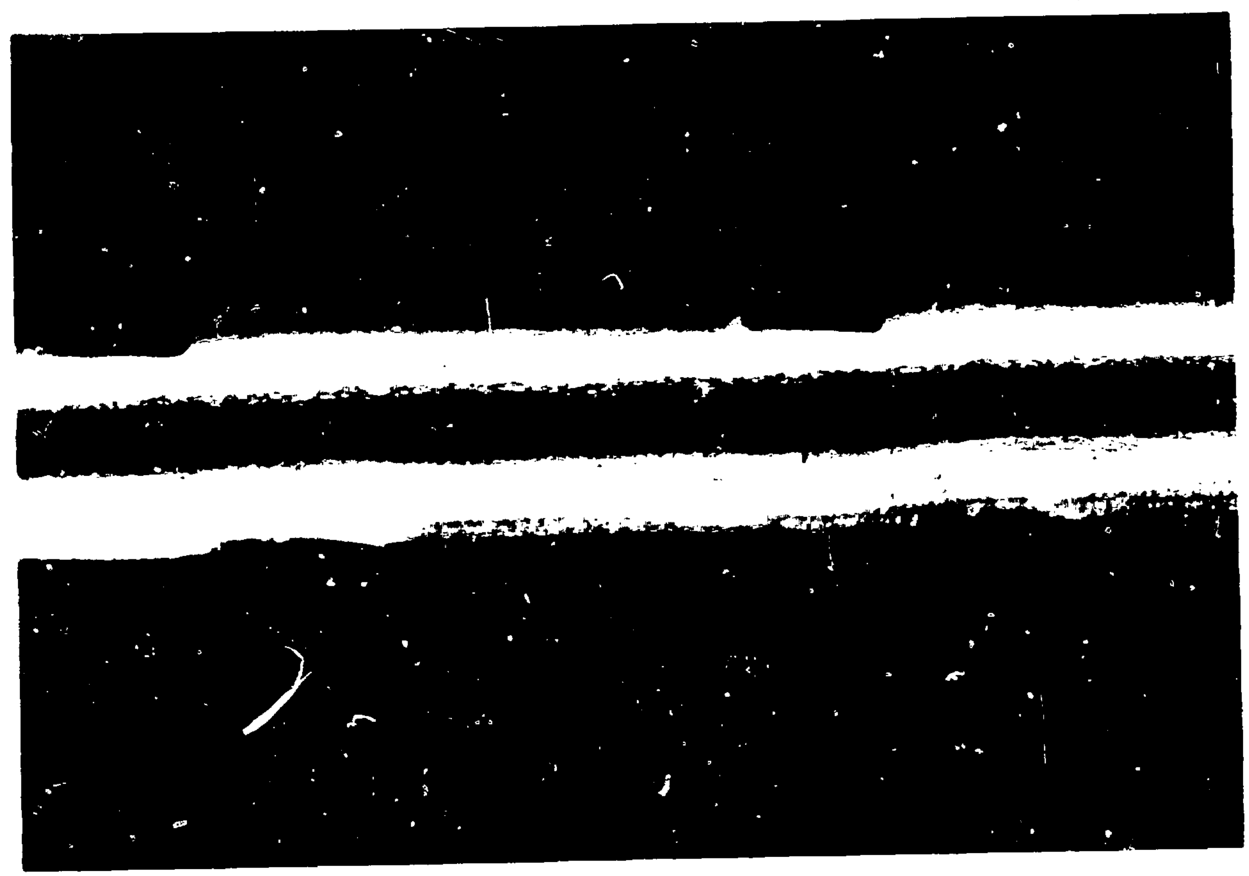

Figure 2-1. Deformed Wire Used to Simulate Reinforcement Bars

Table 2-1. Concrete Mixes

Test No.	1	2	3	4	5	6	7
Mix Ratio (Aggregate, Sand, Concrete)	3-2-1	2-2-1	4-0-1	3-2-1	2-2-1	1-2-1	1-2-1
Concrete Type	III	III	I	I	I	I	I
Type Aggregate	Crushed Pea Gravel	Crushed Pea Gravel	Limestone Gravel	Limestone Gravel	Limestone Gravel	Limestone Gravel	Limestone Gravel
Aggregate Size (Percent)	10% - on 6 35% - on 10 45% - on 20 10% - on 40	10% - on 6 35% - on 10 45% - on 20 10% - on 40	— 20% - on 10 60% - on 20 20% - on 40	— 20% - on 10 60% - on 20 20% - on 40	— 20% - on 10 60% - on 20 20% - on 40	— 20% - on 10 60% - on 20 20% - on 40	— 20% - on 10 60% - on 20 20% - on 40
Sand Size	-40 on 60	-40 + 60	N/A	-40 + 60	-40 + 60	Sandblast Sand	Sandblast Sand
Lomar D %	1/4 %	1/4 %	1/4 %	1/4 %	1/4 %	1/4 %	1/4 %
$CaCl_2$	2 %	2 %	2 %	2 %	2 %	2 %	2 %
Water	45 %	45 %	62 %	70 %	62 %	55 %	60 %
Compressive Strength MPa (psi)							
1 Day Break	—	—	—	—	—	14.2 (2060)	10.2 (1480)
3 Day Break	18.95 (2750)	33.4 (4850)	—	—	—	29.2 (4240)	22.5 (3270)
5 Day Break	—	—	27.6 (4000)	17.9 (2600)	27.8 (4040)	—	—
7 Day Break	—	—	29.1 (4230)	20.2 (2930)	29.8 (4320)	35.8 (5190)	30.0 (4360)
10 Day Break	19.1 (2770)	36.9 (5350)	—	—	—	—	—

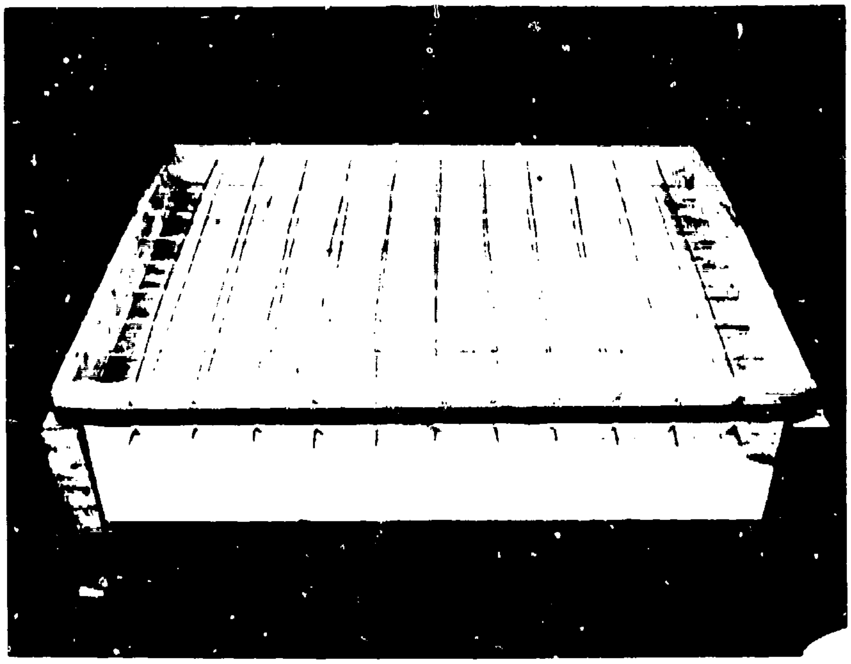

FIGURE 2-2. FABRICATION MOLD FOR REINFORCED CONCRETE PANELS

that walls were poured to allow the determination of the walls' compressive strength at the time of testing. The test walls were allowed to cure for at least seven days prior to testing.

A test fixture was designed to allow for testing the scaled model reinforced concrete walls in two support configurations, i.e., one side supported and three side supported. A design drawing of the mounting fixture has been included in this report as Figure 2-3. This fixture consists of a 15.24 cm (6.0 in) deep horizontal bracket and two removable 7.62 cm (3.0 in) deep side brackets. Walls to be tested with one side fixed were mounted in the horizontal bracket. For tests with three sides fixed, the vertical side brackets were attached to the fixture and the wall was then slipped down between the two side brackets and into the horizontal bracket. Shims were used to secure the wall rigidly inside the frame, both at the sides and at the bottom. Figure 2-4 shows a wall supported on one side, at the base, simulating a wall fixed at the bottom and Figure 2-5 shows a wall supported on three sides.

2.3 Fabrication of Masonry Block Dividing Walls

The primary emphasis of this program was on fragmentation of blast loaded reinforced concrete walls, however, a limited test program, i.e., four tests, was conducted on masonry block dividing walls. Due to the difficulties associated with fabricating 1/6th-scale model masonry blocks and the complexity of the molds that would have to be built, it was decided to use full-scale masonry blocks. The walls fabricated were 163 cm (64.0 in) wide, 142 cm (56.0 in) high and supported only at the base. A review of design drawings for typical masonry walls showed that these walls normally have No. 6 rebar at 122 cm (48.0 in) centers as well as a wall/foundation tie-down. The masonry block dividing walls built for this program had this reinforcement as shown in Figure 2-6. Two dividing walls were built using the standard haydite blocks and two walls were built using the stronger concrete blocks. Each of the walls was allowed to cure for at least three days prior to testing. The two tests performed on the haydite block walls used the same charge weight, 0.454 kg (1 lb) of C-4 explosive; however, the standoff distance was varied. One of the tests on the concrete block wall was performed using 0.454 kg (1 lb) of C-4 charge and at the same standoff as the haydite block tests for comparison purposes and the second test was performed using a 1.362 kg (3.0 lb) of C-4 charge. Details of the test program are provided in a later section.

2.4 Test Setup and Procedures

A detailed test program was developed for this study and is summarized in Table 2-2. Tests were conducted varying the reinforced concrete wall thickness, the percent reinforcement, the charge size, the standoff distance and the constraint conditions. The initial values for the peak specific impulse delivered to the panels were calculated

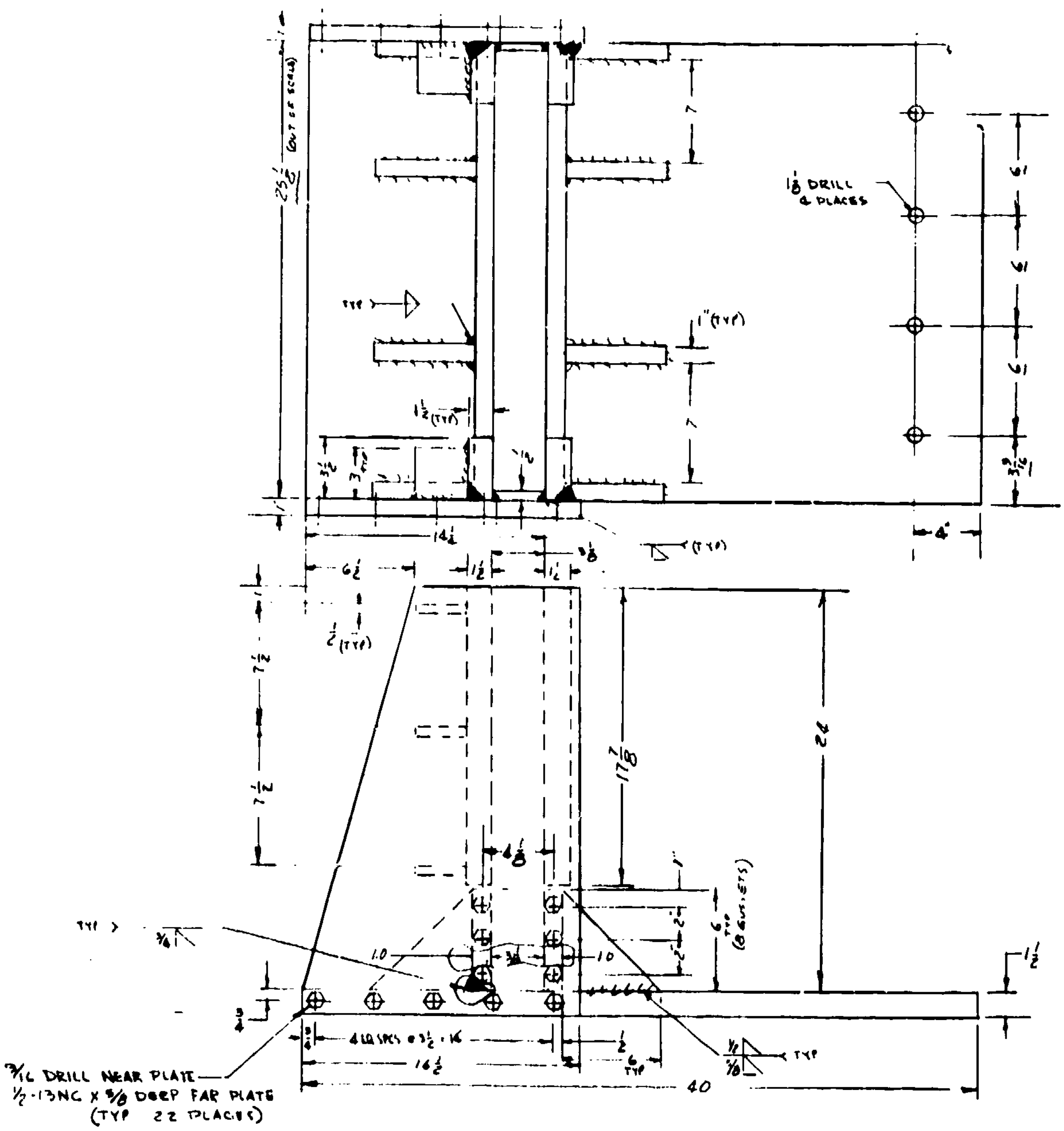

FIGURE 2-3. SCHEMATIC DRAWING OF THE REINFORCED CONCRETE PANEL MOUNTING FIXTURE

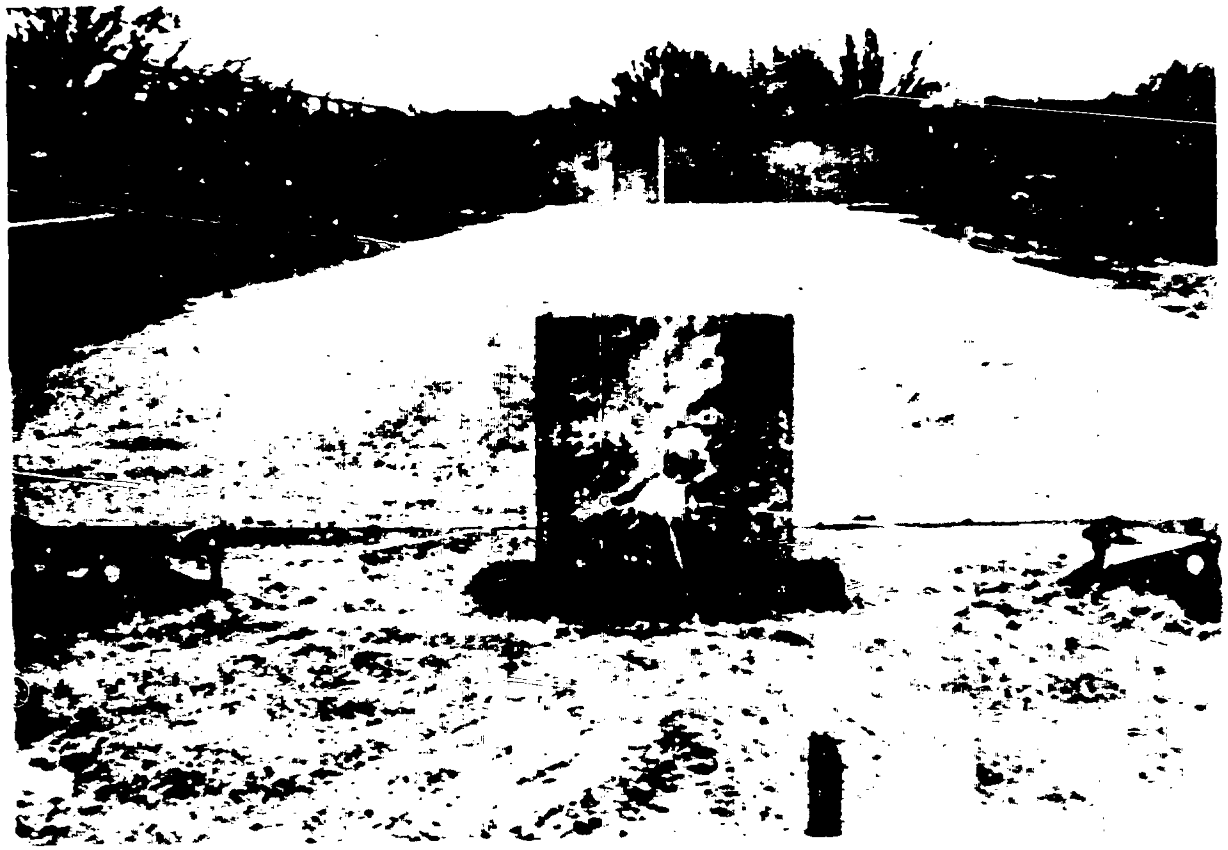

FIGURE 2-4. PHOTOGRAPH OF THE TEST FIXTURE FOR A SINGLE SIDE SUPPORTED TEST

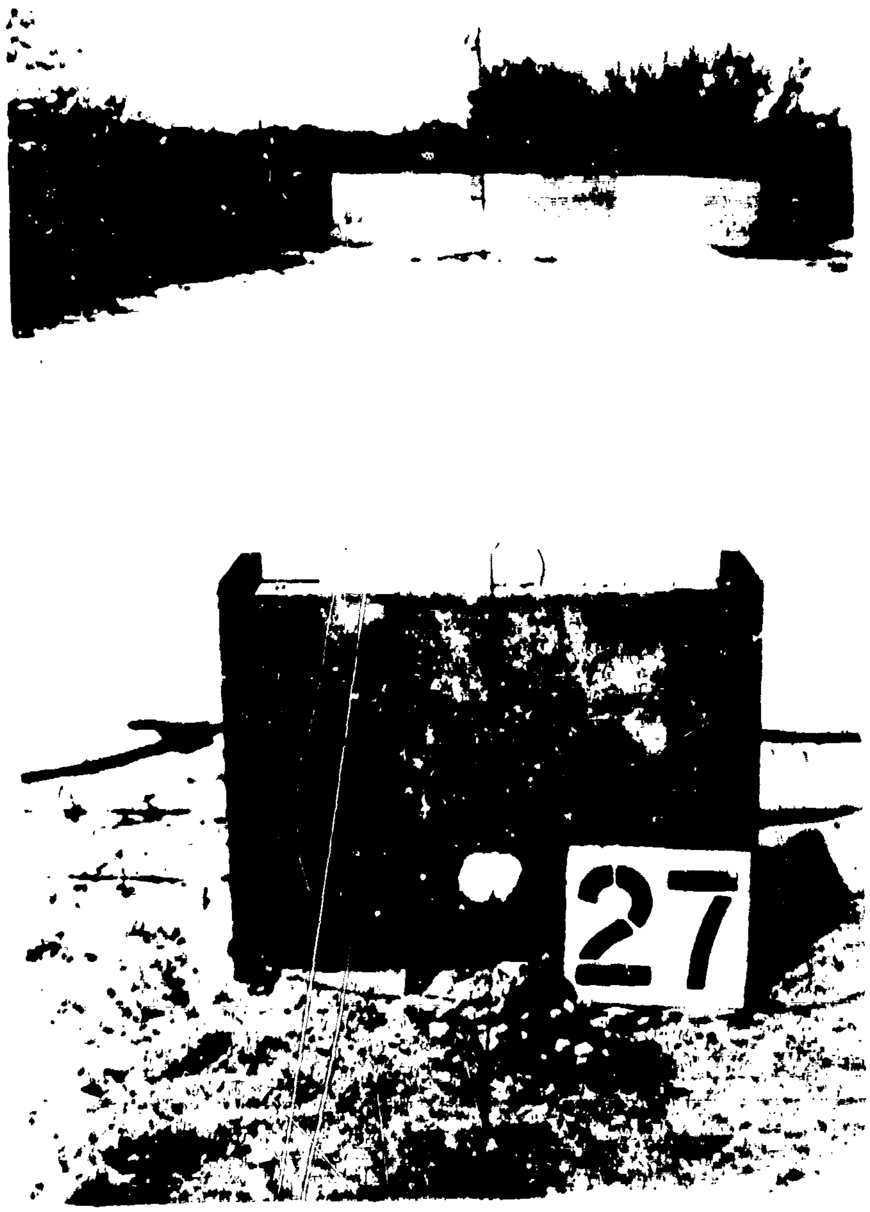

FIGURE 2-5. PHOTOGRAPH OF THE TEST FIXTURE FOR A THREE SIDE SUPPORTED TEST

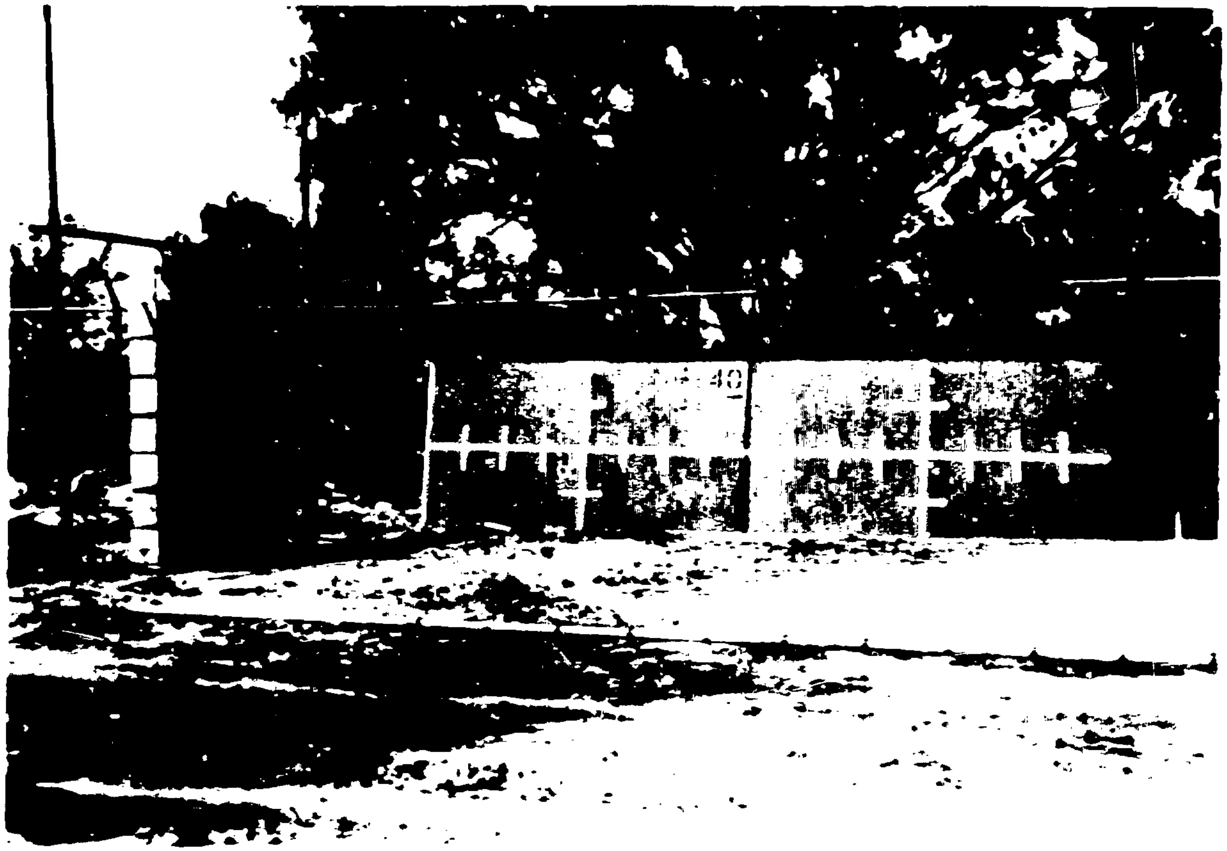

FIGURE 2-6. TEST ARRANGEMENT FOR A MASONRY BLOCK WALL

Table 2-2. Program Test Plan

Wall Type	Test Series	Wall Support	Nominal Thickness (cm)	Rebar Spacing (cm)	Charge Weight (g)	Scaled Specific Impulse Range $\frac{\text{Nt-ms}}{\text{kg}^{1/3}}$
Reinforced Concrete	1	1 side	5.08	2.54	227.0	2.78 - 3.59
Reinforced Concrete	1	1 side	5.08	2.54	454.0	2.84 - 4.28
Reinforced Concrete	2	1 side	5.08	5.08	227.0	2.61 - 10.40
Reinforced Concrete	2	1 side	5.08	5.08	454.0	2.84
Reinforced Concrete	2	1 side	5.08	5.08	1360.0	1.97
Reinforced Concrete	3	1 side	7.62	2.54	454.0	2.84 - 5.67
Reinforced Concrete	4	1 side	7.62	5.08	454.0	2.84 - 5.67
Reinforced Concrete	4	1 side	7.62	5.08	1360.0	3.94
Reinforced Concrete	5	3 side	5.08	2.54	454.0	2.03 - 4.34
Reinforced Concrete	5	3 side	5.08	2.54	1360.0	1.45
Reinforced Concrete	6	3 side	5.08	5.08	454.0	1.45 - 4.34
Reinforced Concrete	7	3 side	5.08	2.54	454.0	2.03 - 5.67
Reinforced Concrete	7	3 side	5.08	2.54	1360.0	1.97
Reinforced Concrete	8	3 side	5.08	5.08	454.0	2.03 - 4.34
Masonry (Haydite)	9	1 side	20.30	122.00	454.0	0.81
Masonry (Haydite)	9	1 side	20.30	122.00	1360.0	1.39
Masonry (Concrete)	10	1 side	20.30	122.00	454.0	0.81 - 1.16

using the TM 5-1300 criteria given in Appendix A as equation (A-2). The actual standoff distances and charge weights employed in these tests were determined from the impulse versus scaled distance curves in Reference 2. The tests were conducted utilizing the test setup and procedures as described below.

The setup used for the testing of the reinforced concrete walls consisted of a mounting fixture, a fragment recovery pit, camera emplacements, velocity grid sheets, and an explosive charge support frame. The fragment recovery area consisted of a fine sand runway 4.9 m (16.0 ft) wide and 33 m (108.0 ft) long, and the support frame was mounted at the head of this recovery area. The test setup is shown schematically in Figure 2-7. A gridded background was positioned directly across from a high-speed camera and a witness camera, used in determining fragment velocities. The high-speed camera normally was run at 400 frames per second while the witness camera was run at 64 frames per second. The scale model wall was divided into quadrants and each quarter was painted with a different color, i.e., blue, green, red, and white, in an effort to determine better the fragmentation pattern downrange, i.e., which quadrant did the fragments come from, and how many fragments were produced from each quadrant. Briefly, the test sequence consisted of mounting the test wall in the support frame, loading and positioning the cameras across from the gridded backgound, and then positioning the C-4 explosive charge. For the majority of the tests, the C-4 charge was positioned 0.18 m (0.6 ft) from the base of the wall to simulate a charge located 0.9 m (3.0 ft) from the floor of a full-scale building. After the charge was detonated, the resulting fragments were numbered, their position in the recovery pit was recorded, and the fragments were collected for later data reduction. The data reduction consisted of sizing and weighing each fragment, determining whether the fragments were chunky, i.e., large drag area and a very small lift area, or pancake, i.e., large lift area and a small drag area, and determining the fragment velocities. As previously mentioned, the high-speed camera and the gridded background were used to determine fragment velocities. The velocity of a fragment was calculated by measuring the time, i.e., the number of frames on the high-speed film, that it took the fragment to travel a specific distance as referenced on the gridded background. Since the gridded background was 1.2 m (4.0 ft) from the center of the panel, the distance traveled by a fragment as measured on the grid was adjusted to account for the depth of field errors. For example, Figure 2-8 shows a setup for a typical test, with the cameras located 6.6 m (21.5 ft) from the center of the test wall, and the gridded background located 1.2 m (4.0 ft) from the center of the wall. If the fragment traveled 1.2 m (4.0 ft) as referenced by the grid, the fragment will actually travel only 0.85 m (2.8 ft). Whenever possible, velocities were calculated for several fragments for each test. A summary of the velocities for all of the tests is given in a later section of this report.

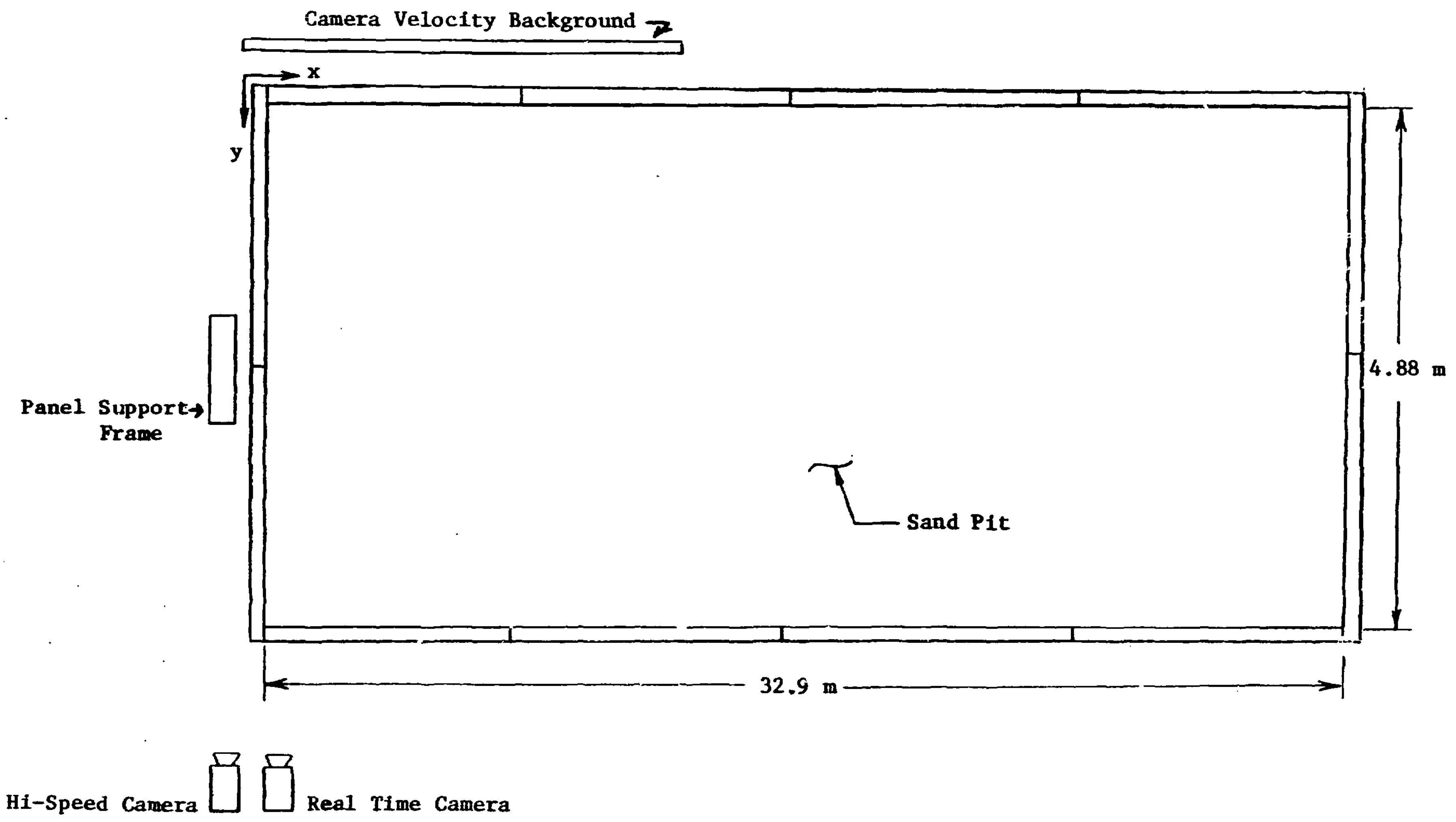

FIGURE 2-7. TEST SETUP

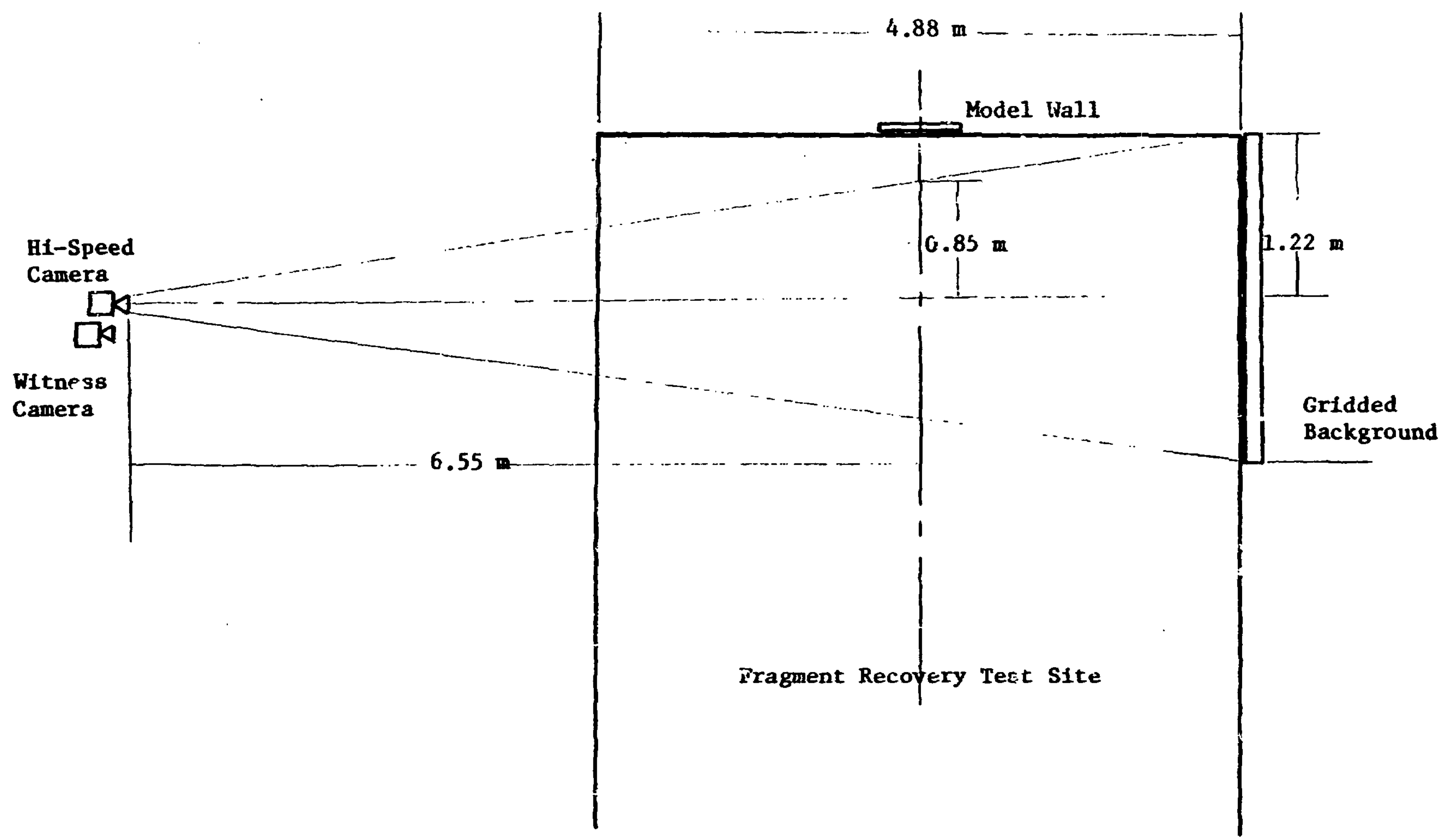

FIGURE 2-8. TYPICAL CAMERA SETUP

3.0 TEST RESULTS

3.1 General

Tests were conducted against 1/6th-scale reinforced concrete walls and against full-scale masonry block walls during this program. In each test, the fragment velocity was recorded using high-speed 16 mm cameras. The fragments were collected in a fine sand runway and the mass, dimensions and range traveled for each fragment were recorded. In addition, the geometric shape of the fragment, and the color of the fragment was recorded. The information collected on each test was entered into a computer for data reduction. Because of the large number of fragments collected in these tests, it is impractical to present all of the data collected during this effort. Instead, statistical summaries of the fragments collected and variations in the maximum responses will be presented.

3.2 Reinforced Concrete Panel Test Results

Failure Patterns

Appendix B presents a detailed description of the results of each test, with emphasis on the panel failure patterns. Panel failure modes are quite complex, and depend primarily on the impulse applied to the panel, the edge conditions, wall thickness, amount of reinforcing, and the concrete strength. As the impulse applied to the panel is varied, the wall response can vary from little or no response, incipient spallation, localized spallation similar to ballistic plugging behavior, massive spallation and even the shearing of the panel out of its support. Panels supported on one edge often have a tendency, at moderate impulse levels, to fail at the base so that the panel undergoes a net rotation, away from the charge. Usually, the panel perimeter is relatively intact except at the center where a localized volume of interior concrete* and a large portion of the surface concrete† has been ejected. As the impulse level is increased, the panel will often fail both at the bottom support and on a line parallel to the bottom support near the level of the charge as is shown in Figure 3-1. This type of dual hinge failure is associated with a large number of high velocity, but moderate mass

*Interior fragments - fragments originating from the concrete between the reinforcement layers. Generally, these fragments are chunky and of a size less than the reinforcement spacing.

†Surface fragments - fragments originating from the thin layer of concrete between the panel surface and the nearest reinforcement layer. Generally, they are pancake shaped.

FIGURE 3-1. DUAL HINGE FAILURE OF A SINGLE SIDE SUPPORTED REINFORCED CONCRETE PANEL

fragments. At higher impulse levels, the wall is sheared completely from the support. Often major pieces of the wall (1/4 to 3/4 of the panel) remain intact and can travel substantial distances, albeit at low velocities. The trajectory of these extremely large fragments is very flat so that they usually roll end over end, much like a wheel. Also associated with these high impulse tests are a very high number of fragments, many with significant and potentially damaging masses and velocities.

Panels supported on three edges exhibit failure patterns that are markedly different than panels supported only on one edge. At low impulse levels, the panels fail at all three supports and at the center along a line parallel to the two upright supports. A small volume of interior concrete and a large portion of the surface concrete is usually ejected as was the case in the test panel shown in Figure 3-2. As the impulse increases to moderate levels, more fragments with larger masses and higher velocities are ejected. At large impulses, the panel may shear completely off at the supports as was the case in Test 36 (see Figure 3-3). In this test, the lower two quadrants were massively fractured and most of this material has separated from the bulk of the panel. The upper right quadrant tumbled in a low trajectory and landed 17 m (56.0 ft) downrange. The top left quadrant traveled in a low trajectory to a point 4.3 m (14.1 ft) downrange.

3.3 General Summary of Test Results

For each test, a general summary of the test results was prepared. This summary contains information about all aspects of the tests including a description of the panel, the charge and the fragments produced. The fragment characteristic summary contains the number of fragments recovered, the average and largest mass, the average and the longest range for each of three fragment categories: source, shape and total. "Source" refers to the probable origin of the fragment. Possible sources are interior fragments, fragments from the acceptor side of the panel, and fragments from the front face of the panel. This latter category is further subdivided into quadrants of the panel from which the fragments originated, as determined by the fragment color. The bottom quadrants were painted red or white, and the top quadrants were painted blue and green. The shape category has two possiblities: "chunky" or "pancake." A fragment is characterized as being a "pancake" if the ratio of the largest fragment dimensions to the smallest dimension exceeds 2.0. All other fragments are considered "chunky." The final fragment category is labeled total. As its name implies, this category summarizes the data collected for every test.

The general test summaries are found in Appendix C organized by test number. Several general observations can be drawn from the summaries in Appendix C. First, all "pancake" fragments usually outnumber "chunky" fragments by a better than 2 to 1 margin. However,

FIGURE 3-2. MULTIPLE HINGE FAILURE OF A THREE SIDE SUPPORTED PANEL AT LOW IMPULSE LEVELS

FIGURE 3-3. FAILURE PATTERN OF A THREE SIDE SUPPORTED PANEL AT HIGH IMPULSE LEVELS

the "chunky" fragments average range is almost always greater than the average range of the "pancake" fragments. In single side supported tests, the average range for "chunky" fragments averaged approximately 1.75 times that for "pancake" fragments. In three side supported tests, "chunky" fragments averaged only 1.2 times the "pancake" fragment average range. Fragments originating from the interior of the panel or from the front face, the painted side, each represent about 40% of the fragments generated on a given test. The remaining 20% originate from the acceptor side of the panel. On tests where the charge was centered on the exposed part of the wall (Tests 1, 2, and 3), the majority of the fragments originate from the lower two quadrants, i.e., about twice as many fragments originated from the lower half of the panel as from the upper portion of the panel. When the charge was lowered to one-third the height of the panel, the majority of the fragments originated from the lower quadrant, i.e., approximately three times as many fragments were produced from the lower quadrants of the wall as from the upper quadrants.

3.4 Fragment Mass Distributions

The mass distribution of fragments emanating from the reinforced concrete walls are plotted in Figures 3-4 through 3-8. The format of the curves is the same as used in arena tests of bombs and large caliber projectiles: Mott distribution (Reference 3). These curves consist of plotting the number of fragments with a mass greater than a given mass, M. The mass distributions are plotted in several sets depending on the wall strength, the charge placement and the number of sides supported. The test series number in the plot title (see Table 2-2), is used to group tests with similar panel geometry. For example, test series 3 consists of all single side supported panels, 7.62 cm (3.0 in) thick and rebar spacing of 2.54 cm (1.0 in). If the charge was centered on the panel, a "C" is appended to the test series number. If the panel strength, as measured in static compression, exceeds 27.6 MPa (4000 psi), an "S" for strong is appended to the test series number. Otherwise, a "W" for weak is used. Figure 3-4 presents the mass distributions for the three tests with the charge centered on the panel. Figures 3-5 and 3-6 present the mass distribution for weak and strong panels supported on one edge. Figures 3-7 and 3-8 present the same distribution for weak and strong panels supported on three edges. The effect of panel strength on mass distribution can be observed by comparing the data for Test 4 [f_c' = 9.2 MPa (1330 psi)] and Test 9 [f_c' = 33 MPa (4800 psi)] (See Figures 3-5b and 3-6b). The two curves are nearly parallel with the weaker panel producing more fragments in each size range than the strong panel for the same impulse applied to the panel. The effect of reinforcement spacing can be observed by comparing Tests 8 [R_s = 2.54 cm (1.0 in)] and 9 [R_s = 5.09 cm (2.0 in)] (See Figures 3-6a and 3-6b). Again, the curves are essentially parallel with the tests using widely spaced rebar producing more fragments than in the closely spaced rebar tests. The effect of panel restraint can be

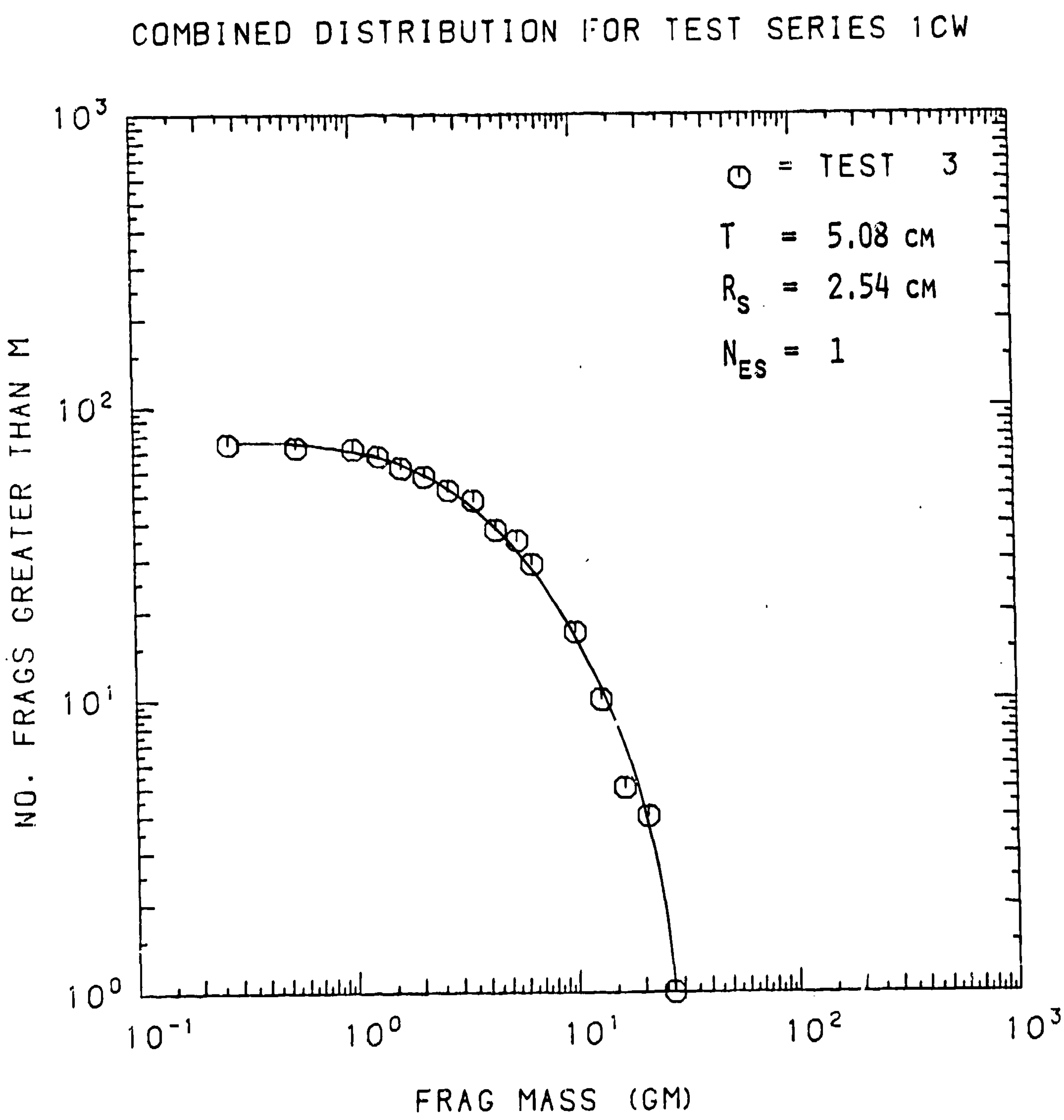

FIGURE 3-4A. MASS DISTRIBUTION FOR TEST SERIES 1CW

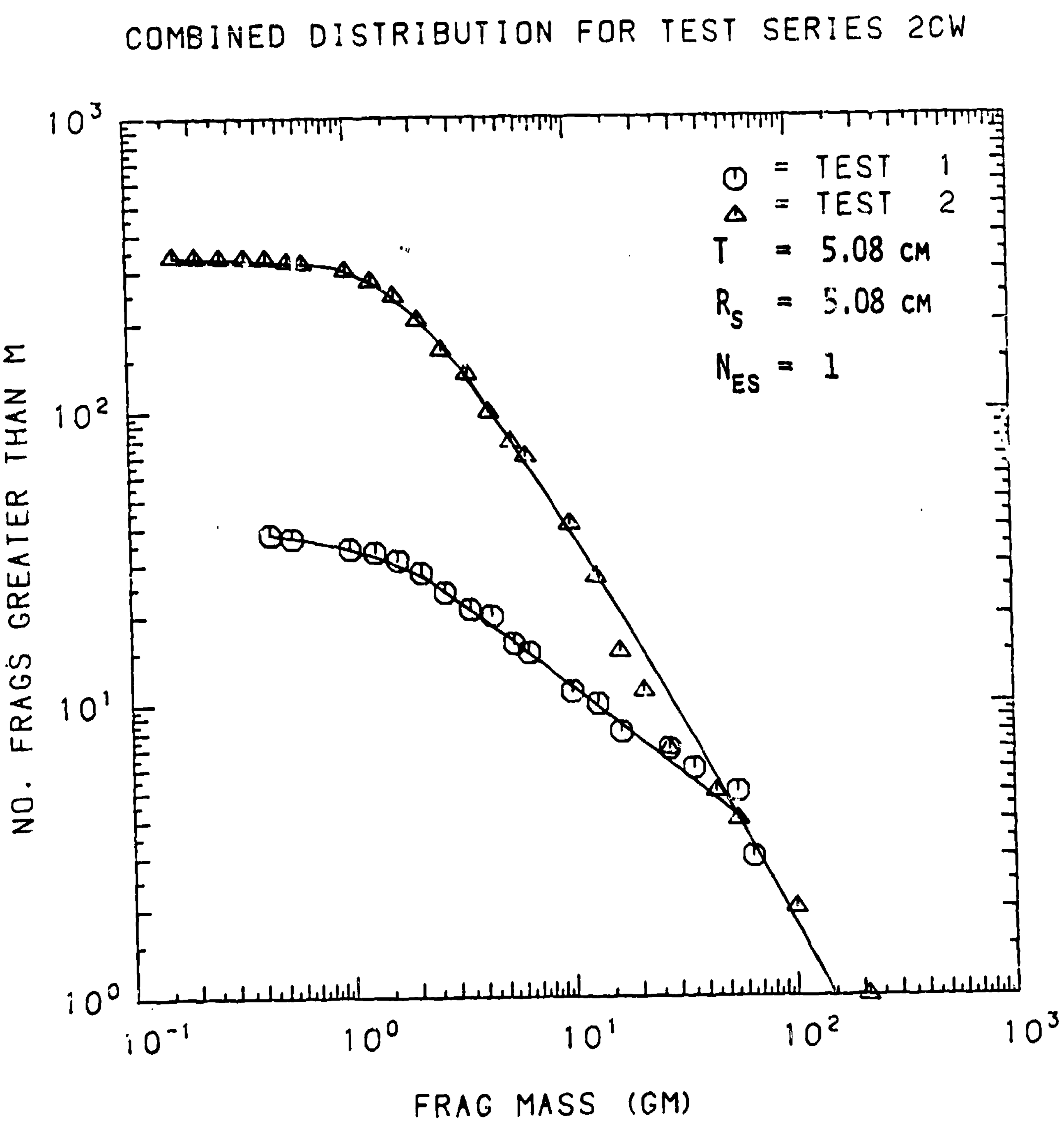

FIGURE 3-4B. MASS DISTRIBUTION FOR TEST SERIES 2CW

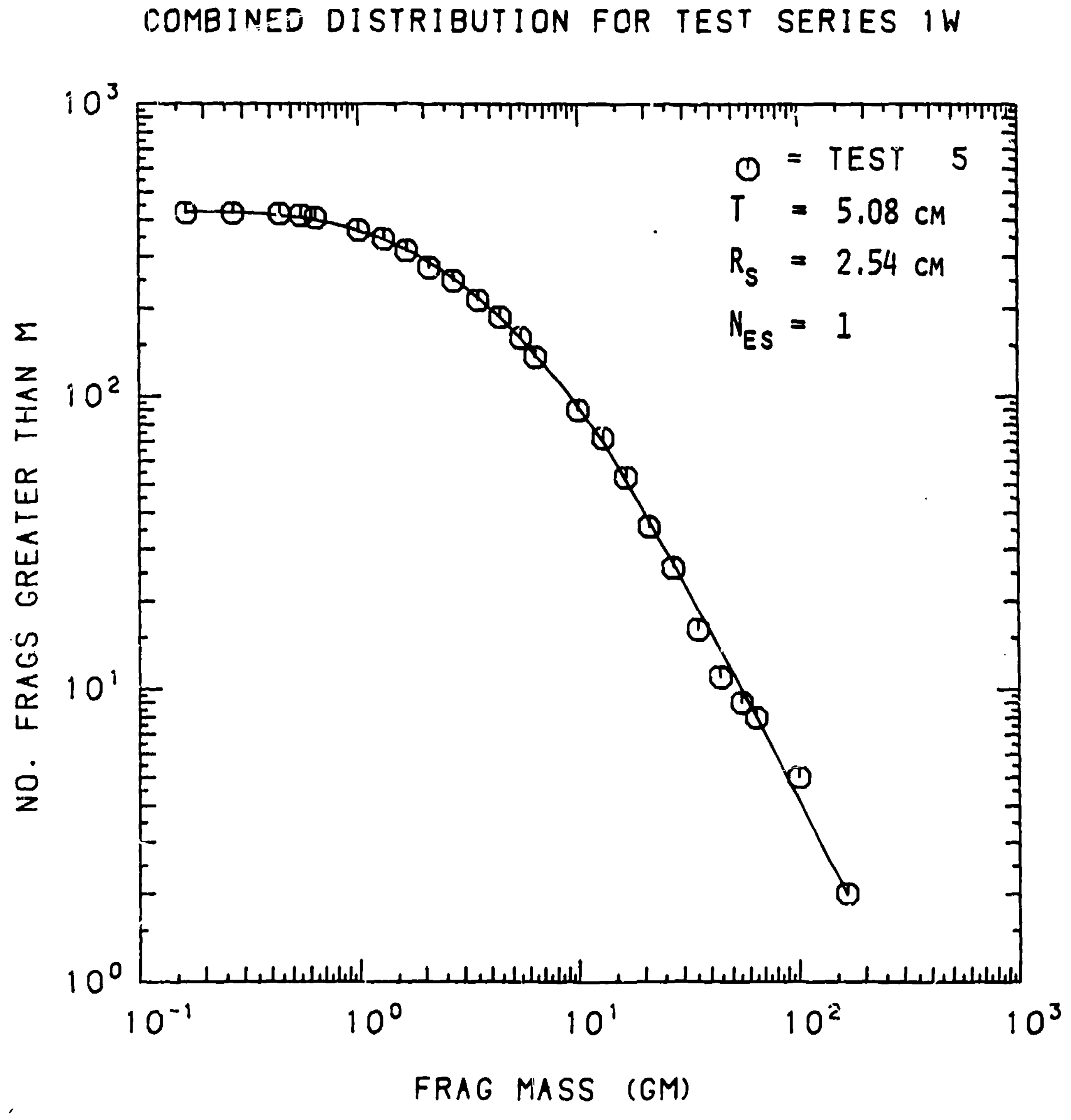

FIGURE 3-5A. MASS DISTRIBUTION FOR TEST SERIES 1W

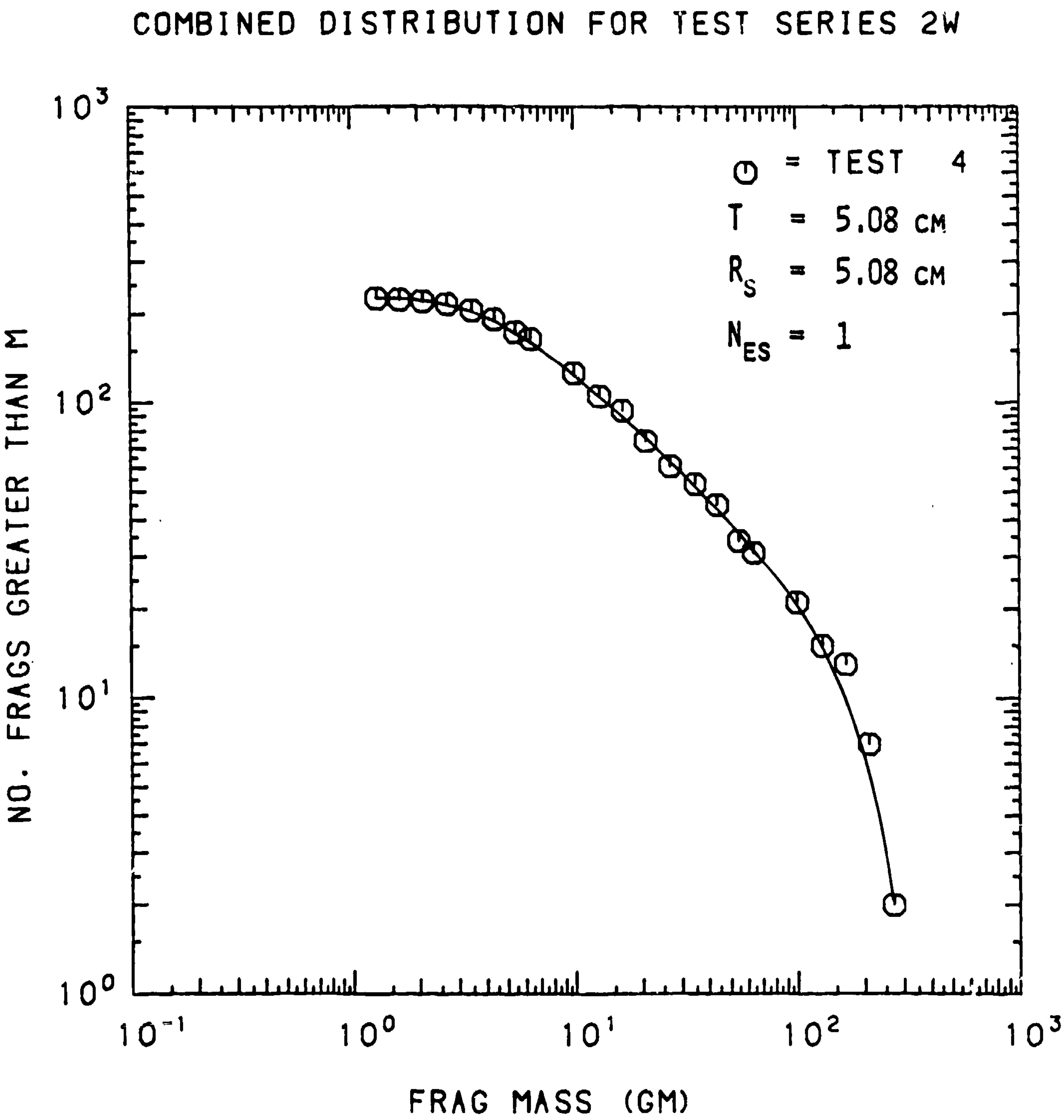

FIGURE 3-5B. MASS DISTRIBUTION FOR TEST SERIES 2W

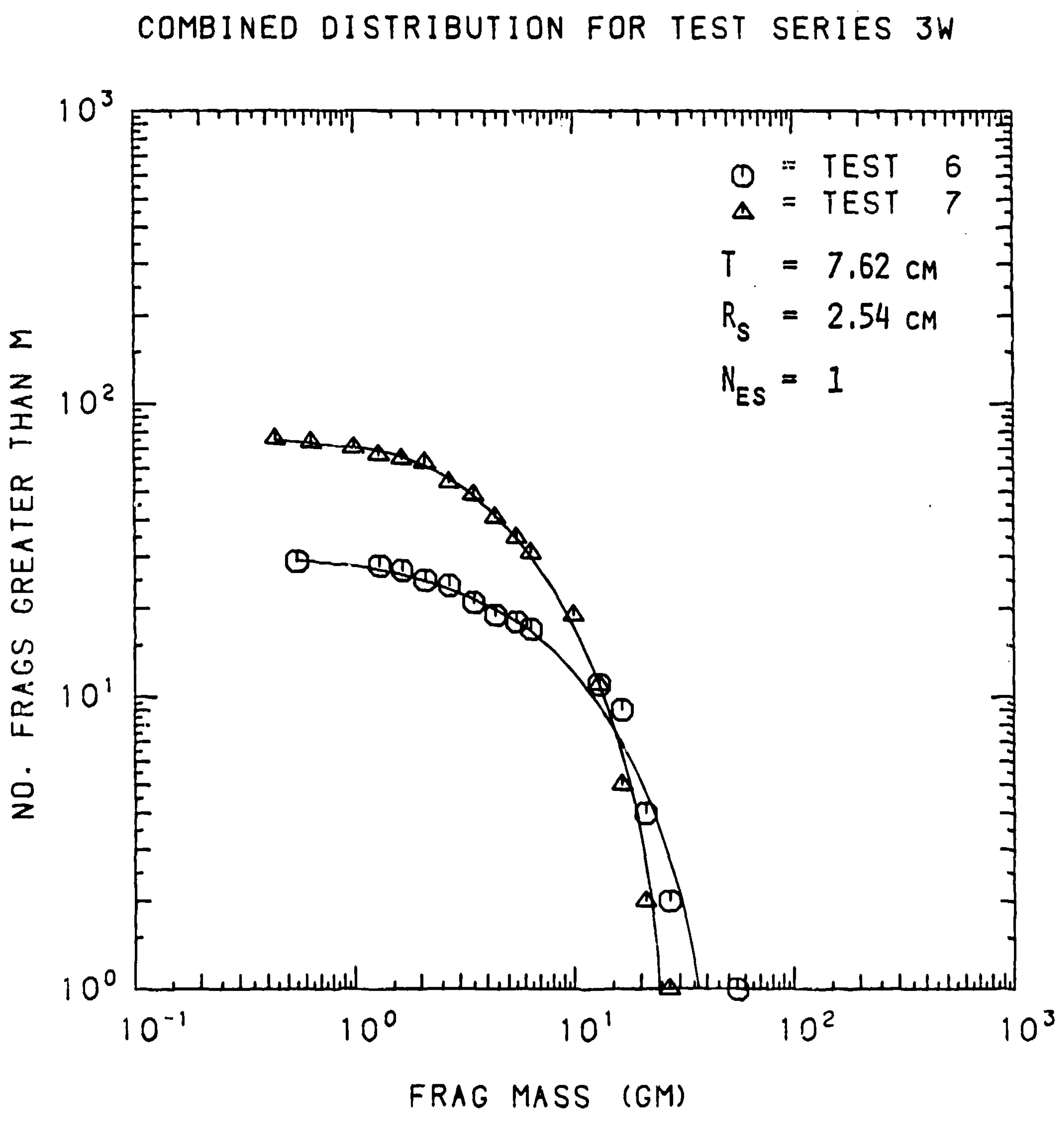

FIGURE 3-5c. MASS DISTRIBUTION FOR TEST SERIES 3W

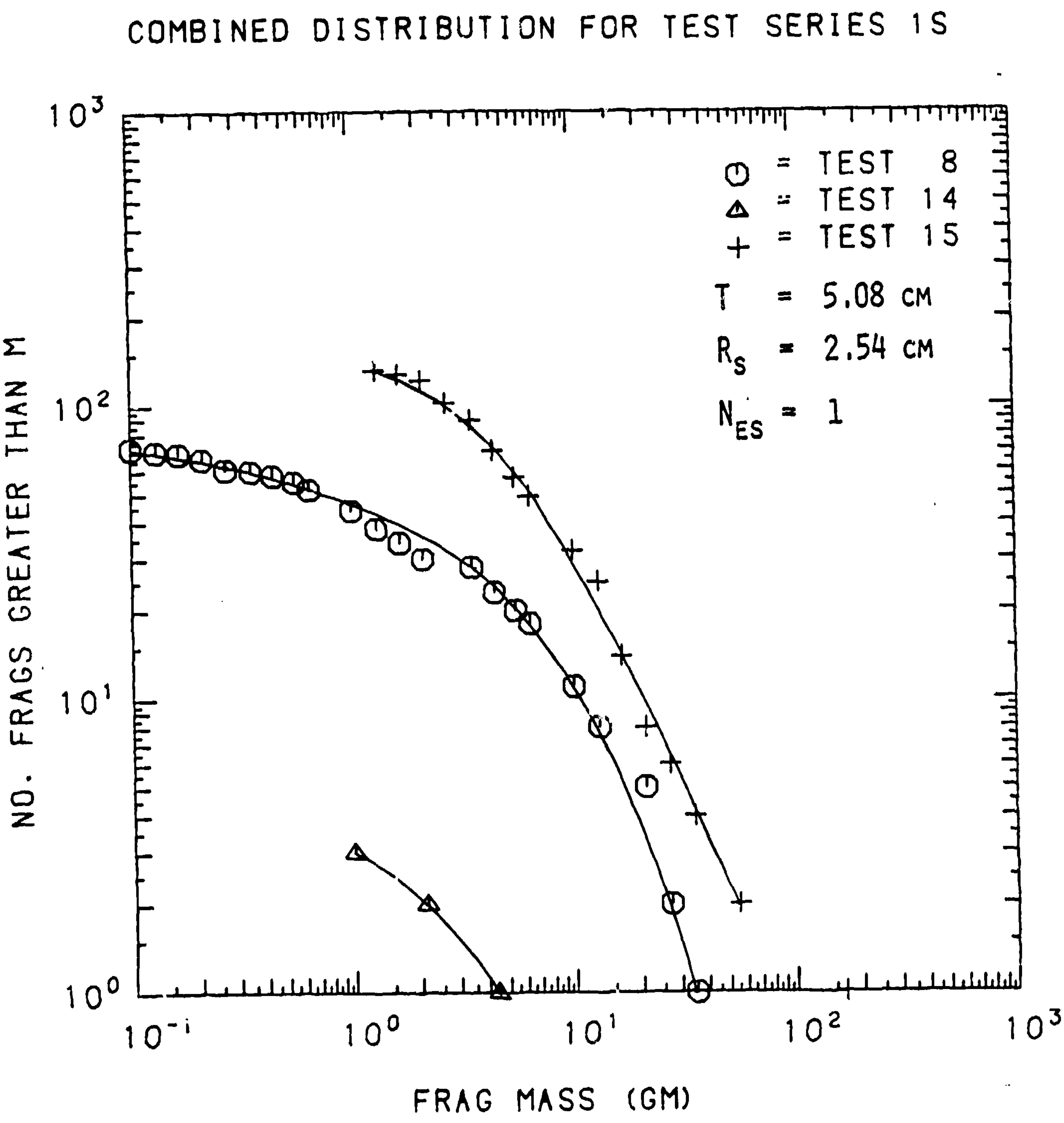

FIGURE 3-6A. MASS DISTRIBUTION FOR TEST SERIES 1S

COMBINED DISTRIBUTION FOR TEST SERIES 2S

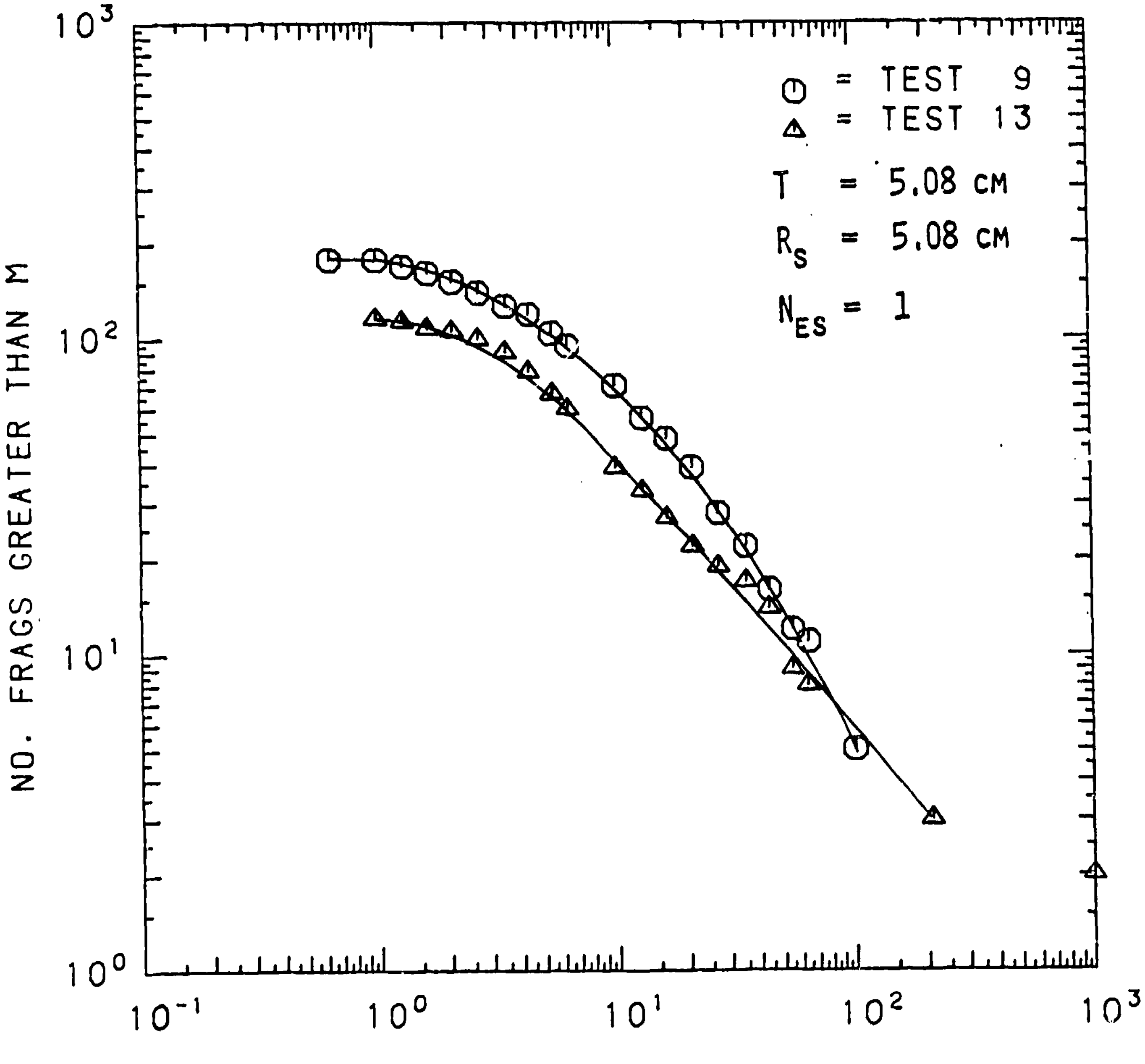

FIGURE 3-6B. MASS DISTRIBUTION FOR TEST SERIES 2S

COMBINED DISTRIBUTION FOR TEST SERIES 3S

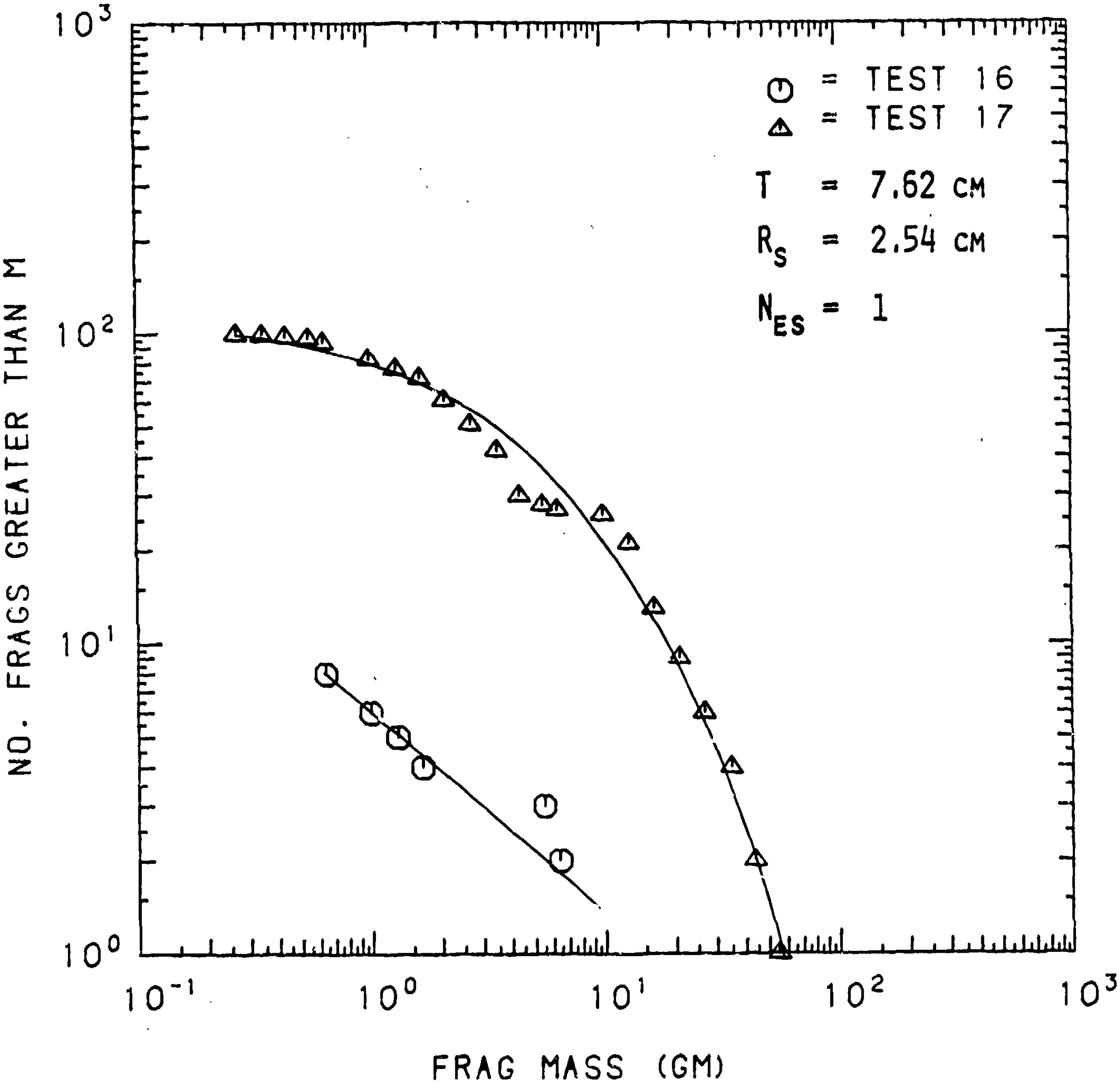

FIGURE 3-6c. MASS DISTRIBUTION FOR TEST SERIES 3S

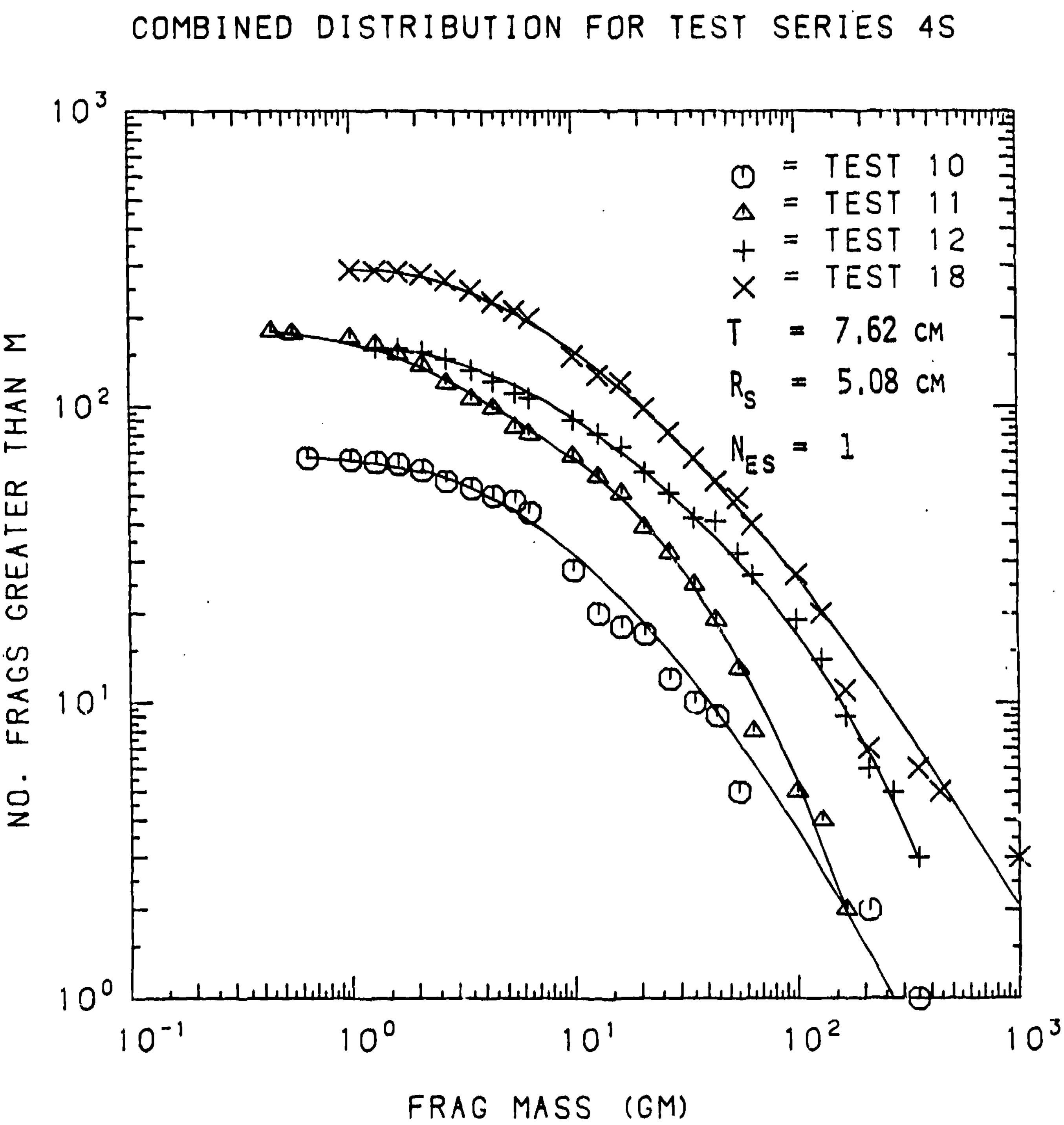

FIGURE 3-6D. MASS DISTRIBUTION FOR TEST SERIES 4S

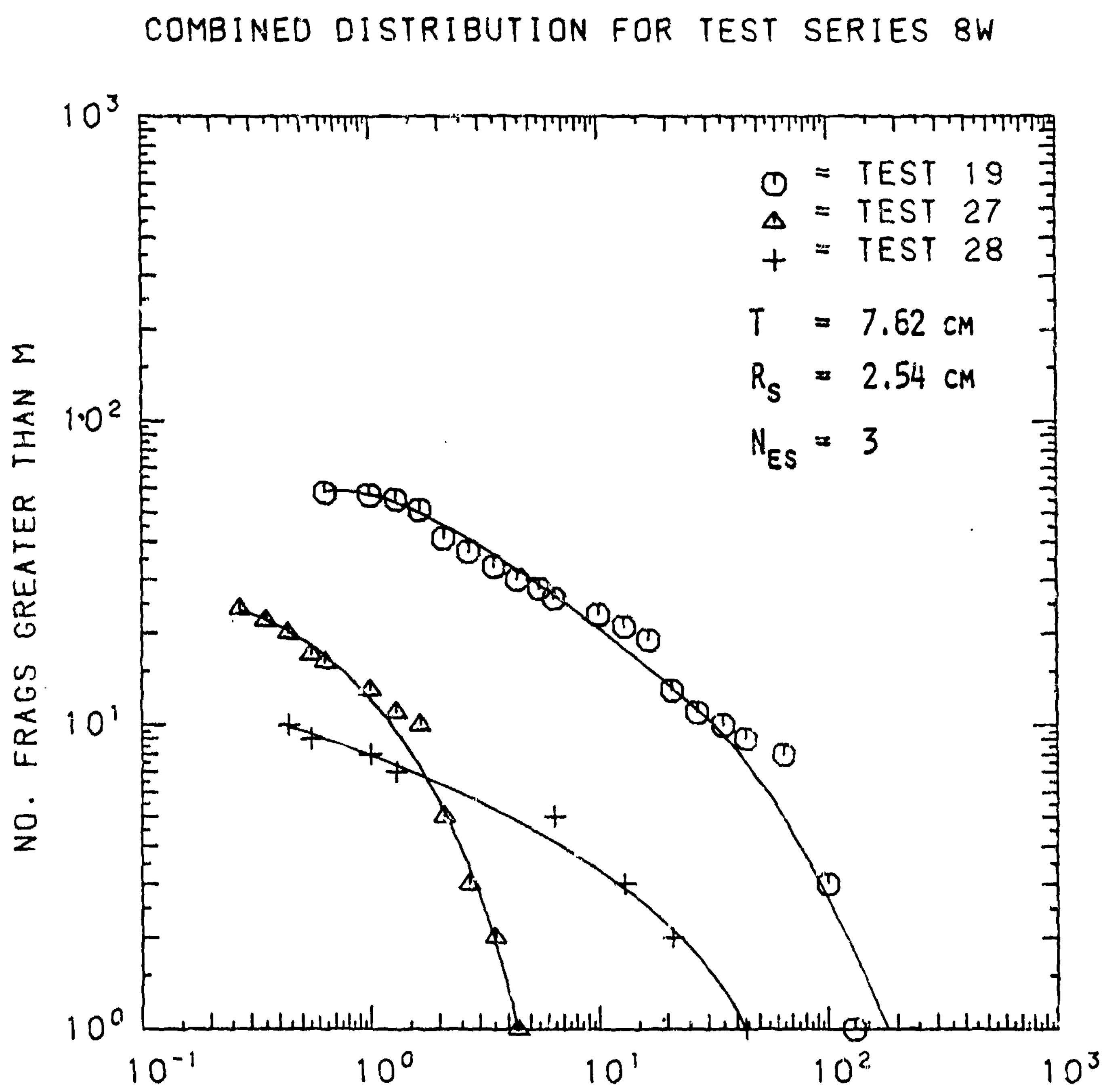

FIGURE 3-7. MASS DISTRIBUTION FOR TEST SERIES 8W

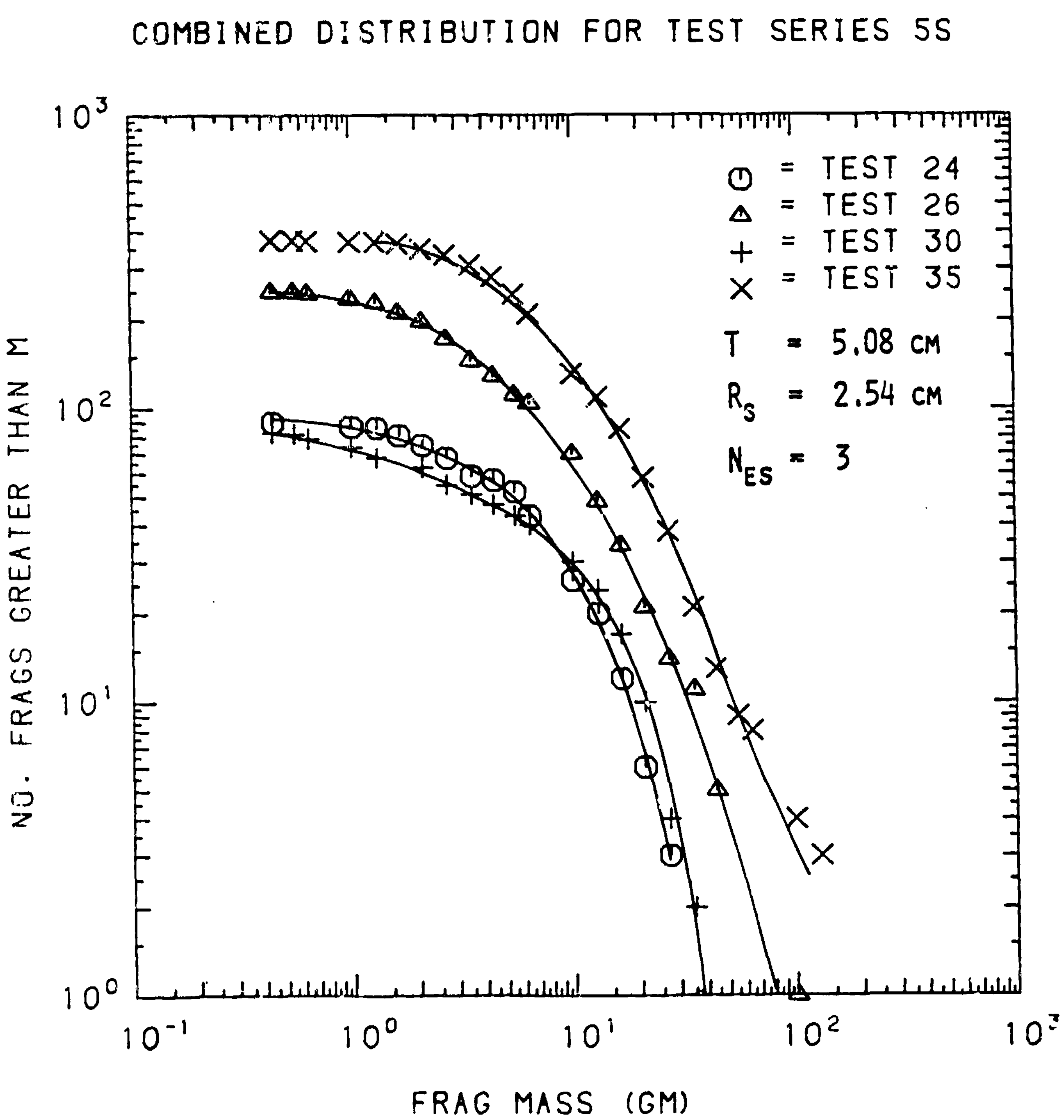

FIGURE 3-8A. MASS DISTRIBUTION FOR TEST SERIES 5S

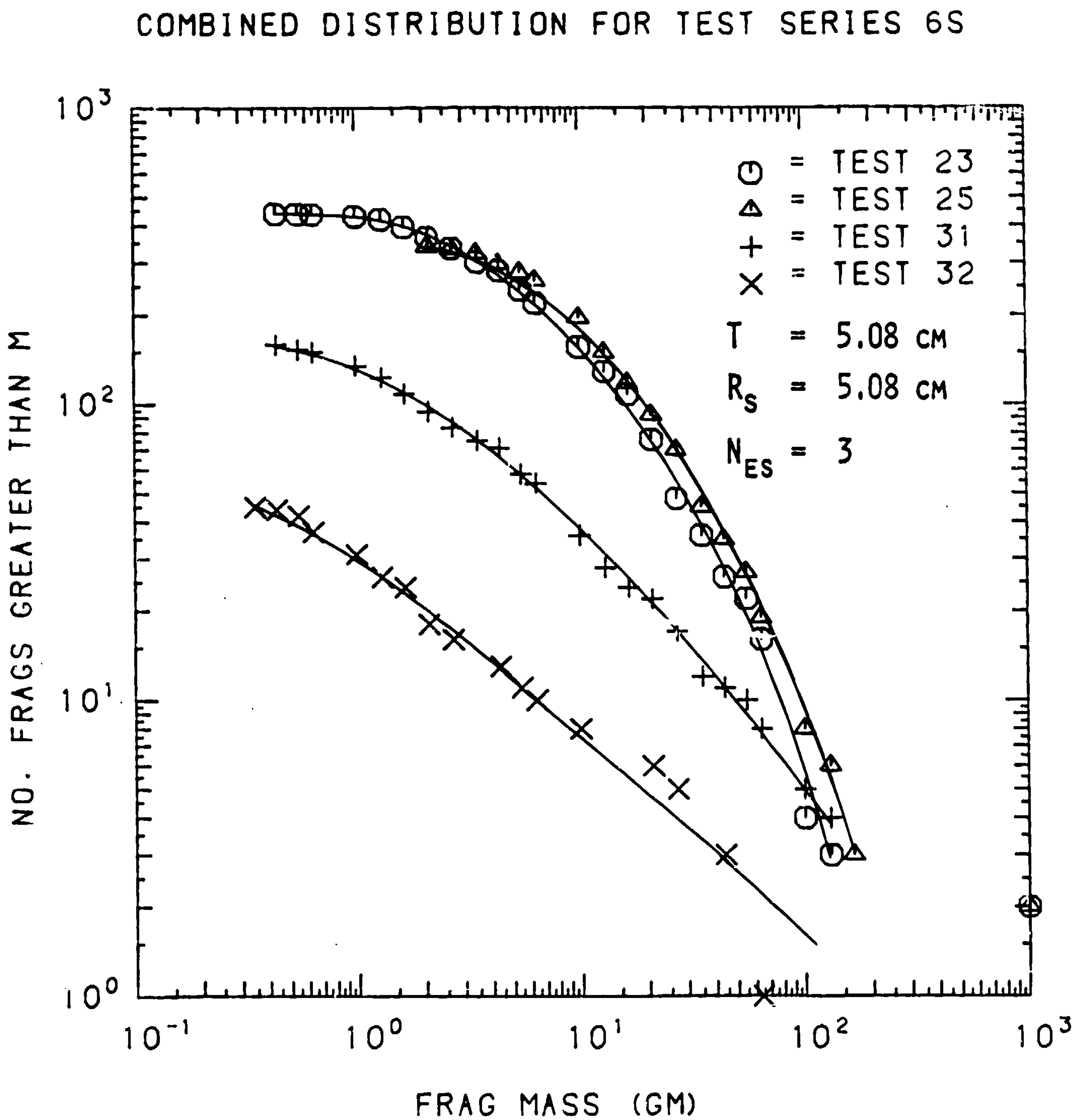

FIGURE 3-8B. MASS DISTRIBUTION FOR TEST SERIES 6S

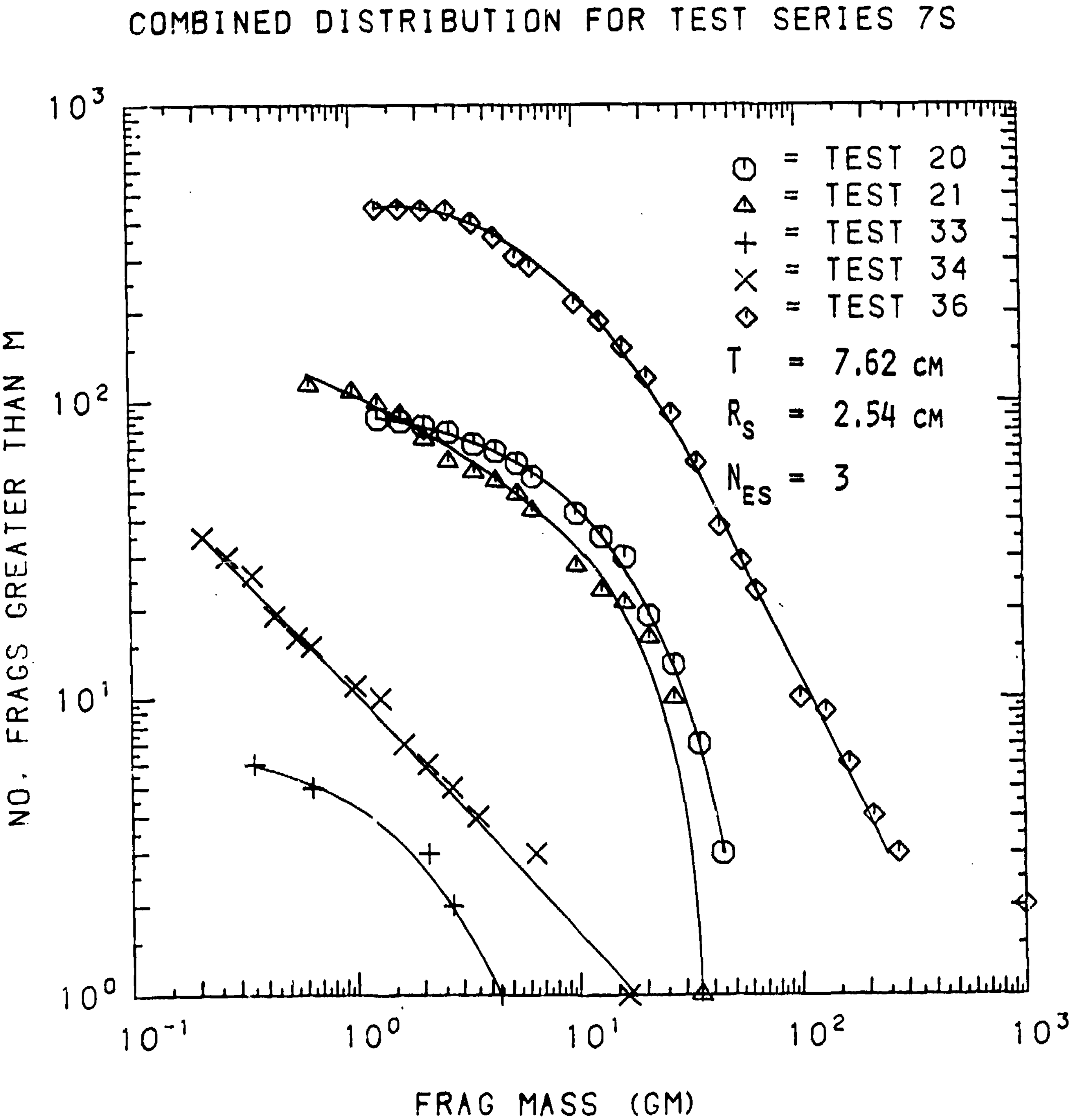

FIGURE 3-8C. MASS DISTRIBUTION FOR TEST SERIES 7S

COMBINED DISTRIBUTION FOR TEST SERIES 8S

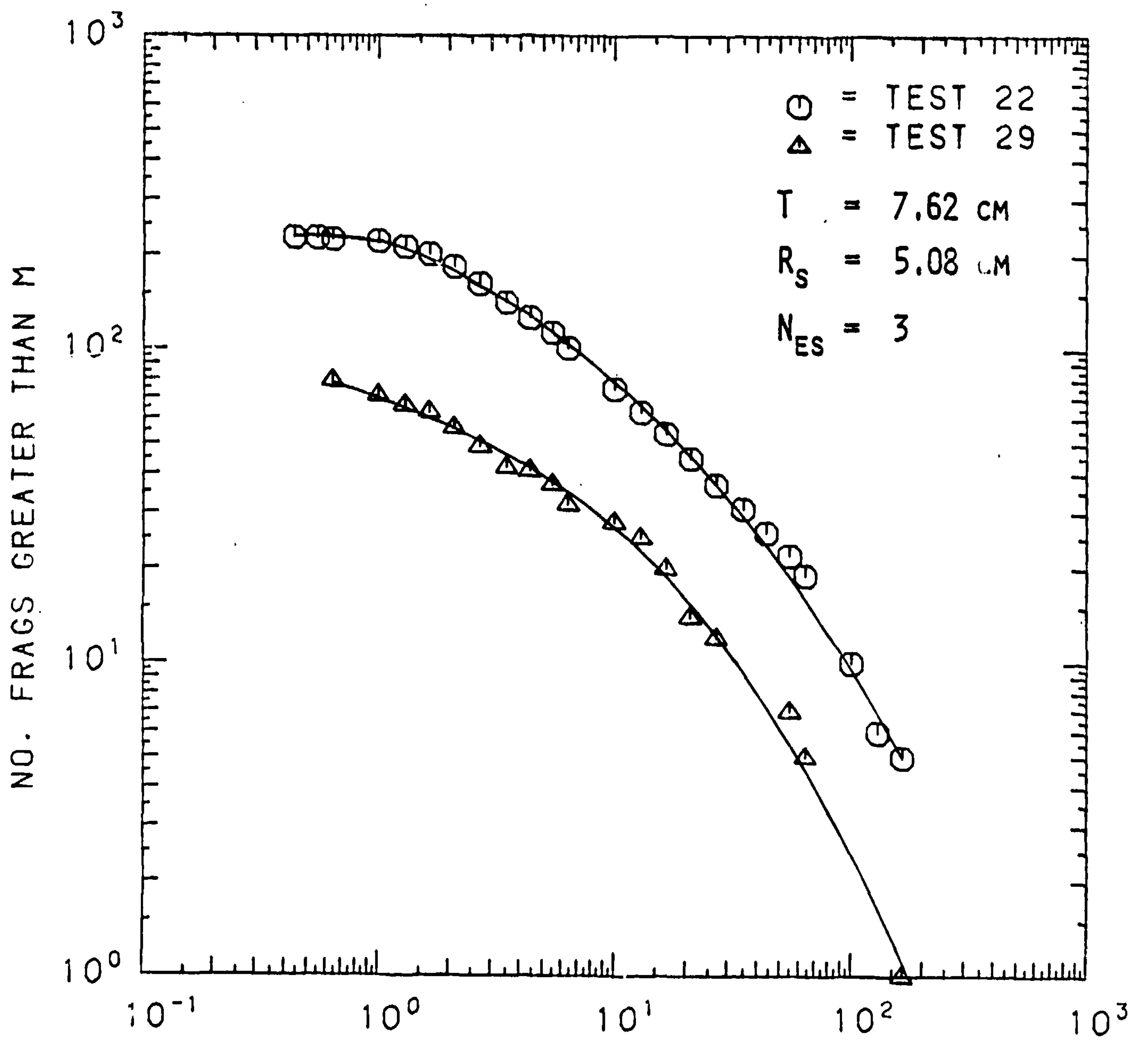

FIGURE 3-8D. MASS DISTRIBUTION FOR TEST SERIES 8S observed by comparing Tests 21 (three side supported) and 17 (one side supported). In this case, three side supported panels produced more fragments in each mass range. The effect of increasing the impulse can be clearly seen on Figure 3-6d. Each test corresponds to an increasing total impulse level ranging from 2.53 x 10^5 to 6.18 x 10^5 Nt-sec (56,900 for Test 10 to 139,000 lb_f-sec for Test 18). Note that Test 18 had a 1.362 kg (3.0 lb) charge while the remaining tests had 0.454 kg (1.0 lb) charges. In summary, more fragments at each mass level are produced, all other parameters held constant, when:

- the total impulse applied to the panel is increased,
- the panel compressive strength is decreased,
- the reinforcement spacing is increased, or
- the number of supporting edges is increased.

3.5 Fragment Range Distributions

Fragment range distributions are presented in Figures 3-9 through 3-13 in a format similar to that used to present the mass distributions. Figure 3-9 presents the range distributions for tests with the explosive charge centered on the panel. Figures 3-10 and 3-11 present the range distributions for weak and strong single edge supported panels. Figures 3-12 and 3-13 are the range data for weak and strong panels supported on three edges. The effect of varying the various test parameters on the range distribution was examined using the same tests for a comparison basis as in the mass distribution discussion. It was found that more fragments at each range level were produced when:

- the total impulse was increased,
- the panel compressive strength was decreased,
- the reinforcement spacing was increased, or
- the number of supporting edges was increased.

The ranges presented in this section represent 1/6th-scale test results. Direct extrapolation to full-scale range is not possible since the acceleration due to gravity was not properly scaled. The qualitative results, that is, the effect of changing the various test parameters, are thought to be accurate.

3.6 Velocity Distributions

Table 3-1 summarizes the fragment velocity data accumulated during this program. The number of fragment velocities reduced for each test range from one to ten readings, which is a small percentage of the total number of fragments produced on a test. The fragments selected were chosen to obtain a cross section of the velocities present on each test, but the choice of fragments selected was biased towards the fastest fragments to ensure that the highest velocity was reduced. For this reason, no statistical analysis of fragment velocities was performed.

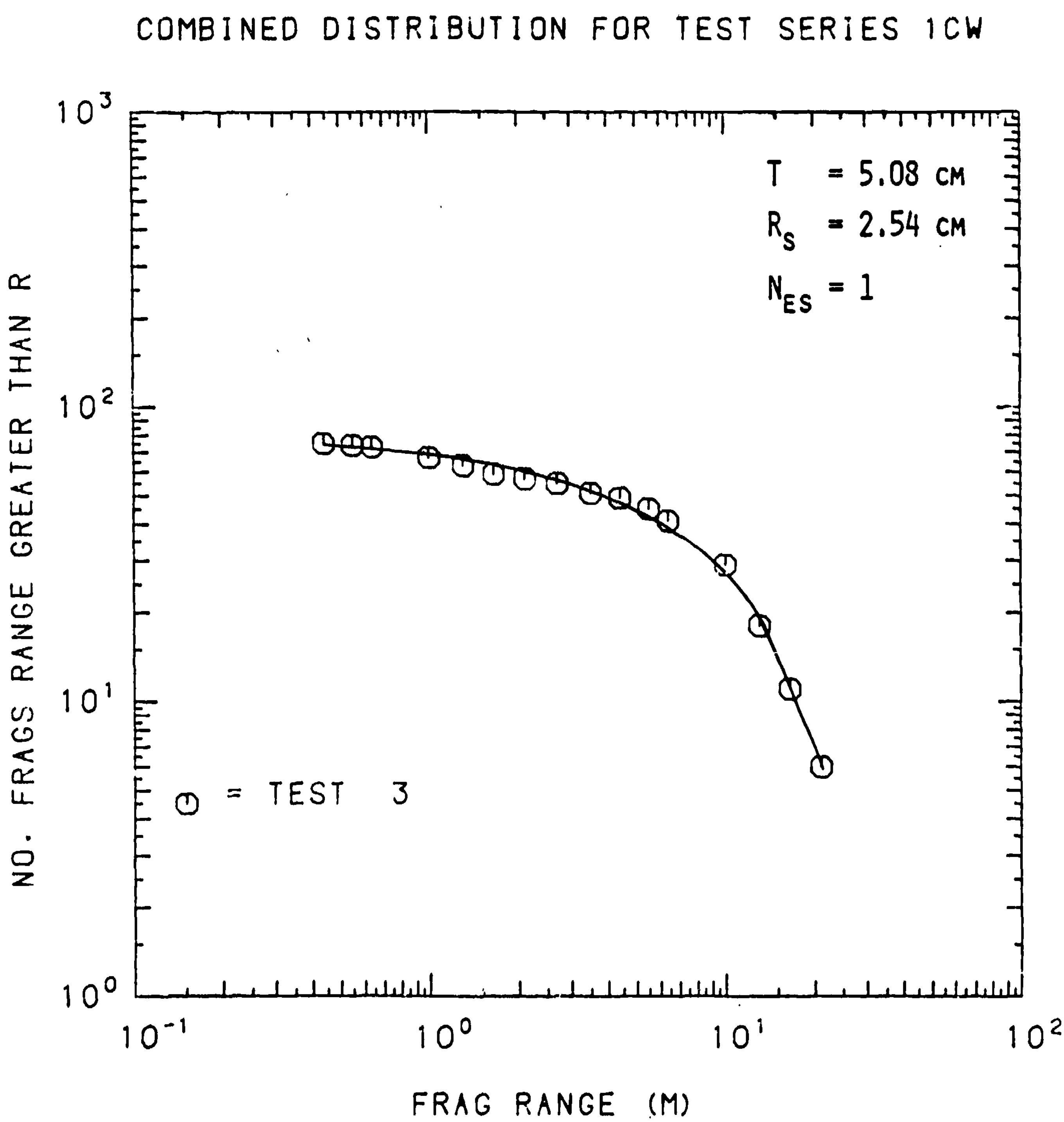

FIGURE 3-9A. RANGE DISTRIBUTION FOR TEST SERIES 1CW

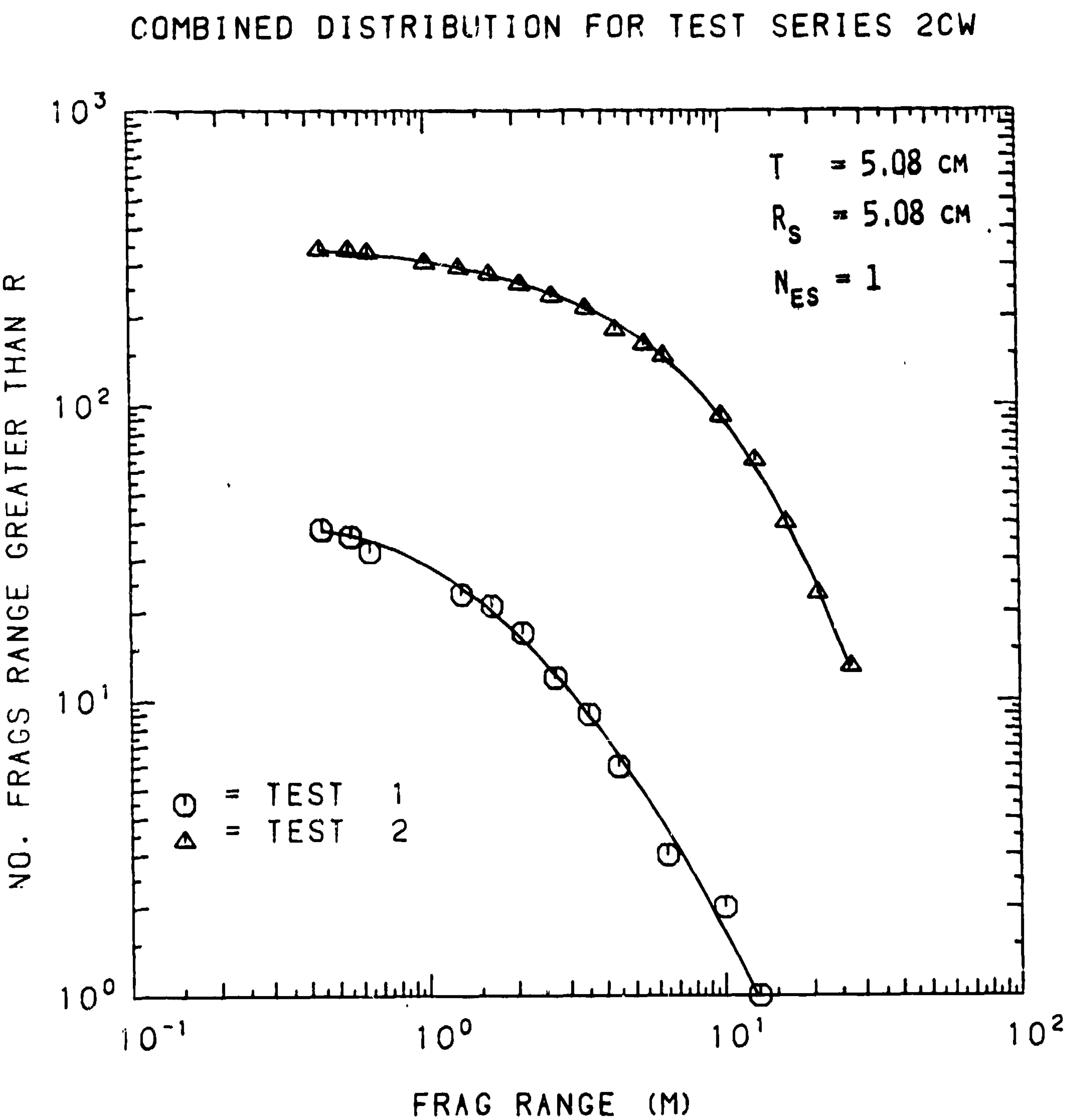

FIGURE 3-9B. RANGE DISTRIBUTION FOR TEST SERIES 2CW

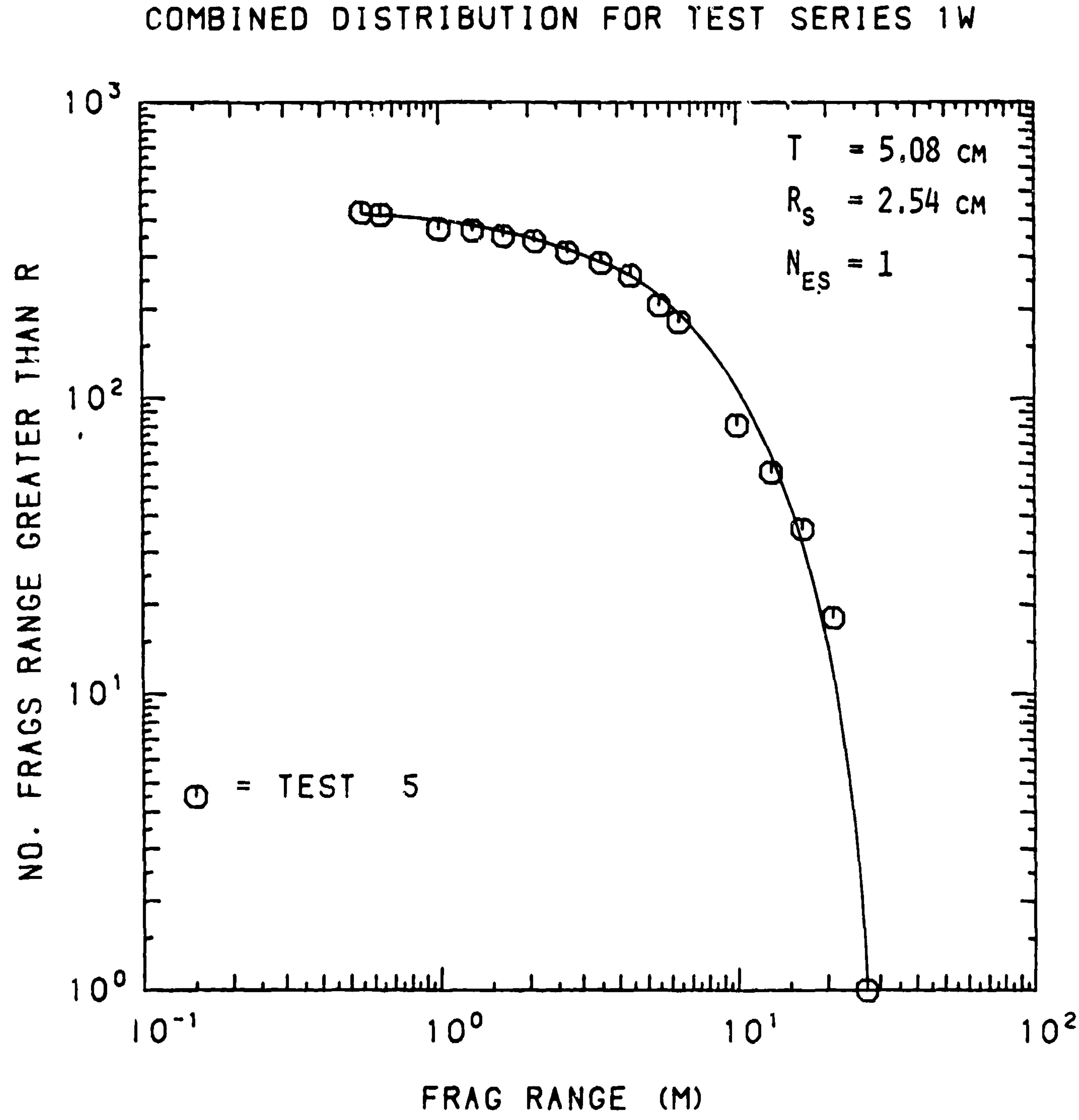

FIGURE 3-10A. RANGE DISTRIBUTION FOR TEST SERIES 1W

COMBINED DISTRIBUTION FOR TEST SERIES 2W

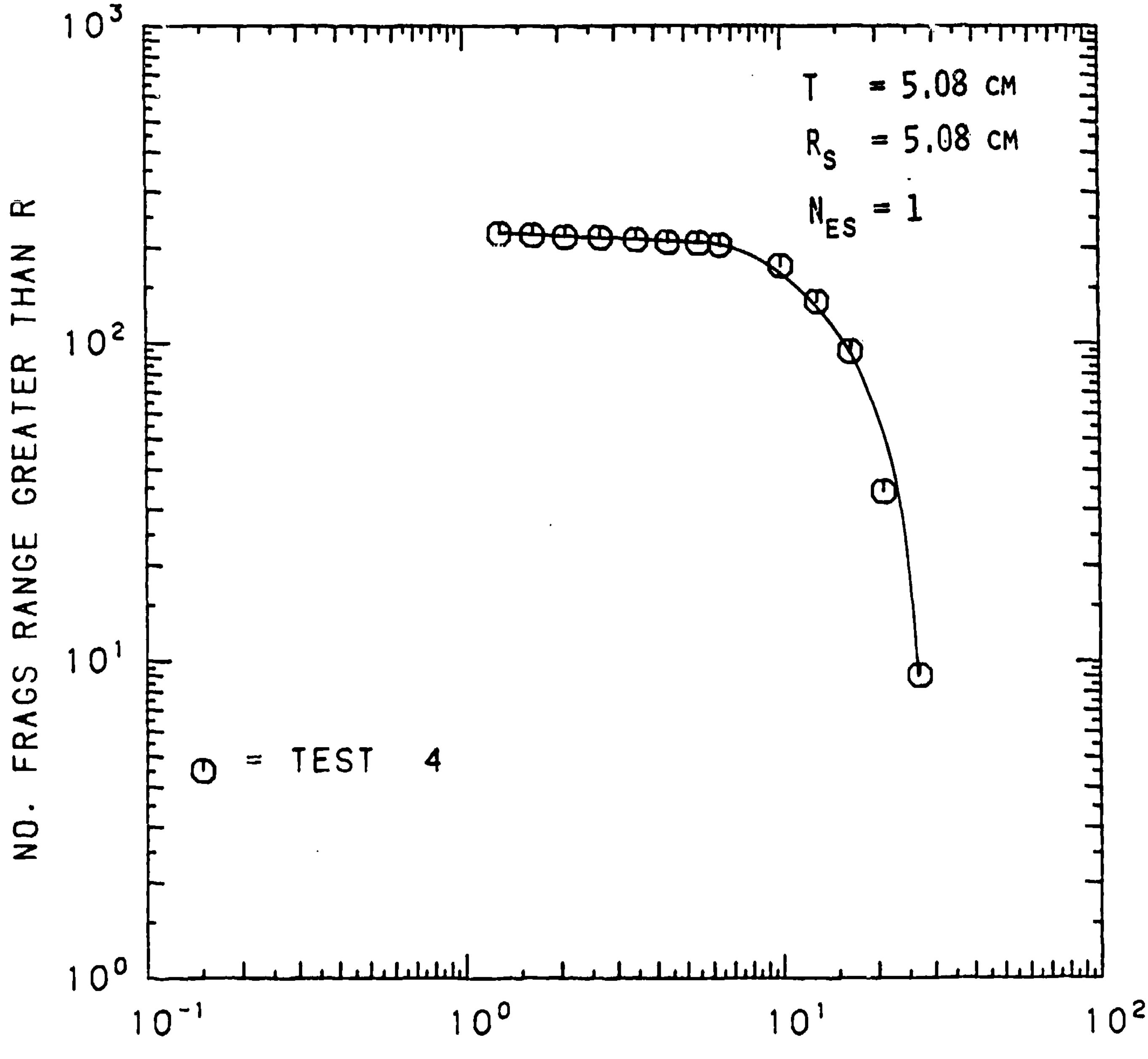

FRAG RANGE (M)

FIGURE 3-10B. RANGE DISTRIBUTION FOR TEST SERIES 2W

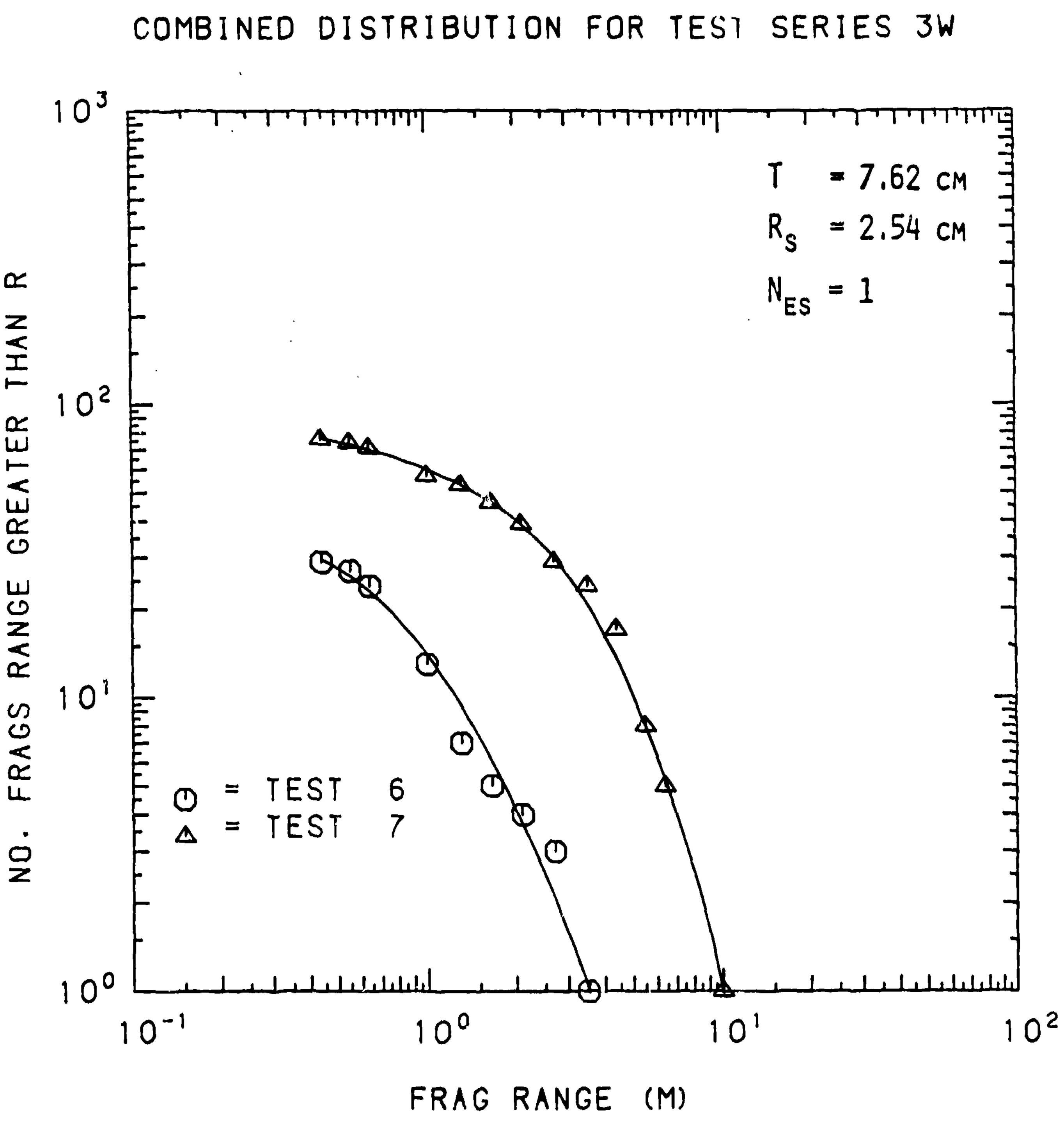

FIGURE 3-10C. RANGE DISTRIBUTION FOR TEST SERIES 3W

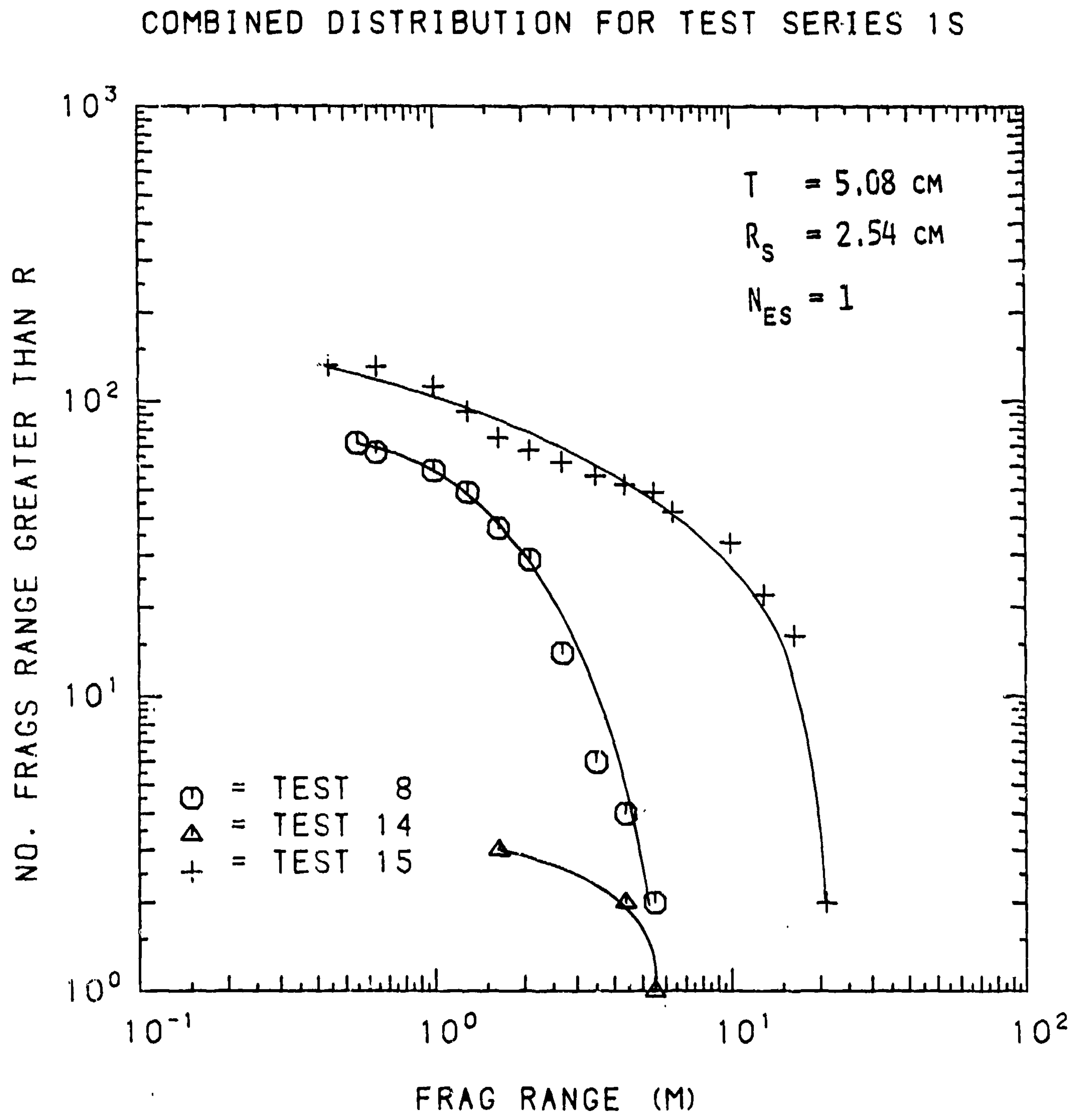

FIGURE 3-11A. RANGE DISTRIBUTION FOR TEST SERIES 1S

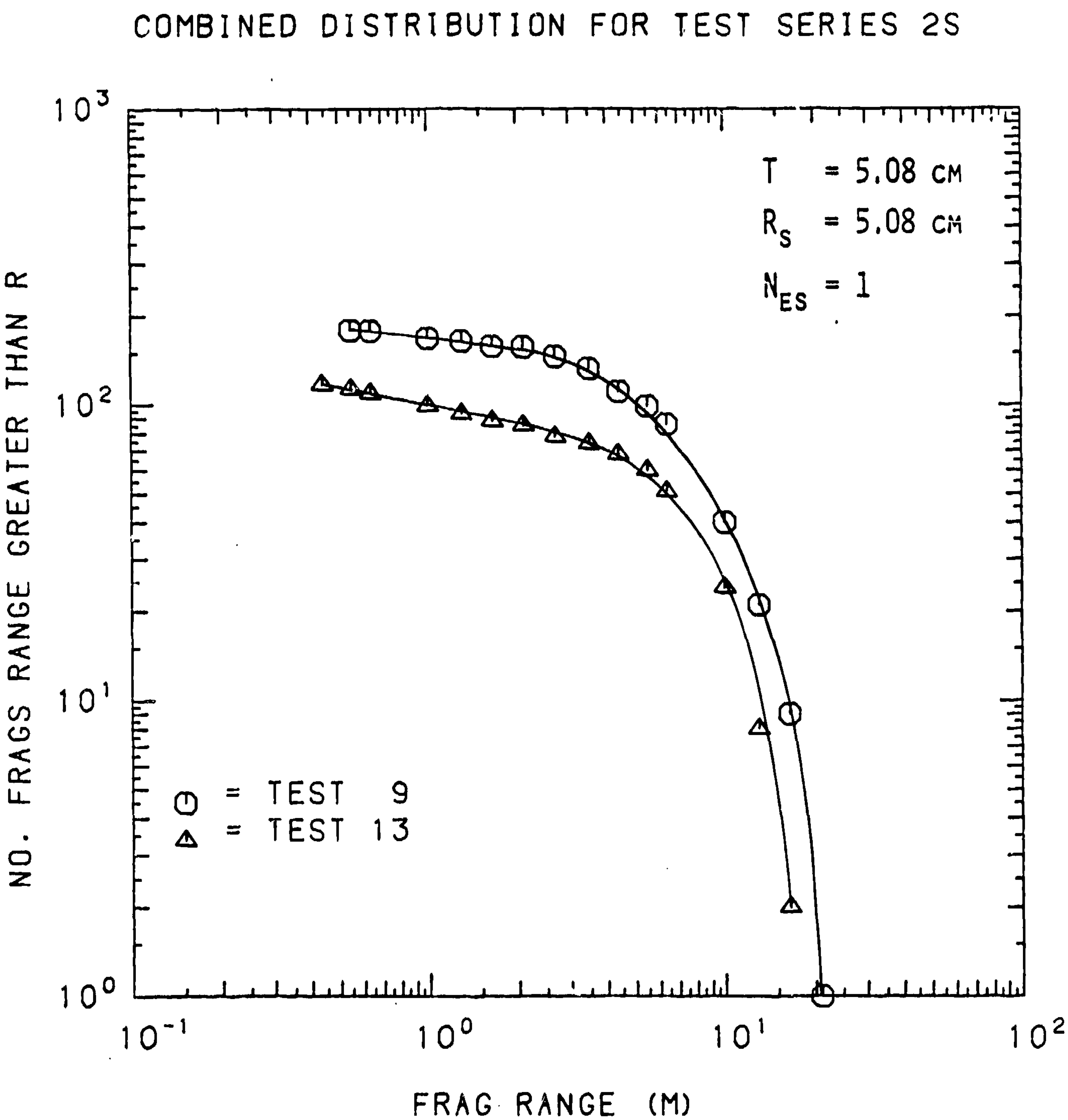

FIGURE 3-11B. RANGE DISTRIBUTION FOR TEST SERIES 2S

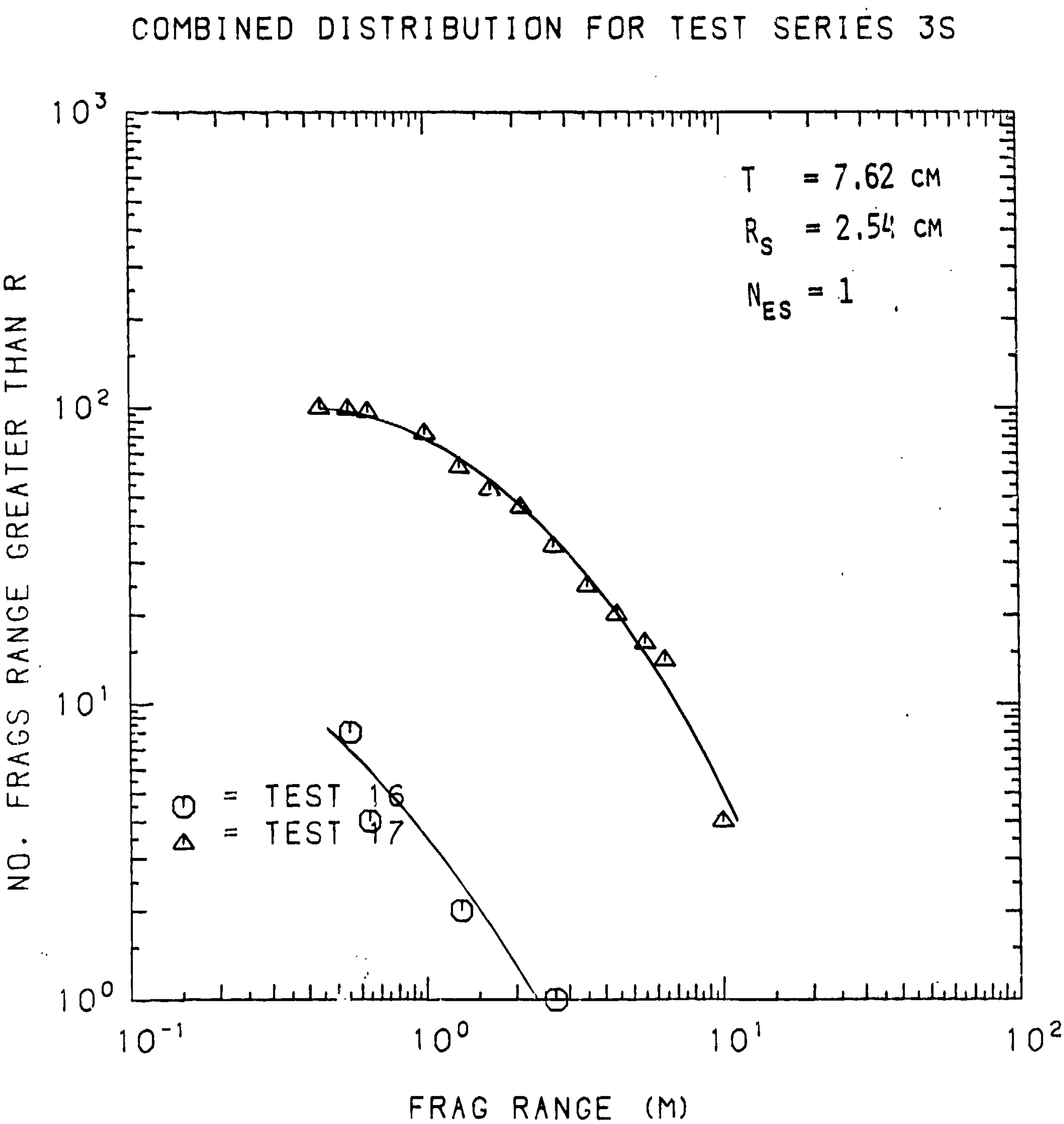

FIGURE 3-11c. RANGE DISTRIBUTION FOR TEST SERIES 3S

COMBINED DISTRIBUTION FOR TEST SERIES 4S

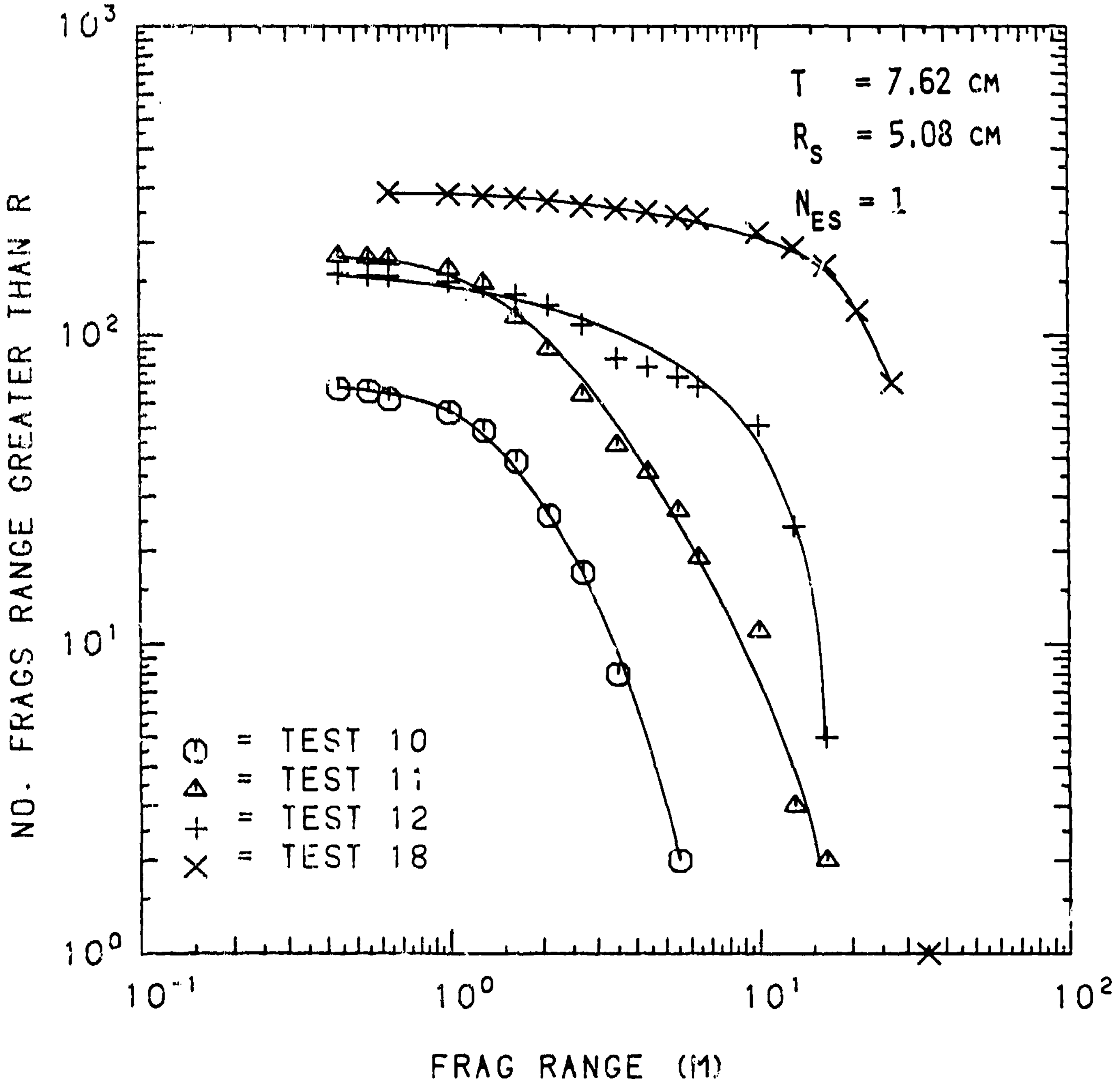

FIGURE 3-11D. RANGE DISTRIBUTION FOR TEST SERIES 4S

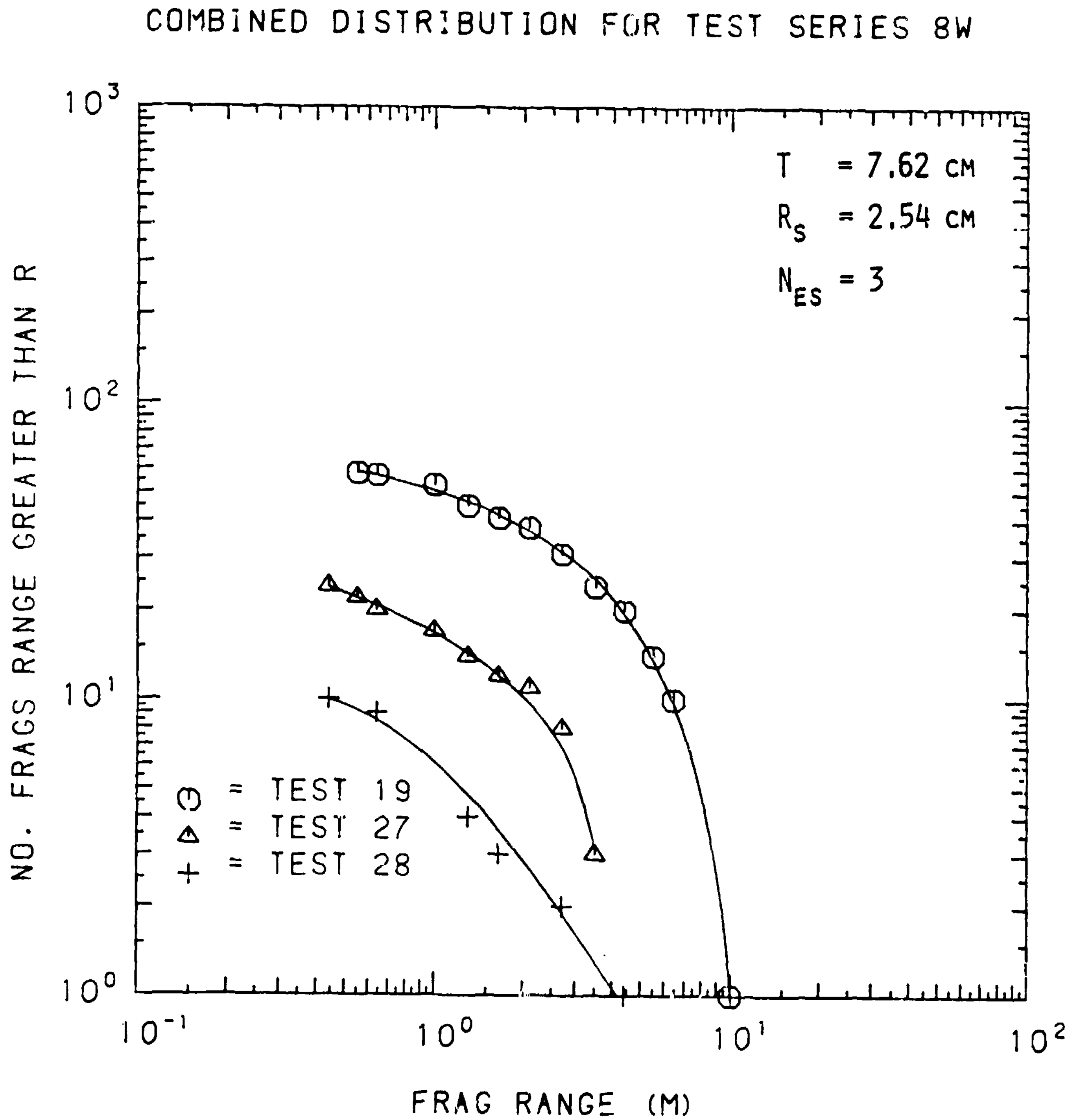

FIGURE 3-12. RANGE DISTRIBUTION FOR TEST SERIES 8W

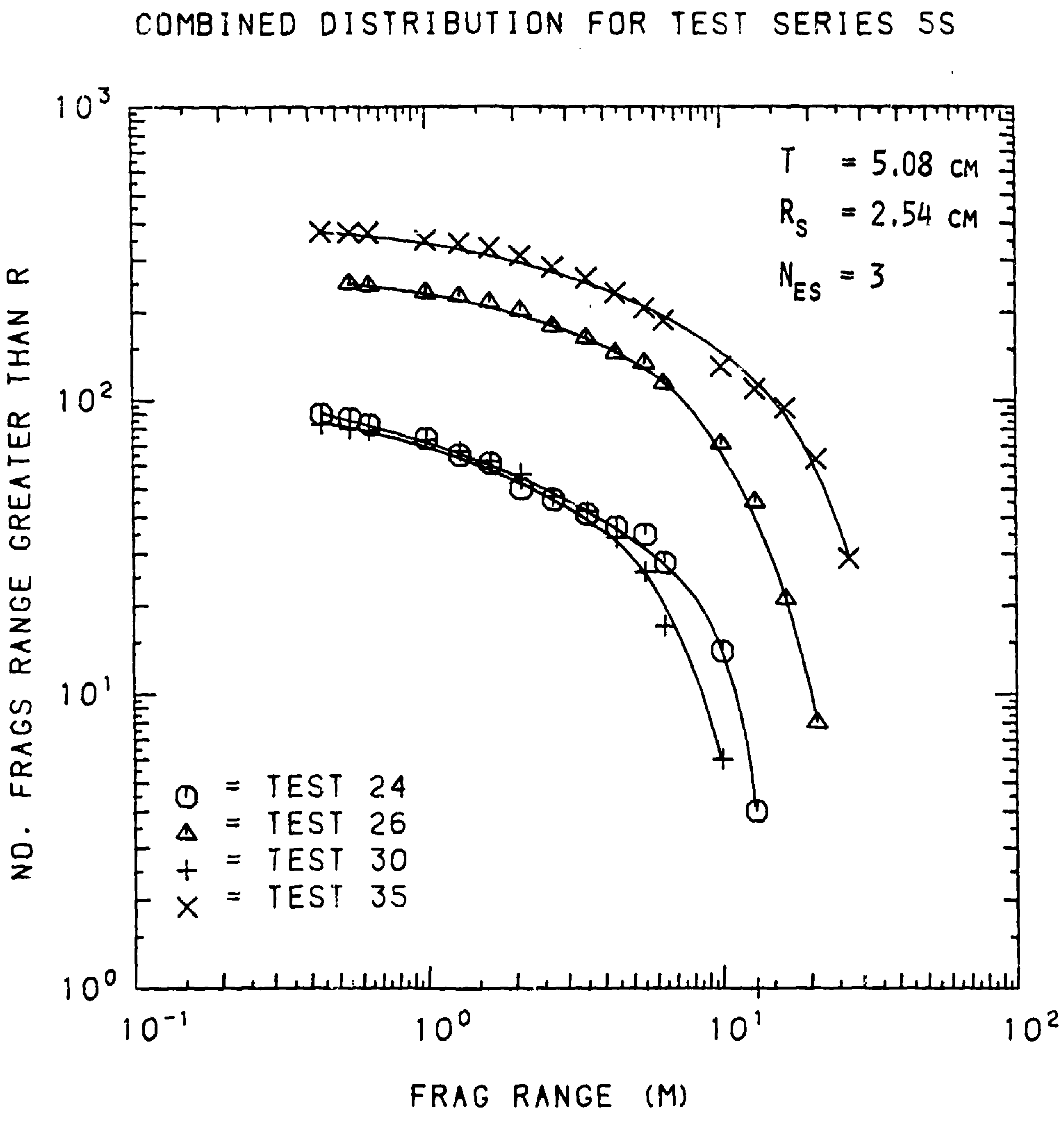

FIGURE 3-13A. RANGE DISTRIBUTION FOR TEST SERIES 5S

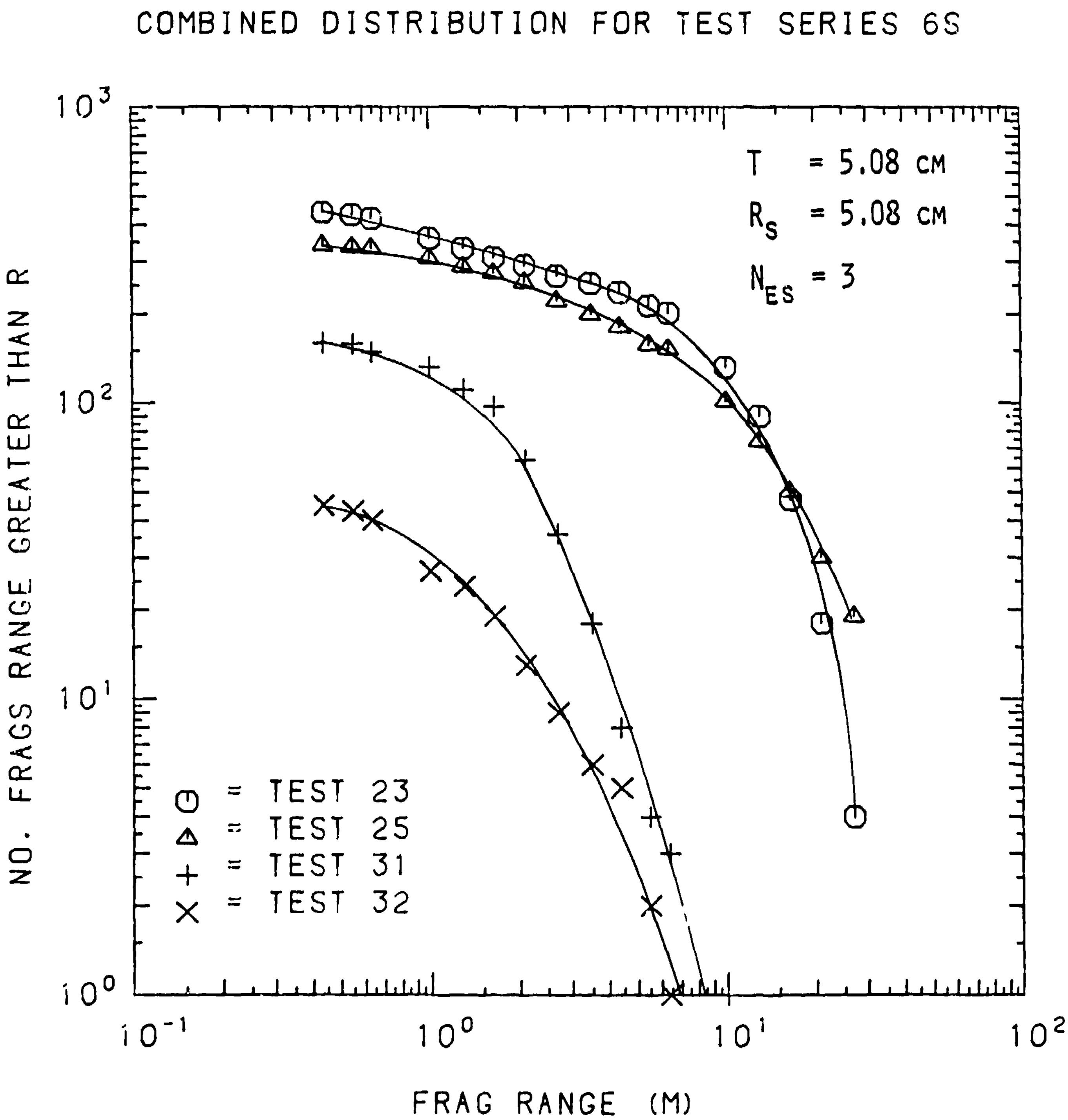

FIGURE 3-13B. RANGE DISTRIBUTION FOR TEST SERIES 6S

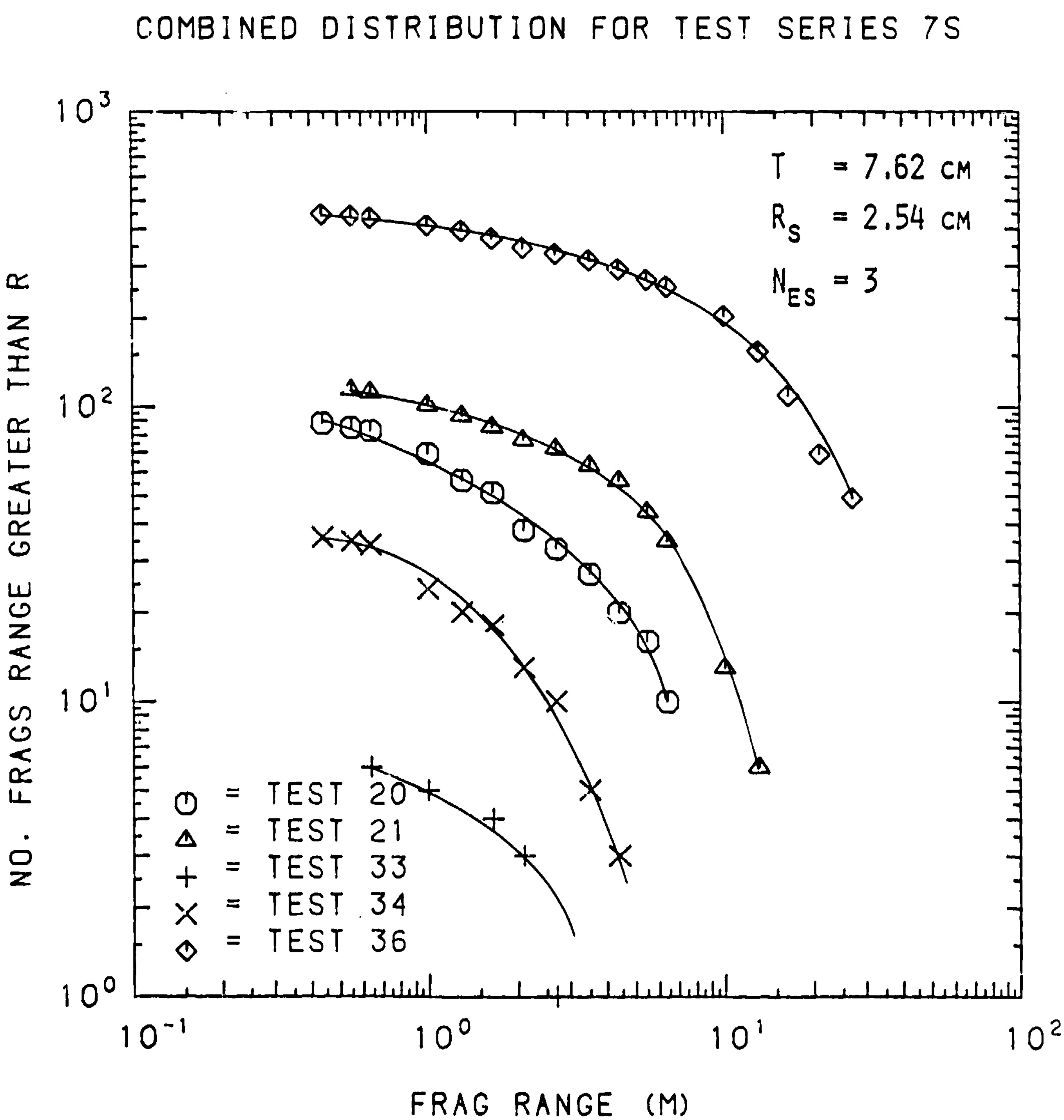

FIGURE 3-13c. RANGE DISTRIBUTION FOR TEST SERIES 7S

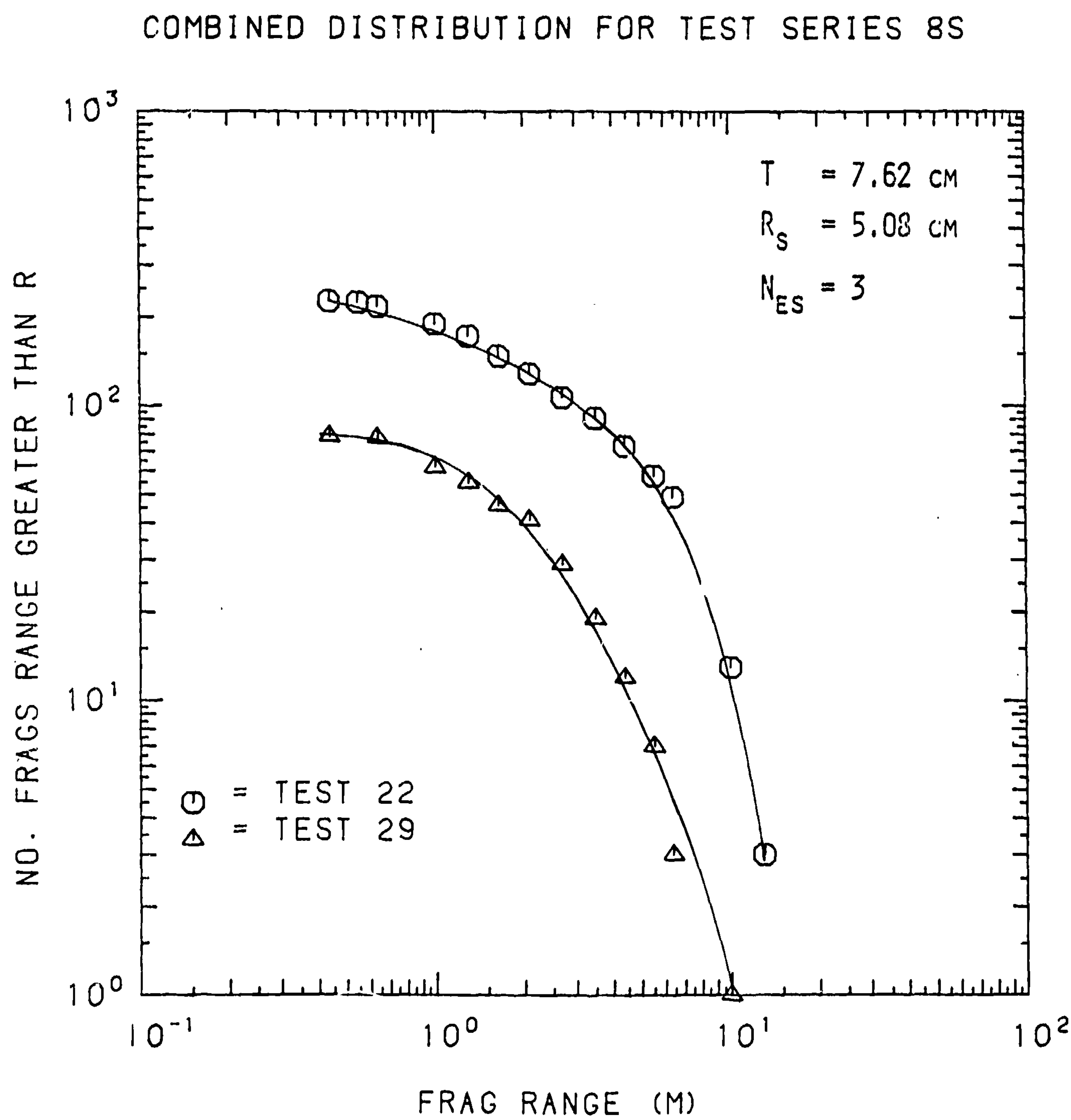

FIGURE 3-13D. RANGE DISTRIBUTION FOR TEST SERIES 8S

Table 3-1. Fragment Velocity Computation Summary

Test No.	NFrag	Fragment Velocity, (m/s)									
		1	2	3	4	5	6	7	8	9	10
1	1	11.278									
2	6	10.881	12.192	13.686	24.171	33.558	41.636				
3	2	14.783	19.964								
4	6	10.546	13.716	15.880	16.398	20.604	26.243				
5	6	4.785	5.852	9.906	10.028	10.119	15.850				
6	1	1.494									
7	5	3.734	10.546	13.106	13.137	24.018					
8	3	7.437	5.502	4.886							
9	8	6.9799	8.0467	9.845	11.491	17.922	18.166	19.599	20.025		
10	3	4.023	8.5039	9.388							
11	5	5.425	8.839	15.545	15.545	19.233					
12	7	2.518	4.694	7.559	10.790	10.820	10.820	20.361			
13	8	2.883	6.492	8.809	9.997	10.424	20.513	26.944	31.364		
14	1	11.186									
15	7	4.572	15.453	19.416	19.660	20.269	21.732	23.652			
16	6	1.981	2.874	3.627	4.237	5.425	8.839				
17	7	6.919	7.193	9.845	12.466	12.527	15.240	20.086			
18	7	22.372	27.310	31.242	31.852	32.796	33.101	35.692			
19	5	6.949	9.601	10.241	11.460	11.582					
20	7	4.877	6.157	8.108	10.942	11.064	11.918	12.954			
21	8	4.115	5.761	6.066	6.828	8.656	8.748	14.387	17.556		
22	7	3.475	10.577	11.399	13.198	13.807	14.173	15.240			
23	8	6.858	9.296	10.698	16.855	20.665	24.933	26.396	27.80		
24	9	8.443	9.083	1[illegible].758	16.734	18.318	18.959	19.812	19.873	20.726	
25	8	7.071	16.124	18.898	21.092	23.927	26.792	26.853	28.011		
26	10	2.774	3.170	5.090	12.131	15.545	15.850	19.141	19.568	20.391	23.470
27	7	3.292	4.328	4.572	4.633	5.486	7.224	9.632			
28	3	6.404	6.440	7.437							
29	6	7.193	7.346	7.894	8.595	10.241	13.045				
30	6	10.638	11.156	12.405	12.893	13.198	13.807				
31	5	3.962	7.620	8.199	12.616	12.774					
32	3	3.078	3.685	8.382							
33	3	2.569	2.905	7.166							
34	4	4.481	6.949	8.217	10.272						
35	5	13.106	14.905	21.610	27.554	35.052					
36	8	4.907	12.710	16.002	21.031	21.031	26.274	27.005	31.181		

3.7 Maximum Responses

In the following paragraphs the largest velocity, range and mass observed in the reinforced concrete tests will be discussed. These responses are given in Tables 3-2 and 3-3 for the single and three side supported test series. The responses are presented graphically in an empirically derived format. The plots are all a function of a parameter which we call the impulse factor. Equation 3-1, the impulse factor, is defined as the total impulse applied to the panel I_{TOT}, divided by the square root of the effective panel thickness. The effective thickness is, in turn, defined as the total panel thickness, t, minus the amount of concrete covering the rebar on the front (painted side, opposite the charge) face of the panel, d_c.

$$\text{Impulse Factor} = \frac{I_{TOT}}{\sqrt{t - d_c}}. \qquad (3\text{-}1)$$

In some cases, a scaled impulse factor, defined as the impulse factor divided by the square root of the explosive weight, is used. In each case two plots are given, one for strong [$f_c' > 27.6$ MPa (4000 psi)] panels supported on one edge and one for the panels supported on three edges. Also in figures which follow, 1.362 kg (3.0 lb) charges are denoted by a plot symbol which has been colored in; 0.454 kg (1.0 lb) charges are open and 0.227 kg (0.5 lb) are partially colored.

The total impulse was obtained by integrating the impulse distribution over the surface of the panel. Reference 4 provides some experimentally derived curves which give the impulse distribution over a plot surface as a function of the scaled standoff distance. The curves from Reference 4 were curve fitted to obtain a mathematical expression which can be used to evaluate the impulse at any one point on the panel surface. The resulting curve fit expression is given by equation (3-2) and is displayed in Figure 3-14.

$$\frac{I\ (Z,\phi)}{W^{1/3}} = \exp\ (A\ \mathrm{Sech}\ \ (B)),\ \left(\frac{\text{lb-sec}}{\text{lb}^{1/3}}\right) \qquad (3\text{-}2)$$

where $A = 5.232 - 1.627 \ln Z + 0.3346 (\ln Z)^2$
$B = [0.751 + 0.0958\ Z - (0.134 + 0.0211\ Z)\ \phi]\ \phi$
Z = Scaled standoff distance, in ft/lb$^{1/3}$
ϕ = Scaled position, X/R, (see insert in Figure 3-14).

This equation can be used to obtain reasonable estimates for the impulse at any point on a flat surface subject to the following constraints:

Scaled distance: $0.3 \leq R/W^{1/3} < 3.0$, ft/lb$^{1/3}$
Scaled position: $0 \leq \phi < 3.0$
Charge weight: $0.5 < \quad < 3.0$, lb

To obtain the total impulse acting on the panel, equation (3-2) was integrated over the surface area of the panel. For a square panel with a length of one side of ℓ, and the charge located at one half the height of the panel, the total impulse is given by:

Table 3-2

SUMMARY OF SINGLE SIDE SUPPORT TESTS

TEST NO.	REBAR SP. (MM)	THICK-NESS (MM)	COMPRESSIVE STRENGTH (MPA)	R (M)	W (KG)	ITOT (KNT-S)	NO. FRAGS	MASS LG (KG)	MASS AV (KG)	RANGE LG (M)	RANGE AV (M)	LARGEST VELOCITY (M/S)
3	25.40	57.15	8.57	0.127	0.227	0.175	75	0.030	0.007	24.92	8.62	19.96
5	25.40	52.39	11.54	0.183	0.454	0.253	423	0.173	0.009	27.15	6.84	15.85
8	25.40	52.39	33.07	0.183	0.454	0.253	72	0.035	0.005	5.80	1.95	7.44
14	25.40	52.39	40.59	0.147	0.227	0.155	3	0.005	0.003	5.80	4.01	11.19
15	25.40	52.39	40.88	0.147	0.454	0.296	132	0.166	0.009	23.73	5.86	23.65
1	50.80	52.39	7.17	0.152	0.227	0.157	38	0.077	0.015	14.42	2.65	11.28
2	50.80	53.97	8.57	0.076	0.227	0.253	338	0.226	0.006	31.89	7.70	41.64
4	50.80	53.97	9.17	0.183	0.454	0.253	225	0.345	0.034	31.62	14.79	26.24
9	50.80	50.80	33.07	0.183	0.454	0.253	179	19.005	0.122	24.96	6.97	20.03
13	50.80	53.97	40.31	0.320	1.361	0.418	117	16.329	0.167	19.51	5.78	31.36
6	25.40	80.96	8.61	0.183	0.454	0.253	29	0.064	0.012	3.64	1.23	1.49
7	25.40	80.96	8.61	0.147	0.454	0.296	76	0.027	0.007	11.25	2.87	24.09
16	25.40	80.96	41.44	0.183	0.454	0.253	8	0.007	0.003	2.97	1.01	8.84
17	25.40	80.96	41.44	0.128	0.454	0.326	100	0.057	0.007	12.12	2.96	20.09
10	50.80	77.79	33.38	0.183	0.454	0.253	67	0.366	0.024	5.92	2.07	9.39
11	50.80	76.20	33.38	0.147	0.454	0.296	180	22.317	0.140	17.98	3.16	19.23
12	50.80	80.96	40.65	0.127	0.454	0.328	158	0.439	0.042	18.77	6.61	20.35
18	50.80	80.96	37.38	0.219	1.361	0.619	289	11.113	0.109	37.00	17.89	35.69

Table 3-3

SUMMARY OF THREE SIDE SUPPORT TESTS

TEST NO.	REBAR SP. (MM)	THICK-NESS (MM)	COMPRESSIVE STRENGTH (MPA)	R (M)	W (KG)	ITOT (KNT-S)	NO. FRAGS	MASS (KG) LG	MASS (KG) AV	RANGE (M) LG	RANGE (M) AV	LARGEST VELOCITY (M/S)
24	25.40	50.80	41.00	0.183	0.454	0.253	90	0.032	0.008	16.11	4.79	20.73
26	25.40	55.56	35.40	0.146	0.454	0.297	250	0.122	0.009	25.79	7.32	23.47
30	25.40	52.39	39.79	0.219	0.454	0.219	83	0.044	0.009	13.10	4.14	13.81
35	25.40	50.80	48.23	0.387	1.361	0.338	375	16.864	0.057	32.28	10.02	35.05
23	50.80	50.80	41.00	0.183	0.454	0.253	440	6.169	0.040	30.46	7.20	27.80
25	50.80	50.80	40.48	0.146	0.454	0.297	341	5.216	0.050	32.19	8.10	28.01
31	50.80	50.80	39.79	0.219	0.454	0.219	159	0.165	0.013	10.91	2.11	12.77
32	50.80	53.97	45.82	0.268	0.454	0.185	45	0.068	0.008	7.30	1.92	8.38
20	25.40	80.96	43.38	0.146	0.454	0.297	88	0.089	0.014	9.02	2.91	12.95
21	25.40	77.79	36.73	0.128	0.454	0.326	114	0.038	0.008	14.92	5.01	17.56
33	25.40	77.79	49.35	0.219	0.454	0.219	6	0.005	0.002	2.93	1.90	7.16
34	25.40	79.38	49.35	0.183	0.454	0.253	36	0.019	0.002	4.93	1.94	10.27
36	25.40	77.79	49.35	0.320	1.361	0.418	444	10.954	0.058	31.82	10.85	31.18
19	50.80	80.96	16.32	0.183	0.454	0.253	58	0.161	0.021	11.34	3.68	11.58
22	50.80	80.96	36.73	0.146	0.454	0.297	227	0.205	0.018	14.81	3.69	15.24
27	50.80	77.79	27.22	0.219	0.454	0.219	24	0.005	0.001	4.28	1.94	9.63
28	50.80	76.20	27.22	0.198	0.454	0.238	10	0.052	0.011	4.65	1.51	7.44
29	50.80	77.79	28.08	0.160	0.454	0.279	79	0.167	0.015	10.34	2.57	13.05

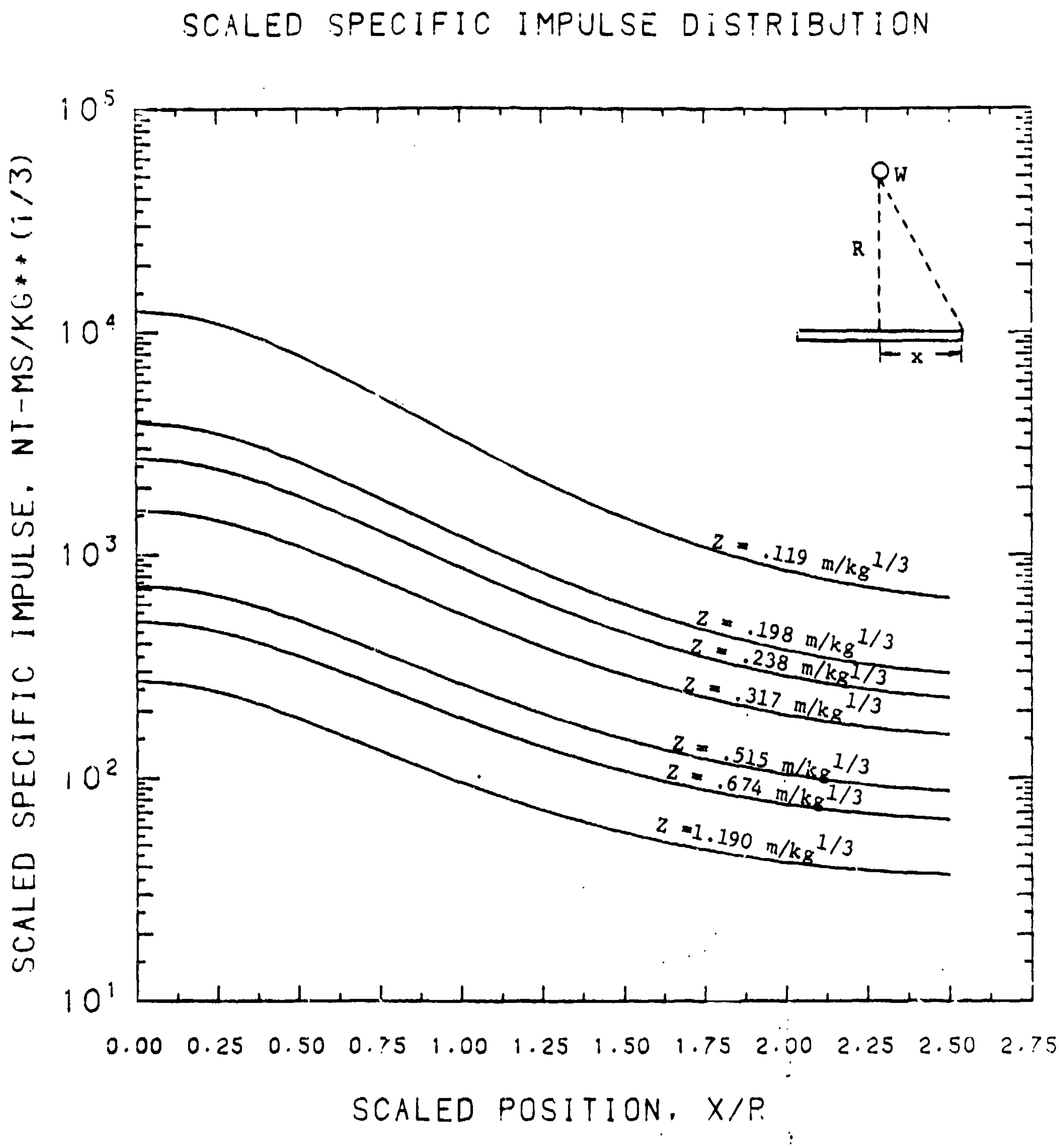

SCALED SPECIFIC IMPULSE DISTRIBUTION
SCALED SPECIFIC IMPULSE, NT-MS/KG** (1/3)
10^5
10^4
10^3
10^2
10^1
W
R
x
Z = .119 m/kg^1/3
Z = .198 m/kg^1/3
Z = .238 m/kg^1/3
Z = .317 m/kg^1/3
Z = .515 m/kg^1/3
Z = .674 m/kg^1/3
Z =1.190 m/kg^1/3
0.00 0.25 0.50 0.75 1.00 1.25 1.50 1.75 2.00 2.25 2.50 2.75
SCALED POSITION, X/R

FIGURE 3-14.

$$\frac{I_{TOT}}{W^{1/3}} = 4 \int_{o}^{\ell/2} \int_{o}^{\ell/2} \frac{I\ (Z,\phi)}{W^{1/3}}\ dx\ dy \qquad (3\text{-}3)$$

Equation (3-3) cannot be integrated directly, so the numerical procedure given by equation (3-4) was devised. As long as Δx and Δy are sufficiently small, equation (3-4) will provide a reasonably accurate estimate for the total impulse acting on a panel.

$$\frac{I_{TOT}}{W^{1/3}} = 4 \sum_{x=o}^{\ell/2} \sum_{y=o}^{\ell/2} \frac{I\ (Z,\phi)}{W^{1/3}}\ \Delta x\ \Delta y \qquad (3\text{-}4)$$

The total impulse was calculated for each of the 36 reinforced concrete tests using Δx and Δy of one-hundredth of the length of one panel side. The total impulse for the one and three side supported panels was summarized in Tables 3-1 and 3-2.

3.7.1 Largest Velocity

Figures 3-15a and 3-15b present the largest velocity data for the single and three side supported tests. In both cases, the largest velocity increases roughly linearly with the impulse factor, I_{TOT}. Both sets of data were curve fit and the resulting linear equations are shown on the respective plots. Also shown on the figures are the standard deviation σ, and the multiple correlation coefficient r of the curve fits. The fit for the three side support curve is better than the one for one edge supported, as evidenced by the lower standard deviation and multiple correlation coefficient. At low impulse levels, the largest velocity is about the same for both kinds of supporting arrangements. For high impulse levels, above approximately 14.0 x 10^5 Nt-s/$m^{½}$ (1.8 x 10^5 psi-s/$ft^{½}$), the largest velocity for three side supported panels begins to exceed that for the single side supported panels. Note that the 0.227 kg (0.5 lb) and 1.36 kg (3.0 lb) charges on both graphs follow the trend line of the 0.454 kg (1.0 lb) charge data.

3.7.2 Largest Range

Figures 3-16a and 3-16b present the curves for the largest range for fragments emanating from panels supported on one and three sides. The use of the scaled range defined as the largest range R_L, divided by the rebar spacing R_S, appears to correlate the test data adequately

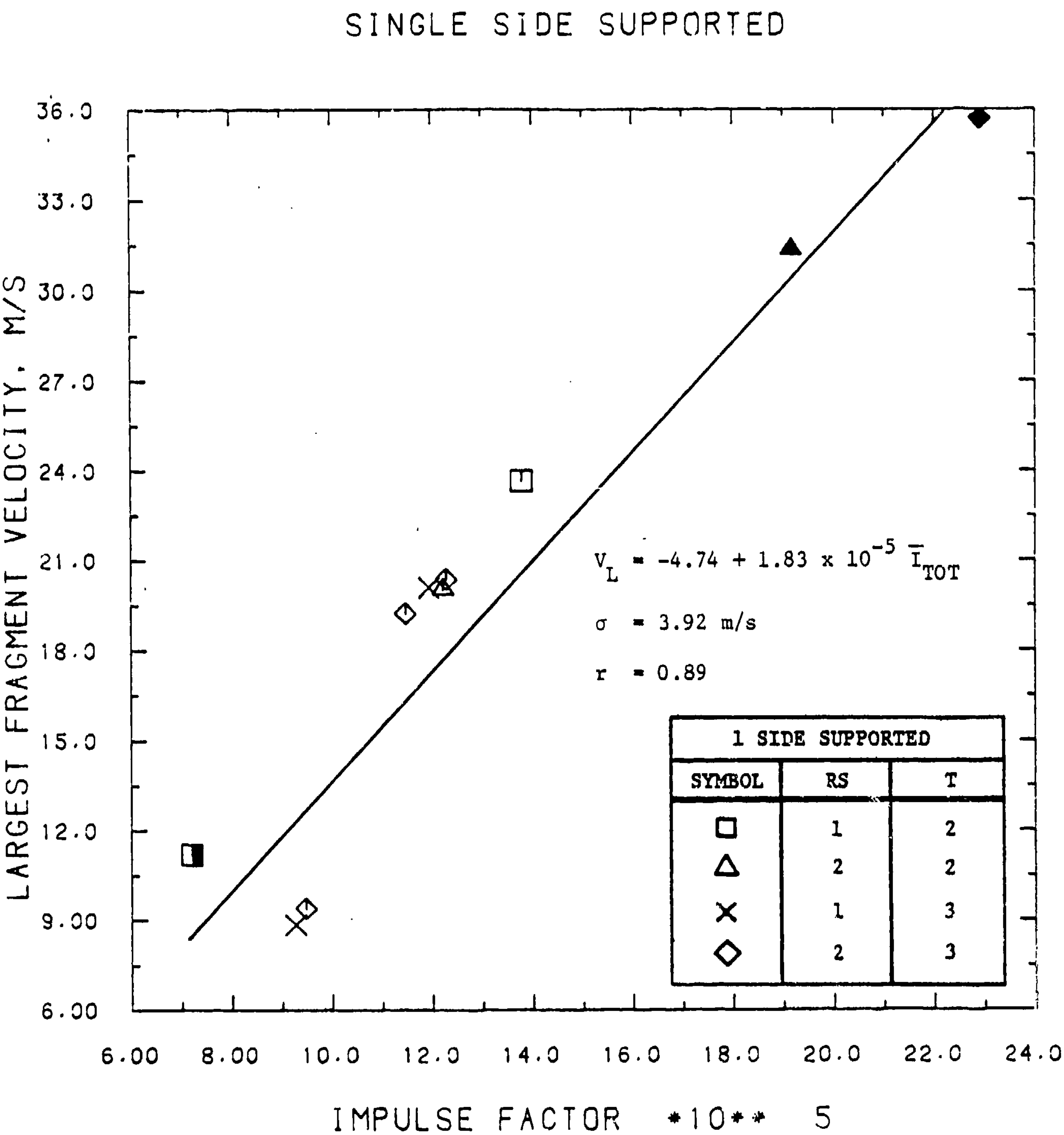

Figure 3-15A. The Largest Fragment Velocity as a Function of the Impulse Factor for Single Side Supported Panels

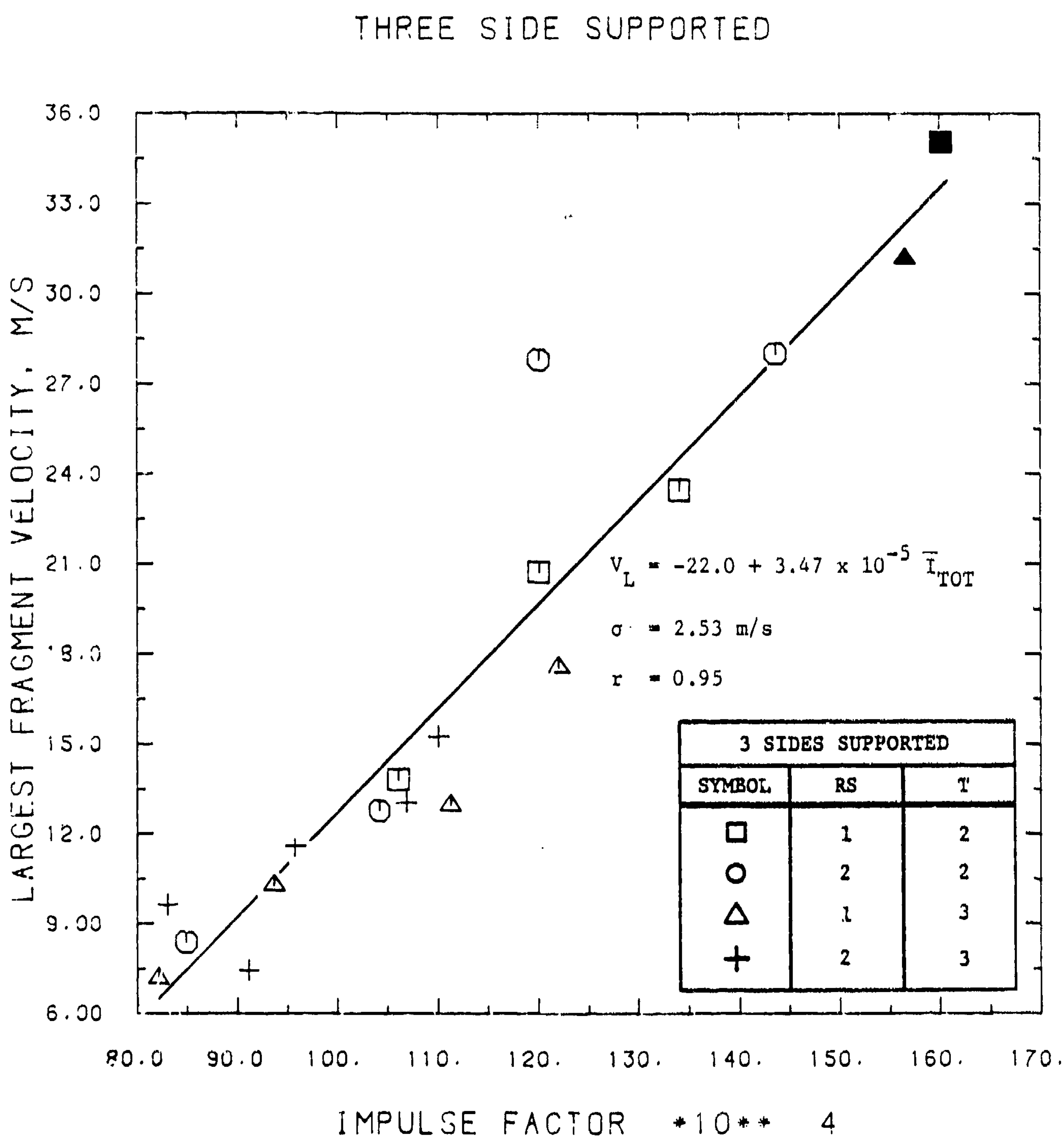

FIGURE 3-15B. THE LARGEST FRAGMENT VELOCITY AS A FUNCTION OF THE IMPULSE FACTOR FOR THREE SIDE SUPPORTED PANELS

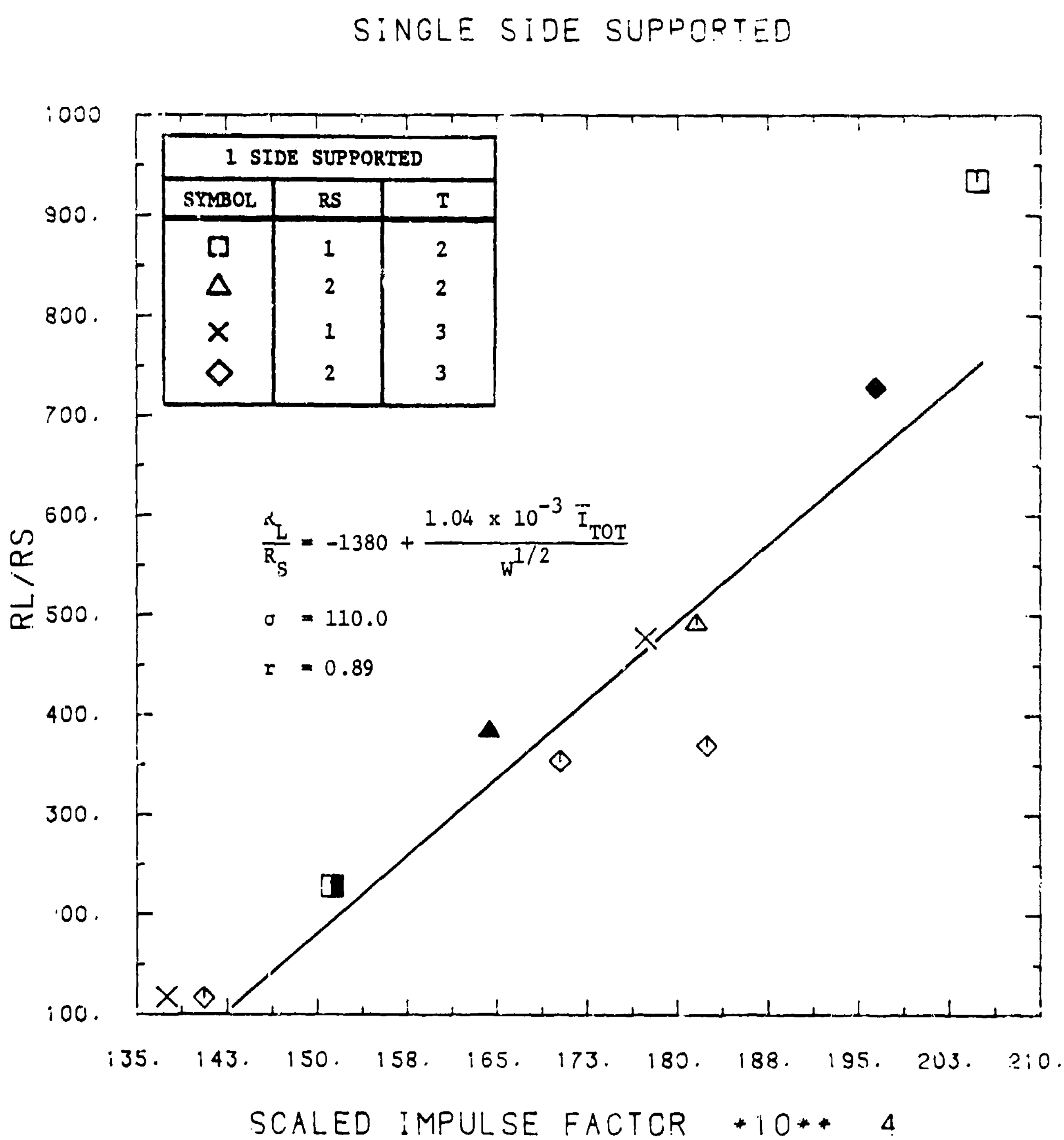

FIGURE 3-16A. THE LARGEST FRAGMENT RANGE AS A FUNCTION OF THE SCALED IMPULSE FACTOR FOR SINGLE SIDE SUPPORTED PANELS

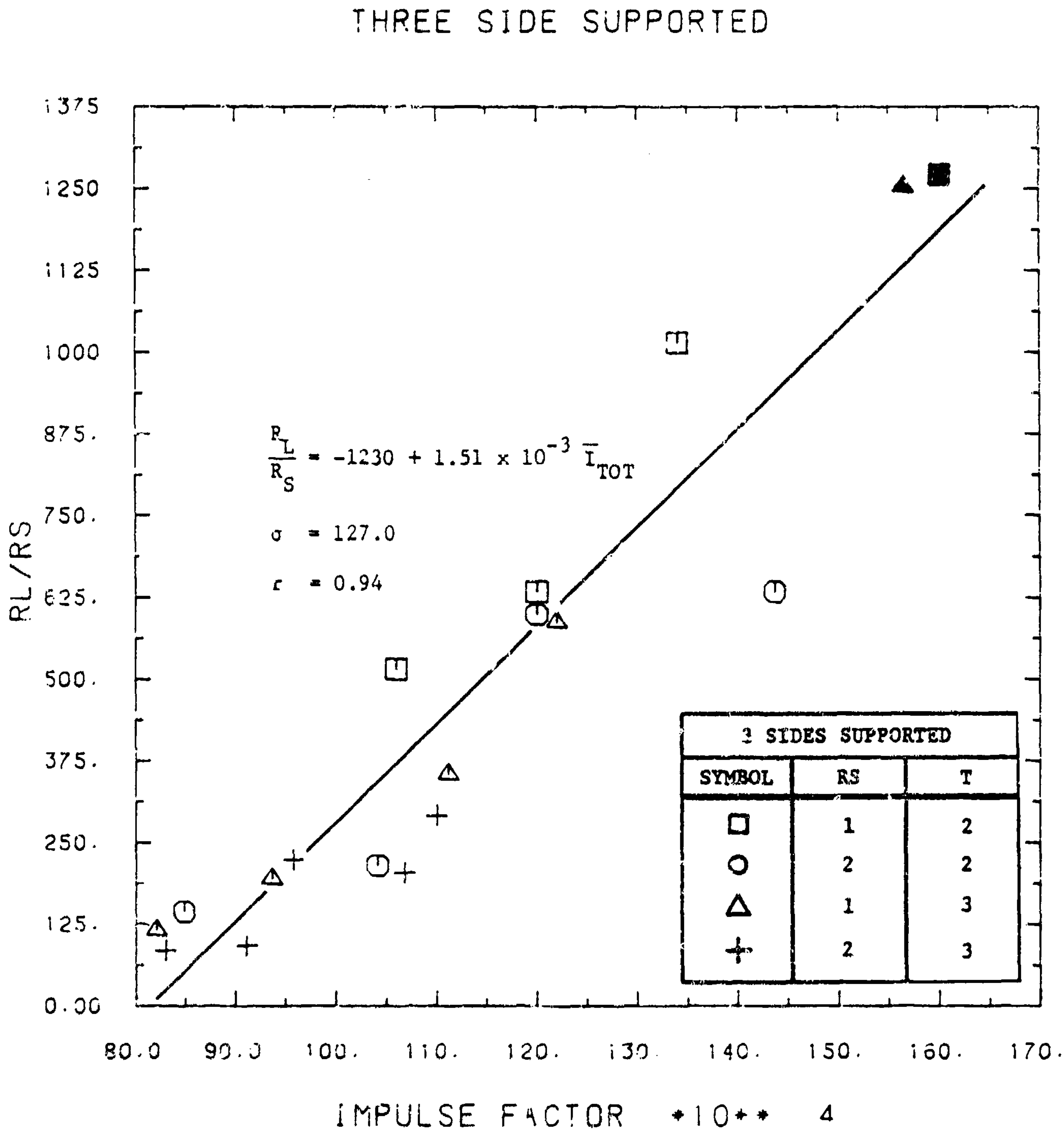

FIGURE 3-16B. THE LARGEST FRAGMENT RANGE AS A FUNCTION OF THE IMPULSE FACTOR FOR THREE SIDE SUPPORTED PANELS with the scaled impulse factor for the single side supported panels, and the impulse factor for the panels supported on three sides. This implies that at equivalent impulse levels, the largest range will be about twice as long for panels with rebar spacing of 5.08 cm (2.0 in) as than for panels with R_S = 2.54 cm (1.0 in) at equivalent impulse levels. Although the graphs are on different scales, it is clear that the largest range for fragments emanating from three side supported panels exceeds that of the panels supported on one edge. The difference is negligible at low impulse levels, but increases as the total impulse on the panel increases. The curve fit for the three side supported panels is better than that for the cantilevered panel data as evidenced by the higher multiple correlation coefficient.

3.7.3 Number of Fragments Produced

Figures 3-17a and 3-17b present the curves for the number of fragments produced from panels with one and three sides supported. The data were found to correlate well when the number of fragments, N_f, divided by the rebar spacing, R_s, was plotted as a function of the scaled impulse factor for cantilevered panels, and the impulse factor for the panels supported on one edge. This implies that at equivalent impulse levels, the number of fragments produced in tests with R_S = 5.08 cm (2.0 in) will be roughly twice that for panels with R_S = 2.54 cm (1.0 in).

3.7.4 Largest Mass

Figure 3-18 presents the curves for the largest mass recovered in experiments with the cantilevered and three side supported panels. The y-axis on the plots is the largest mass, M_L, divided by the rebar spacing, R_S. The x-axis is the scaled impulse factor for the single side supported panels or the impulse factor for the three side supported panels. The data correlation is better for the largest mass for the three side supported panels as evidenced by the higher multiple correlation coefficient. It is apparent that at equivalent scaled impulses, the largest mass produced in experiments with reinforcement spacings of 5.08 cm (2.0 in) will be roughly twice that for tests with R_S = 2.54 cm (1.0 in).

3.8 Masonry Wall Test Results

Four tests were performed on full-scale masonry walls, two tests on walls built using haydite blocks and two tests on walls built using concrete blocks. Summaries of these four tests were prepared and have been included here as Table 3-4. Included in these summaries are a description of the wall parameters, charge size, standoff distance, impulse, number of fragments recovered, maximum fragment range, maximum fragment mass, average fragment velocity, and a short description of the test results.

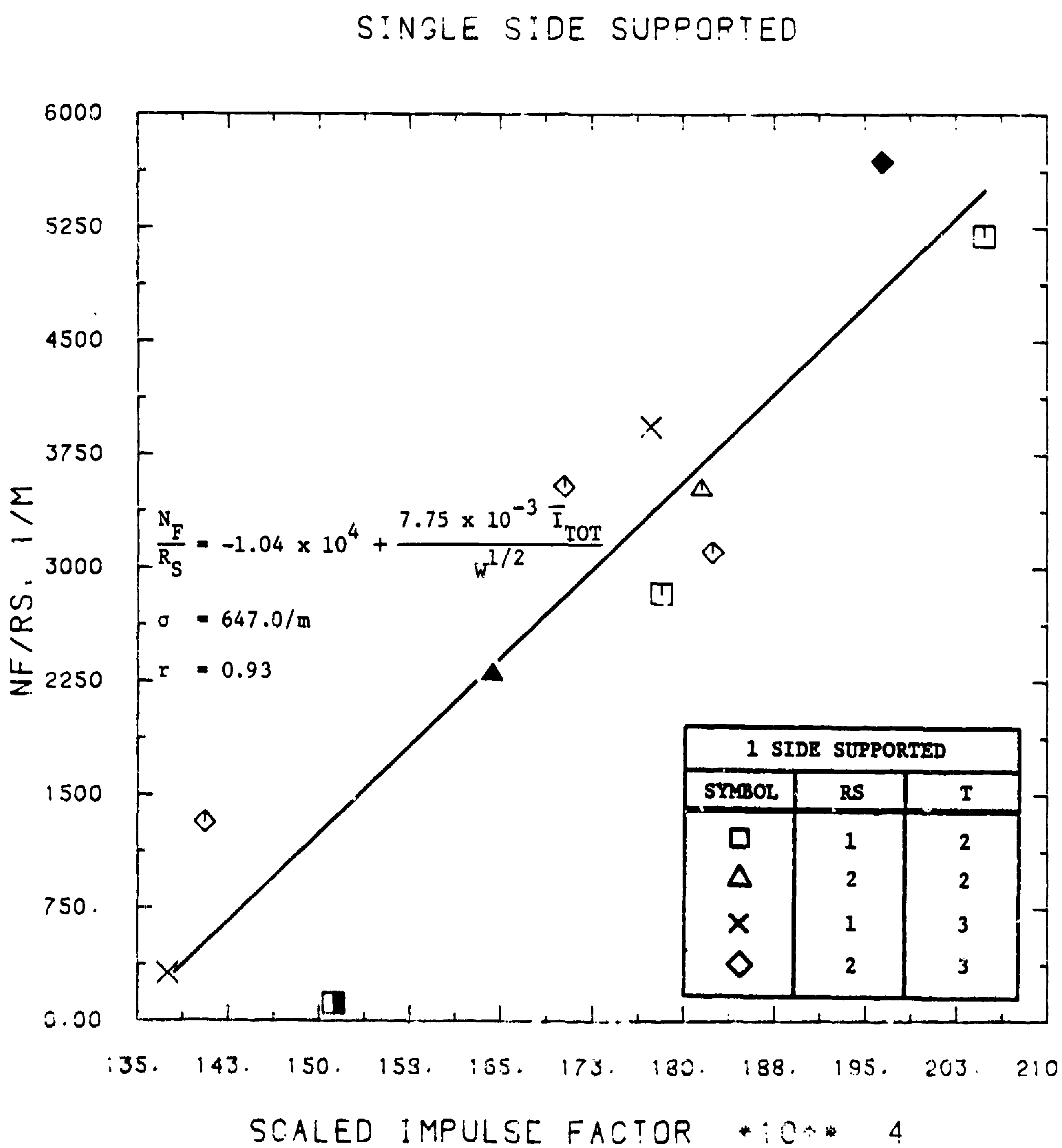

FIGURE 3-17A. NUMBER OF FRAGMENTS PRODUCED AS A FUNCTION OF THE SCALED IMPULSE FACTOR FOR SINGLE SIDE SUPPORTED PANELS

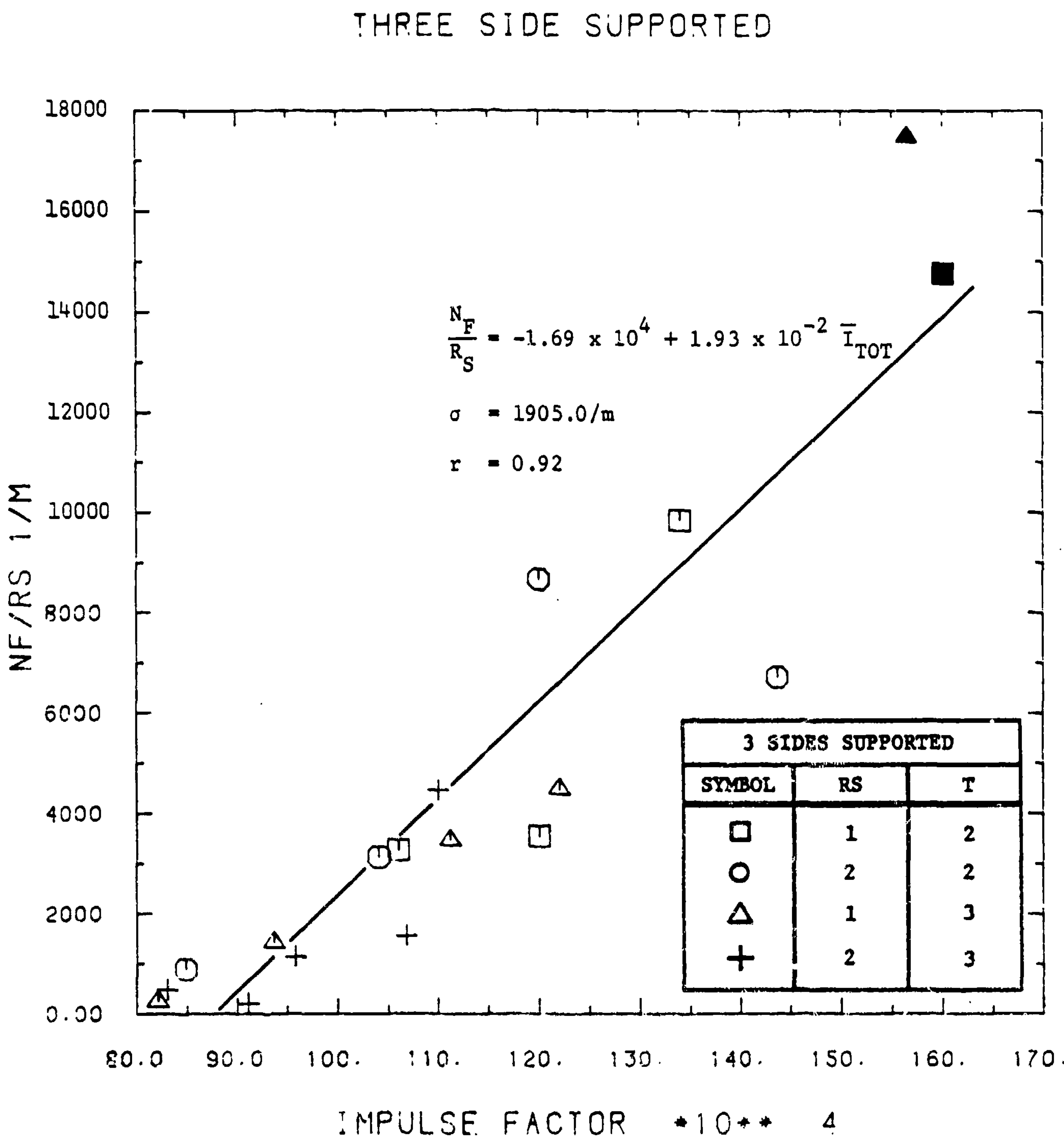

FIGURE 3-17B. NUMBER OF FRAGMENTS PRODUCED AS A FUNCTION OF THE IMPULSE FACTOR FOR THREE SIDE SUPPORTED PANELS

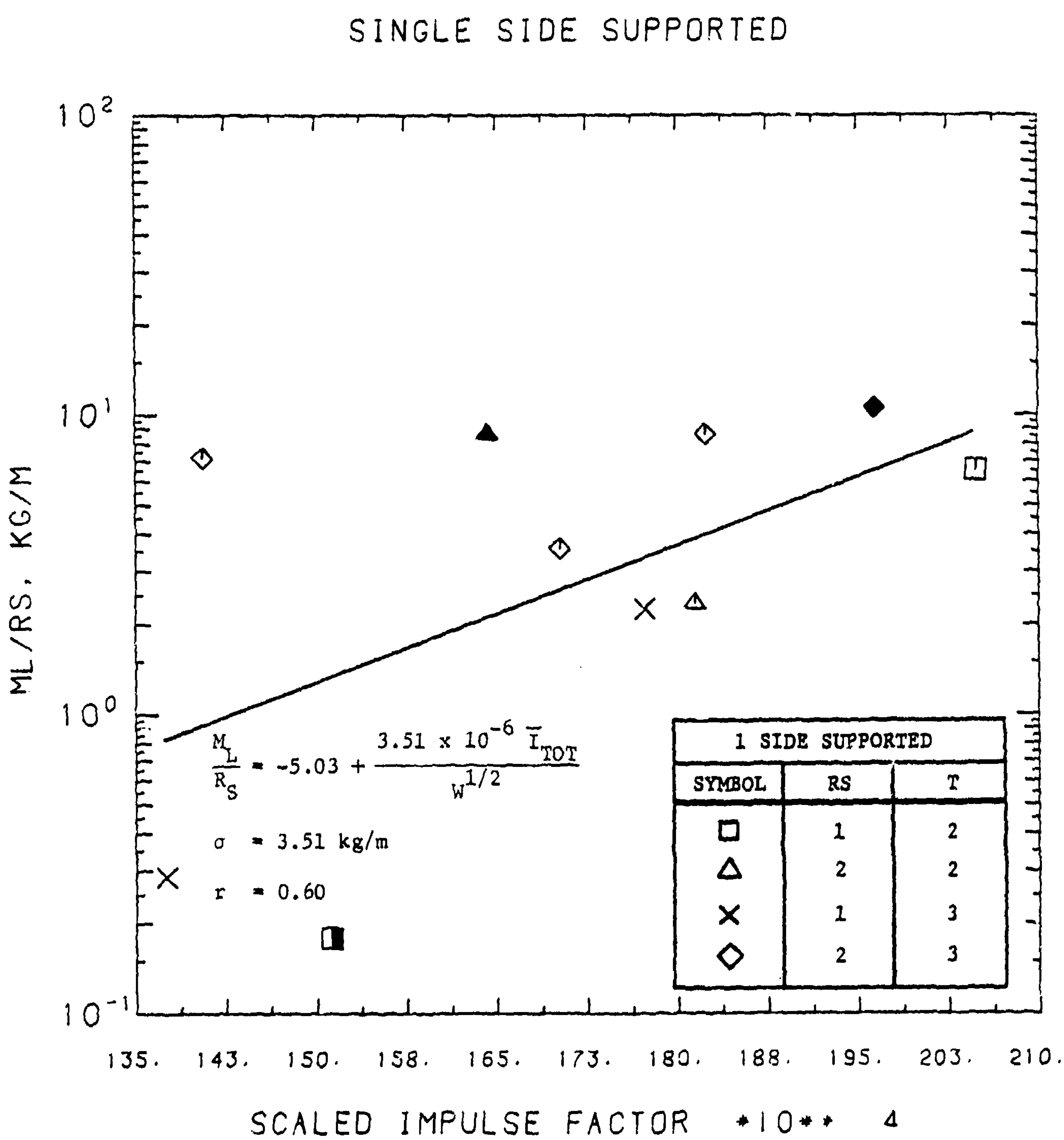

FIGURE 3-18A. LARGEST RECOVERED MASS AS A FUNCTION OF THE SCALED IMPULSE FACTOR FOR SINGLE SIDE SUPPORTED PANELS

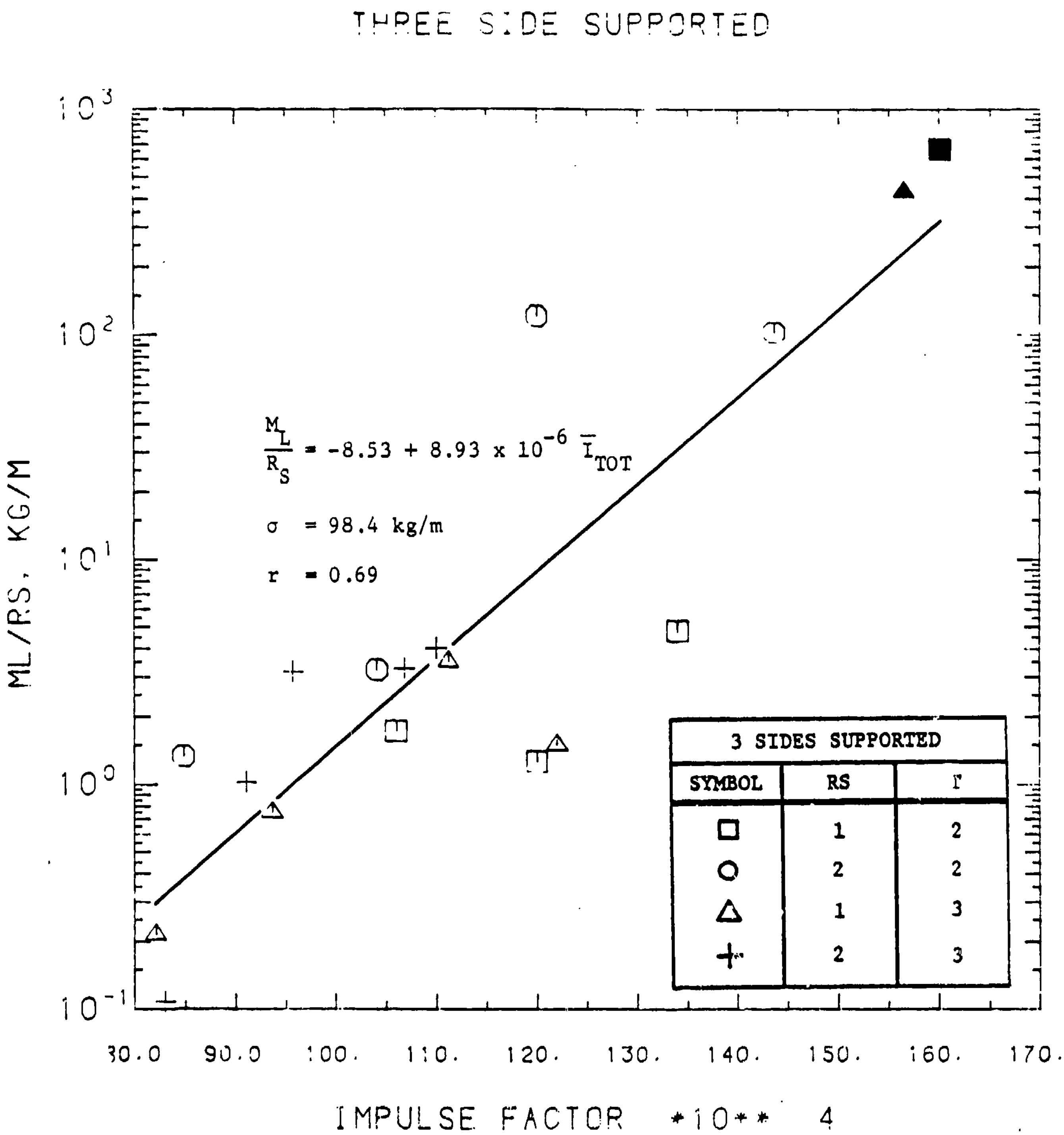

FIGURE 3-18B. LARGEST RECOVERED MASS AS A FUNCTION OF THE IMPULSE FACTOR FOR THREE SIDE SUPPORTED PANELS

Table 3-4. Masonry Dividing Wall Test Results

Test No.	Wall Dim (m)	Type of Block	Charge Weight (kg)	Charge Height (mm)	Standoff Distance (mm)	Z $(m/kg^{1/3})$	$I/W^{1/3}$ $Nt\text{-}s/kg^{1/3}$	Largest Velocity	No of Frags	Max Frag Range (m)	Max Frag Weight (kg)	Comments
37	1.63 x 1.42	Haydite	0.453	483	381	0.496	0.834	—	0	—	—	Wall is severely cracked and deformed. Little deformation near the base. Deformation increases evenly towards the top. Maximum deformation is about 18-30 cm (7-12 inches) from the top.
38	1.63 x 1.42	Haydite	1.36	508	381	0.345	1.39	11.3	229	12.8	13.1	Side columns of the wall (½-1 block in width) is intact. Bottom row of blocks is intact. Majority of the debris fell in the first 2.4 m (8 ft) with little velocity. One full block and one complete half block fragments intact. Very little lateral dispersion of the fragments.
39	1.63 x 1.42	Concrete	0.454	508	382	0.496	0.834	10.3	78	4.05	17.2	Wall has a hole blown out of the center. Two blocks were blown out intact. Farthest fragment went approximately 0.3 m (13 inches) with the majority of the fragments inside of 0.25 m (10 inches) downrange. Very small lateral dispersion of fragments. Remaining columns of blocks were deformed approximately 15 degrees.
40	1.63 x 1.42	Concrete	0.454	508	381	0.397	1.16	—	0	—	—	Wall is intact; however, a vertical crack at the wall center was created. Top block at center of the wall is loose and was popped up about 1.3 cm (½ inch). No fragments were created.

Test No's. 37 and 38 were performed on walls built using haydite blocks. Test No. 37 was performed using a 0.454 kg (1.0 lb) charge at a standoff distance of 0.38 m (1.25 ft). The wall was severely cracked and deformed at the top, but the lower rows of blocks were fairly intact, as can be seen in Figure 3-19. Test No. 38 was performed using a 1.362 kg (3.0 lb) charge at the same standoff distance as that of Test No. 37. Since the scaled impulse was significantly higher, a greater degree of fragmentation was expected and did in fact result. A total of 229 fragments were produced, with the majority of the fragments coming from the center of the wall.

Test No's. 39 and 40 were performed on walls built with the concrete blocks. Test No. 39 was performed using the same charge weight and standoff distance used in Test No. 37 in order to obtain a comparison between the haydite and concrete blocks. A total of 78 fragments were produced in this test, with the majority of fragments originating from the center of the wall (see Figure 3-20). Several complete blocks were launched downrange and only the side columns remained upright. Test No. 40 was performed using a 0.454 kg (1.0 lb) charge and a standoff distance of 0.3 m (0.98 ft). No fragments were produced; however, the wall did sustain a vertical crack at the wall center.

Even though a very limited number of tests on masonry walls were performed, some observations and general conclusions can be drawn:

1) the masonry block walls do not break up as drastically as do the reinforced concrete walls,

2) fragments produced have a much lower velocity than do fragments produced from reinforced concrete walls, and

3) masonry wall fragments have a much shorter range.

FIGURE 3-19. FAILURE PATTERN FOR A HAYDITE BLOCK DIVIDING WALL TEST

FIGURE 3-20. FAILURE PATTERN FOR A CONCRETE BLOCK DIVIDING WALL TEST

4.0 CONCLUSIONS

A small scale test program of reinforced concrete and masonry dividing walls was performed in order to determine the fragmentation characteristics of the reinforced concrete and masonry walls subjected to close-in blast effects. Parameters of prime importance were: fragment velocity, fragment shape and size, and fragment density downrange. This test program has been the most highly documented wall fragmentation test program to date and several important innovations were made. The color coding of the wall panel allowed the origin of the fragments to be recorded. Complete documentation of every fragment collected including fragment dimensional size, mass, shape and recovery location enabled statistical evaluation of the debris that was formed in each experiment.

Based on the fragment characteristics data generated during these experiments on reinforced concrete panels and masonry walls, a number of general conclusions can be drawn which could be beneficial to designers:

- Fragments produced as a result of a dividing wall failure can be classified as either "chunky" or "pancake" in shape with the "chunky" fragments traveling 20 to 50 percent further than the "pancake" fragments.

- A wide range of velocities and initial trajectory angles are present in every test, however, the predominant trajectory of the higher velocity fragments is normal to the panel surface.

- Walls supported on three sides as compared to cantilevered walls were found to present the greatest hazard due to higher fragment velocities at equivalent impulse levels.

- For charges located at one-half of the height of the panel above the ground, approximately twice as many fragments originated from the lower half of the panel as from the upper half. In addition, it was found that the panel underwent a net rotation, prior to fragment ejection, thereby directing the majority of the fragments into the ground.

- For charges located at one-third the height of the panel above the ground, i.e., simulating a charge located 0.9 m (three feet) from the floor of a full scale building, three times as many fragments originated from the lower half of the panel as from the top half with a greater number traveling downrange.

- Masonry block walls do not fragment as drastically as do reinforced concrete walls. The fragments generally are quite large, often consisting of one or more complete blocks, but the velocities and ranges appear much lower.

Based on the statistical distributions of fragment range, mass, and velocity, the following conclusions can be drawn:

- Fragments emanating from the interior of the panel comprise 40% of the number of fragments produced in any test. Fragments originating from the front face (opposite the charge) comprise another 40% of the fragments. The remaining 20% of the fragments are produced from the acceptor (charge side) of the panel.

- Mass and range distributions in the format of Mott Distributions for arena fragmentation tests were prepared. The resulting distributions for fragment range and mass are qualitatively similar, and similar observations were drawn. More fragments at each mass level, and more fragments at each range level are produced, all other parameters held constant, when:

  a) the total impulse applied to the panel is increased,
  b) the panel compressive strength is decreased,
  c) the reinforcement spacing is increased, or
  d) the number of supporting edges is increased.

Based on the empirical analysis of the response parameters, the following conclusions can be drawn:

- The total impulse applied to the wall was discovered to be an important and controlling parameter in wall fragmentation.

- The failure mechanism for cantilevered walls was qualitatively different than the failure mechanism for walls supported on three edges.

- The largest velocity was found to be independent of the rebar spacing, but dependent on the total impulse acting on the wall, the effective wall thickness, and the restraint conditions.

- For walls supported on one edge, the total impulse acting on the wall, the rebar spacing, explosive weight and the effective wall thickness were the primary factors controlling the largest range, the number of fragments, the largest mass and the average mass. The fragmentation hazard, as evidenced by the number of fragments, the average and largest mass and the largest range, is increased when:

  a) the total impulse is increased,
  b) the rebar spacing is increased,
  c) the panel thickness is decreased,
  d) the explosive weight is increased, or
  e) the panel compressive strength is decreased.

- Charge weight had no appreciable effect on walls supported on three edges, outside of controlling the total impulse applied to the wall. All other fragmentation hazard trends for walls supported on three sides were qualitatively similar to those for the cantilevered walls.
- Concrete blocks appear to be superior to haydite blocks in resisting fragmentation.

5.0 RECOMMENDATIONS

Based on the results of this program and the subsequent data analysis, the following recommendations are being made:

- arger scale, or near full-scale tests on reinforced concrete dividing walls should be conducted to verify and improve the empirical scaling laws presented in this report.

- Additional tests of masonry walls should be conducted to verify the results of the limited test program conducted here and to improve the scaling laws.

- Conduct experimental programs to investigate more fully the effect of the total impulse on the wall fragmentation patterns. Specifically, investigate the difference between large charges at large standoffs versus smaller charges located closer to the panel.

- Conduct experimental programs to investigate the effect of off-center charge placement on wall fragmentation.

- Dividing walls should be built with only one side supported instead of three sides supported to reduce potential fragmentation hazards.

- Design and test the effectiveness of new dividing wall concepts such as:

  a) Hollow-walled reinforced concrete dividing wall similar in design to a masonry block, see Figure 5-1a.

  b) Solid reinforced concrete walls designed to rotate on failure as shown in Figure 5-1b. This rotation of the wall will direct the fragments into the ground thereby reducing the potential fragment hazard downrange.

- The data collected on this program are quite extensive, however, all aspects of the data have not been analyzed. It is recommended that formal statistical distributions of the mass, and range as a function of the fragment origin, or fragment shape be performed. Polar plots or fragment density contours should be produced. The effect of the concrete compressive strength should be formally introduced into the empirical analysis, as well as attempts to correlate the test results with full-scale test data or analytical procedures. These topics are suggested for further data analysis.

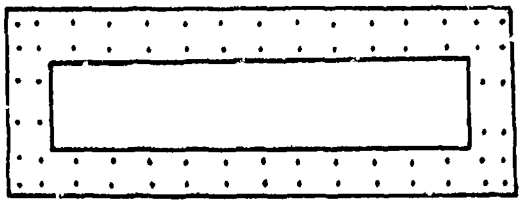

a) Hollow Reinforced Concrete Wall

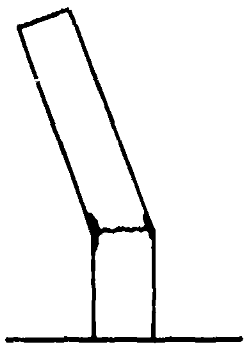

b) Hinge Failure Reinforced Concrete Wall

FIGURE 5-1. SUGGESTED DIVIDING WALL CONCEPTS

6.0 REFERENCES

1. Department of the Army, "Structures to Resist the Effects of Accidental Explosions," TM 5-1300, U. S. Government Printing Office, Washington, D.C., June 1969.

2. Baker, W. E., Explosions in Air, The University of Texas Press, Austin, Texas, 1973.

3. Johnson, C. and Moseley, J. W., "Preliminary Warhead and Terminal Ballistics Handbook," Naval Weapon Laboratory, Report 1821, March 1964.

4. Hokanson, J. C., Esparza, E. D. and Wenzel, A. B., "Measurement of Blast Parameters on a Barricade Due to Simultaneous Detonations of Multiple Charges," Final Report for Contract No. DAAA21-76-C-0254, Prepared for the U.S. Army Research and Development Command, Dover, New Jersey, July 15, 1977.

APPENDIX A

RESULTS OF LITERATURE SEARCH AND MODEL ANALYSIS

PRECEDING PAGE BLANK-NOT FILMED

APPENDIX A

A.1 General

This section of the report summarizes the results of the literature search conducted for this program and presents a model analysis developed for fragmentation of reinforced concrete. A brief discussion of the uses of dividing walls and the fragmentation of reinforced concrete has also been included in this section.

A.2 Background Information

In munition manufacturing facilities, reinforced concrete dividing walls are used as shields for personnel protection and as physical barriers between explosive production steps. If an explosion should occur, the dividing wall may break up under the overpressure loading. Fragments emerging from the back side of the wall may impact an adjacent explosive source with sufficient energy to cause a secondary initiation, or may be a hazard for nearby inhabited buildings. The sensitivity of selected munitions and explosives to fragment impact is being investigated and sufficient data are available to predict threshold initiation conditions (Reference 1). However, the fragment hazard associated with wall breakup under blast loadings is an area which has not been extensively studied. Current predictive techniques for determining wall fragmentation are based solely on analytical studies which have limited scopes and few practical design applications (for example, C. A. Kot in References 2 and 3 provides a means for calculating spall fragment thickness and velocity for blast-loaded concrete panels which have no reinforcing). For these reasons, the current safety regulations which have evolved are quite conservative:

1) building must be located such that less than one fragment per 55.7 m^2 (600 ft^2) exposed building area with an energy greater than 78.6 J (58 foot pounds) strikes the structure;

2) if the above criteria (1) cannot be met, then inhabited building distance of 381 m (1250 ft) minimum is required for siting quantities greater than 45.4 kg (100 lb).

In the majority of design applications, the spall fragment density is not known, so the second and most costly requirement is usually enforced.

A.2.1 Mechanisms for Fragment Formation

When a reinforced concrete element is overloaded by a blast wave, the element fails and concrete fragments are formed. Depending on the degree of blast overload, the mechanism for fragment formation may be either spalling, scabbing or the generation of post-failure fragments.

PRECEDING PAGE BLANK-NOT FILMED

A.2.2 Spalling of Concrete

One mechanism of fragment generation for concrete or masonry walls loaded by strong air blast waves can be spalling. This physical process is well described in the literature (see References 4 and 5), and is shown schematically in Figure A-1. The reflected air blast wave is transmitted through the wall as a compressive wave, with velocity U and normal stress σ. The shock velocity is somewhat greater than sound velocity in the concrete, i.e.,

$$U > a_c = (E/\rho)^{1/2} \tag{A-1}$$

For some types of masonry, there are data which give U as a function of shock strength. The wave enters the wall with initial compressive stress $\sigma_1 = P_r$, the reflected air shock overpressure. The profile of stress in this shock is determined by the time history of the reflected overpressure. As the wave passes through the wall, it may decay slightly [see Figure A-1(a)].

On reflection from the rear face, the normal stress must drop to zero, and this boundary condition is accommodated by a reflected tensile wave which at first exactly cancels the compressive stress in the transmitted wave. But, as the tensile wave continues back through the wall, a net tensile stress develops, and failure will occur at a location where this stress exceeds the tensile strength of the concrete, e.g., where σ_4 or σ_5 in Figure A-1(b) exceeds tensile strength.

The spalling process we have just described is essentially independent of wall boundary conditions, provided the wall lateral dimensions are much greater than the thickness. It is predictable, and it is possible to estimate spall thickness and velocity, if wave profiles and wall material properties are known. Actual fragment masses cannot be accurately predicted, however, and one must rely on test results to determine these masses.

A.2.3 Scabbing of Concrete

From Reference 6, scabbing of reinforced concrete elements is described as the end result of a tension failure in the concrete normal to its free surface. Scabbing is associated with large deflections which occur in the later stages of the ductile response mode of the reinforced concrete element. In general, the velocities of the scabbed fragments are lower than the velocities of spalled fragments.

A.2.4 Post-Failure Concrete Fragments

In the situation where a reinforced concrete element is failed by exposure to a substantial blast overload, fragments are formed and

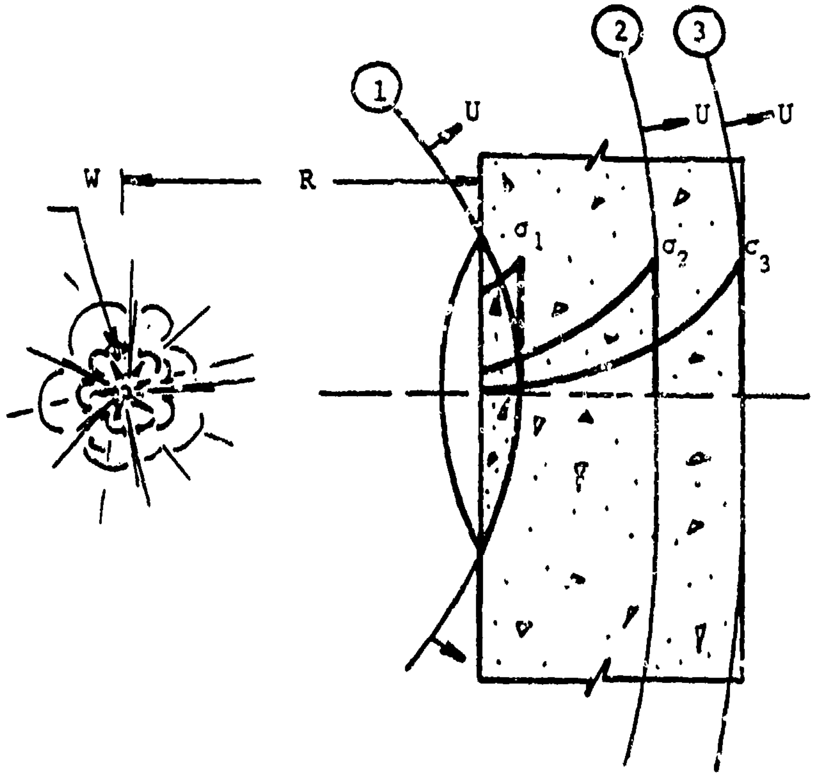

a) Transmission of Incident Shock

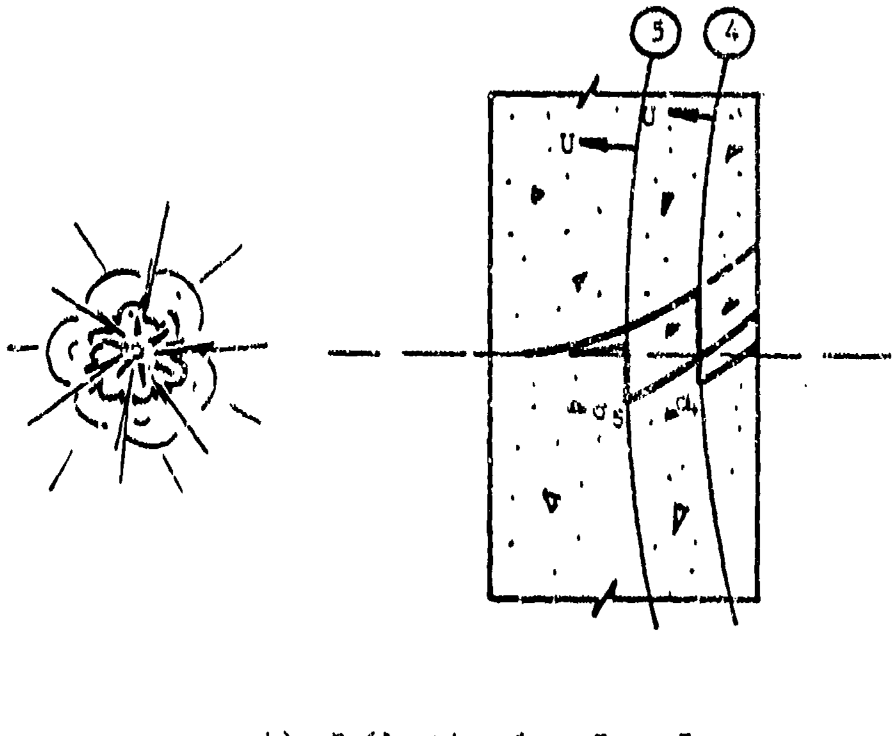

b) Reflection from Rear Face

FIGURE A-1. SCHEMATIC OF SHOCK TRANSMISSION AND REFLECTION IN CONCRETE WALL displaced at high velocities (Reference 6). Failure of an element is characterized by the dispersal of concrete fragments formed by the cracking and displacement of the concrete between the donor and receiver layers of the reinforcement. As an element deflects and the concrete begins to crush, the compression stresses normally resisted by the concrete are transferred to the reinforcement. With increased deflections, these compression forces tend to buckle the reinforcement outward thereby initiating the rapid disintegration of the element.

The velocity of individual fragments varies and depends on: (1) the magnitude of the excess impulse defined as the blast impulse minus the flexural impulse capacity of the element (area under the resistance-time curve), (2) the mass of the fragment, (3) the location of the fragment prior to collapse, (4) the interaction between the fragments during their flight and (5) the strength and time history of the compressive stress wave transmitted through the dividing wall as the blast wave is reflected. Although the velocities of individual fragments differ, the average translational velocity V_f of the debris after complete failure can be approximated from the excess impulse i_e, and the momentum of the wall after collapse. Equation (A-2), taken from Reference 6, provides a means of estimating the fragment velocities from the blast impulse and a knowledge of the dividing wall geometry.

$$i_b^{\,2} = C_u \left(\frac{p_H d_c^{\,3} f_{ds}}{H}\right) + C_f d_c^{\,2} v_f^{\,2} \qquad \text{(A-2)}$$

where i_b = applied unit blast impulse
p_H = reinforcement ratio in the horizontal direction
d_c = distance between the centroids of the compression and tension reinforcement
f_{ds} = dynamic design stress for the reinforcement
H = span height
v_f = maximum velocity of the post-failure fragments
C_u = impulse coefficient
C_f = post-failure fragment coefficient

A.3 Literature Search

A number of documents were reviewed for information pertinent to this program and a list of these documents is presented here as Table A-1. In addition to providing data on tests of reinforced concrete, these reports provided information on areas such as: the use of deformed reinforcement wire to simulate full-size reinforcement bars; predictive techniques for calculating the fragmentation characteristics of reinforced concrete walls; predictive techniques for calculating spall fragment thickness and velocity for blast-loaded concrete panels without reinforcement; and actual designs of reinforced concrete and masonry dividing walls.

Table A-1. List of Reports

Rindner, R. M. and Schwartz, A. H., "Establishment of Safety Design Criteria for Use in Engineering of Explosives Facilities and Operations, Report No. 5," Technical Report No. 3267, Ammunition Engineering Directorate, Picatinny Arsenal, Dover, New Jersey, June 1965.

Rindner, R. M., Wachtell, S. and Saffian, L. W., "Establishment of Safety Design Criteria for Use in Engineering of Explosive Facilities and Operations," Technical Report No. 3712, Ammunition Engineering Directorate, Picatinny Arsenal, Dover, New Jersey, September 1968.

Willoughby, A. B., Wilton, C., Gabrielsen, B. L. and Zaccor, J. V., "A Study of Loading, Structural Response, and Debris Characteristics of Wall Panels," URS Research Company Report No. URS-680-5, Contract No. 11618, (6300A-250), July 1969.

Gabrielsen, B. and Wilton, C., "Shock Tunnel Tests of Arched Wall Panels," URS Research Company, Report No. URS-7030-19, Contract No. DACH20-71-C-0223, December 1974.

Kot, C. A. and Turula, P., "Air Blast Effects on Concrete Walls," Argonne National Laboratory, Report No. ANL-CT-76-50, July 1976.

Kot, C. A., Valentin, R. A., McLennan, D. A. and Turula, P., "Effects of Air Blast on Power Plant Structures and Components," Argonne National Laboratory, Report No. ANL-CT-78-41, October 1978.

Kot, C. A., "Spalling of Concrete Walls Under Blast Loads," Components Technology Division, Argonne National Laboratory, Argonne, Illinois.

Kaplan, K., "Dangers of Secondary Missiles," Minutes of the Seventeenth Explosives Safety Seminar, Volume II, September 1976.

Robins, P. J. and Calderwood, R. W., "Explosive Testing of Fiber-Reinforced Concrete," British Concrete Journal, Volume 12, No. 1, January 1978.

Cohen, E. and Dobbs, N., "Models for Determining the Response of Reinforced Concrete Structures to Blast Loads," Annals New York Academy of Sciences, Volume 152, Art. 1, October 28, 1968.

Cohen, E. and Dobbs, N., "Design Procedures and Details for Reinforced Concrete Structures Utilized in Explosive Storage and Manufacturing Facilities," Annals New York Academy of Sciences, Volume 152, Art. 1, October 28, 1968.

Harris, H. G., Sabnis, G. M. and White, R. N., "Reinforcement for Small Scale Direct Models of Concrete Structures," Models for Concrete Structures, Paper SP 24-6.

Table A-1 (Continued)

Zia, P., White, R. N. and Vanhorn, D. A., "Principles of Model Analysis," Models for Concrete Structures, Paper SP 24-2.

Chowdhury, A. H. and White, R. N., "Materials and Modeling Techniques for Reinforced Concrete Frames," ACI Journal, Title No. 74-50, November 1, 1977.

U. S. Energy Research and Development Administration, Albuquerque Operations Office, "Report of Investigation of the Explosion with Fatal Injuries in Building 11-14A on March 30, 1977 at the Pantex Plant-Amarillo, Texas," June 28, 1977.

White, R. N. and Sabnis, G. M., "Size Effects on Gypsum Mortars," Authorized Reprint from the Copyrighted Journal of Materials, Volume 3, No. 1, Published by the American Society for Testing and Materials, 1968.

Sabnis, G. M. and White, R. N., "A Gypsum Mortar for Small-Scale Models," ACI Journal, November 1977.

Baker, C. F. and Mullins, R. K., "Design of a Building Wall Subject to Blast Loading," UCID-16275, Lawrence Livermore Laboratory, Livermore, California, June 1973.

Saucier, K. L., "Dynamic Properties of Mass Concrete," U.S. Army Engineer Waterways Experiment Station, Vicksburg, Mississippi, AD-A043 004, June 1977.

"Study to Determine the Optimum Section of Reinforced Concrete Beams Subjected to Blast Loads," U.S. Naval Civil Engineering Laboratory, Port Hueneme, California, AD 636 284, February 1959.

Criswell, M. E., "Strength and Behavior of Reinforced Concrete Slab-Column Connections Subjected to Static and Dynamic Loading," U.S. Army Engineer Waterways Station, Vicksburg, Mississippi, December 1979.

"A Study of Loading, Structural Response, and Debris Characteristics of Wall Panels," Final Report, URS Research Company, July 1969.

"Analysis of Non-Reinforced Masonry Building Response to Abnormal Loading and Resistance to Progressive Collapse," National Bureau of Standards, COM-75-10087, November 1974.

The information found in the literature was used as a basis for the model analysis developed by SwRI for reinforced concrete walls, the test plan developed to validate the analytical results, and the performance of the validation tests and the associated data reduction.

A.4 Model Analysis

The model analysis for fragmentation of reinforced concrete elements overloaded by blast impulse is presented in this section. The model analysis begins with a description of the pertinent geometry, constitutive and mechanical properties for the problem at hand. The next step is to derive the nondimensional pi terms from the previously developed list of parameters. The similitude relationships are summarized and a discussion of the requirements for replica modeling is presented. The implications of the model analysis and potential problems are described.

Table A-2 presents the list of parameters for the problem of fragmentation of reinforced concrete dividing walls overloaded by blast impulse. For convenience, the parameters are categorized by the concrete, rebar and explosive source characteristics and responses. The parameters describing the concrete, rebar, and the explosive source are self-explanatory; however, the response parameters require further clarification. The damage caused to the panel consists of (a) fragmentation and (b) distortion of the remaining panel. Distortion of the panel remnant can be characterized by deflection, rotation and strain of the concrete and steel components. The fragmentation response may be characterized by the fragment velocity, mass, dimension range, trajectory angle and the number of fragments. Obviously, the fragments emerging from the dividing wall are not identical, so the parameters v_f, m_f, d_f, β_f represent average fragment characteristics, and statistical distribution functions, ψ, will be used to represent the variability in the fragment characteristics.

The second step in performing a model analysis is to develop the similitude relationships. These relationships are nondimensional ratios of physical parameters, such as those listed in Table A-3, which must be held invariant between the model and prototype systems if the model scale test results are to be representative of the full-scale responses. The procedure for obtaining the nondimensional ratios, and a formal discussion of their application is given in Reference 7. Leondi, in Reference 8, provides a step-by-step description of the procedure for obtaining the nondimensional ratios for the problem of dividing wall fragmentation. Since the mechanism for deriving the nondimensional ratio (pi terms) is so adequately explained in these references, only the resulting terms are presented in this report. Table A-3 lists the pi terms for the dividing and fragmentation problem. In this table, the pi terms are grouped according to the type of similarity represented.

The first four pi terms and terms π_{16} through π_{22} are statements of geometric similarity . Pi term 5 relates the density of the rebar to that of the concrete. Thus, all densities must be scaled by the same factor γ, between the model and prototype systems. Pi terms 7, 8, 9,

Table A-2. List of Parameters

PARAMETER	SYMBOL	DIMENSION
Concrete		
characteristic dimension (span, thickness)	L_c	L
aggregate size	L_A	L
density	ρ_c	FT^2/L^4
compressive strength	C_c	F/L^2
tensile strength	T_c	F/L^2
elastic modulus	E_c	F/L^2
Poisson's ratio	ν_c	-
Rebar		
characteristic dimension (diameter, spacing)	L_r	L
reinforcement ratio	r_r	-
density	ρ_s	FT^2/L^4
ultimate strength	V_s	F/L^2
tensile strength	T_s	F/L^2
elastic moduli	E_s	F/L^2
Explosive		
energy in source	W	FL
standoff distance	R	L
blast pressure	P	F/L^2
blast impulse	I	FT/L^2
loading time	T	T
Responses		
deflection of concrete	D_c	L
rotation of concrete	θ_c	-
deformation of rebar	D_s	L
rotation of rebar	θ_s	-
strain in concrete	ϵ_c	-
strain in rebar	ϵ_s	-
trajectory angle	θ_f	-
fragment velocity	V_f	L/T
fragment mass	M_f	FT^2/L
distribution functions	ψ	-
fragment characteristic size	d_f	L
fragment range	R_L	L
number of fragments	N_f	-

Table A-3. List of Pi Terms

$$\left.\begin{aligned}
\pi_1 &= L_c/R \\
\pi_2 &= L_A/R \\
\pi_3 &= L_r/R \\
\pi_4 &= t_r
\end{aligned}\right\}\ \text{geometric similarity}$$

$$\left.\begin{aligned}
\pi_5 &= \rho_s/\rho_c \\
\pi_6 &= R^3C_c/W \\
\pi_7 &= T_c/C_c \\
\pi_8 &= T_s/C_c \\
\pi_9 &= U_s/C_c \\
\pi_{10} &= E_c/C_c \\
\pi_{11} &= E_s/E_c \\
\pi_{12} &= \nu_c
\end{aligned}\right\}\ \text{constitutive similarity}$$

$$\left.\begin{aligned}
\pi_{13} &= PR^3/W \\
\pi_{14} &= I^2R/\rho_c W \\
\pi_{15} &= E_c T^2/\rho_c R^2
\end{aligned}\right\}\ \text{explosive blast output}$$

$$\left.\begin{aligned}
\pi_{16} &= D_c/R \\
\pi_{17} &= D_s/R \\
\pi_{18} &= d_f/R \\
\pi_{19} &= \theta_c \\
\pi_{20} &= \theta_s \\
\pi_{21} &= \beta^2 \\
\pi_{22} &= R_L/L_r \\
\pi_{23} &= N_f
\end{aligned}\right\}\ \text{geometric similarity of the responses}$$

$$\left.\begin{aligned}
\pi_{24} &= \epsilon_c \\
\pi_{25} &= \epsilon_s \\
\pi_{26} &= m_f/d_f^3\rho_c
\end{aligned}\right\}\ \text{constitutive similarity of the responses}$$

$$\left.\begin{aligned}
\pi_{27} &= \psi \\
\pi_{28} &= V_f^2 m_f/W
\end{aligned}\right\}\ \text{kinematic similarity}$$

10 and 11 require that the strength and moduli of the concrete and steel be scaled by the same factor, ψ. Ideally, this implies that the stress-strain curve of the concrete and steel should scale between the model and prototype. Additionally, π_{24}, π_{25} and π_{12} require that the strain in the concrete and steel, and Poisson's ratio of the concrete all be invariant between model and prototype systems. The only practical way to maintain the invariance of the density, strength, strain and Poisson's ratio between the two systems is to construct both the model and prototype out of the same materials. A model of this type is called a replica model. Obviously, to maintain geometric similarity as well, not only is it necessary to shrink down the rebar size and panel dimensions, it is also necessary to use scaled concrete aggregates. Scaled aggregates in modeling of reinforced concrete has been successfully employed by a variety of researchers to predict full-scale penetration by missiles as well as wall fragmentation accurately.

The requirements for similarity of the explosive charge are given by pi terms 6, 13, 14, 15 and 28. Pi term 6 can be used to fix the scale factor of the energy in the explosive source. Since the scale factor for the geometric length is λ and for stress is ψ, the scale factor for energy must be $\lambda^3\psi$. For a replica model, ψ is 1.0 and the scale factor for energy is λ^3. Similarly, the scale factors for blast pressure, impulse and loading time can be established from terms π_{13}, π_{14}, and π_{15} as 1.0, $\gamma^{1/2}\lambda$, and $\lambda\ (\gamma/\psi)^{1/2}$ (1.0, λ and λ for replica modeling).

The scale factor for mass and velocity can be derived from π_{26} and π_{28}, respectively. The scale factors for these quantities are $\lambda^3\gamma$ and $\gamma^{-1/2}$ (λ^3 and 1.0 for replica modeling). The scale factors for all physical quantities are summarized in Table A-4. Although the intention is to build replica models in this program, the scaling law for a dissimilar model is given in the table. Note that an entry of 1.0 in the table implies that this parameter, e.g., pressure, is the same in the model and the prototype. The model analysis can be used to suggest a possible representation of the physical process of wall fragmentation. This is done by grouping the response parameters together on the left side of an equality and the remaining parameters on the right side:

$$\text{(RESPONSES)} = f\left(\frac{\rho_s}{\rho_c},\ \frac{R^3 C_c}{W},\ \ldots\right) \qquad \text{(A-3)}$$

Responses measured during this program consisted of the fragment mass, velocity, dimensional size and range, and the number of fragments generated. Because of the large quantity of data obtained in the tests, attempts to correlate the data with the test conditions should consist of two parts:

- correlation of maximum responses (maximum velocity, maximum range, etc.)

Table A-4. Model Law for Dividing Wall Fragmentation

Parameter	Replica Scaling Law	Dissimilar Material Scaling Law
Lengths	λ	λ
Angles	1.0	1.0
Densities	1.0	γ
Strengths, moduli	1.0	ψ
Poisson's ratio	1.0	1.0
Strains	1.0	1.0
Velocities	1.0	$\gamma^{-1/2}$
Mass	λ^3	$\lambda^3\gamma$
Reinforcement ratio	1.0	1.0
Explosive energy	λ^3	λ^3
Pressure	1.0	1.0
Impulse	λ	$\gamma^{1/2}\lambda$
Time	λ	$\lambda(\gamma/\psi)^{1/2}$
Number of fragments	1.0	1.0

- statistical distribution of the fragment characteristics (mass, range).

A functional format relating the above responses and parameters describing the concrete wall and the explosive charge is given in equation (A-4):

$$\begin{bmatrix} M_L \\ V_L \\ R_L \\ N_f \\ \psi(M) \\ \psi(R) \end{bmatrix} = f\left(I_{TOT}, W, R_s, C_c, n_{ss}\right) \qquad \text{(A-4)}$$

where M_L = largest recovered fragment mass
V_L = largest fragment velocity
R_L = largest fragment range
N_f = total number of fragments recovered
$\psi(M)$ = fragment mass distribution
$\psi(R)$ = fragment range distribution
I_{TOT} = total impulse delivered to the wall
W = charge weight
R_s = rebar spacing
C_c = concrete thickness covering rebar
n_{ss} = number of supported edges of the panel

REFERENCES

1. Petino, G., Jr., "Sensitivity of Cased Charges of Molten and Solid Composition B to Impact by Primary Steel Fragments," Technical Report No. 4975, Picatinny Arsenal, June 1976.

2. Kot, C. A., "Spalling of Concrete Walls Under Blast Load," Transactions of the 4th International Conference on Structural Mechanics in Reactor Technology, Volume J(b), Paper 10/5, San Francisco, California, August 1977.

3. Kot, C. A., Valentin, R. A., McLennan, D. A. and Turula, P., "Effects of Air Blast on Power Plant Structures and Components," Argonne National Laboratory, Report ANC-CT-78-41, October 1978.

4. Rinehart, J. S., Stress Transitions in Solids, Hyperdynamics, Santa Fe, New Mexico, 1975.

5. Davids, N. (ed.), International Symposium on Stress Wave Propagation in Materials, Interscience Publishers, Inc. New York, New York, 1960.

6. Department of the Army, "Structures to Resist the Effects of Accidental Explosions," TM 5-1300, U. S. Government Printing Office, Washington, D.C., June 1969.

7. Baker, W. E., Westine, P. S. and Dodge, F. T., Similarity Methods in Engineering Dynamics, Hayden Book Company, Inc., New Rochelle, New Jersey, 1973.

8. Baker, W. E., Explosions in Air, The University of Texas Press, Austin, Texas, 1973.

APPENDIX B

TEST SUMMARIES

TEST SUMMARIES FOR CANTILEVERED WALLS
NOMINALLY 50 mm (2 in) THICK

Test No.	Rebar Spacing (mm)	Thickness (mm)	W (kg)	R (m)	Summary
1	50.8	52.39	0.227	0.152	Charge was centered vertically behind the wall. Wall was blown down by the blast but it did not start to fragment until the wall had started to collapse. Fragments were directed into the sand within a few feet of ground zero and skipped downrange.
2	50.8	53.97	0.227	0.076	Charge was centered vertically behind the wall. Center of the wall was blown out by the blast. Fragments traveled parallel to the ground surface before coming to rest.
4	50.8	53.97	0.454	0.183	Charge was positioned 1/3 of the way up the bottom of the wall. Wall sheared off completely at the base. Approximately half of the wall was still attached but severely cracked and traveled about 3.0 meters downrange.
9	50.8	50.8	0.454	0.183	Wall sheared off completely at the base and traveled about 4.9 meters downrange. Wall broke up into three major pieces but all three pieces were still attached to one another by the rebar. The top half of the wall (green and blue quarters) were almost intact. A large number of charge-side fragments were found in the pit.

Test No.	Rebar Spacing (mm)	Thickness (mm)	W (kg)	R (m)	Summary
3	25.4	57.15	0.227	0.127	Wall was broken at the base and at the center but did not shear off. Majority of the fragments originated from the center of the wall and were ejected normal to the wall surface.
5	25.4	52.39	0.454	0.183	Wall sheared off at the base; however, the vertical reinforcement on the charge side remained attached to both the wall and the base. Majority of the fragments came from the lower portion of the wall near the base.
8	25.4	52.39	0.454	0.183	Wall broke at the base but did not shear off. Wall had a horizontal break approximately 28 cm from the top of the wall. Fragments originated from the center of the wall; however, a number of charge-side fragments were found in the pit.
14	25.4	52.39	0.227	0.147	Wall cracked at the base and slumped over about 30°. Only three fragments were produced and these originated from the center of the wall.
15	25.4	52.39	0.454	0.147	Wall cracked at the base and completely collapsed. Wall was attached to the base by the vertical rebar. Majority of the fragments originated from the center of the wall.

Test No.	Rebar Spacing (mm)	Thickness (mm)	W (kg)	R (m)	Summary
13	50.8	53.97	1.361	0.320	Wall sheared off completely at the base. Wall was uniformly cut about 7.62 cm below the center of the wall. Upper portion flew about 14 m downrange. Upper quadrants (blue and green) were attached to one another and did not fragment even though they did crack. Wall section skipped eight times before coming to rest.

TEST SUMMARIES FOR CANTILEVERED WALLS
NOMINALLY 80 mm (3 in) THICK

Test No.	Rebar Spacing (mm)	Thickness (mm)	W (kg)	R (m)	Summary
6	25.4	80.96	0.454	0.183	Wall failed at the base but did not shear off. Center of the wall was well broken up and the majority of the fragments came from the center of the wall.
7	25.4	80.96	0.454	0.147	Wall failed at the base but did not shear off. Majority of the fragments came from the center of the wall. This test was a repeat of Test No. 6 but with a higher impulse. More fragments were produced and the fragments had a larger average mass and a greater range than those observed in Test No. 6.
16	25.4	80.96	0.454	0.183	Wall failed at the base and fell forward, but did not shear off. Very few fragments were produced and most came from the charge side. No fragments from the backside of the wall were produced.
17	25.4	80.96	0.454	0.128	Wall failed at the base but did not shear off. A large number of fragments were produced, the majority coming from the lower portion of the wall.

Test No.	Rebar Spacing (mm)	Thickness (mm)	W (kg)	R (m)	Summary
10	50.80	77.79	0.454	0.183	Panel sheared off at the base. Panel was broken into two pieces with the larger piece landing about 0.7 m into the pit and the small piece landing just inside the edge of the pit. Most of the fragments came from the lower center of the panel (red and white quadrants). Upper part of panel was intact (green and blue quadrants).
11	50.80	76.20	0.454	0.147	Panel sheared off at the base and landed about 1 m into the pit. The top portion of the panel (green and blue quadrants) were still attached; however, there was a crack between the two quadrants. Portions of the red and white quadrants were still attached to the base by the rebar. Most of the fragments came from the lower center section of the panel (red and white quadrants). Three fragments landed outside of the recovery pit on the left hand side.
12	50.80	80.96	0.454	0.127	Wall sheared off at the base and the upper two thirds landed 2.1 m downrange. The upper quadrant (blue and green) was basically intact but was cracked at the center. Large number of fragments were produced and several large fragments traveled approximately 18 m.

Test No.	Rebar Spacing (mm)	Thickness (mm)	W (kg)	R (m)	Summary
18	50.80	80.96	1.361	0.219	Wall completely sheared off and was broken up extensively. Large fragment from white quadrant flew 15 m. Large blue and red fragment flew 17 m. Several large fragments (red quadrant) flew about 31 m (next to back fence). Backstop at fence had numerous fragment hits.

TEST SUMMARIES FOR THREE SIDE SUPPORTED WALLS
NOMINALLY 50 mm (2 in) THICK

PRECEDING PAGE BLANK-NOT FILMED

Test No.	Rebar Spacing (mm)	Thickness (mm)	W (kg)	R (m)	Summary
24	25.4	50.80	0.454	0.183	Lower center of the wall was blown out, leaving the rebar on each face. The upper 0.3 m of the panel were relatively intact, except for a vertical crack at the wall midspan and cracks at the edges of the side retainers. Relatively few fragments were produced and the majority of those produced were relatively small and only about as thick as the rebar cover.
26	25.4	55.56	0.454	0.146	Wall was well broken up but did not shear off. Wall was severely cracked at the sides and translated forward but the rebar held it to the frame. Majority of fragments are from the lower center (red and white quadrants).
30	25.4	52.39	0.454	0.219	Wall did not shear off but was severely broken and had a large vertical crack at the center. Sides at the restraints were also cracked severely. Center of wall translated towards the pit and the wall ended up being "V" shaped. Majority of fragments are red and white with a few green.

Test No.	Rebar Spacing (mm)	Thickness (mm)	W (kg)	R (m)	Summary
35	25.4	50.80	1.361	0.387	Wall was completely sheared off at the base and sides and flew 26 m downrange. Wall was broken vertically and horizontally but was relatively intact. Fragments flew outside of sandpit and some hit the plywood backstop at fence.

Test No.	Rebar Spacing (mm)	Thickness (mm)	W (kg)	R (m)	Summary
23	50.8	50.80	0.454	0.183	Wall sheared off completely at the base and at the side restraints. Large section of upper wall (blue and red quadrant) landed about 1 m in the pit. A large piece, mostly green and some white, landed about 2 m into the pit. Concrete was stripped off of the rebar at some places.
25	50.8	50.80	0.454	0.146	Entire exposed portion of the wall was blown down out of the frame. One large piece (mostly blue with some red) traveled 7 m. A second large piece (mostly green) went 8 m. The blue fragment hit at 4.5 m and rolled the rest of the way. The green fragment hit and also rolled. There was a very large angular dispersion of fragments. Many fragments were found outside of the sand pit (especially to the right) and several fragments hit the backstop at the end of the sand runway.
31	50.8	50.80	0.454	0.219	Wall did not shear off but was again cracked in the center ("V" shaped). Sides at the restraints were cracked. The majority of the fragments originated from the lower center of the wall.

Test No.	Rebar Spacing (mm)	Thickness (mm)	W (kg)	R (m)	Summary
32	50.8	53.97	0.454	0.219	Wall was completely broken in half at the center but remained attached at the sides by the rebar. Wall is in a "V" shape with about a 2.5 cm gap at the top of the Vee. Few fragments were produced, mostly red and white. Large number of fragments on the charge side but all fell at the base.

TEST SUMMARIES FOR THREE SIDE SUPPORTED WALLS
NOMINALLY 80 mm (3 in) THICK

Test No.	Rebar Spacing (mm)	Thickness (mm)	W (kg)	R (m)	Summary
20	25.4	80.96	0.454	0.146	Wall is cracked at the base and at both side restraints but did not shear off. Wall has a vertical crack at the midspan. Majority of the fragments are from the wall's lower center (white and red quadrants). Some fragments were produced from the upper quadrants (blue and green). The white quadrant fragments are mostly the rebar covering.
21	25.4	77.79	0.454	0.128	Wall is cracked at the base and at the side restraints but was held in place by the rebar. Wall has a vertical crack at the midspan. Majority of the fragments were from the lower center; however, some fragments were produced from the upper quadrants.
33	25.4	77.79	0.454	0.219	Wall has a vertical crack at the center and is cracked at the sides but is relatively intact. No large fragments of any color. Wall has a 4 inch circular area broken up on the charge side (concrete cover over the rebar is broken out).
34	25.4	79.38	0.454	0.183	Wall has a vertical crack at the midspan and is cracked at the side restraints. One edge of the break is displaced about 2.5 cm. Very few fragments were produced. Charge side is well broken up but fragments fell at the base.

PRECEDING PAGE BLANK-NOT FILMED

Test No.	Rebar Spacing (mm)	Thickness (mm)	W (kg)	R (m)	Summary
36	25.4	77.79	1.361	0.320	Wall was completely sheared off at the base and sides. Two large pieces flew downrange. One piece, the green and white half, landed 17 m downrange and approximately 1 m on the left side outside of the recovery pit. Blue quadrant, with about 5 cm of the red quadrant, flew approximately 4.3 m downrange.

Test No.	Rebar Spacing (mm)	Thickness (mm)	W (kg)	R (m)	Summary
19	50.8	80.96	0.454	0.183	Wall sheared off on both side restraints and at the base but was held by the rebar. Wall had vertical crack at the midspan and was well broken up. Most of the fragments were from the lower center. Charge side is also well fractured but most of these fragments remained on the charge side at the base of the wall.
22	50.8	80.96	0.454	0.146	Wall is completely fractured and the upper part sheared off at both side restraints and translated approximately 20 cm. Lower part of wall is still attached at the base by the rebar. Wall has a large vertical crack at the midspan and most of the fragments are from the lower center.
27	50.8	77.79	0.454	0.219	Wall did not shear off. Wall has a vertical crack at the center and cracks at each side (support sides). Fragments are from the lower center and are mostly red with some white and a few blue.
28	50.8	76.20	0.454	0.198	Wall did not shear off but has a vertical crack at the center. Wall is cracked at the restraints but not broken up badly. Very few fragments . The fragments are from the lower center (mostly red and white). A small pile of fragments found on the ground at the base (backface side).

Test No.	Rebar Spacing (mm)	Thickness (mm)	W (kg)	R (m)	Summary
29	50.8	77.79	0.454	0.160	Wall did not shear off but has a vertical crack at the center and the sides are cracked at the restraints. Hole blown out of the lower center of the wall. Majority of fragments are red on white.

APPENDIX C

GENERAL SUMMARY OF TEST RESULTS

GENERAL SUMMARY FOR TEST 1

PANEL CHARACTERISTICS

PANEL SPAN	0.46 M	PANEL THICKNESS	52.4 MM
REBAR DIAMETER	2.11 MM	REBAR SPACING	50.8 MM
REBAR COVER	7.94 MM	NO. EDGES SUPPORTED	1
CONCRETE COMPR. STR.	7.17 MPA		

CHARGE CHARACTERISTICS

CHARGE TYPE	C-4	INITIATOR	M-6
CHARGE WEIGHT	226.80 GM	STANDOFF DISTANCE	0.152 M
REFL. IMPULSE	2.46 KPA-S	CHARGE HEIGHT	0.229 M

FRAGMENT CHARACTERISTICS

TYPE		NO. FRAGS RECOVERED	MASS (GM) LG	MASS (GM) AVG	RANGE (M) LG	RANGE (M) AVG
SOURCE						
	RED	7	65.23	17.45	2.28	1.33
	WHITE	10	64.69	27.63	14.42	5.65
	GREEN	3	76.90	27.14	4.68	2.38
	INTERIOR	10	6.57	2.08	4.70	2.12
	ACCEPTOR	8	32.06	6.29	2.19	0.85
SHAPE						
	PANCAKE	26	76.90	16.00	14.42	2.18
	CHUNKY	12	62.76	11.24	11.23	3.68
TOTAL		38	76.90	14.50	14.42	2.66

GENERAL SUMMARY FOR TEST 2

PANEL CHARACTERISTICS

PANEL SPAN	0.46 M	PANEL THICKNESS	54.0 MM
REBAR DIAMETER	2.11 MM	REBAR SPACING	50.8 MM
REBAR COVER	7.94 MM	NO. EDGES SUPPORTED	1
CONCRETE COMPR. STR.	8.58 MPA		

CHARGE CHARACTERISTICS

CHARGE TYPE	C-4	INITIATOR	M-6
CHARGE WEIGHT	226.80 GM	STANDOFF DISTANCE	0.076 M
REFL. IMPULSE	9.86 KPA-S	CHARGE HEIGHT	0.229 M

FRAGMENT CHARACTERISTICS

TYPE	NO. FRAGS RECOVERED	MASS (GM) LG	MASS (GM) AVG	RANGE (M) LG	RANGE (M) AVG
SOURCE					
RED	43	15.78	2.80	31.89	10.34
WHITE	27	8.10	2.59	31.89	8.85
BLUE	25	26&30	4.60	31.79	14.19
GREEN	29	226.30	18.92	25.76	7.83
INTERIOR	184	58.39	5.25	23.41	7.05
ACCEPTOR	30	25.09	6.15	2.75	1.30
SHAPE					
PANCAKE	295	58.39	4.70	31.89	7.21
CHUNKY	43	226.30	14.34	31.89	11.04
TOTAL	338	226.30	5.93	31.89	7.70

GENERAL SUMMARY FOR TEST 3

PANEL CHARACTERISTICS

PANEL SPAN	0.46 M	PANEL THICKNESS	57.1 MM
REBAR DIAMETER	2.11 MM	REBAR SPACING	25.4 MM
REBAR COVER	7.94 MM	NO. EDGES SUPPORTED	[illegible]
CONCRETE COMPR. STR.	8.58 MPA		

CHARGE CHARACTERISTICS

CHARGE TYPE	C-4	INITIATOR	M-6
CHARGE WEIGHT	226.80 GM	STANDOFF DISTANCE	0.127 M
REFL. IMPULSE	3.38 KPA-S	CHARGE HEIGHT	0.229 M

FRAGMENT CHARACTERISTICS

TYPE		NO. FRAGS RECOVERED	MASS (GM) LG	MASS (GM) AVG	RANGE (M) LG	RANGE (M) AVG
SOURCE	RED	26	29.75	7.92	20.68	7.44
	WHITE	23	24.06	5.64	24.92	7.28
	BLUE	14	19.45	6.42	23.52	11.12
	GREEN	10	15.93	6.87	21.23	11.81
	INTERIOR	2	7.08	4.70	10.47	5.82
SHAPE	PANCAKE	41	29.75	8.44	23.52	5.98
	CHUNKY	34	24.39	4.64	24.92	11.80
TOTAL		75	29.75	6.72	24.92	8.62

GENERAL SUMMARY FOR TEST 4

PANEL CHARACTERISTICS

PANEL SPAN	0.46 M	PANEL THICKNESS	54.0 MM
REBAR DIAMETER	2.11 MM	REBAR SPACING	50.8 MM
REBAR COVER	9.52 MM	NO. EDGES SUPPORTED	1
CONCRETE COMPR. STR.	9.18 MPA		

CHARGE CHARACTERISTICS

CHARGE TYPE	C-4	INITIATOR	M-6
CHARGE WEIGHT	453.60 GM	STANDOFF DISTANCE	0.183 M
REFL. IMPULSE	3.38 KPA-S	CHARGE HEIGHT	0.152 M

FRAGMENT CHARACTERISTICS

TYPE	NO. FRAGS RECOVERED	MASS (GM) LG	MASS (GM) AVG	RANGE (M) LG	RANGE (M) AVG
SOURCE					
RED	51	345.40	59.52	30.71	16.76
WHITE	57	215.70	34.06	31.62	17.99
BLUE	18	98.44	23.04	23.62	10.02
GREEN	10	100.10	30.95	20.92	11.62
INTERIOR	79	118.69	19.37	23.44	13.52
ACCEPTOR	10	183.32	35.37	15.14	8.20
SHAPE					
PANCAKE	132	345.40	27.44	28.90	13.43
CHUNKY	93	333.50	42.62	31.62	16.71
TOTAL	225	345.40	33.71	31.62	14.79

GENERAL SUMMARY FOR TEST 5

PANEL CHARACTERISTICS

PANEL SPAN	0.46 M	PANEL THICKNESS	52.4 MM
REBAR DIAMETER	2.11 MM	REBAR SPACING	25.4 MM
REBAR COVER	7.94 MM	NO. EDGES SUPPORTED	1
CONCRETE COMPR. STR.	11.55 MPA		

CHARGE CHARACTERISTICS

CHARGE TYPE	C-4	INITIATOR	M-6
CHARGE WEIGHT	453.60 GM	STANDOFF DISTANCE	0.183 M
REFL. IMPULSE	3.45 KPA-S	CHARGE HEIGHT	0.152 M

FRAGMENT CHARACTERISTICS

TYPE		NO. FRAGS RECOVERED	MASS (GM) LG	MASS (GM) AVG	RANGE (M) LG	RANGE (M) AVG
SOURCE						
	RED	85	34.68	9.94	27.15	11.92
	WHITE	31	33.88	10.35	23.91	7.08
	BLUE	8	8.13	5.11	15.79	4.02
	GREEN	3	4.52	4.38	18.53	6.77
	INTERIOR	261	172.84	8.58	25.17	5.74
	ACCEPTOR	34	33.87	4.80	9.54	3.16
SHAPE						
	PANCAKE	283	165.61	8.95	24.80	5.63
	CHUNKY	140	172.84	8.97	27.15	9.28
TOTAL		423	172.84	8.95	27.15	6.84

GENERAL SUMMARY FOR TEST 6

PANEL CHARACTERISTICS

PANEL SPAN	0.46 M	PANEL THICKNESS	81.0 MM
REBAR DIAMETER	2.11 MM	REBAR SPACING	25.4 MM
REBAR COVER	11.11 MM	NO. EDGES SUPPORTED	1
CONCRETE COMPR. STR.	8.62 MPA		

CHARGE CHARACTERISTICS

CHARGE TYPE	C-4	INITIATOR	M-6
CHARGE WEIGHT	453.60 GM	STANDOFF DISTANCE	0.183 M
REFL. IMPULSE	3.45 KPA-S	CHARGE HEIGHT	0.152 M

FRAGMENT CHARACTERISTICS

TYPE	NO. FRAGS RECOVERED	MASS (GM) LG	MASS (GM) AVG	RANGE (M) LG	RANGE (M) AVG
SOURCE					
RED	11	32.43	11.37	1.37	0.95
WHITE	18	63.41	12.61	3.64	1.40
SHAPE					
PANCAKE	13	63.41	16.31	3.11	1.30
CHUNKY	16	20.55	8.76	3.64	1.18
TOTAL	29	63.41	12.14	3.64	1.23

GENERAL SUMMARY FOR TEST 7

PANEL CHARACTERISTICS

PANEL SPAN	0.46 M	PANEL THICKNESS	81.0 MM
REBAR DIAMETER	2.11 MM	REBAR SPACING	25.4 MM
REBAR COVER	9.52 MM	NO. EDGES SUPPORTED	1
CONCRETE COMPR. STR.	8.62 MPA		

CHARGE CHARACTERISTICS

CHARGE TYPE	C-4	INITIATGR	M-6
CHARGE WEIGHT	453.60 GM	STANDOFF DISTANCE	0.147 M
REFL. IMPULSE	5.17 KPA-S	CHARGE HEIGHT	0.152 M

FRAGMENT CHARACTERISTICS

TYPE	NO. FRAGS RECOVERED	MASS (GM) LG	MASS (GM) AVG	RANGE (M) LG	RANGE (M) AVG
SOURCE					
RED	43	21.26	6&10	9.42	2.94
WHITE	28	27.05	8.30	11.25	2.98
BLUE	1	1.14	1.14	4.31	4&31
INTERIOR	4	5.23	3.26	1.56	0.91
SHAPE					
PANCAKE	34	27.05	8.14	9.42	2.42
CHUNKY	42	17.78	5.53	11.25	3.23
TOTAL	76	27.05	6.70	11.25	2.87

GENERAL SUMMARY FOR TEST 8

PANEL CHARACTERISTICS

PANEL SPAN	0.46 M	PANEL THICKNESS	52.4 MM
REBAR DIAMETER	2.11 MM	REBAR SPACING	25.4 MM
REBAR COVER	7.94 MM	NO. EDGES SUPPORTED	1
CONCRETE COMPR. STR.	33.10 MPA		

CHARGE CHARACTERISTICS

CHARGE TYPE	C-4	INITIATOR	M-6
CHARGE WEIGHT	453.60 GM	STANDOFF DISTANCE	0.183 M
REFL. IMPULSE	3.45 KPA-S	CHARGE HEIGHT	0.152 M

FRAGMENT CHARACTERISTICS

TYPE	NO. FRAGS RECOVERED	MASS (GM) LG	MASS (GM) AVG	RANGE (M) LG	RANGE (M) AVG
SOURCE					
RED	10	7.49	2.35	5.80	2.47
WHITE	9	8.06	2.19	2.93	1.74
INTERIOR	21	6.54	0.97	5.19	2.64
ACCEPTOR	32	35.81	8.91	3.31	1.40
SHAPE					
PANCAKE	58	35.81	5.12	5.19	1.87
CHUNKY	14	28.15	3.71	5.80	2.31
TOTAL	72	35.81	4.84	5.80	1.95

GENERAL SUMMARY FOR TEST 9

PANEL CHARACTERISTICS

PANEL SPAN	0.46 M	PANEL THICKNESS	50.8 MM
REBAR DIAMETER	2.11 MM	REBAR SPACING	50.8 MM
REBAR COVER	6.35 MM	NO. EDGES SUPPORTED	1
CONCRETE COMPR. STR.	33.10 MPA		

CHARGE CHARACTERISTICS

CHARGE TYPE	C-4	INITIATOR	M-6
CHARGE WEIGHT	453.60 GM	STANDOFF DISTANCE	0.183 M
REFL. IMPULSE	3.45 KPA-S	CHARGE HEIGHT	0.152 M

FRAGMENT CHARACTERISTICS

TYPE	NO. FRAGS RECOVERED	MASS (GM) LG	MASS (GM) AVG	RANGE (M) LG	RANGE (M) AVG
SOURCE					
RED	23	19006.00	846.24	17.84	4.86
WHITE	31	102.50	19.69	20.88	10.31
GREEN	2	27.53	16.20	7.36	7.34
INTERIOR	77	119.08	13.33	24.96	7.14
ACCEPTOR	46	105.36	13.17	12.32	5.50
SHAPE					
PANCAKE	117	19006.00	177.89	14.22	5.68
CHUNKY	62	96.02	14.92	24.96	9.41
TOTAL	179	19006.00	121.44	24.96	6.97

GENERAL SUMMARY FOR TEST 10

PANEL CHARACTERISTICS

PANEL SPAN	0.46 M	PANEL THICKNESS	77.8 MM
REBAR DIAMETER	2.11 MM	REBAR SPACING	50.8 MM
REBAR COVER	6.35 MM	NO. EDGES SUPPORTED	1
CONCRETE COMPR. STR.	33.40 MPA		

CHARGE CHARACTERISTICS

CHARGE TYPE	C-4	INITIATOR	M-6
CHARGE WEIGHT	453.60 GM	STANDOFF DISTANCE	0.183 M
REFL. IMPULSE	3.45 KPA-S	CHARGE HEIGHT	0.152 M

FRAGMENT CHARACTERISTICS

TYPE	NO. FRAGS RECOVERED	MASS (GM) LG	MASS (GM) AVG	RANGE (M) LG	RANGE (M) AVG
SOURCE					
RED	4	95.66	27.64	3.71	3.45
GREEN	1	2.34	2.34	5.92	5.92
INTERIOR	22	250.20	23.43	3.48	1.53
ACCEPTOR	39	365.70	24.06	5.67	2.15
SHAPE					
PANCAKE	59	365.70	23.60	5.92	2.09
CHUNKY	8	95.66	24.73	3.71	1.96
TOTAL	67	365.70	23.73	5.92	2.07

GENERAL SUMMARY FOR TEST 11

PANEL CHARACTERISTICS

PANEL SPAN	0.46 M	PANEL THICKNESS	76.2 MM
REBAR DIAMETER	2.11 MM	REBAR SPACING	50.8 MM
REBAR COVER	9.52 MM	NO. EDGES SUPPORTED	1
CONCRETE COMPR. STR.	33.40 MPA		

CHARGE CHARACTERISTICS

CHARGE TYPE	C-4	INITIATOR	M-6
CHARGE WEIGHT	453.60 GM	STANDOFF DISTANCE	0.147 M
REFL. IMPULSE	5.17 KPA-S	CHARGE HEIGHT	0.152 M

FRAGMENT CHARACTERISTICS

TYPE	NO. FRAGS RECOVERED	MASS (GM) LG	MASS (GM) AVG	RANGE (M) LG	RANGE (M) AVG
SOURCE					
RED	12	50.99	18.33	16.51	6.60
WHITE	9	48.75	17.48	17.98	7.29
BLUE	2	1.23	1.16	6.70	5.91
GREEN	1	22317.00	22317.00	1.49	1.49
INTERIOR	89	181.68	15.96	11.97	3.23
ACCEPTOR	67	163.37	15.80	6.17	1.83
SHAPE					
PANCAKE	141	22317.00	172.92	11.06	2.45
CHUNKY	39	163.37	20.36	17.98	5.72
TOTAL	180	22317.00	139.86	17.98	3.16

GENERAL SUMMARY FOR TEST 12

PANEL CHARACTERISTICS

PANEL SPAN	0.46 M	PANEL THICKNESS	81.0 MM
REBAR DIAMETER	2.11 MM	REBAR SPACING	50.8 MM
REBAR COVER	9.52 MM	NO. EDGES SUPPORTED	1
CONCRETE COMPR. STR.	40.68 MPA		

CHARGE CHARACTERISTICS

CHARGE TYPE	C-4	INITIATOR	M-6
CHARGE WEIGHT	453.60 GM	STANDOFF DISTANCE	0.127 M
REFL. IMPULSE	6.89 KPA-S	CHARGE HEIGHT	0.152 M

FRAGMENT CHARACTERISTICS

TYPE	NO. FRAGS RECOVERED	MASS (GM) LG	MASS (GM) AVG	RANGE (M) LG	RANGE (M) AVG
SOURCE					
RED	14	150.85	57.92	16.60	11.76
WHITE	16	425.10	83.36	18.77	9.59
BLUE	6	121.66	47.54	16.23	7.97
GREEN	2	173.59	134.88	13.33	9.64
INTERIOR	86	439.10	34.41	16.43	6.59
ACCEPTOR	34	195.13	27.46	7.26	2.71
SHAPE					
PANCAKE	119	439.10	33.63	17.71	5.65
CHUNKY	39	425.10	66.40	18.77	9.52
TOTAL					
	158	439.10	41.72	18.77	6.61

GENERAL SUMMARY FOR TEST 13

PANEL CHARACTERISTICS

PANEL SPAN	0.46 M	PANEL THICKNESS	54&0 MM
REBAR DIAMETER	2.11 MM	REBAR SPACING	50.8 MM
REBAR COVER	6.35 MM	NO. EDGES SUPPORTED	1
CONCRETE COMPR. STR.	40.34 MPA		

CHARGE CHARACTERISTICS

CHARGE TYPE	C-4	INITIATO	M-6
CHARGE WEIGHT	1360.80 GM	STANDOFF DISTANCE	0.320 M
REFL. IMPULSE	3.45 KPA-S	CHARGE HEIGHT	0.152 M

FRAGMENT CHARACTERISTICS

TYPE	NO. FRAGS RECOVERED	MASS (GM) LG	MASS (GM) AVG	RANGE (M) LG	RANGE (M) AVG
SOURCE					
RED	6	1417.40	254.17	10.76	3.61
WHITE	12	219.00	32.30	19.51	5.72
INTERIOR	39	72.75	10.98	18.72	4.79
ACCEPTOR	59	87.10	14.79	12.26	6.75
SHAPE					
PANCAKE	94	16330.00	200.18	18.72	5.99
CHUNKY	23	219.00	31.60	19.51	4.90
TOTAL	117	16330.00	147.04	19.51	5.78

GENERAL SUMMARY FOR TEST 14

PANEL CHARACTERISTICS

PANEL SPAN	0.46 M	PANEL THICKNESS	52.4 MM
REBAR DIAMETER	2.11 MM	REBAR SPACING	25.4 MM
REBAR COVER	6&35 MM	NO. EDGES SUPPORTED	1
CONCRETE COMPR. STR.	40.62 MPA		

CHARGE CHARACTERISTICS

CHARGE TYPE	C-4	INITIATOR	M-6
CHARGE WEIGHT	226&80 GM	STANDOFF DISTANCE	0.147 M
REFL. IMPULSE	2.62 KPA-S	CHARGE HEIGHT	0.152 M

FRAGMENT CHARACTERISTICS

TYPE	NO. FRAGS RECOVERED	MASS (GM) LG	MASS (GM) AVG	RANGE (M) LG	RANGE (M) AVG
SOURCE					
WHITE	3	4&67	2.69	5.80	4.01
SHAPE					
CHUNKY	3	4&67	2.69	5.80	4.01
TOTAL	3	4&67	2.69	5.80	4.01

GENERAL SUMMARY FOR TEST 15

PANEL CHARACTERISTICS

PANEL SPAN	0.46 M	PANEL THICKNESS	52.4 MM
REBAR DIAMETER	2.11 MM	REBAR SPACING	25.4 MM
REBAR COVER	6&35 MM	NO. EDGES SUPPORTED	1
CONCRETE COMPR. STR.	40.91 MPA		

CHARGE CHARACTERISTICS

CHARGE TYPE	C-4	INITIATGR	M-6
CHARGE WEIGHT	453.60 GM	STANDOFF DISTANCE	0.147 M
REFL. IMPULSE	5.17 KPA-S	CHARGE HEIGHT	0.152 M

FRAGMENT CHARACTERISTICS

TYPE	NO. FRAGS RECOVERED	MASS (GM) LG	MASS (GM) AVG	RANGE (M) LG	RANGE (M) AVG
SOURCE					
RED	30	39.08	7.26	23.74	12.30
WHITE	18	165.44	20.43	22.28	11.21
BLUE	3	10.17	8.08	11.36	6&70
GREEN	2	12.23	11.03	11.93	9.77
INTERIOR	24	7.37	3.39	18.46	3.90
ACCEPTOR	55	62.02	8.95	4&04	1.27
SHAPE					
PANCAKE	90	165.44	8.91	19.69	3.27
CHUNKY	42	43.78	9.61	23.74	11.41
TOTAL	132	165.44	9.13	23.74	5.86

GENERAL SUMMARY FOR TEST 16

PANEL CHARACTERISTICS

PANEL SPAN	0.46 M	PANEL THICKNESS	81.0 MM
REBAR DIAMETER	2.11 MM	REBAR SPACING	25.4 MM
REBAR COVER	6&35 MM	NO. EDGES SUPPORTED	1
CONCRETE COMPR. STR.	41.47 MPA		

CHARGE CHARACTERISTICS

CHARGE TYPE	C-4	INITIATOR	M-6
CHARGE WEIGHT	453.60 GM	STANDOFF DISTANCE	0.183 M
REFL. IMPULSE	3.38 KPA-S	CHARGE HEIGHT	0.152 M

FRAGMENT CHARACTERISTICS

TYPE	NO. FRAGS RECOVERED	MASS (GM) LG	MASS (GM) AVG	RANGE (M) LG	RANGE (M) AVG
SOURCE					
WHITE	1	0.73	0.73	2.98	2.98
INTERIOR	2	6.58	4.34	0.65	0.62
ACCEPTOR	5	7.28	3.35	1.40	0.77
SHAPE					
PANCAKE	7	7.28	3.63	1.40	0.73
CHUNKY	1	0.73	0.73	2.98	2.98
TOTAL					
	8	7.28	3 27	2.98	1.01

GENERAL SUMMARY FOR TEST 17

PANEL CHARACTERISTICS

PANEL SPAN	0.46 M	PANEL THICKNESS	81.0 MM
REBAR DIAMETER	2.11 MM	REBAR SPACING	25.4 MM
REBAR COVER	6.35 MM	NO. EDGES SUPPORTED	1
CONCRETE COMPR. STR.	41.47 MPA		

CHARGE CHARACTERISTICS

CHARGE TYPE	C-4	INITIATOR	M-6
CHARGE WEIGHT	453.60 GM	STANDOFF DISTANCE	0.128 M
REFL. IMPULSE	6.89 KPA-S	CHARGE HEIGHT	0.152 M

FRAGMENT CHARACTERISTICS

TYPE	NO. FRAGS RECOVERED	MASS (GM) LG	MASS (GM) AVG	RANGE (M) LG	RANGE (M) AVG
SOURCE					
RED	25	44.56	8.66	12.12	4.06
WHITE	13	30.76	7.99	11.91	5.94
BLUE	1	0.91	0.91	2.31	2.31
INTERIOR	29	5.76	2.66	4.65	2.14
ACCEPTOR	32	57.22	10.46	7.35	1.64
SHAPE					
PANCAKE	65	57.22	7.24	12.12	2.10
CHUNKY	35	44.56	7.50	11.91	4.54
TOTAL	100	57.22	7.33	12.12	2.96

GENERAL SUMMARY FOR TEST 18

PANEL CHARACTERISTICS

PANEL SPAN	0.46 M	PANEL THICKNESS	81.0 MM
REBAR DIAMETEP	2.11 MM	REBAR SPACING	50.8 MM
REBAR COVER	7.94 MM	NO. EDGES SUPPORTED	1
CONCRETE COMPR. STR.	37.41 MPA		

CHARGE CHARACTERISTICS

CHARGE TYPE	C-4	INITIATOR	M-6
CHARGE WEIGHT	1360.80 GM	STANDOFF DISTANCE	0.220 M
REFL. IMPULSE	6&29 KPA-S	CHARGE HEIGHT	0.152 M

FRAGMENT CHARACTERISTICS

TYPE	NO. FRAGS RECOVERED	MASS (GM) LG	MASS (GM) AVG	RANGE (M) LG	RANGE (M) AVG
SOURCE					
RED	44	465.10	47.33	31.87	18.85
WHITE	42	2336&00	104&13	31.98	19.20
BLUE	10	11113.00	1140.41	31.72	23.88
GREEN	8	8754&50	1176&11	31.89	28.30
INTERIOR	112	148.10	19.52	37.01	16.85
ACCEPTOR	73	158.91	26&75	31.84	16.22
SHAPE					
PANCAKE	185	11113.00	136&26	37.01	16&18
CHUNKY	104	2336&00	59.63	32.13	20.95
TOTAL	289	11113.00	108.68	37.01	17.90

GENERAL SUMMARY FOR TEST 19

PANEL CHARACTERISTICS

PANEL SPAN	0.46 M	PANEL THICKNESS	81.0 MM
REBAR DIAMETER	2.11 MM	REBAR SPACING	50.8 MM
REBAR COVER	11.11 MM	NO. EDGES SUPPORTED	3
CONCRETE COMPR. STR.	16.33 MPA		

CHARGE CHARACTERISTICS

CHARGE TYPE	C-4	INITIATOR	M-6
CHARGE WEIGHT	453.60 GM	STANDOFF DISTANCE	0.183 M
REFL. IMPULSE	3.45 KPA-S	CHARGE HEIGHT	0.152 M

FRAGMENT CHARACTERISTICS

TYPE	NO. FRAGS RECOVERED	MASS (GM) LG	MASS (GM) AVG	RANGE (M) LG	RANGE (M) AVG
SOURCE					
RED	15	123.76	31.61	8.13	3.72
WHITE	18	92.15	24.20	11.34	5.08
BLUE	5	2.69	1.90	3.01	1.78
GREEN	2	161.70	83.98	1.68	1.12
INTERIOR	15	20.54	4.54	7.99	3.19
ACCEPTOR	3	31.44	20.70	5.34	2.34
SHAPE					
PANCAKE	28	161.70	18.10	9.20	3.20
CHUNKY	30	123.76	23.69	11.34	4.12
TOTAL	58	161.70	20.99	11.34	3.68

PANEL CHARACTERISTICS

PANEL SPAN	0.46 M	PANEL THICKNESS	81.0 MM
REBAR DIAMETER	2.11 MM	REBAR SPACING	25.4 MM
REBAR COVER	9.52 MM	NO. EDGES SUPPORTED	3
CONCRETE COMPR. STR.	43.41 MPA		

CHARGE CHARACTERISTICS

CHARGE TYPE	C-4	INITIATOR	M-6
CHARGE WEIGHT	453.60 GM	STANDOFF DISTANCE	0.147 M
REFL. IMPULSE	5.17 KPA-S	CHARGE HEIGHT	0.152 M

FRAGMENT CHARACTERISTICS

TYPE	NO. FRAGS RECOVERED	MASS (GM) LG	MASS (GM) AVG	RANGE (M) LG	RANGE (M) AVG
SOURCE					
RED	13	27.40	11.79	9.02	2.44
WHITE	52	89.41	18.77	8.94	3.56
BLUE	8	29.91	7.52	5.80	2.17
GREEN	6	6.06	4.11	3.02	1.56
INTERIOR	8	8.78	4.07	2.05	1.16
ACCEPTOR	1	8.21	8.21	3.42	3.42
SHAPE					
PANCAKE	48	39.41	16.54	8.94	2.68
CHUNKY	40	36&30	11.52	9.02	3.19
TOTAL	88	89.41	14.26	9.02	2.91

GENERAL SUMMARY FOR TEST 21

PANEL CHARACTERISTICS

PANEL SPAN	0.46 M	PANEL THICKNESS	77.8 MM
REBAR DIAMETER	2.11 MM	REBAR SPACING	25.4 MM
REBAR COVER	6.35 MM	NO. EDGES SUPPORTED	3
CONCRETE COMPR. STR.	36.76 MPA		

CHARGE CHARACTERISTICS

CHARGE TYPE	C-4	INITIATOR	M-6
CHARGE WEIGHT	453.60 GM	STANDOFF DISTANCE	0.128 M
REFL. IMPULSE	6.89 KPA-S	CHARGE HEIGHT	0.152 M

FRAGMENT CHARACTERISTICS

TYPE	NO. FRAGS RECOVERED	MASS (GM) LG	MASS (GM) AVG	RANGE (M) LG	RANGE (M) AVG
SOURCE					
RED	43	38.19	11.46	14.77	6.07
WHITE	28	31.03	9.53	12.27	5.20
BLUE	9	27.59	6.34	5.58	3.52
GREEN	1	7.83	7.83	4.48	4.48
INTERIOR	33	11.34	3.46	14.92	3.90
SHAPE					
PANCAKE	55	38.19	5.65	14.80	4.49
CHUNKY	59	34.78	10.64	14.92	5.50
TOTAL	114	38.19	8.23	14.92	5.01

GENERAL SUMMARY FOR TEST 22

PANEL CHARACTERISTICS

PANEL SPAN	0.46 M	PANEL THICKNESS	77.8 MM
REBAR DIAMETER	2.11 MM	REBAR SPACING	50.8 MM
REBAR COVER	7.94 MM	NO. EDGES SUPPORTED	3
CONCRETE COMPR. STR.	36.76 MPA		

CHARGE CHARACTERISTICS

CHARGE TYPE	C-4	INITIATOR	M-6
CHARGE WEIGHT	453.60 GM	STANDOFF DISTANCE	0.147 M
REFL. IMPULSE	5.17 KPA-S	CHARGE HEIGHT	0.152 M

FRAGMENT CHARACTERISTICS

TYPE	NO. FRAGS RECOVERED	MASS (GM) LG	MASS (GM) AVG	RANGE (M) LG	RANGE (M) AVG
SOURCE					
RED	29	172.79	31.92	13.89	5.13
WHITE	23	170.93	36.05	14.81	7.25
BLUE	25	65.90	15.25	12.82	5.63
GREEN	23	204.50	34.84	8.30	3.92
INTERIOR	102	107.70	8.98	7.82	2.46
ACCEPTOR	24	114.64	12.13	3.07	1.67
SHAPE					
PANCAKE	174	204.50	16.26	14.81	3.36
CHUNKY	53	180.60	25.03	13.89	4.76
TOTAL	227	204.50	18.31	14.81	3.69

GENERAL SUMMARY FOR TEST 23

FANEL CHARACTERISTICS

PANEL SPAN	0.46 M	PANEL THICKNESS	50.8 MM
REBAR DIAMETER	2.11 MM	REBAR SPACING	50.8 MM
REBAR COVER	6&35 MM	NO. EDGES SUPPORTED	3
CONCRETE COMPR. STR.	41.03 MPA		

CHARGE CHARACTERISTICS

CHARGE TYPE	C-4	INITIATOR	M-6
CHARGE WEIGHT	453.60 GM	STANDOFF DISTANCE	0.183 M
REFL. IMPULSE	3.45 KPA-S	CHARGE HEIGHT	0.152 M

FRAGMENT CHARACTERISTICS

TYPE	NO. FRAGS RECOVERED	MASS (GM) LG	MASS (GM) AVG	RANGE (M) LG	RANGE (M) AVG
SOURCE					
RED	46	134&36	16.81	29.51	10.44
WHITE	51	78.28	16&46	28.78	10.31
BLUE	17	5851.00	352.05	3.38	1.77
GREEN	7	6169.00	888.11	2.69	1.33
INTERIOR	230	74&94	10.81	26.20	7.20
ACCEPTGR	88	115.53	13.77	30.46	5.28
SHAPE					
PANCAKE	363	6169.00	45.67	28.78	7.01
CHUNKY	77	115.53	12.26	30.46	8.10
TOTAL	440	6169.00	39.82	30.46	7.20

GENERAL SUMMARY FOR TEST 24

PANEL CHARACTERISTICS

PANEL SPAN	0.46 M	PANEL THICKNESS	50.8 MM
REBAR DIAMETER	2.11 MM	REBAR SPACING	25.4 MM
REBAR COVER	6.35 MM	NO. EDGES SUPPORTED	3
CONCRETE COMPR. STR.	41.03 MPA		

CHARGE CHARACTERISTICS

CHARGE TYPE	C-4	INITIATOR	M-6
CHARGE WEIGHT	453.60 GM	STANDOFF DISTANCE	0.183 M
REFL. IMPULSE	3.45 KPA-S	CHARGE HEIGHT	0.152 M

FRAGMENT CHARACTERISTICS

TYPE	NO. FRAGS RECOVERED	MASS (GM) LG	MASS (GM) AVG	RANGE (M) LG	RANGE (M) AVG
SOURCE					
RED	37	32.22	7.98	16.11	6&10
WHITE	28	30.59	12.36	13.36	4&28
BLUE	2	6.41	4&20	3.31	2.60
GREEN	2	3.23	2.38	0.91	0.91
INTERIOR	16	20.26	4.49	10.45	3.99
ACCEPTOR	5	12.97	5.70	8.81	2.90
SHAPE					
PANCAKE	60	32.22	7.83	16.11	5.30
CHUNKY	30	30.59	9.51	11.82	3.77
TOTAL	90	32.22	8.39	16.11	4.79

GENERAL SUMMARY FOR TEST 25

PANEL CHARACTERISTICS

PANEL SPAN	0.46 M	PANEL THICKNESS	50.8 MM
REBAR DIAMETER	2.11 MM	REBAR SPACING	50.8 MM
REBAR COVER	7.94 MM	NO. EDGES SUPPORTED	3
CONCRETE COMPR. STR.	40.51 MPA		

CHARGE CHARACTERISTICS

CHARGE TYPE	C-4	INITIATOR	M-6
CHARGE WEIGHT	453.60 GM	STANDOFF DISTANCE	0.147 M
REFL. IMPULSE	5.17 KPA-S	CHARGE HEIGHT	0.152 M

FRAGMENT CHARACTERISTICS

TYPE	NO. FRAGS RECOVERED	MASS (GM) LG	MASS (GM) AVG	RANGE (M) LG	RANGE (M) AVG
SOURCE					
RED	40	76.17	22.93	32.20	13.84
WHITE	29	92.82	30.21	31.31	13.00
BLUE	5	5216.00	1050.49	6.90	3.02
GREEN	17	5216.00	322.95	12.38	3.80
INTERIOR	160	183.54	17.61	32.11	7.75
ACCEPTOR	90	69.32	14.71	19.00	5.71
SHAPE					
PANCAKE	262	5216.00	59.55	31.95	7.80
CHUNKY	79	131.43	17.69	32.20	9.12
TOTAL	341	5216.00	49.85	32.20	8.11

GENERAL SUMMARY FOR TEST 26

PANEL CHARACTERISTICS

PANEL SPAN	0.46 M	PANEL THICKNESS	55.6 MM
REBAR DIAMETER	2.11 MM	REBAR SPACING	25.4 MM
REBAR COVER	6.35 MM	NO. EDGES SUPPORTED	3
CONCRETE COMPR. STR.	35.43 MPA		

CHARGE CHARACTERISTICS

CHARGE TYPE	C-4	INITIATOR	M-6
CHARGE WEIGHT	453.60 GM	STANDOFF DISTANCE	0.147 M
REFL. IMPULSE	5.17 KPA-S	CHARGE HEIGHT	0.152 M

FRAGMENT CHARACTERISTICS

TYPE	NO. FRAGS RECOVERED	MASS (GM) LG	MASS (GM) AVG	RANGE (M) LG	RANGE (M) AVG
SOURCE					
RED	79	48.06	7.01	24.15	8.54
WHITE	57	27.51	9.65	25.79	12.59
BLUE	21	39.75	8.20	10.82	3.27
GREEN	8	42.75	7.42	8.26	4.93
INTERIOR	75	121.95	10.05	14&14	4.18
ACCEPTOR	10	18.14	8.29	3.26	1.80
SHAPE					
PANCAKE	156	121.95	9.38	25.79	6.74
CHUNKY	94	48.06	7.55	24&15	8.29
TOTAL					
	250	121.95	8.69	25.79	7.32

GENERAL SUMMARY FOR TEST 27

PANEL CHARACTERISTICS

PANEL SPAN	0.46 M	PANEL THICKNESS	77.8 MM
REBAR DIAMETER	2.11 MM	REBAR SPACING	50.8 MM
REBAR COVER	7.94 MM	NO. EDGES SUPPORTED	3
CONCRETE COMPR. STR.	27.24 MPA		

CHARGE CHARACTERISTICS

CHARGE TYPE	C-4	INITIATOR	M-6
CHARGE WEIGHT	453.60 GM	STANDOFF DISTANCE	0.219 M
REFL. IMPULSE	2.46 KPA-S	CHARGE HEIGHT	0.152 M

FRAGMENT CHARACTERISTICS

TYPE	NO. FRAGS RECOVERED	MASS (GM) LG	MASS (GM) AVG	RANGE (M) LG	RANGE (M) AVG
SOURCE					
RED	8	5.40	2.05	3.59	1.88
WHITE	1	3.21	3.21	1.06	1.06
BLUE	6	1.50	0.80	4.28	1.87
GREEN	1	0.47	0.47	1.07	1.07
INTERIOR	6	4.11	1.53	3.25	2.23
ACCEPTOR	2	1.86	1.09	3.85	2.46
SHAPE					
PANCAKE	19	5.40	1.40	4.28	1.83
CHUNKY	5	4.11	1.91	3.59	2.36
TOTAL	24	5.40	1.51	4.28	1.94

GENERAL SUMMARY FOR TEST 28

PANEL CHARACTERISTICS

PANEL SPAN	0.46 M	PANEL THICKNESS	76.2 MM
REBAR DIAMETER	2.11 MM	REBAR SPACING	50.8 MM
REBAR COVER	7.94 MM	NO. EDGES SUPPORTED	3
CONCRETE COMPR. STR.	27.24 MPA		

CHARGE CHARACTERISTICS

CHARGE TYPE	C-4	INITIATOR	M-6
CHARGE WEIGHT	453.60 GM	STANDOFF DISTANCE	0.198 M
REFL. IMPULSE	2.96 KPA-S	CHARGE HEIGHT	0.152 M

FRAGMENT CHARACTERISTICS

TYPE	NO. FRAGS RECOVERED	MASS (GM) LG	MASS (GM) AVG	RANGE (M) LG	RANGE (M) AVG
SOURCE					
RED	1	7.51	7.51	2.97	2.97
WHITE	3	52.30	30.04	4.65	2.34
BLUE	5	8.26	2.41	1.45	0.87
INTERIOR	1	1.01	1.01	0.73	0.73
SHAPE					
PANCAKE	9	52.30	10.63	4.65	1.49
CHUNKY	1	14.97	14.97	1.70	1.70
TOTAL	10	52.30	11.07	4.65	1.51

GENERAL SUMMARY FOR TEST 29

PANEL CHARACTERISTICS

PANEL SPAN	0.46 M	PANEL THICKNESS	77.8 MM
REBAR DIAMETER	2.11 MM	REBAR SPACING	50.8 MM
REBAR COVER	9.52 MM	NO. EDGES SUPPORTED	3
CONCRETE COMPR. STR.	28.10 MPA		

CHARGE CHARACTERISTICS

CHARGE TYPE	C-4	INITIATOR	M-6
CHARGE WEIGHT	453.60 GM	STANDOFF DISTANCE	0.160 M
REFL. IMPULSE	4.27 KPA-S	CHARGE HEIGHT	0.152 M

FRAGMENT CHARACTERISTICS

TYPE	NO. FRAGS RECOVERED	MASS (GM) LG	MASS (GM) AVG	RANGE (M) LG	RANGE (M) AVG
SOURCE					
RED	12	81.91	20.53	6&27	2.55
WHITE	15	166.97	43.71	10.33	3.76
BLUE	5	19.32	8.96	1.69	0.94
GREEN	3	9.91	3.69	5.45	4.43
INTERIOR	44	21.12	5.13	5.51	2.23
SHAPE					
PANCAKE	50	166.97	14.27	6&61	2.42
CHUNKY	29	81.91	16.23	10.33	2.84
TOTAL	79	166.97	14.99	10.33	2.57

GENERAL SUMMARY FOR TEST 30

PANEL CHARACTERISTICS

PANEL SPAN	0.46 M	PANEL THICKNESS	52.4 MM
REBAR DIAMETER	2.11 MM	REBAR SPACING	25.4 MM
REBAR COVER	9.52 MM	NO. EDGES SUPPORTED	3
CONCRETE COMPR. STR.	39.82 MPA		

CHARGE CHARACTERISTICS

CHARGE TYPE	C-4	INITIATOR	M-6
CHARGE WEIGHT	453.60 GM	STANDOFF DISTANCE	0.219 M
REFL. IMPULSE	2.46 KPA-S	CHARGE HEIGHT	0.152 M

FRAGMENT CHARACTERISTICS

TYPE	NO. FRAGS RECOVERED	MASS (GM) LG	MASS (GM) AVG	RANGE (M) LG	RANGE (M) AVG
SOURCE					
RED	17	25.05	10.52	11.15	5.03
WHITE	29	27.69	9.17	13.10	5.62
BLUE	2	1.00	0.86	4.44	3.36
GREEN	19	26.29	9.12	10.33	3.06
INTERIOR	7	5.03	2.01	4.44	1.55
ACCEPTOR	9	43.88	14.82	5.12	2.14
SHAPE					
PANCAKE	53	39.69	9.48	13.10	4.32
CHUNKY	30	43.88	8.82	12.23	3.82
TOTAL	83	43.88	9.24	13.10	4.14

GENERAL SUMMARY FOR TEST 31

PANEL CHARACTERISTICS

PANEL SPAN	0.46 M	PANEL THICKNESS	50.8 MM
REBAR DIAMETER	2.11 MM	REBAR SPACING	50.8 MM
REBAR COVER	6.35 MM	NO. EDGES SUPPORTED	3
CONCRETE COMPR. STR.	39.82 MPA		

CHARGE CHARACTERISTICS

CHARGE TYPE	C-4	INITIATOR	M-6
CHARGE WEIGHT	453.60 GM	STANDOFF DISTANCE	0.219 M
REFL. IMPULSE	2.46 KPA-S	CHARGE HEIGHT	0.152 M

FRAGMENT CHARACTERISTICS

TYPE	NO. FRAGS RECOVERED	MASS (GM) LG	MASS (GM) AVG	RANGE (M) LG	RANGE (M) AVG
SOURCE					
RED	5	131.58	53.10	6.45	3.51
WHITE	5	164.69	97.27	10.90	4.36
BLUE	10	34.17	6.77	3.00	1.56
GREEN	3	78.12	32.13	3.55	2.23
INTERIOR	49	46.74	6.06	5.44	2.17
ACCEPTOR	86	92.59	9.57	6.94	1.93
SHAPE					
PANCAKE	131	127.58	8.41	6.94	2.05
CHUNKY	28	164%69	33.50	10.90	2.38
TOTAL	159	164%69	12.83	10.90	2.11

GENERAL SUMMARY FOR TEST 32

PANEL CHARACTERISTICS

PANEL SPAN	0.46 M	PANEL THICKNESS	54&0 MM
REBAR DIAMETER	2.11 MM	REBAR SPACING	50.8 MM
REBAR COVER	6.35 MM	NO. EDGES SUPPORTED	3
CONCRETE COMPR. STR.	45.85 MPA		

CHARGE CHARACTERISTICS

CHARGE TYPE	C-4	INITIATOR	M-6
CHARGE WEIGHT	453.60 GM	STANDOFF DISTANCE	0.219 M
REFL. IMPULSE	1.72 KPA-S	CHARGE HEIGHT	0.152 M

FRAGMENT CHARACTERISTICS

TYPE	NO. FRAGS RECOVERED	MASS (GM) LG	MASS (GM) AVG	RANGE (M) LG	RANGE (M) AVG
SOURCE					
RED	7	10.47	3.08	7.30	3.96
WHITE	9	67.99	22.76	4&92	2.14
BLUE	3	0.76	0.63	4.33	2.86
INTERIOR	12	34.43	5.41	3.06	1.02
ACCEPTOR	14	21.61	3.80	2.46	1.31
SHAPE					
PANCAKE	33	34.43	3.03	7.30	1.83
CHUNKY	12	67.99	20.53	5.29	2.17
TOTAL					
	45	67.99	7.70	7.30	1.92

GENERAL SUMMARY FOR TEST 33

PANEL CHARACTERISTICS

PANEL SPAN	0.46 M	PANEL THICKNESS	77.8 MM
REBAR DIAMETER	2.11 MM	REBAR SPACING	25.4 MM
REBAR COVER	6.35 MM	NO. EDGES SUPPORTED	3
CONCRETE COMPR. STR.	49.39 MPA		

CHARGE CHARACTERISTICS

CHARGE TYPE	C-4	INITIATOR	M-6
CHARGE WEIGHT	453.60 GM	STANDOFF DISTANCE	0.219 M
REFL. IMPULSE	2.46 KPA-S	CHARGE HEIGHT	0.152 M

FRAGMENT CHARACTERISTICS

TYPE	NO. FRAGS RECOVERED	MASS (GM) LG	MASS (GM) AVG	RANGE (M) LG	RANGE (M) AVG
SOURCE					
WHITE	2	0.72	0.57	1.81	1.48
GREEN	1	3.33	3.33	0.69	0.69
INTERIOR	1	0.82	0.82	2.48	2.48
ACCEPTOR	2	5.31	3.80	2.93	2.63
SHAPE					
PANCAKE	5	5.31	2.41	2.93	1.78
CHUNKY	1	0.82	0.82	2.48	2.48
TOTAL	6	5.31	2.15	2.93	1.90

GENERAL SUMMARY FOR TEST 34

PANEL CHARACTERISTICS

PANEL SPAN	0.46 M	PANEL THICKNESS	79.4 MM
REBAR DIAMETER	2.11 MM	REBAR SPACING	25.4 MM
REBAR COVER	6.35 MM	NO. EDGES SUPPORTED	3
CONCRETE COMPR. STR.	49.39 MPA		

CHARGE CHARACTERISTICS

CHARGE TYPE	C-4	INITIATOR	M-6
CHARGE WEIGHT	453.60 GM	STANDOFF DISTANCE	0.183 M
REFL. IMPULSE	3.45 KPA-S	CHARGE HEIGHT	0.152 M

FRAGMENT CHARACTERISTICS

TYPE	NO. FRAGS RECOVERED	MASS (GM) LG	MASS (GM) AVG	RANGE (M) LG	RANGE (M) AVG
SOURCE					
RED	4	1.26	0.75	4.61	1.69
WHITE	10	7.61	1.69	4.93	2.45
BLUE	4	2.35	0.78	3.50	2.25
GREEN	5	0.96	0.51	2.47	1.69
INTERIOR	7	0.74	0.43	2.76	1.75
ACCEPTOR	6	18.90	5.25	3.42	1.50
SHAPE					
PANCAKE	24	7.61	1.06	4&51	1.78
CHUNKY	12	18.90	2.88	4&93	2.26
TOTAL	36	18.90	1.67	4&93	1.94

GENERAL SUMMARY FOR TEST 35

PANEL CHARACTERISTICS

PANEL SPAN	0.46 M	PANEL THICKNESS	50.8 MM
REBAR DIAMETER	2.11 MM	REBAR SPACING	25.4 MM
REBAR COVER	6.35 MM	NO. EDGES SUPPORTED	3
CONCRETE COMPR. STR.	48.26 MPA		

CHARGE CHARACTERISTICS

CHARGE TYPE	C-4	INITIATOR	M-6
CHARGE WEIGHT	1360.80 GM	STANDOFF DISTANCE	0.387 M
REFL. IMPULSE	2.48 KPA-S	CHARGE HEIGHT	0.152 M

FRAGMENT CHARACTERISTICS

TYPE	NO. FRAGS RECOVERED	MASS (GM) LG	MASS (GM) AVG	RANGE (M) LG	RANGE (M) AVG
SOURCE					
RED	33	116&50	18.32	31.91	14.15
WHITE	46	82.01	10.27	31.60	14.75
BLUE	7	16865.70	2419.25	26.40	13.24
GREEN	3	37.52	23.27	26.58	12.62
INTERIOR	150	150.11	14.41	32.26	8.36
ACCEPTOR	136	35.64	9.36	31.63	8.48
SHAPE					
PANCAKE	290	16865.70	69.68	32.26	9.83
CHUNKY	85	116&50	15.40	31.91	10.68
TOTAL	375	16865.70	57.37	32.26	10.02

GENERAL SUMMARY FOR TEST 36

PANEL CHARACTERISTICS

PANEL SPAN	0.46 M	PANEL THICKNESS	77.8 MM
REBAR DIAMETER	2.11 MM	REBAR SPACING	25.4 MM
REBAR COVER	6.35 MM	NO. EDGES SUPPORTED	3
CONCRETE COMPR. STR.	49.39 MPA		

CHARGE CHARACTERISTICS

CHARGE TYPE	C-4	INITIATOR	M-6
CHARGE WEIGHT	1360.80 GM	STANDOFF DISTANCE	0.320 M
REFL. IMPULSE	3.38 KPA-S	CHARGE HEIGHT	0.152 M

FRAGMENT CHARACTERISTICS

TYPE	NO. FRAGS RECOVERED	MASS (GM) LG	MASS (GM) AVG	RANGE (M) LG	RANGE (M) AVG
SOURCE					
RED	38	60.40	23.79	31.45	20.82
WHITE	27	95.27	25.19	19.54	9.83
BLUE	7	6273.50	900.01	11.39	6.03
GREEN	9	10955.90	1228.55	13.30	6.16
INTERIOR	305	290.90	19.90	31.81	11.25
ACCEPTOR	62	77.63	11.99	19.78	4.12
SHAPE					
PANCAKE	336	10955.90	68.83	31.81	9.40
CHUNKY	112	171.46	23.47	31.60	15.02
TOTAL	448	10955.90	57.49	31.81	10.80

GENERAL SUMMARY FOR TEST 38

PANEL CHARACTERISTICS

PANEL SPAN	0.00 M	PANEL THICKNESS	0.0 MM
REBAR DIAMETER	0.00 MM	REBAR SPACING	0.0 MM
REBAR COVER	0.00 MM	NO. EDGES SUPPORTED	0
CONCRETE COMPR. STR.	0.00 MPA		

CHARGE CHARACTERISTICS

CHARGE TYPE	C-4	INITIATOR	M-6
CHARGE WEIGHT	0.00 GM	STANDOFF DISTANCE	0.000 M
REFL. IMPULSE	0.00 KPA-S	CHARGE HEIGHT	0.000 M

FRAGMENT CHARACTERISTICS

TYPE	NO. FRAGS RECOVERED	MASS (GM) LG	MASS (GM) AVG	RANGE (M) LG	RANGE (M) AVG
SOURCE					
RED	14	3084.43	734.30	13.26	3.99
WHITE	10	3923.57	1353.81	9.35	2.56
BLUE	23	11090.30	1531.13	4.34	1.71
GREEN	19	16102.50	2182.19	4.95	2.14
INTERIOR	103	5533.83	193.47	7.93	2.39
ACCEPTOR	60	9253.28	670.59	8.38	2.26
SHAPE					
PANCAKE	197	16102.50	518.50	13.26	2.44
CHUNKY	32	13063.40	1828.54	5.38	1.94
TOTAL	229	16102.50	701.57	13.26	2.37

GENERAL SUMMARY FOR TEST 39

PANEL CHARACTERISTICS

PANEL SPAN	0.00 M	PANEL THICKNESS	0.0 MM
REBAR DIAMETER	0.00 MM	REBAR SPACING	0.0 MM
REBAR COVER	0.00 MM	NO EDGES SUPPORTED	0
CONCRETE COMPR. STR.	0.00 MPA		

CHARGE CHARACTERISTICS

CHARGE TYPE	C-4	INITIATOR	M-6
CHARGE WEIGHT	0.00 GM	STANDOFF DISTANCE	0.000 M
REFL. IMPULSE	0.00 KPA-S	CHARGE HEIGHT	0.000 M

FRAGMENT CHARACTERISTICS

TYPE	NO. FRAGS RECOVERED	MASS (GM) LG	MASS (GM) AVG	RANGE (M) LG	RANGE (M) AVG
SOURCE					
RED	13	3311.00	1006.98	4&53	2.15
WHITE	8	4445.00	1632.95	4&26	2.00
BLUE	2	7031.00	3538.15	1.81	1.25
GREEN	6	17282.00	3625.38	1.09	0.81
INTERIOR	44	1406.00	279.31	3.32	1.68
ACCEPTOR	5	10659.00	2872.67	0.90	0.77
SHAPE					
PANCAKE	70	7031.00	741.59	4.53	1.66
CHUNKY	8	17282.00	3715.58	2.32	1.59
TOTAL	78	17282.00	1046.61	4.53	1.65

APPENDIX D

FRAGMENT MAPS

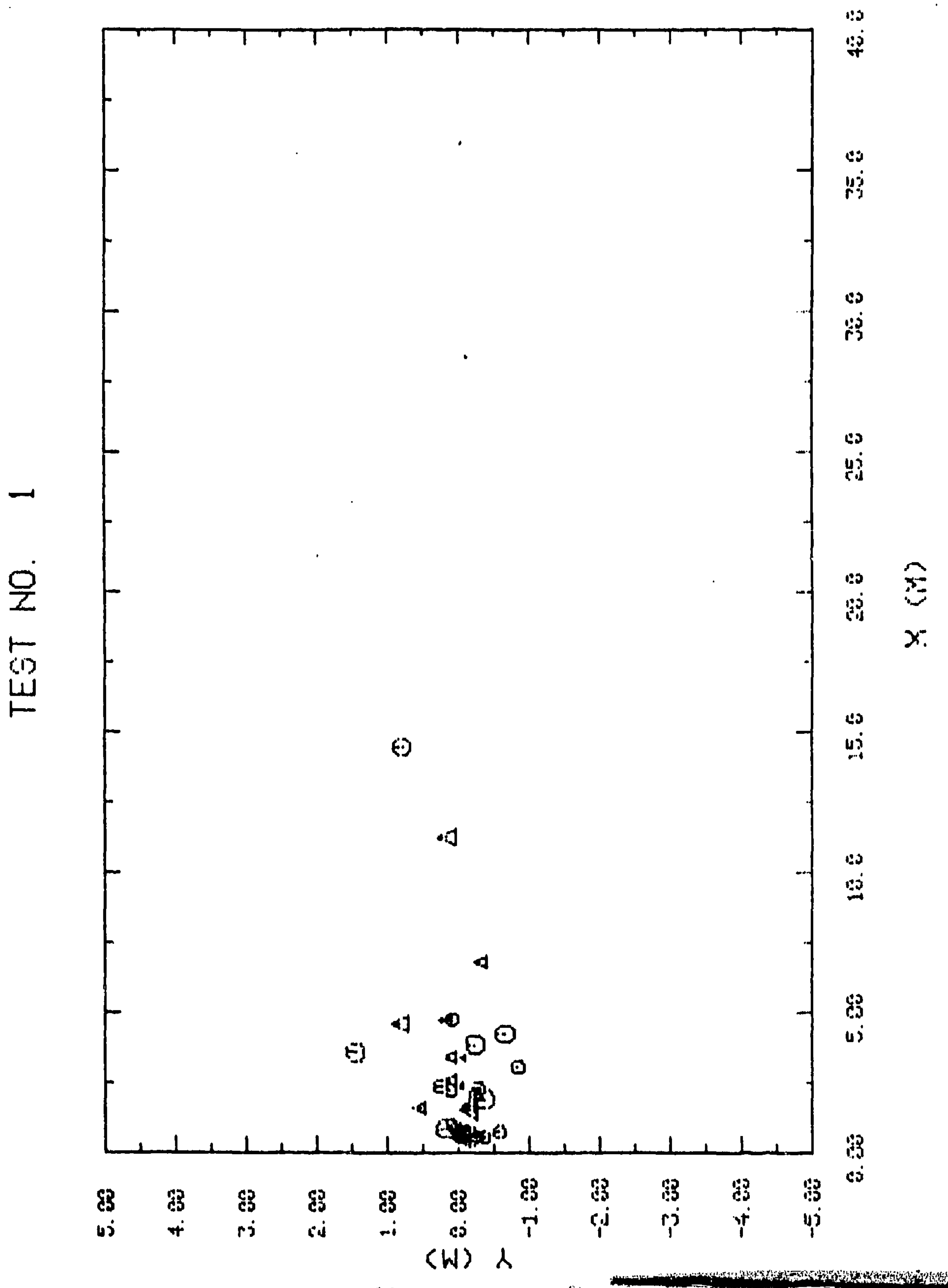
TEST NO. 1
X (M)
Y (M)
0.0
5.0
10.0
15.0
20.0
25.0
30.0
35.0
40.0
5.00
4.00
3.00
2.00
1.00
0.00
-1.00
-2.00
-3.00
-4.00
-5.00

TEST NO. 2

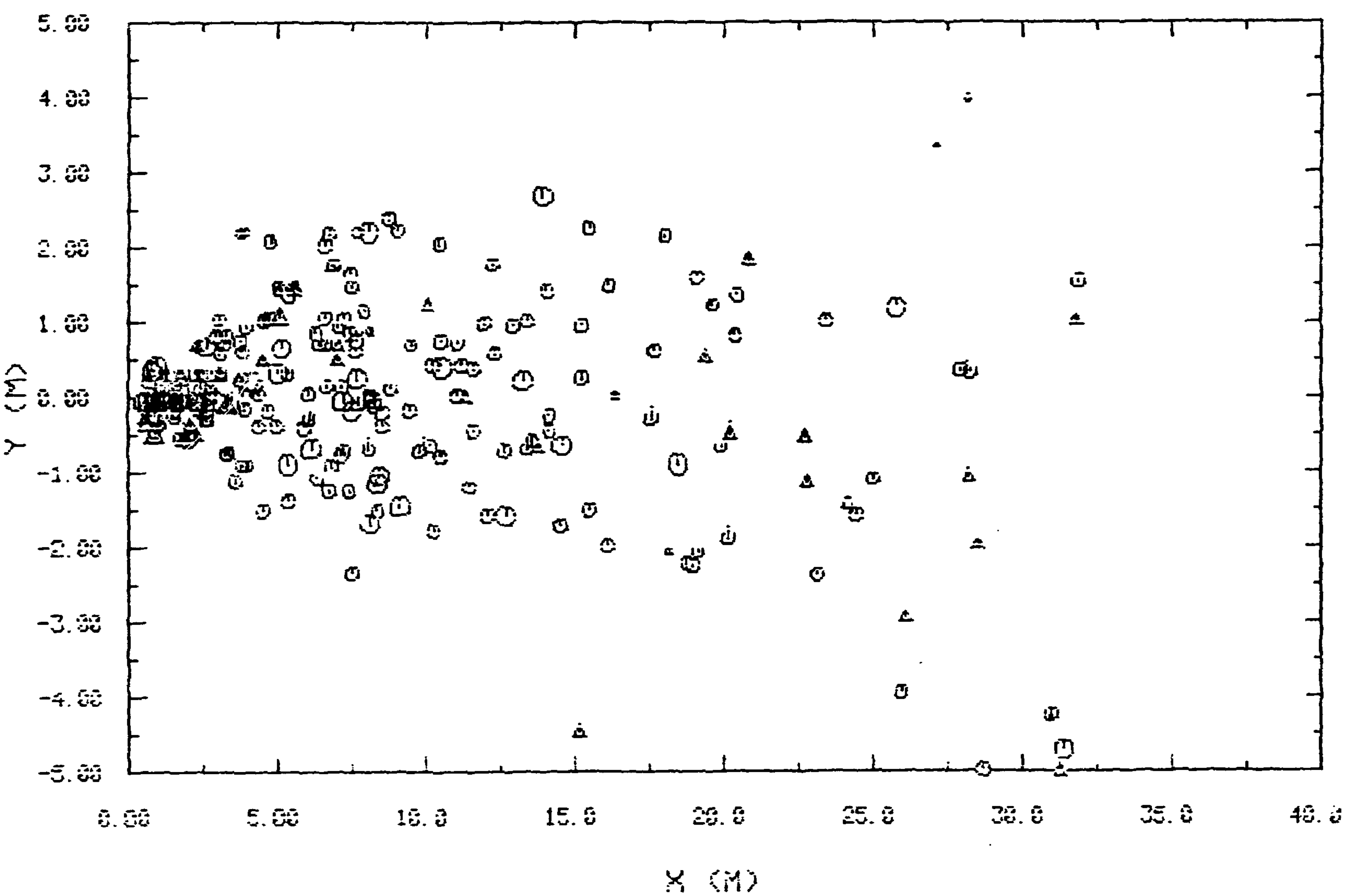

5.00
4.00
3.00
2.00
1.00
0.00
-1.00
-2.00
-3.00
-4.00
-5.00
Y (M)
0.00
5.00
10.0
15.0
20.0
25.0
30.0
35.0
40.0
X (M)

TEST NO. 3

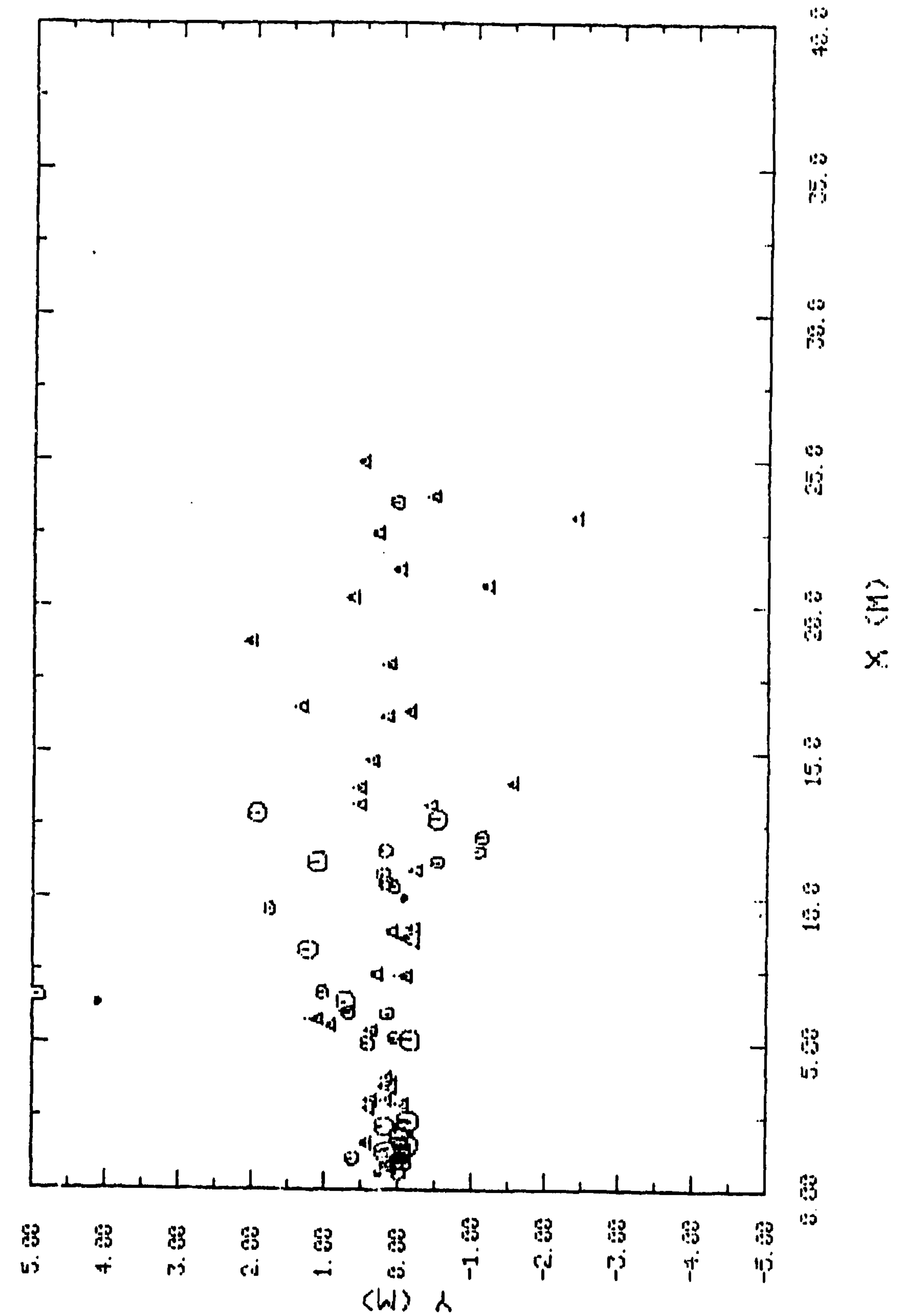

Y (M)
5.00
4.00
3.00
2.00
1.00
.00
-1.00
-2.00
-3.00
-4.00
-5.00
X (M)
0.00
5.00
10.0
15.0
20.0
25.0
30.0
35.0
40.0

TEST NO. 4

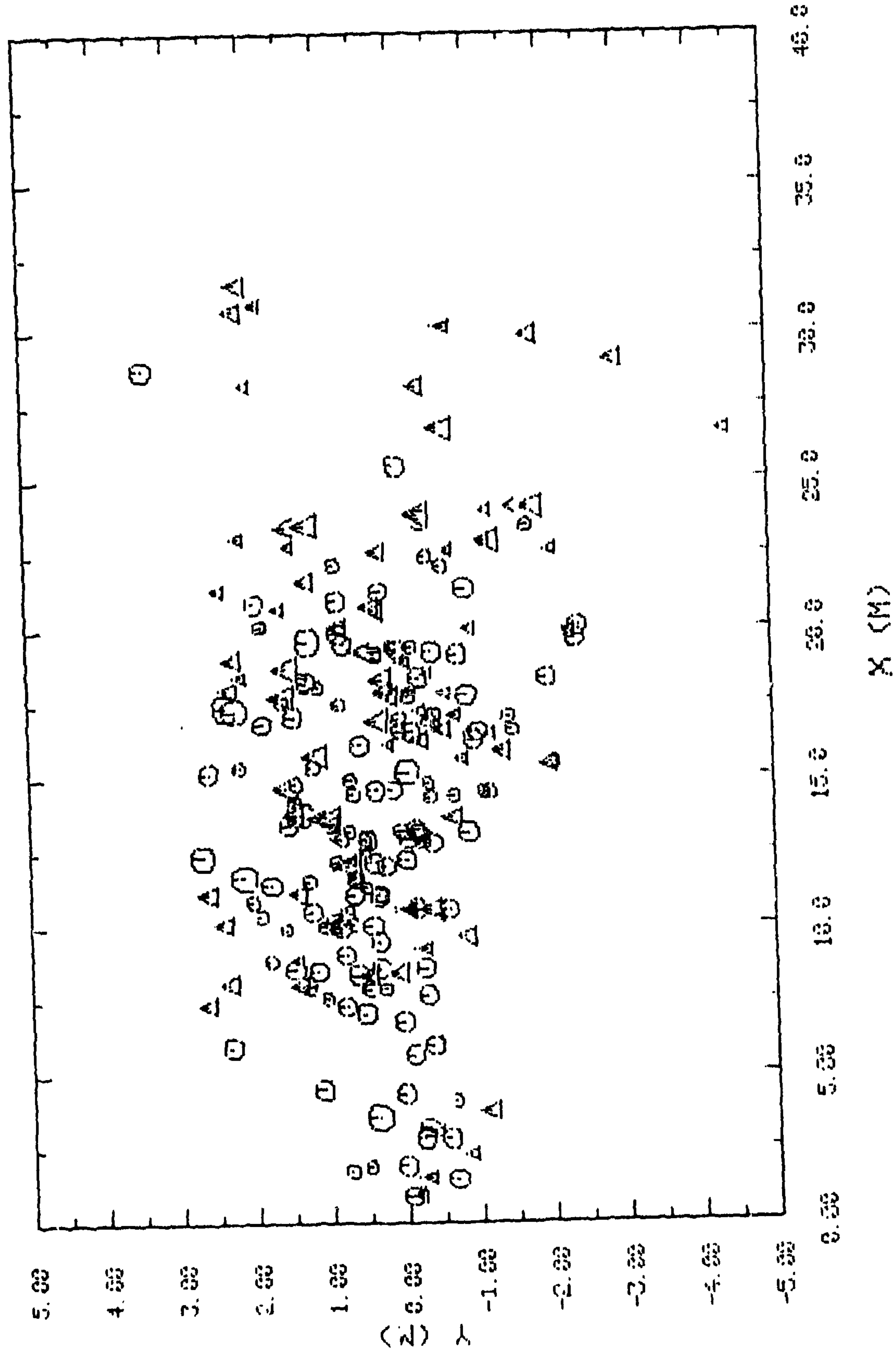
X (M)
0.00
5.00
10.0
15.0
20.0
25.0
30.0
35.0
40.0
Y (M)
5.00
4.00
3.00
2.00
1.00
0.00
-1.00
-2.00
-3.00
-4.00
-5.00

TEST NO. 5

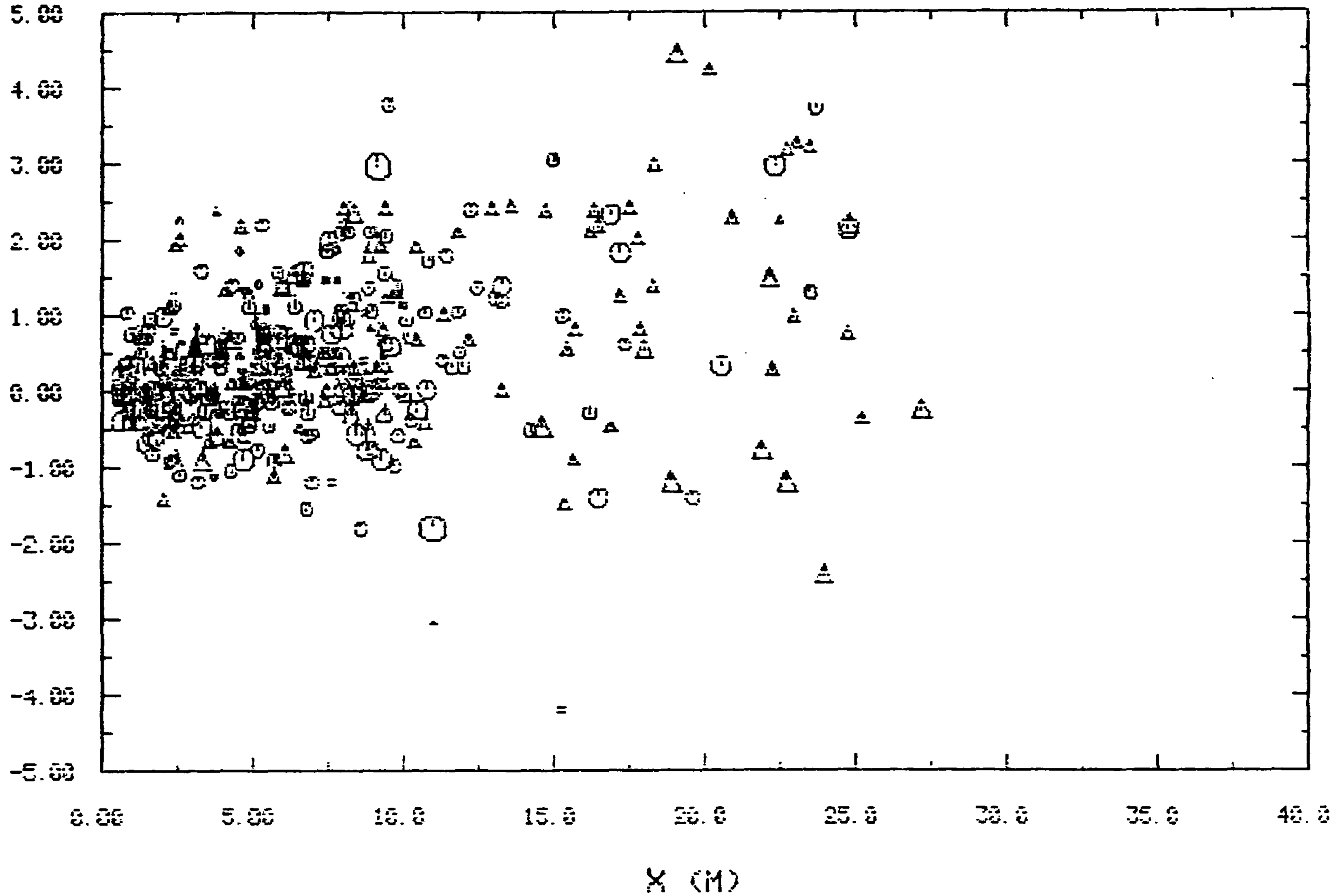

5.00
4.00
3.00
2.00
1.00
0.00
-1.00
-2.00
-3.00
-4.00
-5.00
Y (M)
0.00
5.00
10.0
15.0
20.0
25.0
30.0
35.0
40.0
X (M)

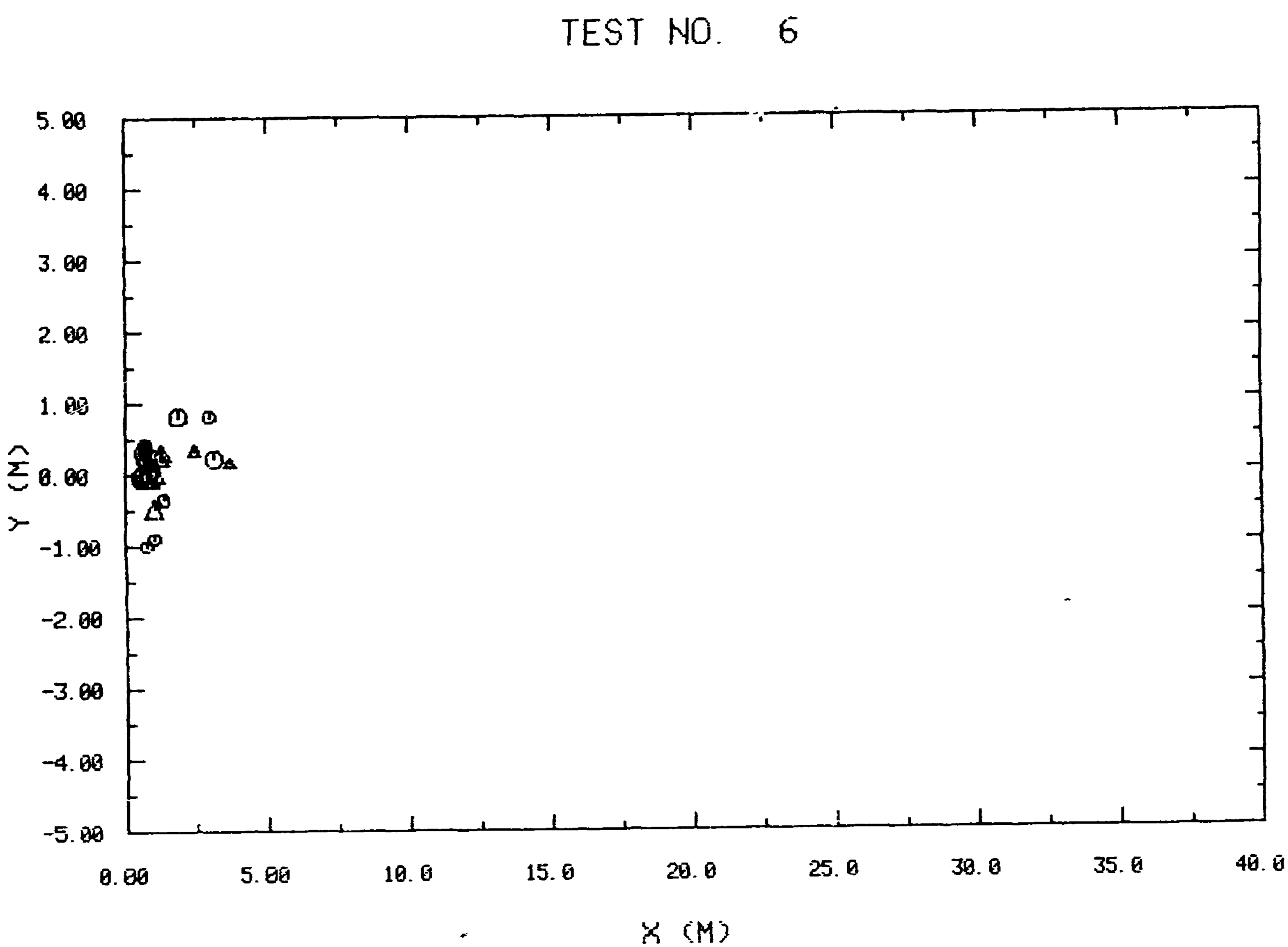
TEST NO. 6
Y (M)
5.00
4.00
3.00
2.00
1.00
0.00
-1.00
-2.00
-3.00
-4.00
-5.00
0.00
5.00
10.0
15.0
20.0
25.0
30.0
35.0
40.0
X (M)

TEST NO. 7

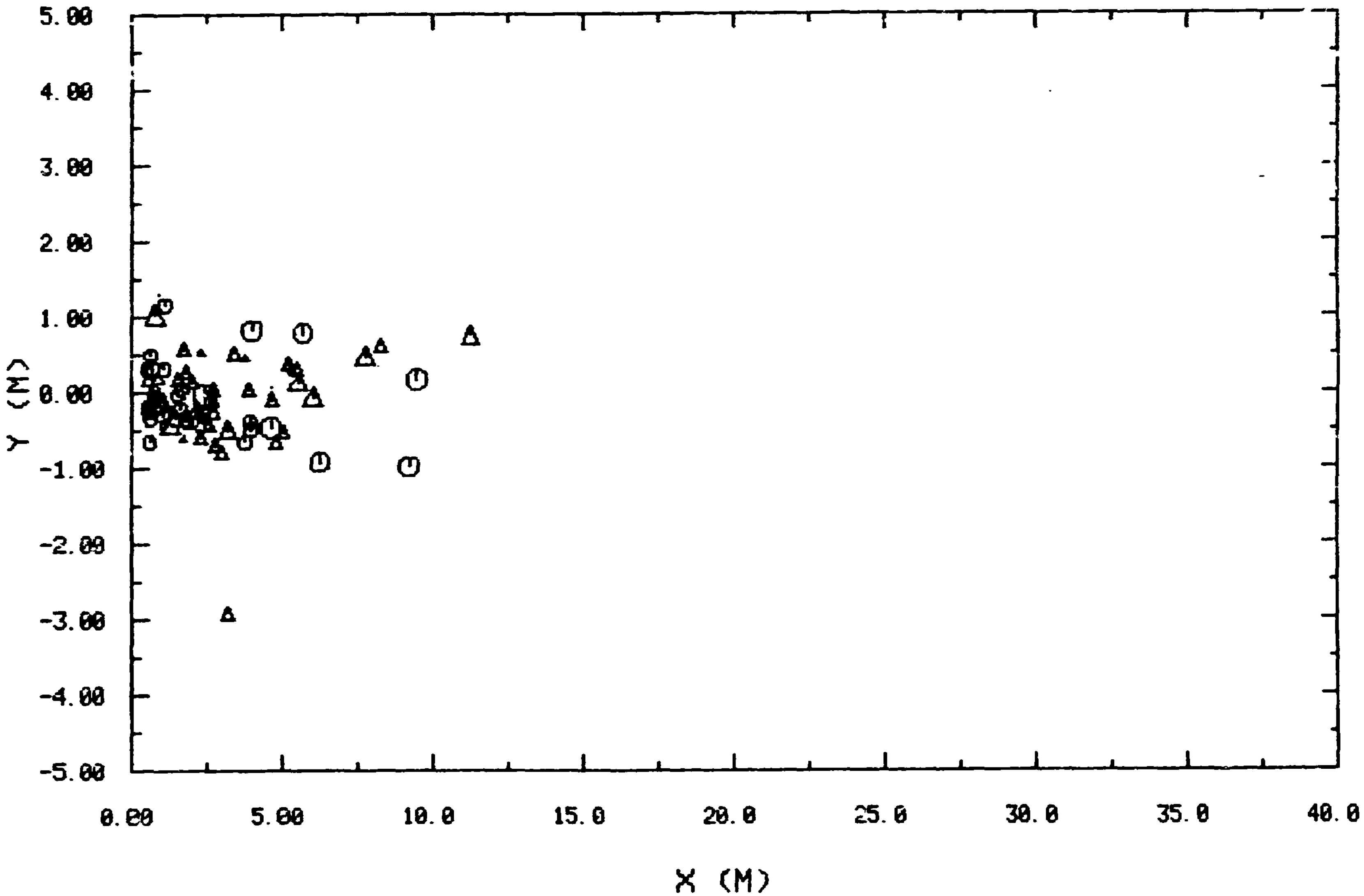

5.00
4.00
3.00
2.00
1.00
0.00
-1.00
-2.00
-3.00
-4.00
-5.00
Y (M)
0.00
5.00
10.0
15.0
20.0
25.0
30.0
35.0
40.0
X (M)

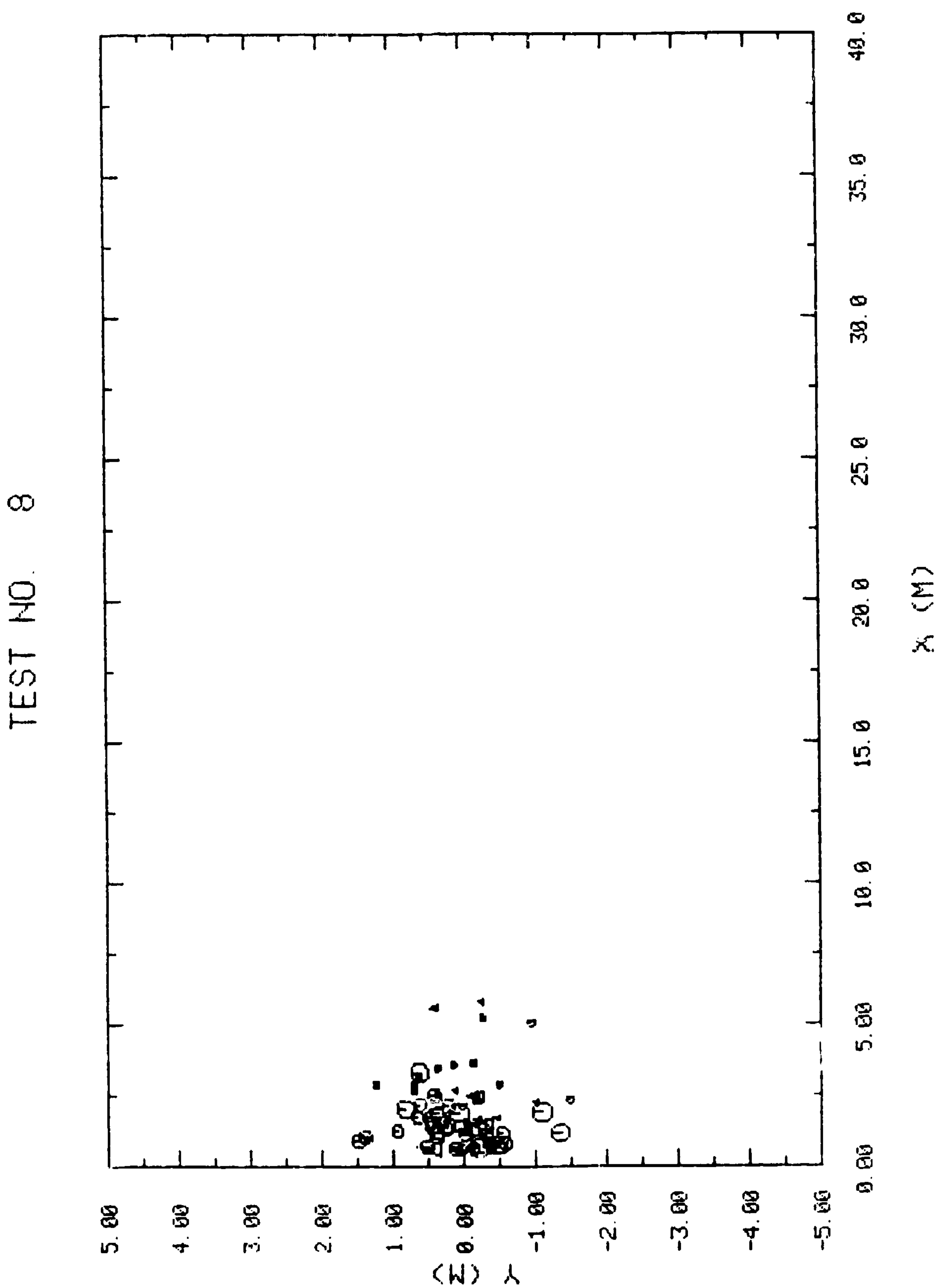
TEST NO. 8
X (M)
Y (M)
0.00
5.00
10.0
15.0
20.0
25.0
30.0
35.0
40.0
5.00
4.00
3.00
2.00
1.00
0.00
-1.00
-2.00
-3.00
-4.00
-5.00

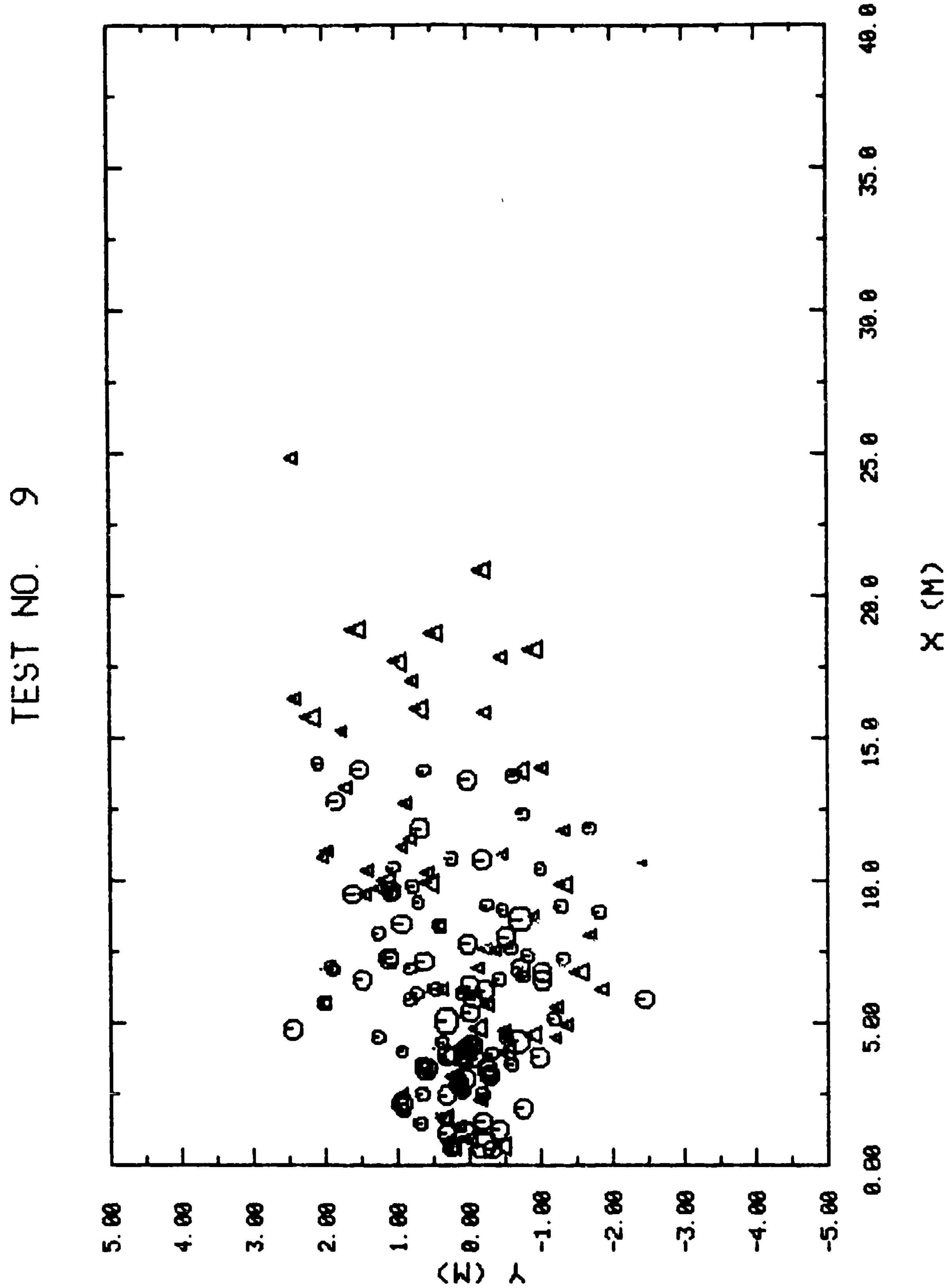
TEST NO. 9
X (M)
Y (M)
0.00
5.00
10.0
15.0
20.0
25.0
30.0
35.0
40.0
5.00
4.00
3.00
2.00
1.00
0.00
-1.00
-2.00
-3.00
-4.00
-5.00

TEST NO. 10

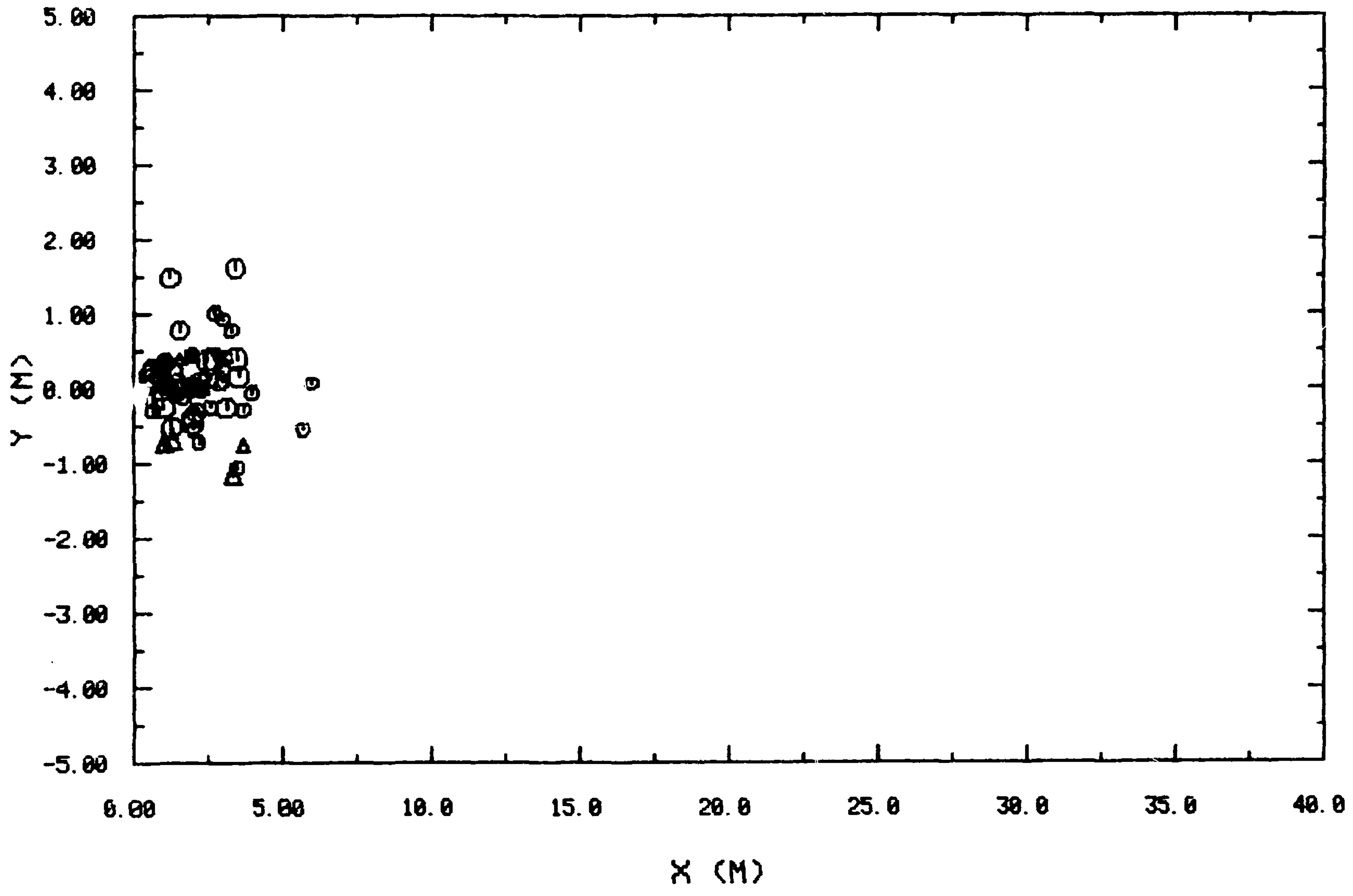

5.00
4.00
3.00
2.00
1.00
0.00
-1.00
-2.00
-3.00
-4.00
-5.00
Y (M)
0.00
5.00
10.0
15.0
20.0
25.0
30.0
35.0
40.0
X (M)

TEST NO. 11

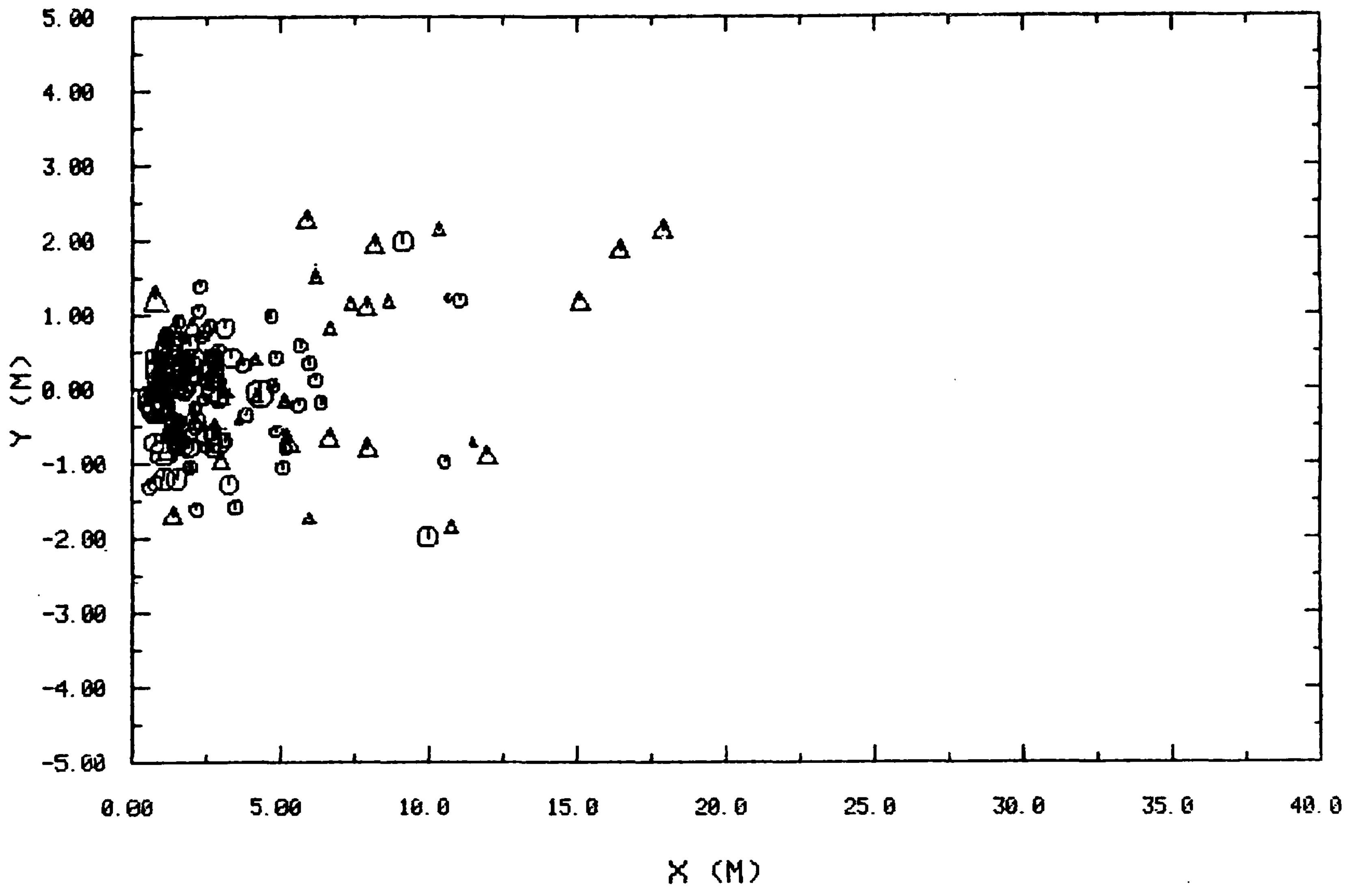

5.00
4.00
3.00
2.00
1.00
0.00
-1.00
-2.00
-3.00
-4.00
-5.00
Y (M)
0.00
5.00
10.0
15.0
20.0
25.0
30.0
35.0
40.0
X (M)

TEST NO. 12

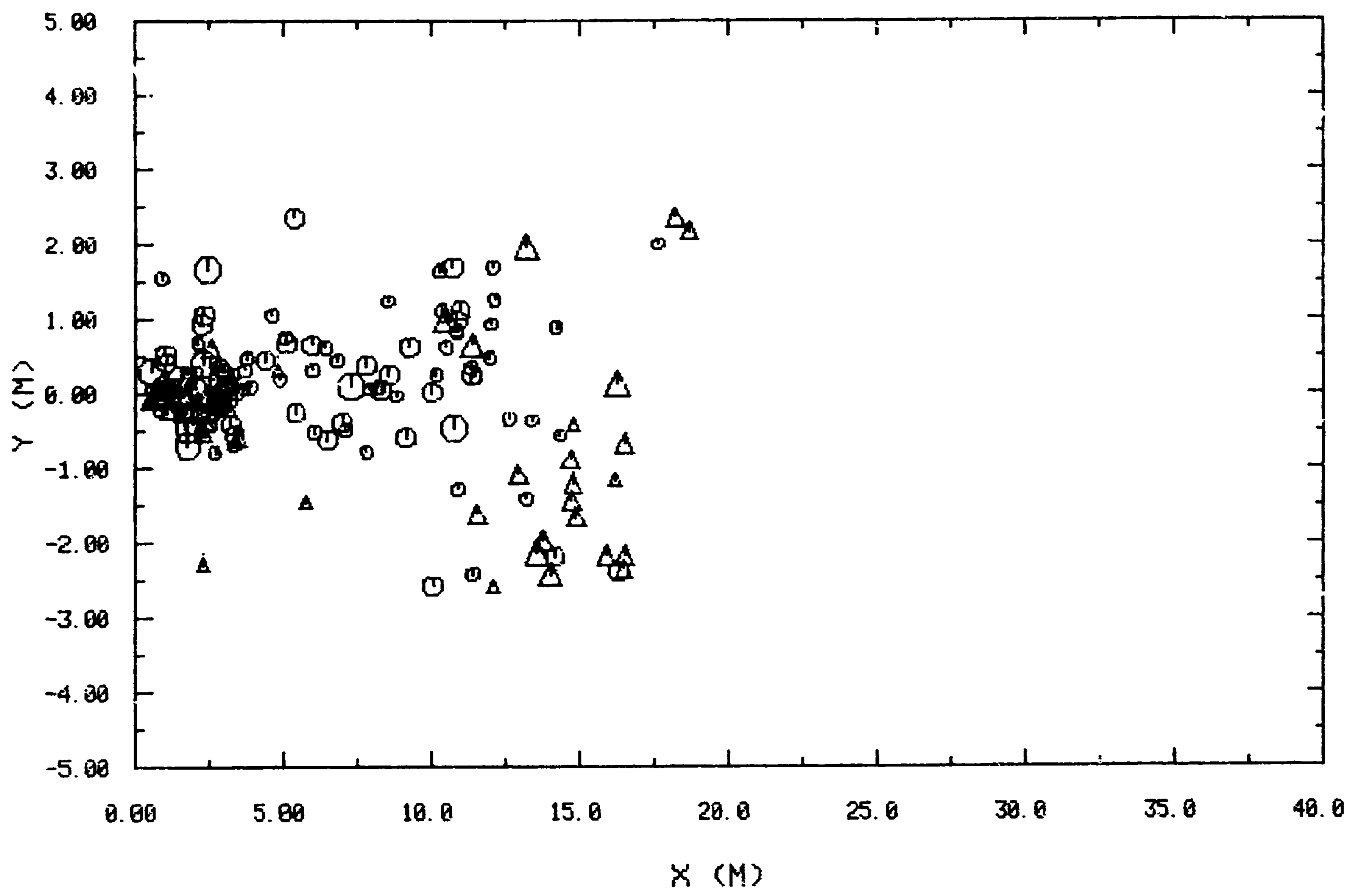

5.00
4.00
3.00
2.00
1.00
0.00
-1.00
-2.00
-3.00
-4.00
-5.00
Y (M)
0.00
5.00
10.0
15.0
20.0
25.0
30.0
35.0
40.0
X (M)

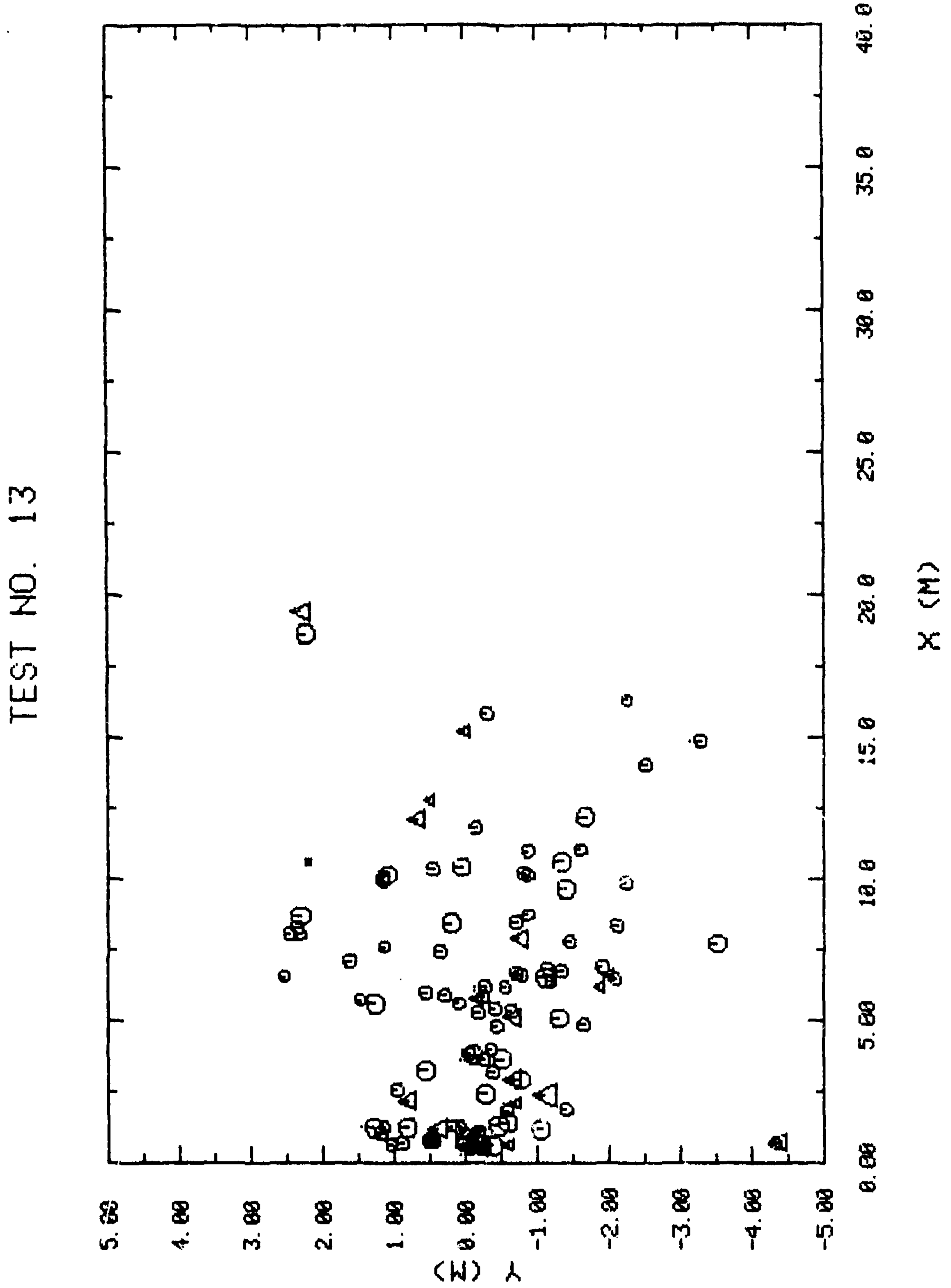
TEST NO. 13
X (M)
Y (M)
0.00
5.00
10.0
15.0
20.0
25.0
30.0
35.0
40.0
5.00
4.00
3.00
2.00
1.00
0.00
-1.00
-2.00
-3.00
-4.00
-5.00

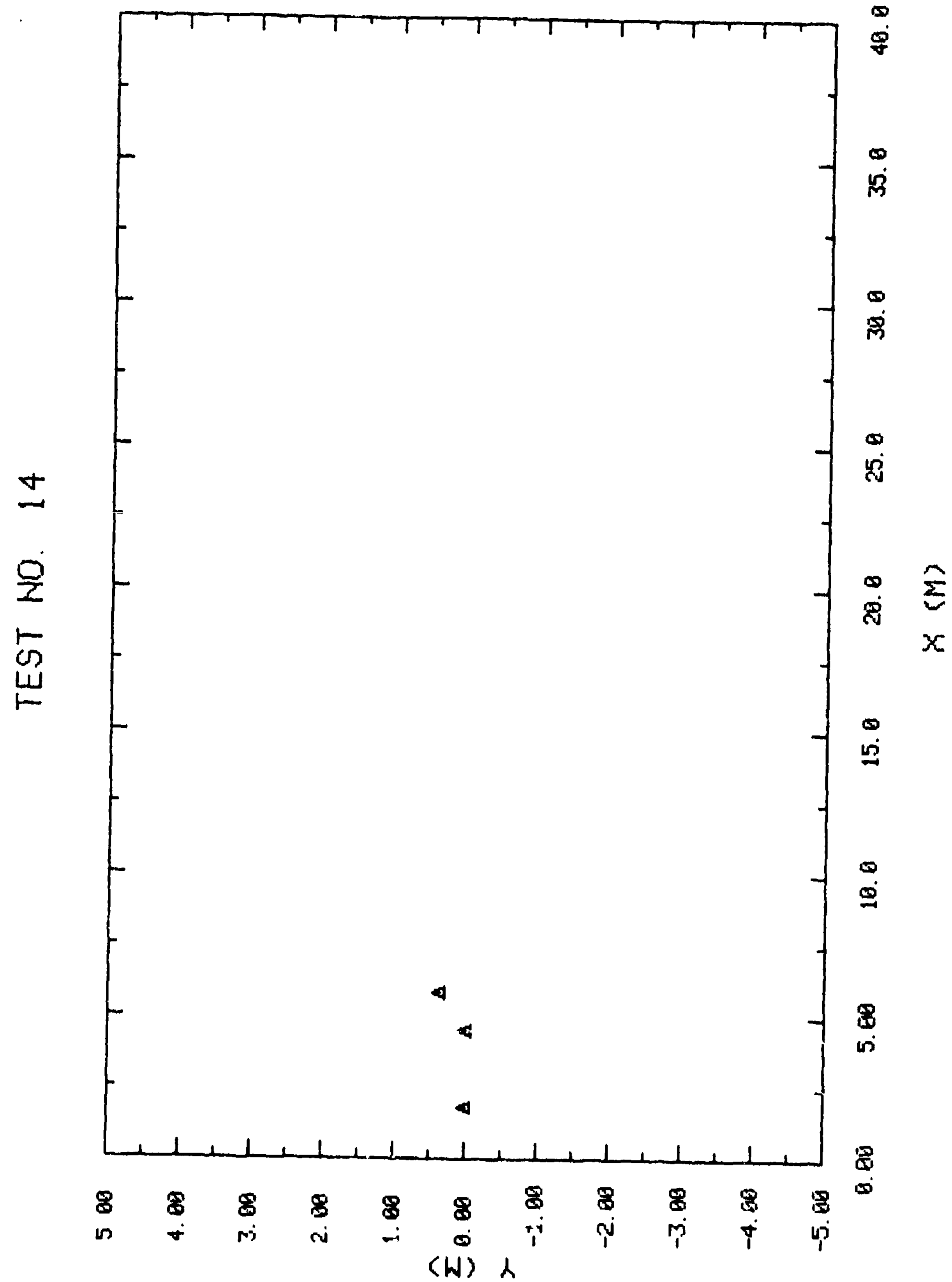
TEST NO. 14
X (M)
Y (M)
0.00
5.00
10.0
15.0
20.0
25.0
30.0
35.0
40.0
5.00
4.00
3.00
2.00
1.00
0.00
-1.00
-2.00
-3.00
-4.00
-5.00
A
A
A

TEST NO. 15

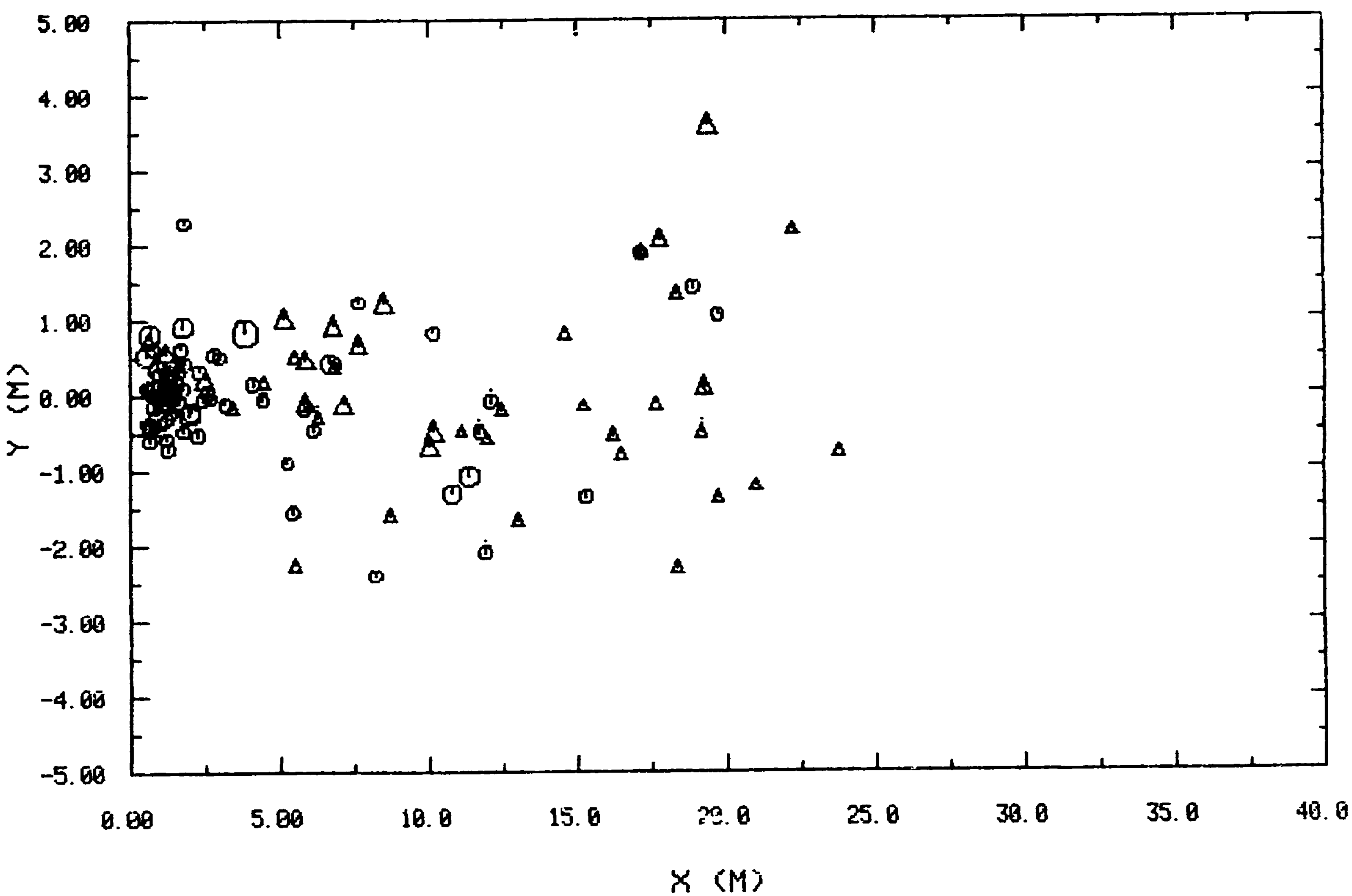
5.00
4.00
3.00
2.00
1.00
0.00
-1.00
-2.00
-3.00
-4.00
-5.00
Y (M)
0.00
5.00
10.0
15.0
20.0
25.0
30.0
35.0
40.0
X (M)

TEST NO. 16

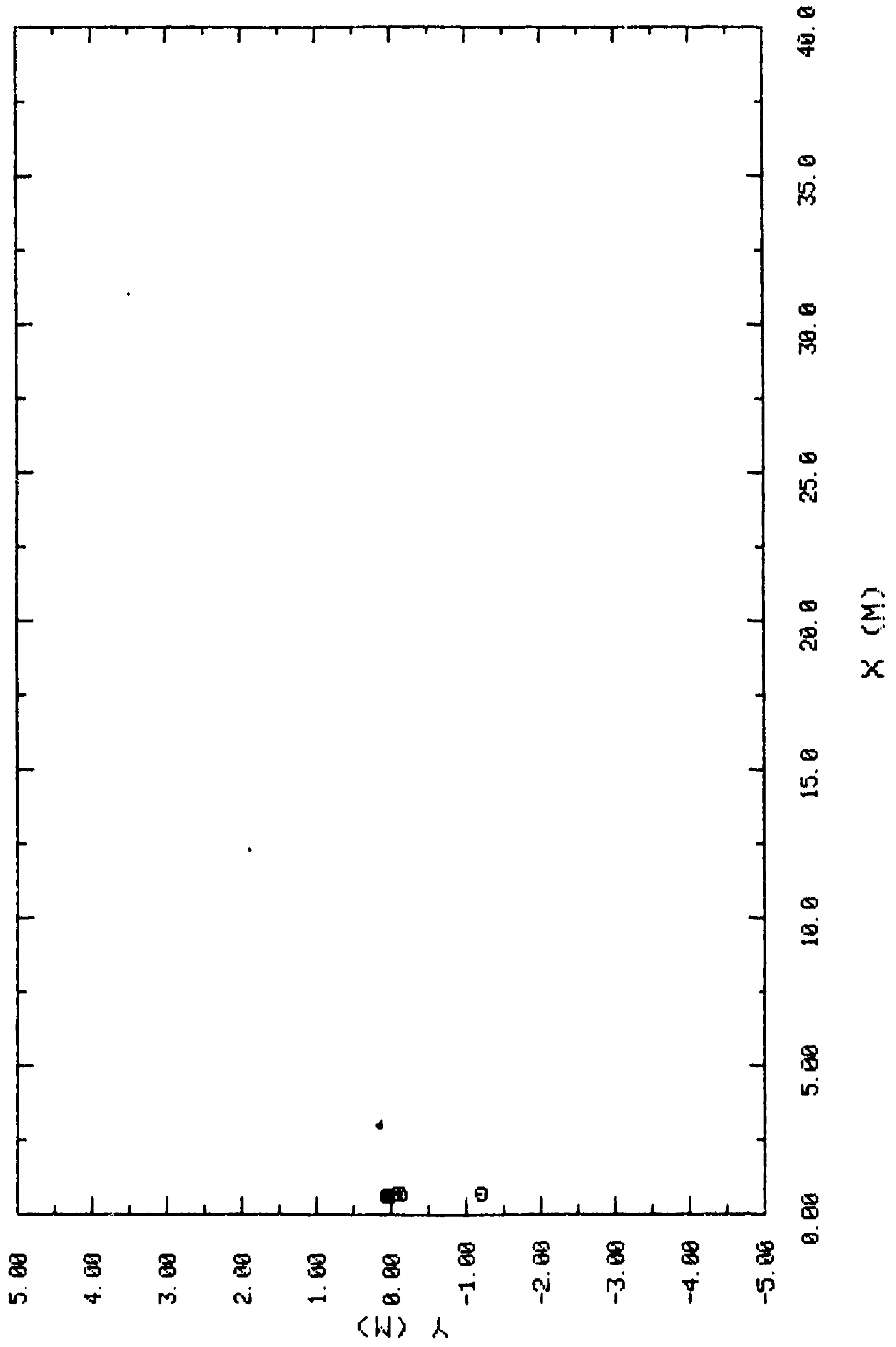
X (M)
Y (M)
0.00
5.00
10.0
15.0
20.0
25.0
30.0
35.0
40.0
5.00
4.00
3.00
2.00
1.00
0.00
-1.00
-2.00
-3.00
-4.00
-5.00

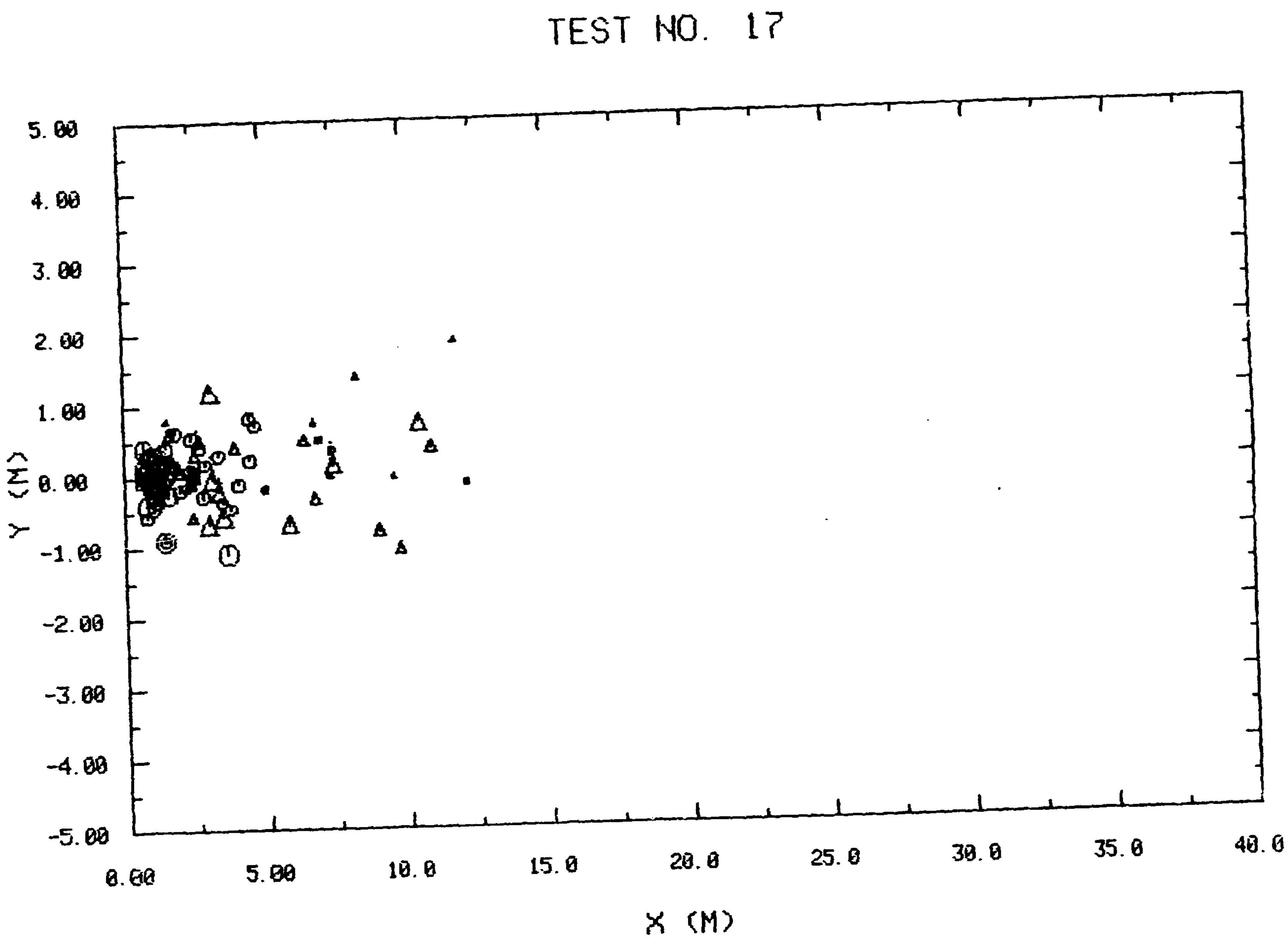
TEST NO. 17
Y (M)
X (M)
5.00
4.00
3.00
2.00
1.00
0.00
-1.00
-2.00
-3.00
-4.00
-5.00
0.00
5.00
10.0
15.0
20.0
25.0
30.0
35.0
40.0

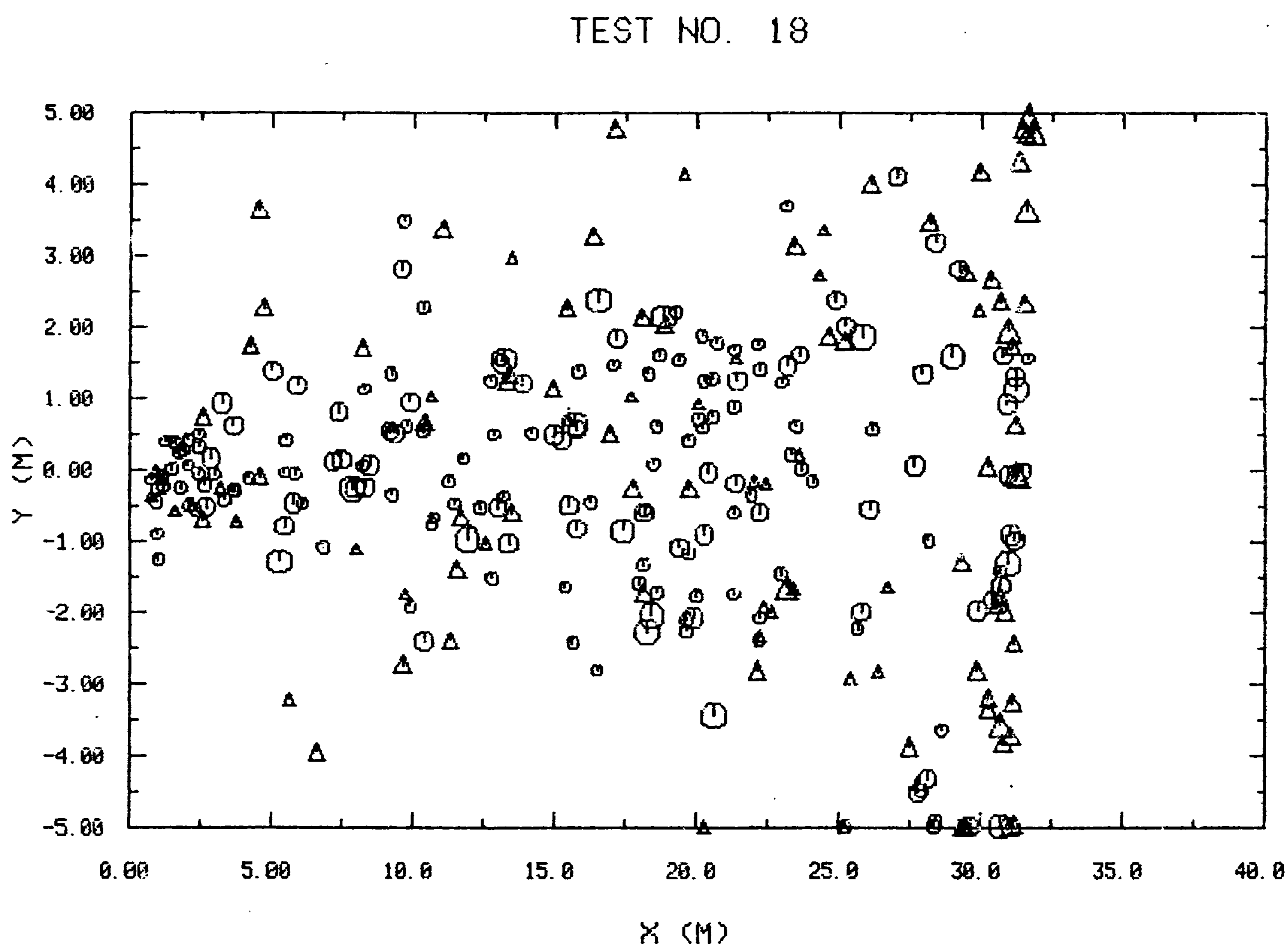

TEST NO. 18
5.00
4.00
3.00
2.00
1.00
0.00
-1.00
-2.00
-3.00
-4.00
-5.00
Y (M)
0.00
5.00
10.0
15.0
20.0
25.0
30.0
35.0
40.0
X (M)

TEST NO. 19

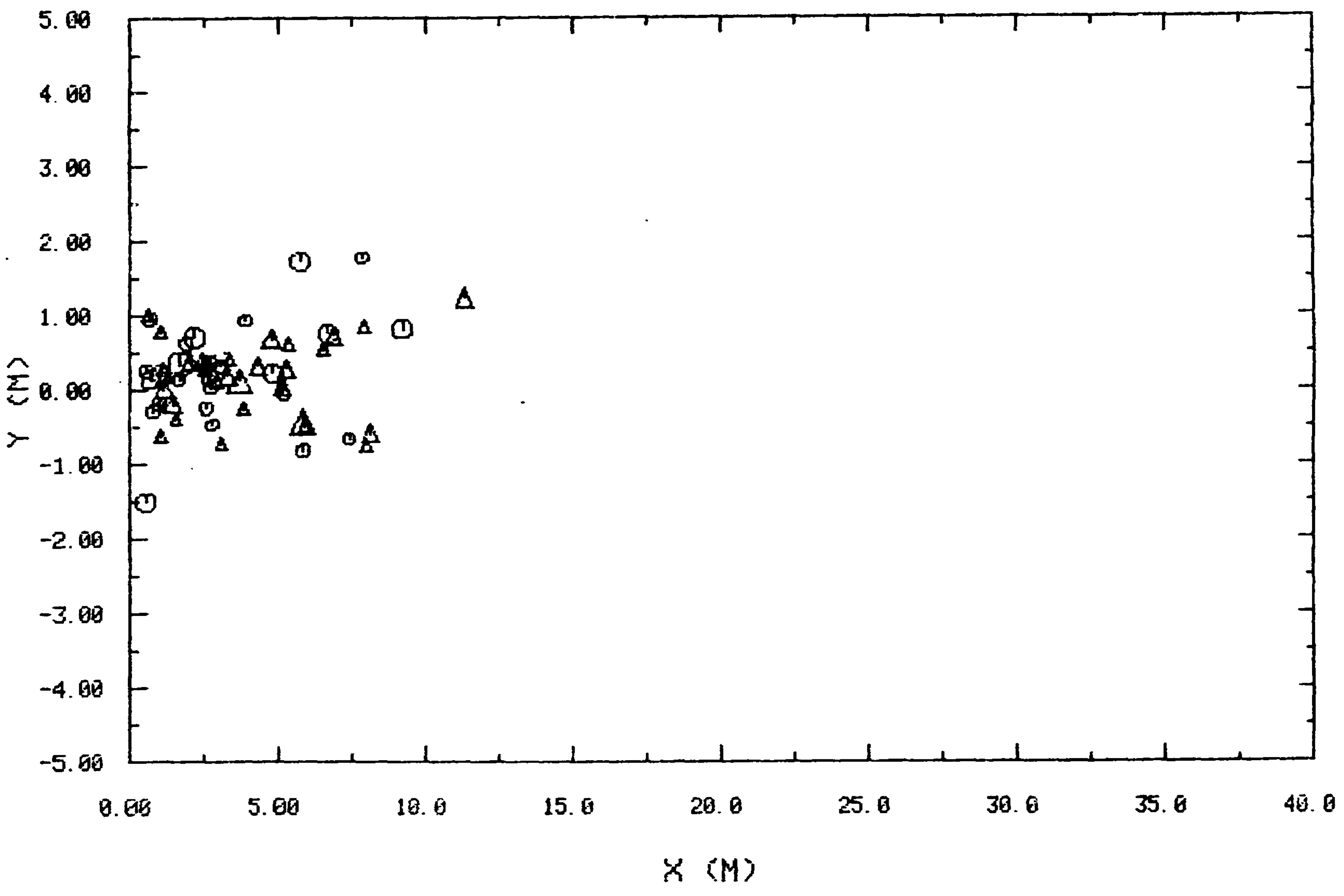

5.00
4.00
3.00
2.00
1.00
0.00
-1.00
-2.00
-3.00
-4.00
-5.00
Y (M)
0.00
5.00
10.0
15.0
20.0
25.0
30.0
35.0
40.0
X (M)

TEST NO. 20

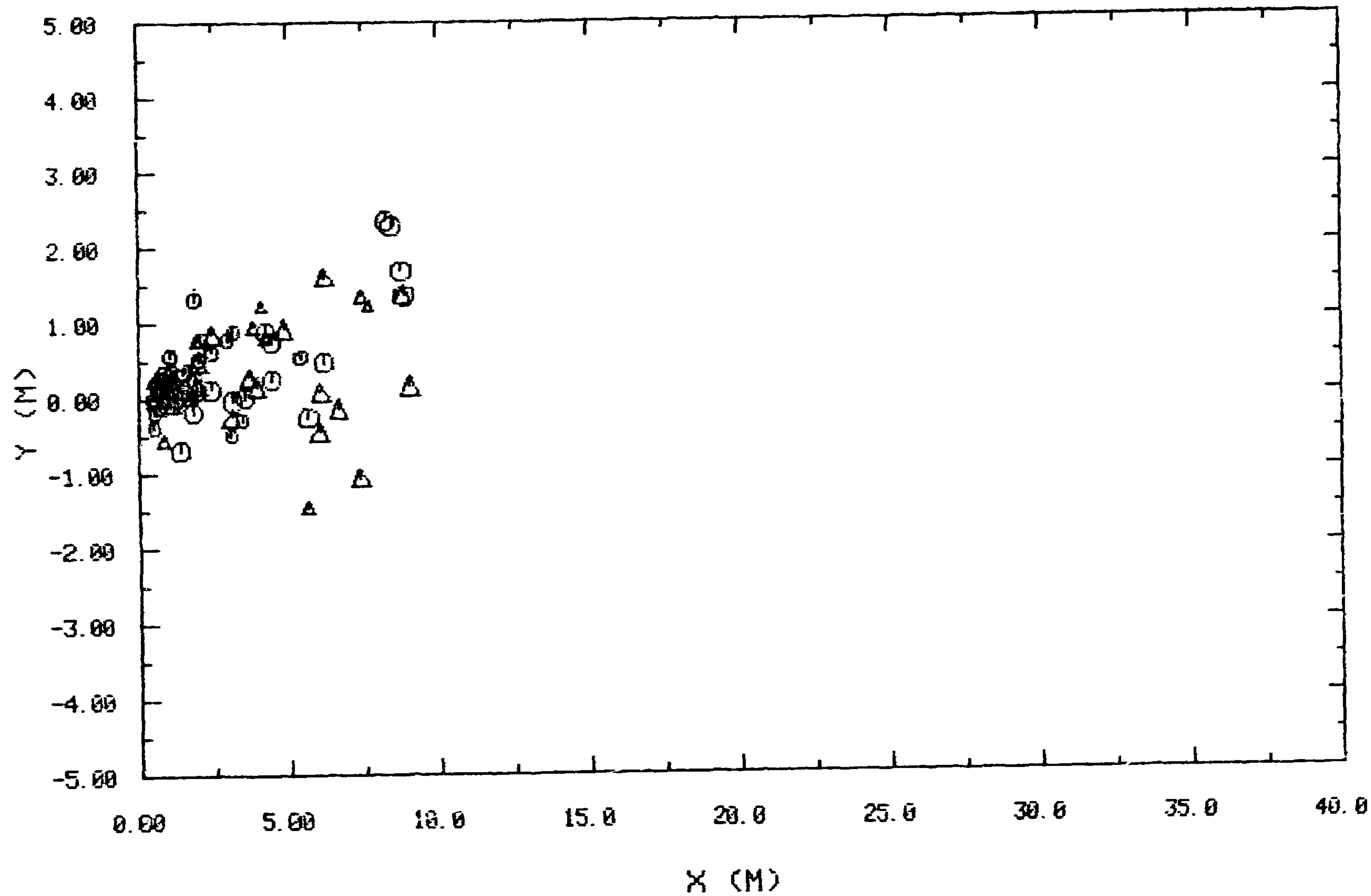

5.00
4.00
3.00
2.00
1.00
0.00
-1.00
-2.00
-3.00
-4.00
-5.00
Y (M)
0.00
5.00
10.0
15.0
20.0
25.0
30.0
35.0
40.0
X (M)

TEST NO. 21

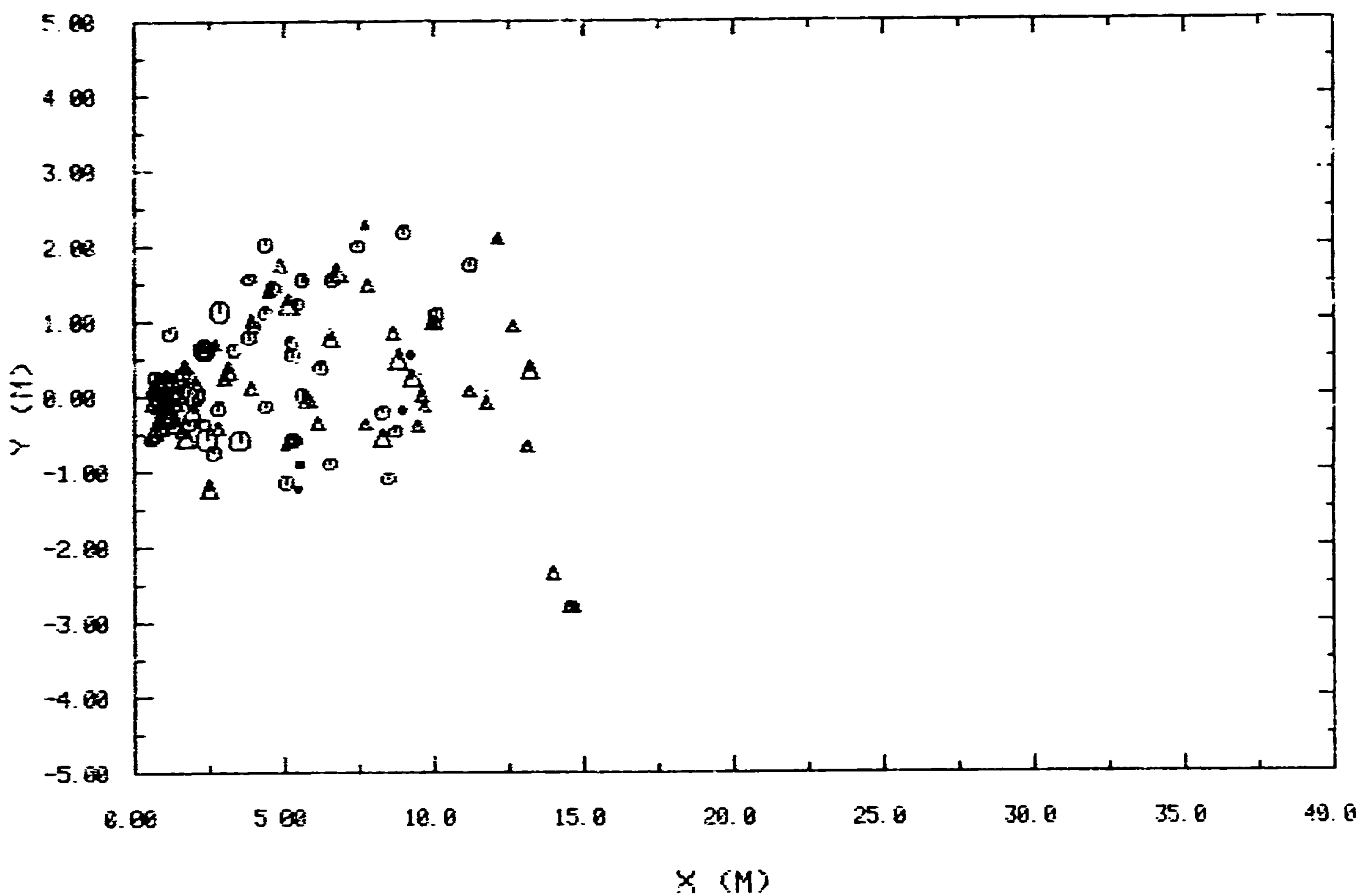

5.00
4.00
3.00
2.00
1.00
0.00
-1.00
-2.00
-3.00
-4.00
-5.00
Y (M)
0.00
5.00
10.0
15.0
20.0
25.0
30.0
35.0
40.0
X (M)

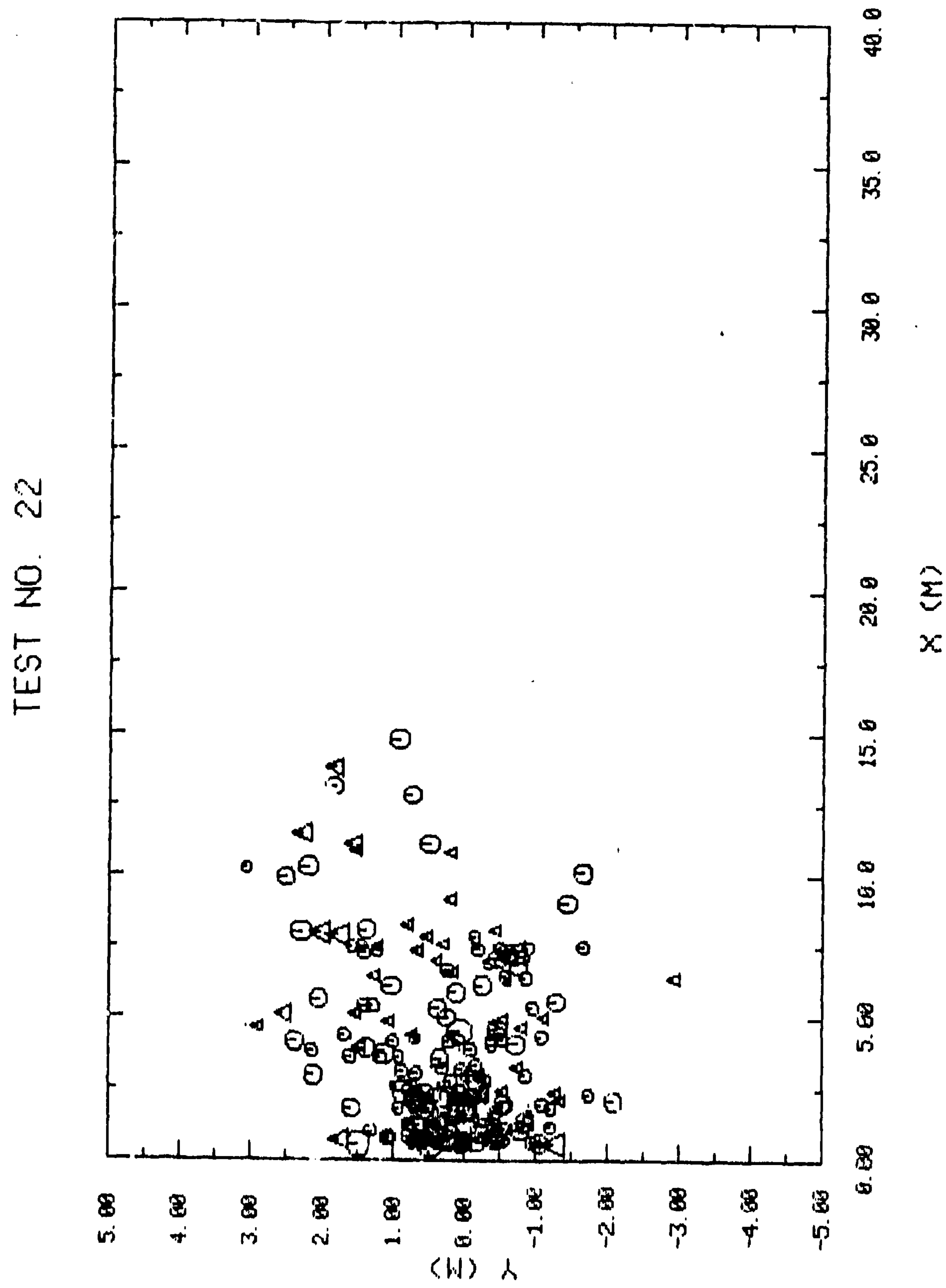

TEST NO. 22
X (M)
Y (M)
0.00
5.00
10.0
15.0
20.0
25.0
30.0
35.0
40.0
5.00
4.00
3.00
2.00
1.00
0.00
-1.00
-2.00
-3.00
-4.00
-5.00

TEST NO. 23

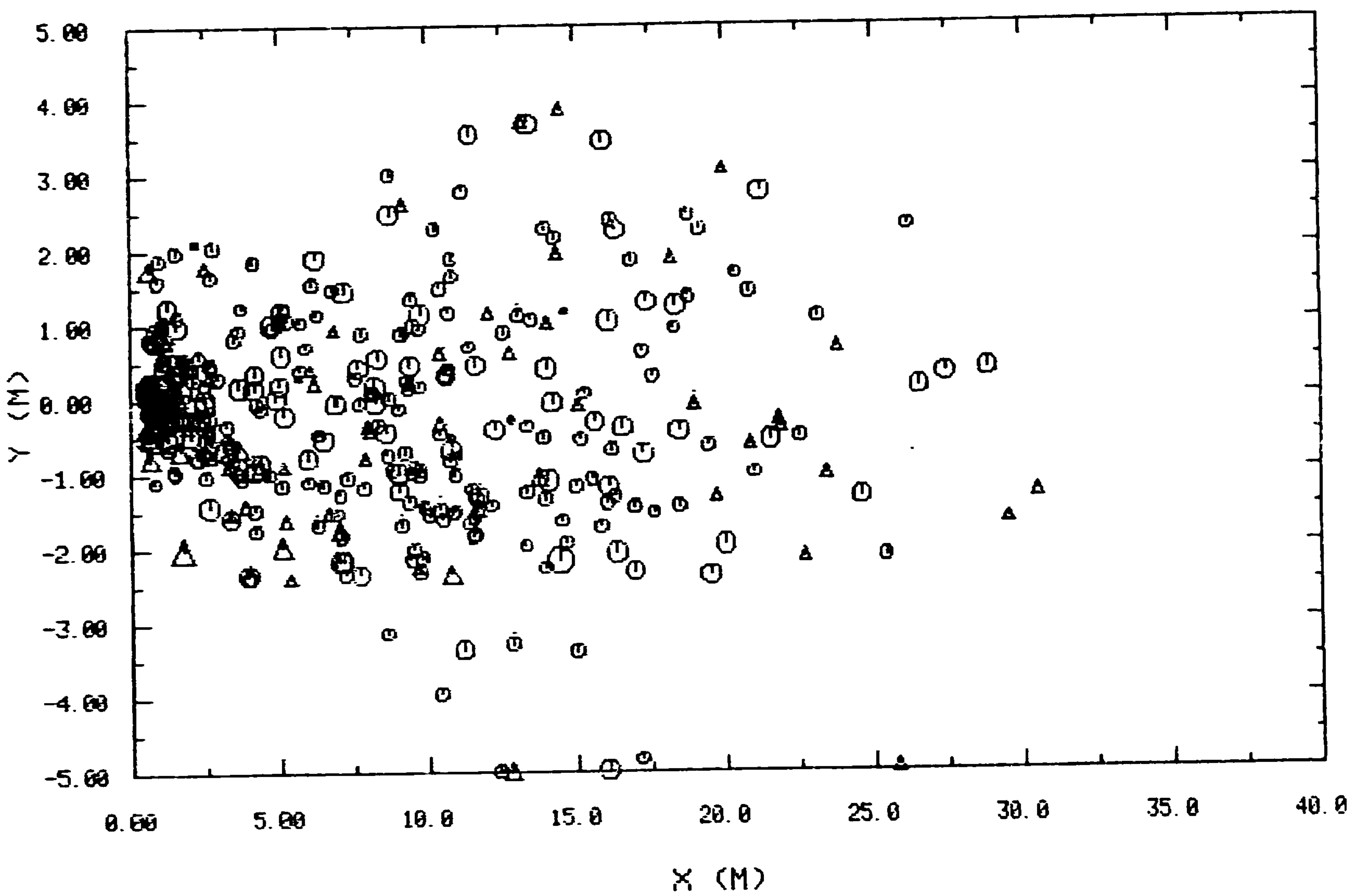
5.00
4.00
3.00
2.00
1.00
0.00
-1.00
-2.00
-3.00
-4.00
-5.00
Y (M)
0.00
5.00
10.0
15.0
20.0
25.0
30.0
35.0
40.0
X (M)

TEST NO. 24

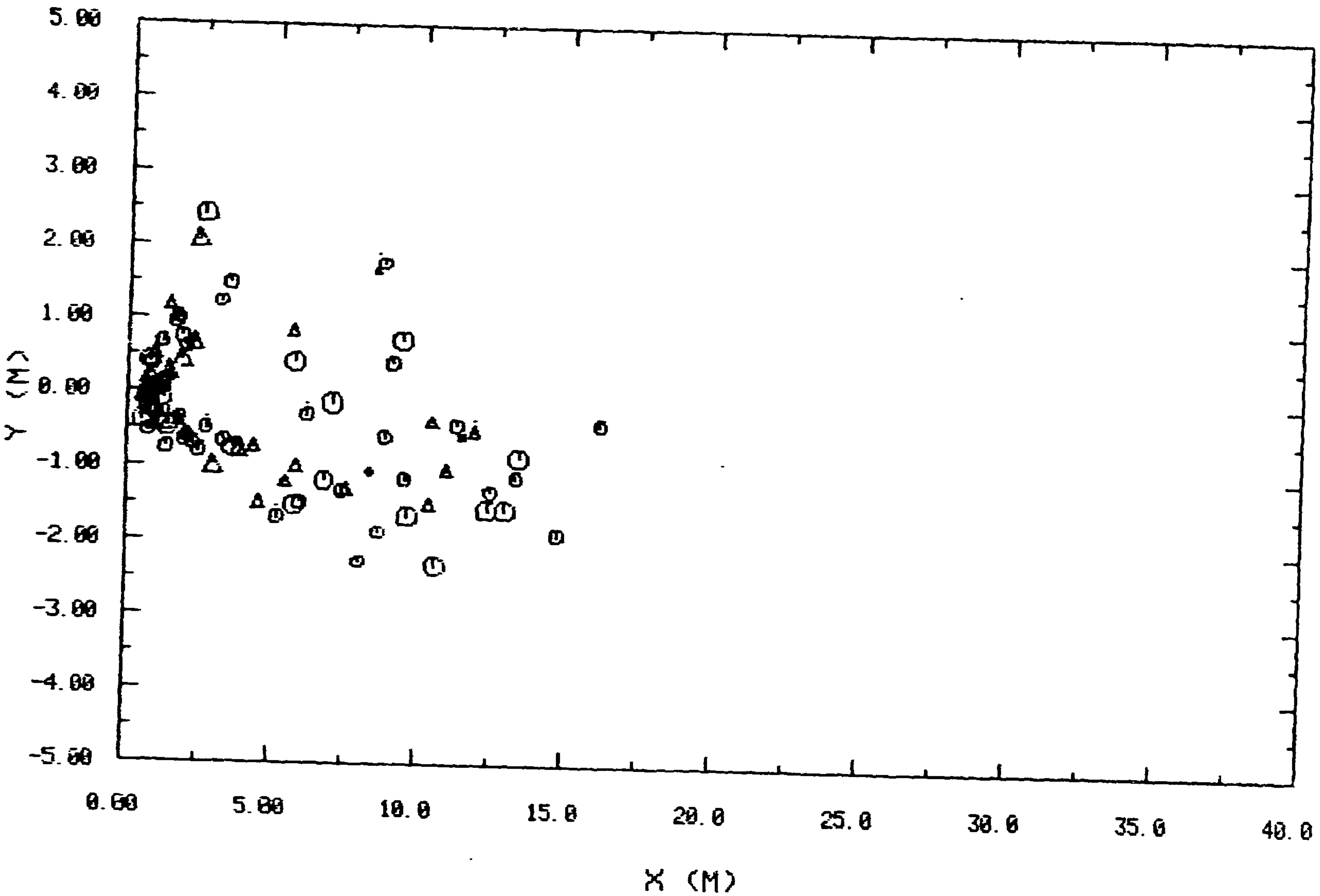

Y (M)
X (M)
5.00
4.00
3.00
2.00
1.00
0.00
-1.00
-2.00
-3.00
-4.00
-5.00
0.00
5.00
10.0
15.0
20.0
25.0
30.0
35.0
40.0

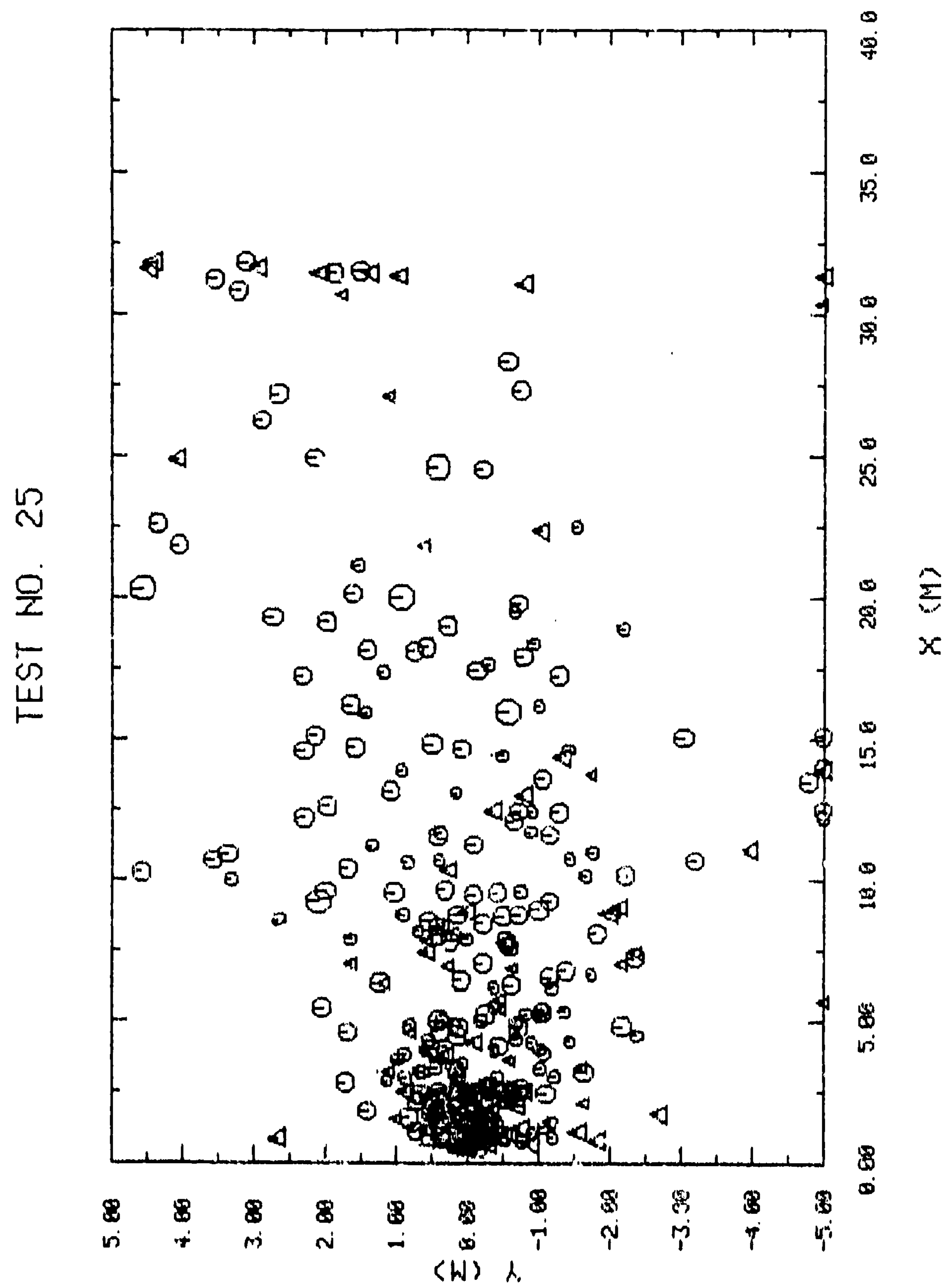
TEST NO. 25
X (M)
Y (M)
0.00
5.00
10.0
15.0
20.0
25.0
30.0
35.0
40.0
5.00
4.00
3.00
2.00
1.00
0.00
-1.00
-2.00
-3.00
-4.00
-5.00

TEST NO. 26

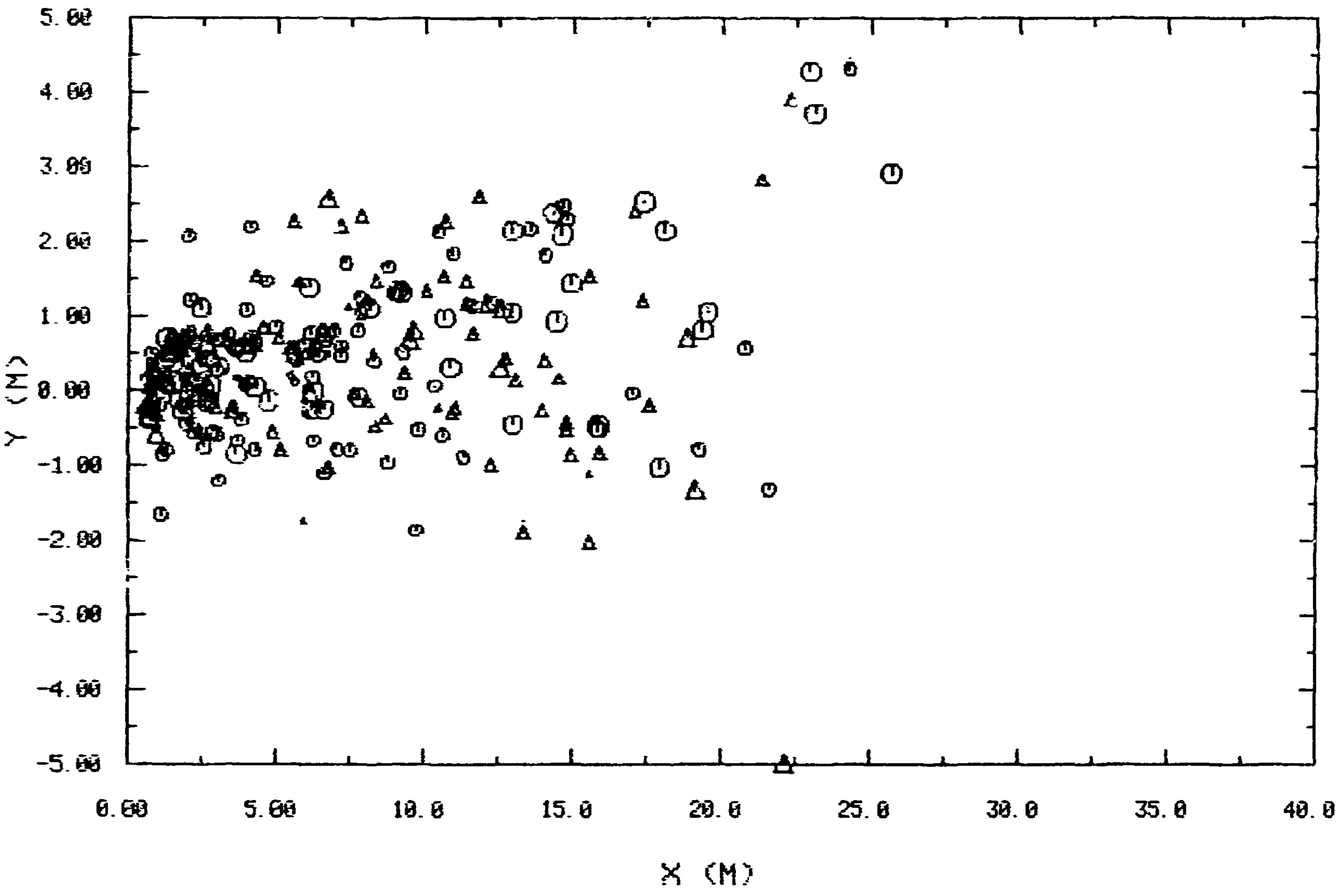
5.00
4.00
3.00
2.00
1.00
0.00
-1.00
-2.00
-3.00
-4.00
-5.00
Y (M)
0.00
5.00
10.0
15.0
20.0
25.0
30.0
35.0
40.0
X (M)

TEST NO. 27

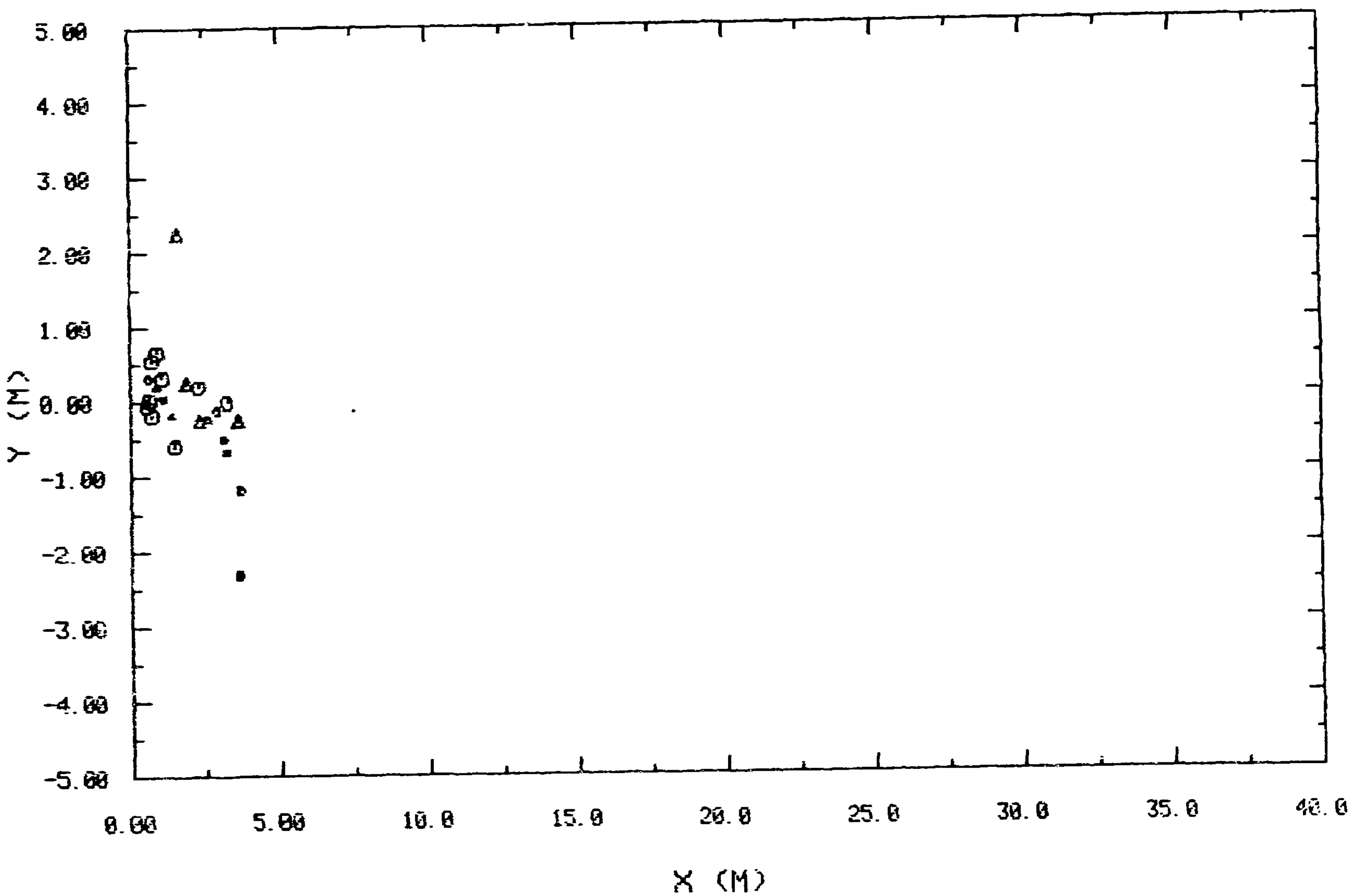

5.00
4.00
3.00
2.00
1.00
0.00
-1.00
-2.00
-3.00
-4.00
-5.00
Y (M)
0.00
5.00
10.0
15.0
20.0
25.0
30.0
35.0
40.0
X (M)

TEST NO. 28

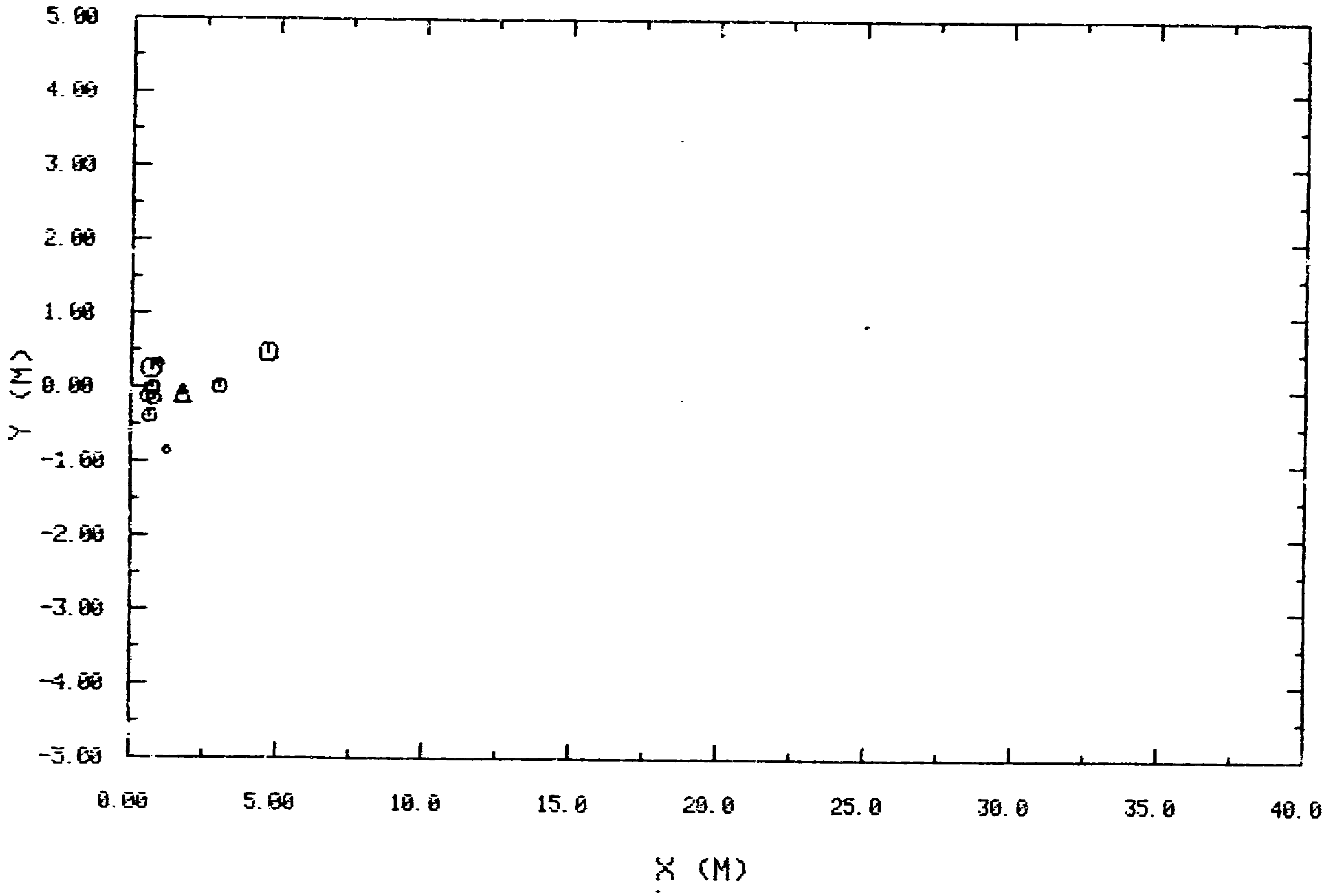

5.00
4.00
3.00
2.00
1.00
0.00
-1.00
-2.00
-3.00
-4.00
-5.00
Y (M)
0.00
5.00
10.0
15.0
20.0
25.0
30.0
35.0
40.0
X (M)

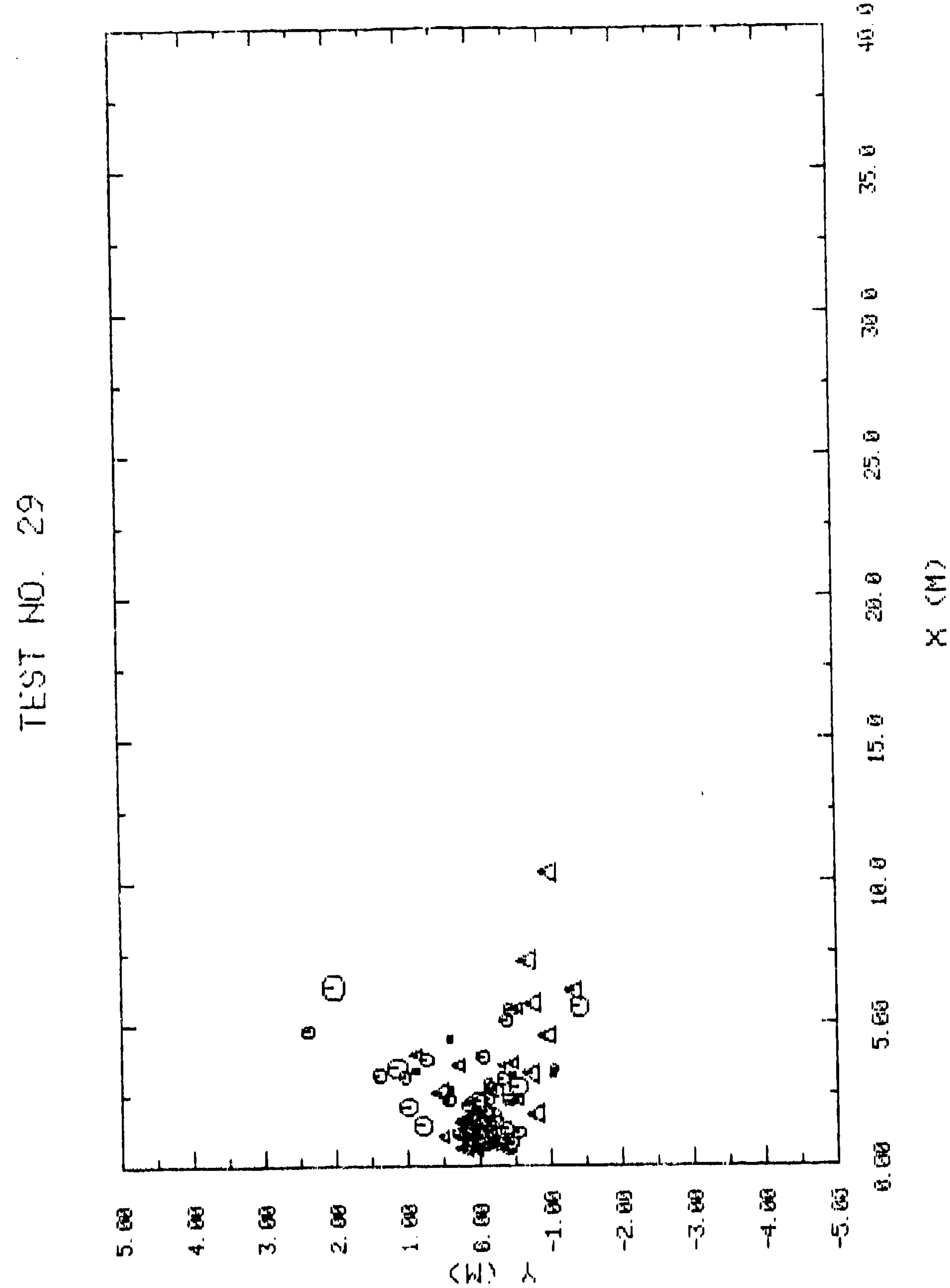
TEST NO. 29
X (M)
Y (M)
0.00
5.00
10.0
15.0
20.0
25.0
30.0
35.0
40.0
5.00
4.00
3.00
2.00
1.00
0.00
-1.00
-2.00
-3.00
-4.00
-5.00

TEST NO. 30

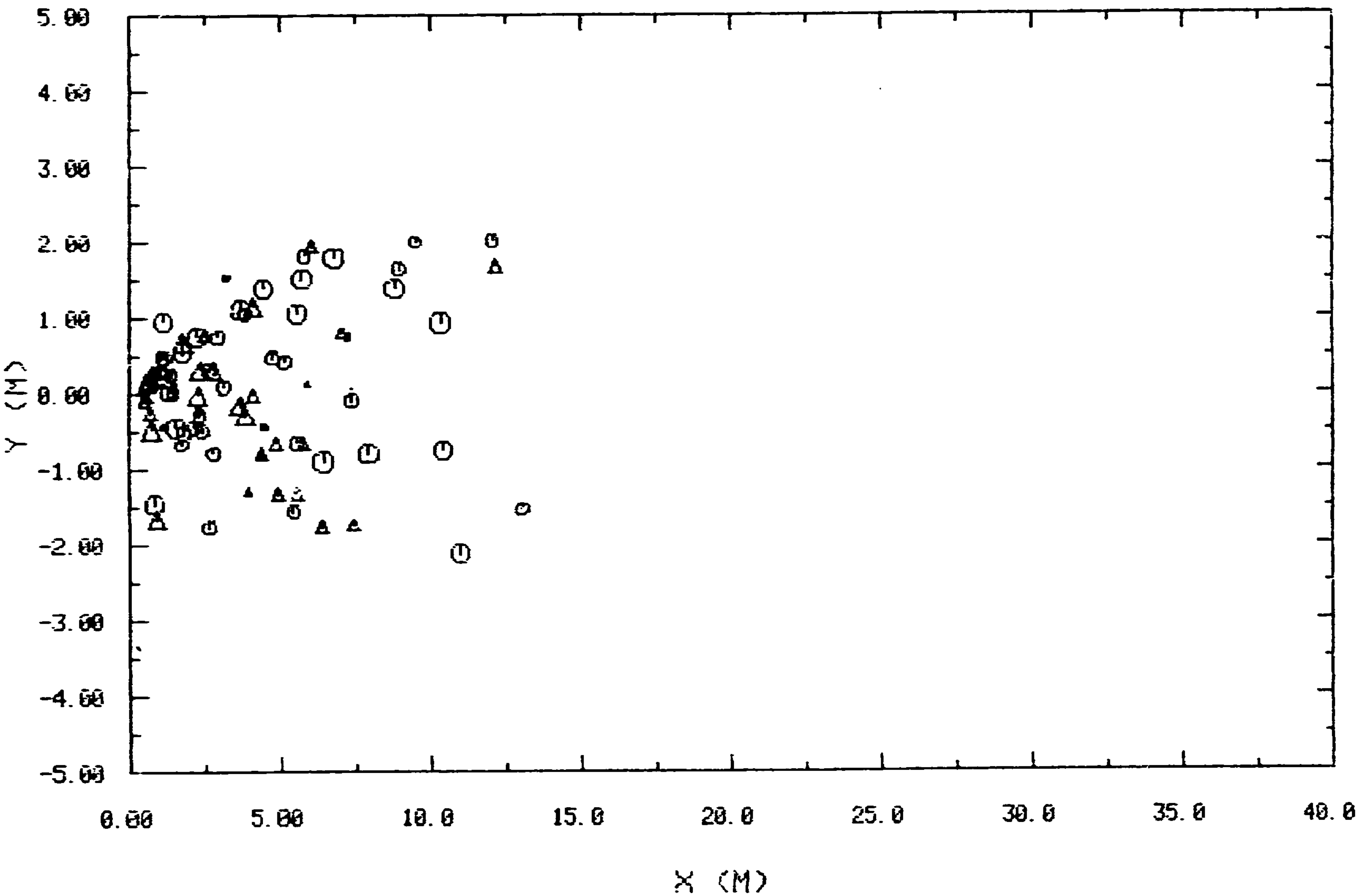

5.00
4.00
3.00
2.00
1.00
0.00
-1.00
-2.00
-3.00
-4.00
-5.00
Y (M)
0.00
5.00
10.0
15.0
20.0
25.0
30.0
35.0
40.0
X (M)

TEST NO. 31

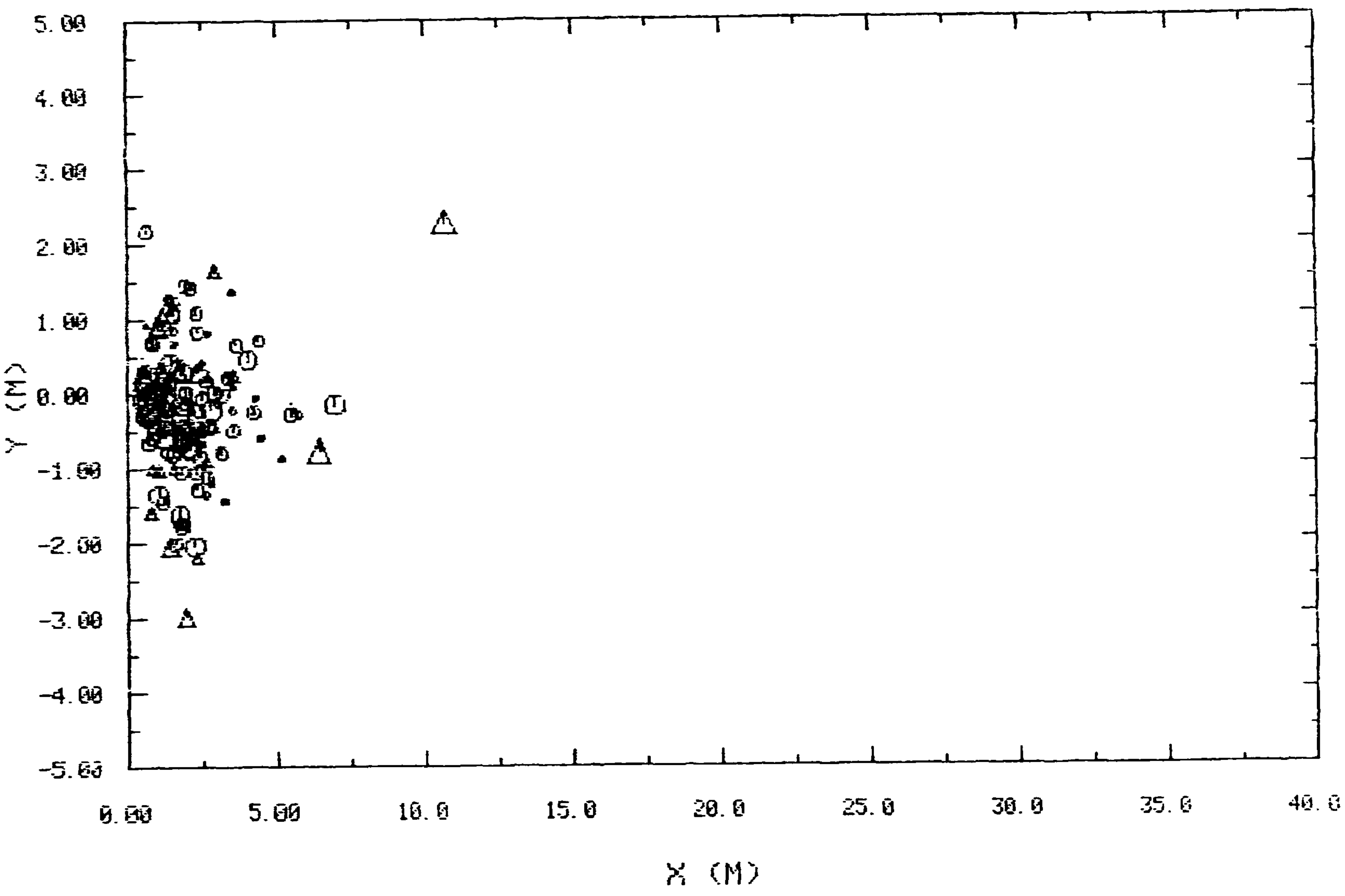
5.00
4.00
3.00
2.00
1.00
0.00
-1.00
-2.00
-3.00
-4.00
-5.00
Y (M)
0.00
5.00
10.0
15.0
20.0
25.0
30.0
35.0
40.0
X (M)

TEST NO. 32

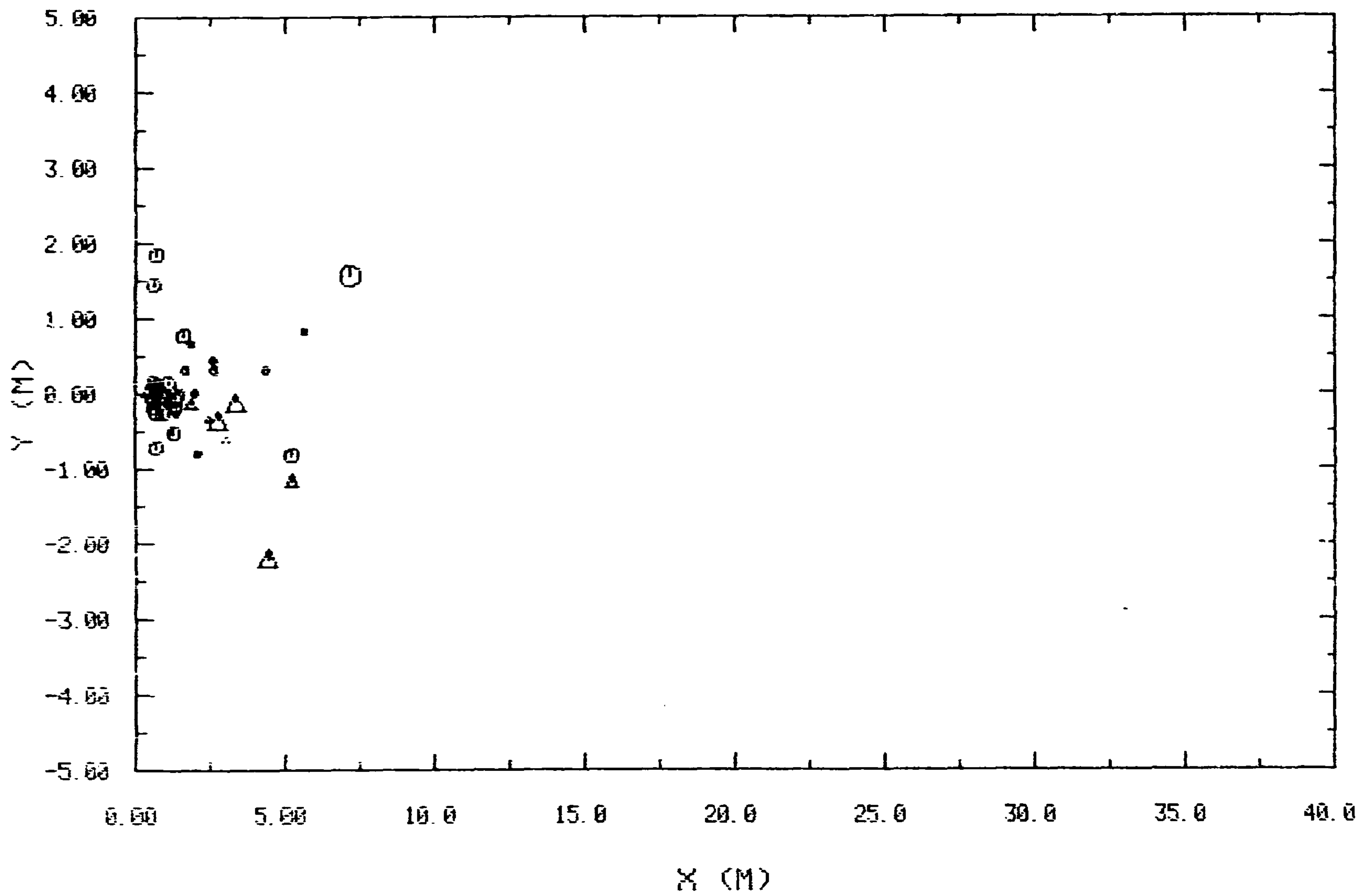

5.00
4.00
3.00
2.00
1.00
0.00
-1.00
-2.00
-3.00
-4.00
-5.00
Y (M)
0.00
5.00
10.0
15.0
20.0
25.0
30.0
35.0
40.0
X (M)

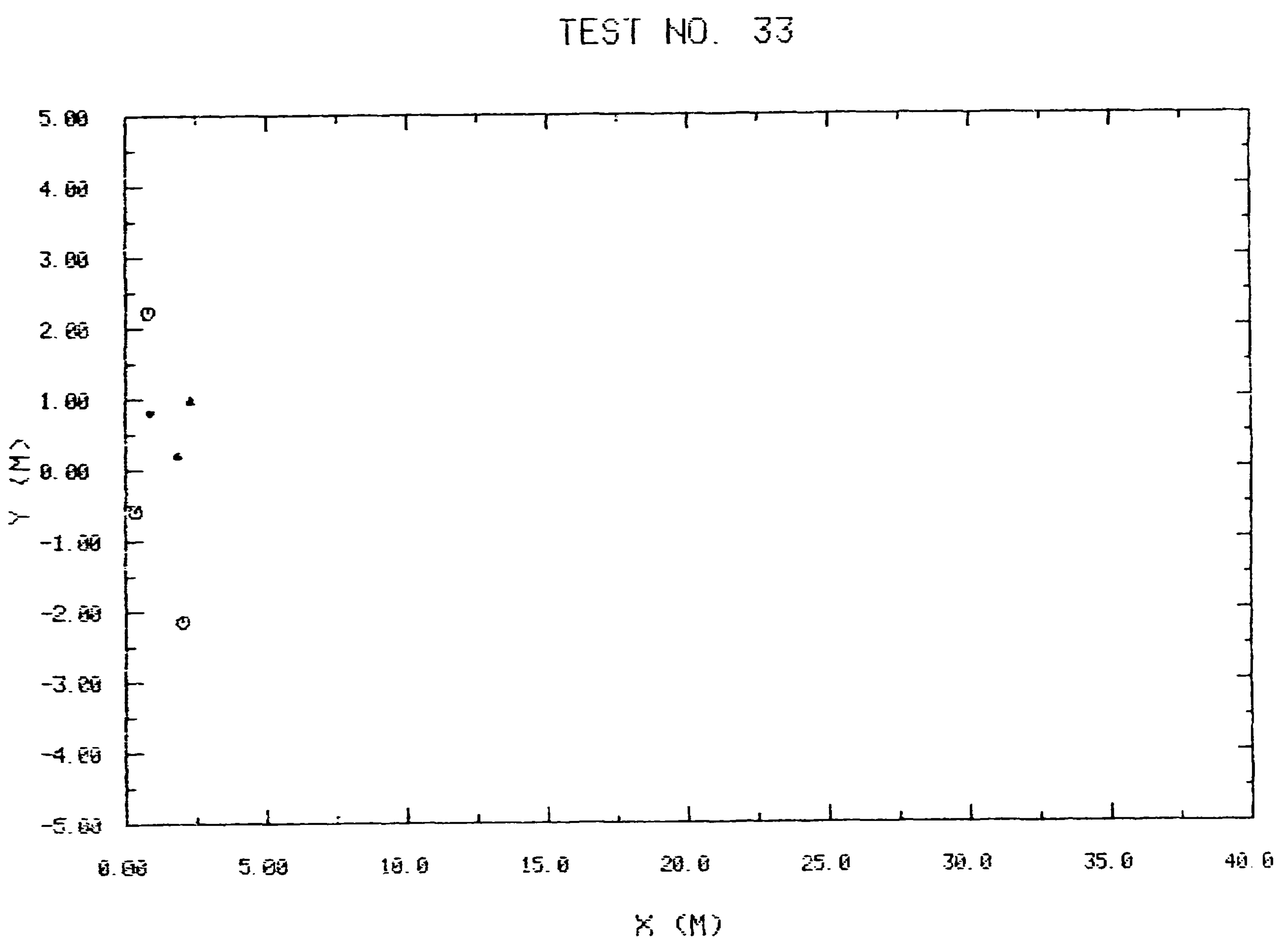
TEST NO. 33
Y (M)
X (M)
5.00
4.00
3.00
2.00
1.00
0.00
-1.00
-2.00
-3.00
-4.00
-5.00
0.00
5.00
10.0
15.0
20.0
25.0
30.0
35.0
40.0

TEST NO. 34

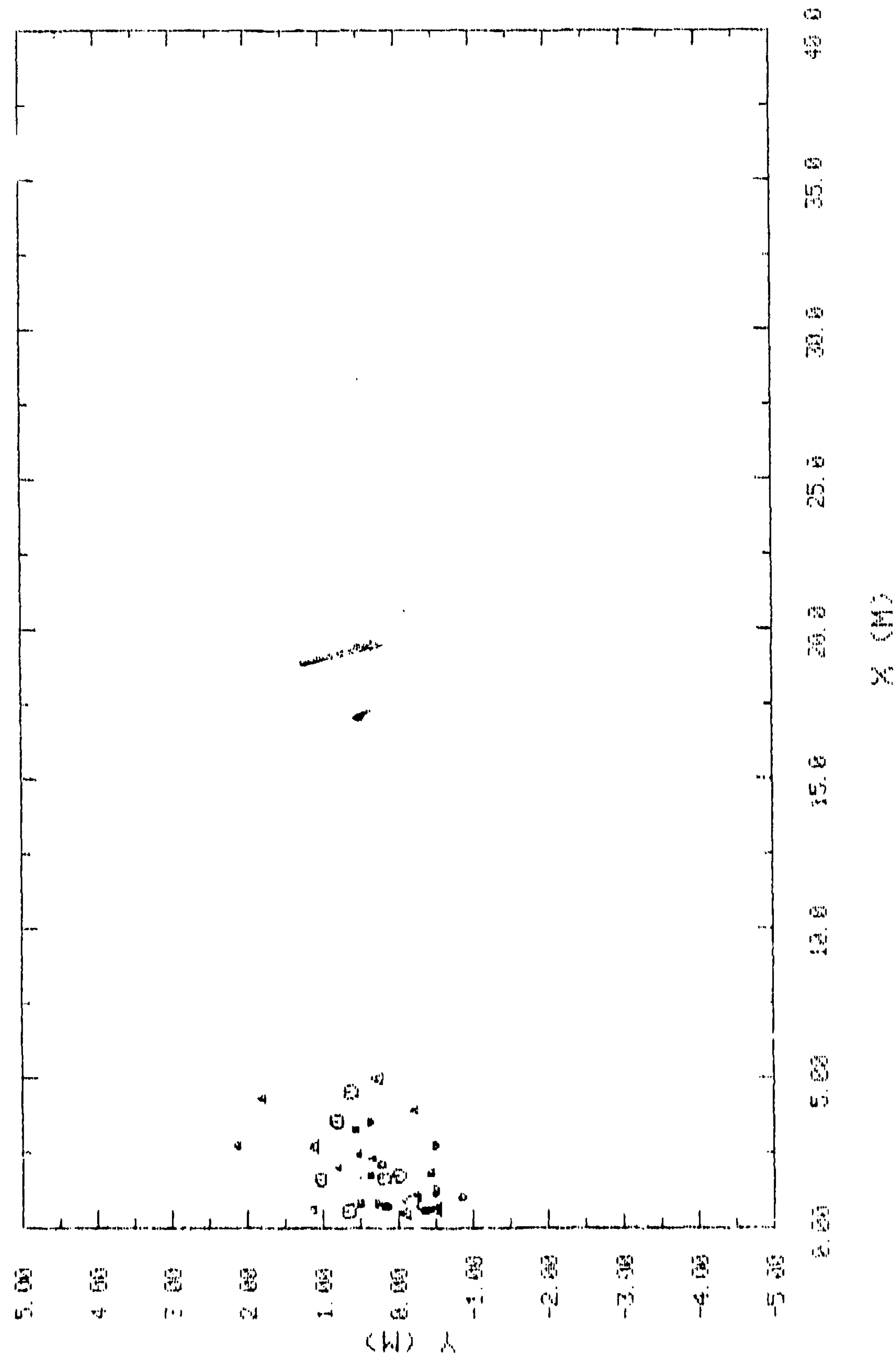

X (M)
Y (M)
0.00
5.00
10.0
15.0
20.0
25.0
30.0
35.0
40.0
5.00
4.00
3.00
2.00
1.00
0.00
-1.00
-2.00
-3.00
-4.00
-5.00

TEST NO. 35

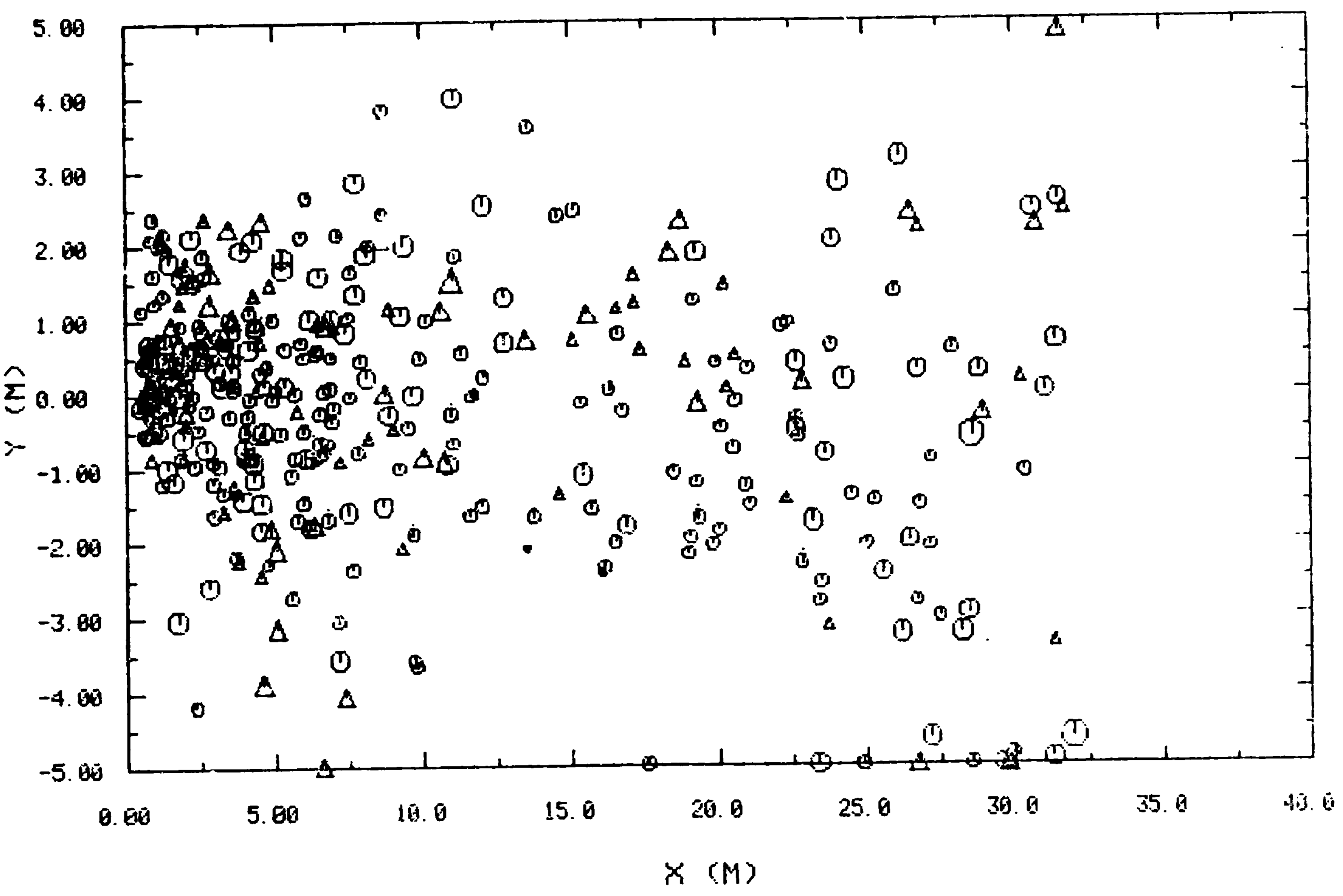
5.00
4.00
3.00
2.00
1.00
0.00
-1.00
-2.00
-3.00
-4.00
-5.00
Y (M)
0.00
5.00
10.0
15.0
20.0
25.0
30.0
35.0
40.0
X (M)

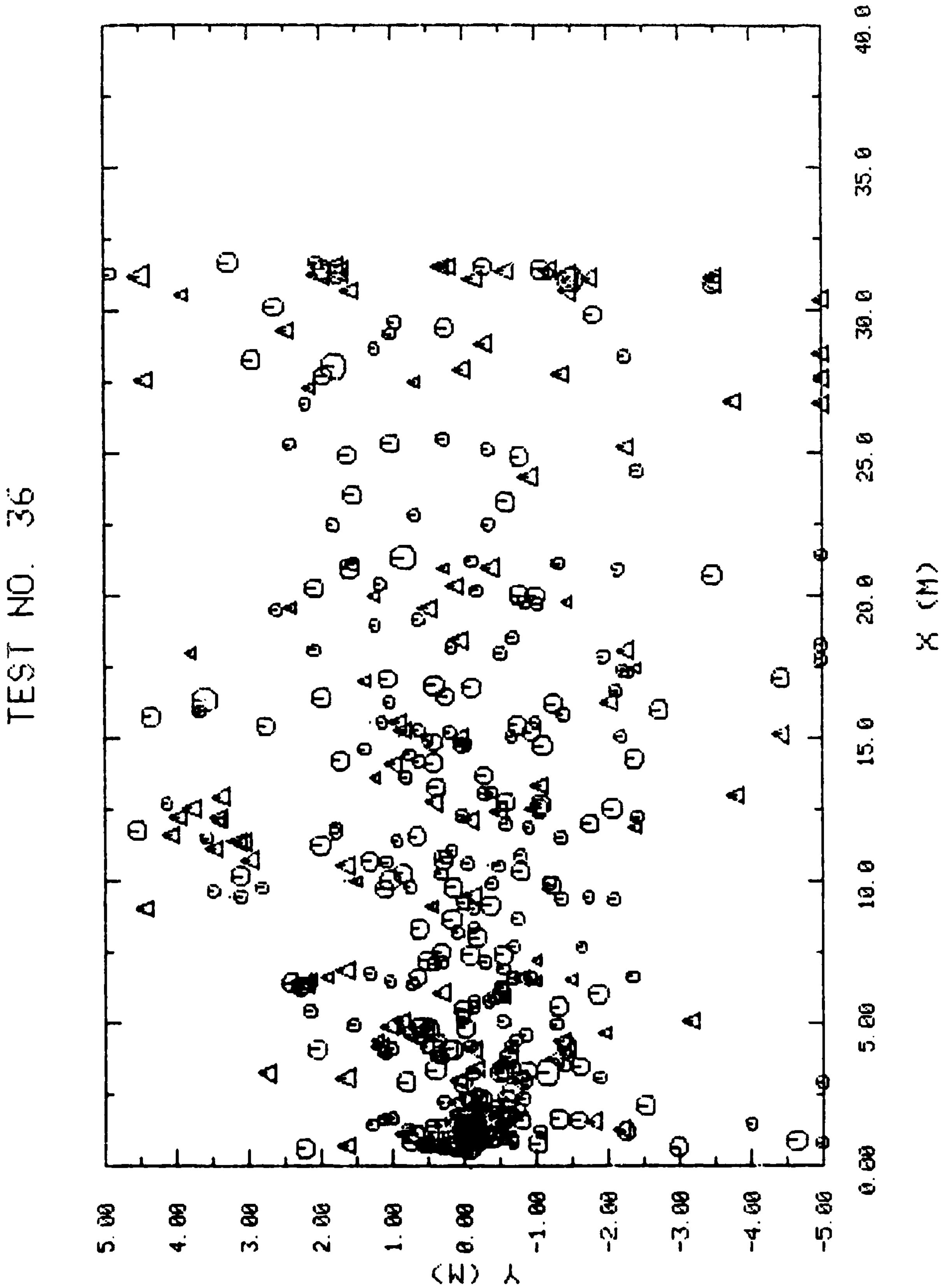
TEST NO. 36
X (M)
Y (M)
0.00
5.00
10.0
15.0
20.0
25.0
30.0
35.0
40.0
5.00
4.00
3.00
2.00
1.00
0.00
-1.00
-2.00
-3.00
-4.00
-5.00

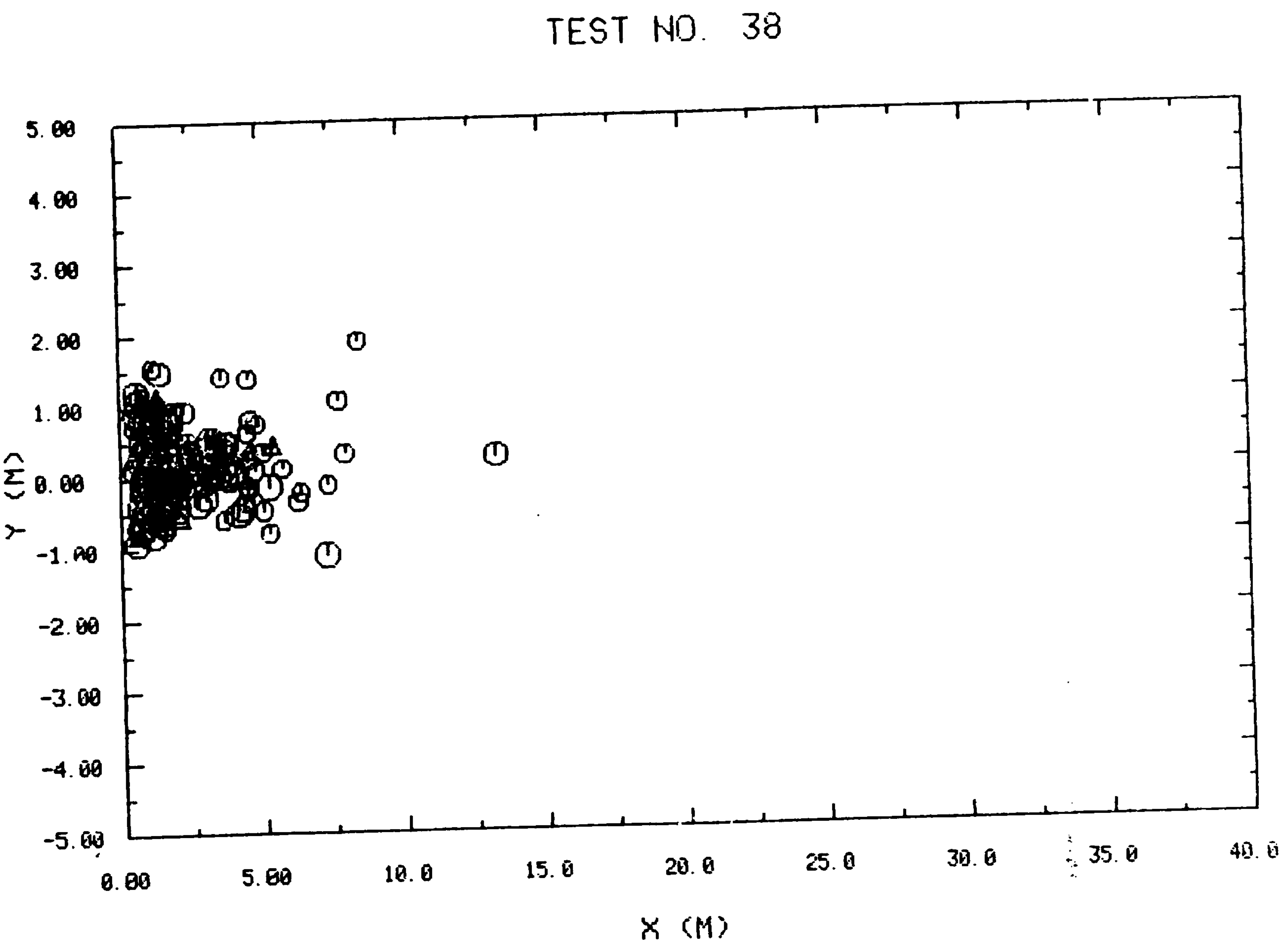
TEST NO. 38
5.00
4.00
3.00
2.00
1.00
0.00
-1.00
-2.00
-3.00
-4.00
-5.00
Y (M)
0.00
5.00
10.0
15.0
20.0
25.0
30.0
35.0
40.0
X (M)

TEST NO. 39

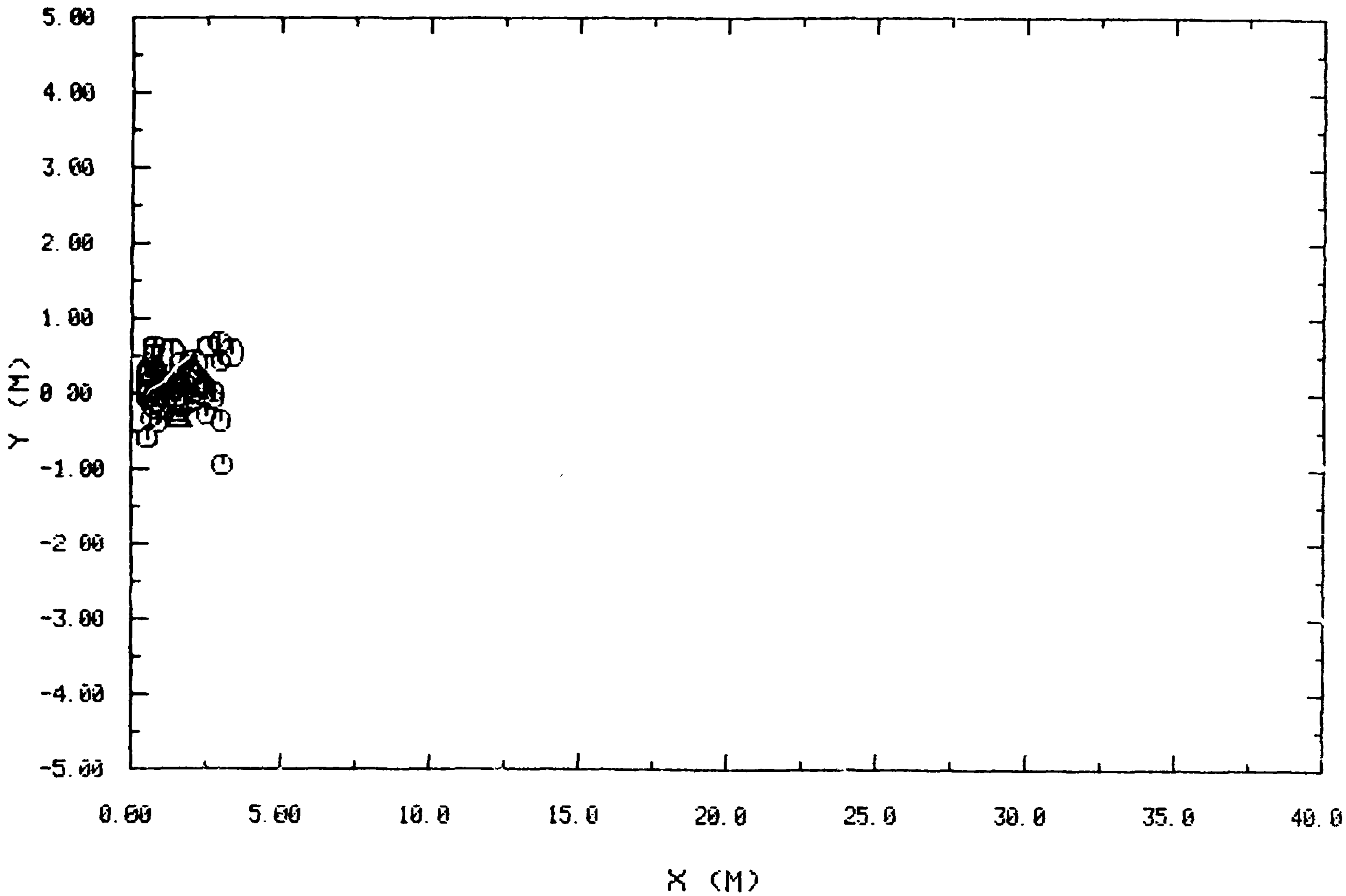

5.00
4.00
3.00
2.00
1.00
0.00
-1.00
-2.00
-3.00
-4.00
-5.00
Y (M)
0.00
5.00
10.0
15.0
20.0
25.0
30.0
35.0
40.0
X (M)

DISTRIBUTION LIST

Commander
U.S. Army Armament Research and
  Development Command
ATTN: DRDAR-CG
      DRDAR-LC
      DRDAR-LCM
      DRDAR-LCM-S (12)
      DRDAR-SF
      DRDAR-TSS (5)
      DRDAR-GCL
Dover, NJ 07801

Commander
U.S. Army Materiel Development and
  Readiness Command
ATTN: DRCDE
      DRCIS-E
      DRCPA-E
      DRCPP-I
      DRCDL
      DRCSG-S
5001 Eisenhower Avenue
Alexandria, VA 22333

Commander
USDRC Installations and
  Services Agency
ATTN: DRCIS-RI-IU
      DRCIS-RI-IC
Rock Island, IL 61299

Commander
U.S. Army Materiel and
  Readiness Command
ATTN: DRSAR-IR (2)
      DRSAR-IRC
      DRSAR-ISE (2)
      DRSAR-IRC-E
      DRSAR-PDM
      DRSAR-LC (2)
      DRSAR-ASF (2)
      DRSAR-SF (3)
      DRSAR-LEP-L
Rock Island, IL 61299

Chairman
Department of Defense Explosives
Safety Board (2)
Hoffman Bldg 1, Room 856C
2461 Eisenhower Avenue
Alexandria, VA 22331

Commander
U.S. Army Munitions Base
Modernization Agency
ATTN: SARPA-PBM-LA (3)
SARPM-PBM-T-SF
SARPM-PBM-EP (2)
Dover, NJ 07801

Director
Ballistics Research Laboratory
U.S. Army Armament Research and
Development Command
ATTN: DRDAR-TSB-S
DRDAR-BLE (C. Kingery) (2)
Aberdeen Proving Ground, MD 21005

Administrator
Defense Technical Information Center
ATTN: Accessions Division (12)
Cameron Station
Alexandria, VA 22314

Commander
U.S. Army Construction Engineering
Research Laboratory
ATTN: CERL-ER
Champaign, IL 61820

Office, Chief of Engineers
ATTN: DAEN-MZA-E
Washington, DC 20314

U.S. Army Engineer District,
Huntsville
ATTN: Construction Division
HAD-ED (2)
P.O. Box 1600 West Station
Huntsville, AL 35807

Director
U.S. Army Industrial Base
Engineering Activity
ATTN: DRXIB-MT (2)
Rock Island, IL 61299

Director
DARCOM Field Safety Activity
ATTN: DRXOS (5)
Charlestown, IN 47111

Director
U.S. Army Materiel Systems
Analysis Activity
ATTN: DRXSY-MP
Aberdeen Proving Ground, MD 21005

Commander/Director
Chemical Systems Laboratory
U.S. Army Armament Research and
Development Command
ATTN: DRDAR-CLJ-L
DRDR-CLB-PA
APG, Edgewood Area, MD 21010

Chief
Benet Weapons Laboratory, LCWSL
U.S. Army Armament Research and
Development Command
ATTN: DRDAR-LCB-TL
Watervliet, NY 12189